MASS BALANCE OF MERCURY IN THE IDRIJCA RIVER CATCHMENT

Doctoral Dissertation
Jožef Stefan International Postgraduate School
Ljubljana, Slovenia, May 2008

Supervisor: *Prof. Dr., Milena Horvat*

Evaluation Board:

Assist. Prof. Dr., Nives Ogrinc, Chairman, Jožef Stefan Institute, Ljubljana, Slovenia

Prof. Dr. Rudolf Rajar, Member, Faculty of Civil and Geodetic Engineering, Ljubljana, Slovenia

Assist. Prof. Dr., Radmila Milačič, Member, Jožef Stefan Institute, Ljubljana, Slovenia

David Kocman

MASS BALANCE OF MERCURY IN THE IDRIJCA RIVER CATCHMENT

Doctoral Dissertation

SNOVNA BILANCA ŽIVEGA SREBRA V POREČJU REKE IDRIJCE

Doktorska disertacija

Supervisor: Prof. Dr. Milena Horvat

May 2008

MEDNARODNA PODIPLOMSKA ŠOLA JOŽEFA STEFANA
JOŽEF STEFAN INTERNATIONAL POSTGRADUATE SCHOOL
Ljubljana, Slovenia

Index

Abstract

Mercury (Hg) pollution has been investigated in the area of the Idrija mercury mine, Slovenia, where the second largest mercury mine in the world operated for more then 500 years. Although the production of mercury at the Idrija mercury mine stopped in 1994, centuries of mining and ore processing operations left behind intense pollution of all environmental compartments, not only in the vicinity of the mine but also in the wider Idrija area.

The overall objective of this study was to establish the main recent sources and sinks, fate and distribution of mercury in different environmental compartments in the Idrijca River catchment.

Sources of mercury in the Idrijca River catchment were identified by measurements of its concentrations in all environmental compartments including water, soils, river sediments and air. In the river water samples of the Idrijca River and its major tributaries, mercury speciation analyses (THg, PHg, DHg, RHg, DGM, MeHg) as well as general geochemical analysis (pH, O_2, Cl^-, SO_4^{2-}) were performed in order to determine the parameters that influence the chemistry of mercury in river water. The influence of changing hydrological conditions on chemistry and transport of mercury was also investigated. In soil samples, spatial and vertical distribution, binding and mobility of different mercury forms (THg, MeHg, water soluble) was investigated based on the Hg speciation and fractionation analysis. In river sediment samples, total Hg was measured in different size fractions to estimate the mercury pool available for further aquatic transport and transformation processes. With the aim of establishing spatial distribution and major sources of elemental mercury (Hg^0) in the atmosphere, Hg^0 geochemical mapping was used. To better understand the fate and behavior of atmospheric mercury, different mercury species (RGM, TPM, GEM) in air over Idrija were determined. In order to determine the rates of atmospheric mercury deposition, concentrations of different mercury species (THg, PHg, DHg, RHg, DGM, MeHg) in precipitation were measured. Furthermore, the magnitude and the influence of different environmental parameters (temperature, moisture and solar radiation) on the mercury soil-atmosphere exchange were investigated during the laboratory flux measurement system experiment.

Based on the experimental results, a mass-balance model of sources, sinks and mercury transport process at the Idrijca River catchment was developed. The processes that were taken into account in the model include erosion of contaminated soils, surface runoff, riverine transport, atmospheric deposition and mercury emissions from the surface. The model is based upon mercury mass-balance calculations as a combination of different approaches. Mercury loads due to the atmospheric deposition and riverine transport were calculated based on the measurements of Hg in precipitation and river water. For the calculation of mercury terrestrial loads to the water system, a WCS mercury tool (Dai and Manguerra, 2000) was used and adopted for site specific conditions. Sediment production was estimated by the Erosion Potential Method (EPM) (Gavrilović, 1988). Based on the results of the laboratory flux chamber experiment Hg emission model was developed. The results of the mercury mass balance model revealed that in the Idrijca River catchment erosion of mercury contaminated soils and surface runoff remain the main inputs of mercury into the Idrijca River tributary system. Taking the calculated inputs and outputs of mercury to/from the catchment into account, it can be concluded that without the suitable remediation actions a reduction of mercury pollution in the area can not be expected.

Keywords: mercury, mass-balance, modeling, Idrijca River catchment

Povzetek

Pričujoče delo obravnava raziskave onesnaženja z živim srebrom (Hg) na območju Idrijskega rudnika živega srebra, kjer je več kot 500 let obratoval drugi največji rudnik živega srebra na svetu. Kljub temu, da je bila proizvodnja živega srebra v rudniku Idrija leta 1994 končana, je posledica stoletnega rudarjenja in predelave rude onesnaženje z živim srebrom v vseh segmentih okolja. Onesnaženje ni omejeno zgolj na bližino rudnika pač pa na širše območje Idrije.

Glavni cilj doktorske naloge je določitev največjih trenutnih izvorov in ponorov, usode in porazdelitve živega srebra v različnih okoljskih segmentih na območju porečja reke Idrijce.

Z namenom določitve glavnih izvorov živega srebra na porečju Idrijce so bile opravljene meritve koncentracij živega srebra v rečni vodi, tleh, rečnem sedimentu in zraku. V vzorcih vod iz reke Idrijce in njenih največjih pritokih so bile vzporedno s speciacijo živega srebra (THg, PHg, DHg, RHg, DGM, MeHg) opravljene splošne geokemične meritve (pH, O_2, Cl^-, SO_4^{2-}). Na ta način so bili določeni parametri, ki najbolj vplivajo na kemizem živega srebra v vodnem okolju. Preučevan je bil tudi vpliv spremenjenih hidroloških razmer na kemizem in transport živega srebra. Na vzorcih tal je bila opravljena speciacija in frakcionacija živega srebra (THg, MeHg, vodotopna frakcija) z namenom ugotavljanja prostorske in vertikalne porazdelitve živega srebra v tleh, njegove vezave in mobilnosti. Za oceno količine živega srebra, ki je na razpolago za transport in pretvorbe v vodnem okolju, so bile izmerjene koncentracije Hg v rečnih sedimentih različnega velikostnega razreda. Za določitev prostorske porazdelitve in glavnih virov elementarnega živega srebra (Hg^0) v zraku je bila uporabljena metoda geokemijskega kartiranja, za razumevanje usode in obnašanja živega srebra v atmosferi pa so bile izmerjene različne oblike Hg v zraku (RGM, TPM, GEM). Stopnja atmosferskega odlaganja živega srebra je bila preučevana na podlagi meritev različnih oblik živega srebra v padavinah (THg, PHg, DHg, RHg, DGM, MeHg). Izmenjava živega srebra med tlemi in atmosfero ter vpliv različnih okoljskih parametrov (temperatura, vlaga, sončno obsevanje) na ta proces so bili merjeni s pomočjo t.i. »flux-chamber« metode v laboratorijskih pogojih.

Na podlagi eksperimentalno pridobljenih podatkov je bil za porečje reke Idrijce izdelan model izvorov, ponorov in transporta živega srebra. Model vključuje naslednje procese: erozijo kontaminiranih tal, površinski odtok, rečni transport, atmosfersko odlaganje ter emisije živega srebra iz tal. Model temelji na izračunu snovnih tokov živega srebra in je kombinacija različnih pristopov. Doprinos živega srebra z atmosferskim odlaganjem ter rečni transport sta bila izračunana na podlagi meritev vsebnosti živega srebra v padavinah in rečni vodi. Za izračun terestričnega vnosa živega srebra v vodno okolje je bil uporabljen t.i. WCS mercury tool model (Dai and Manguerra, 2000) prilagojen razmeram na območju porečja Idrijce. Povprečno letno sproščanje zemljin zaradi erozije je bilo ocenjeno s pomočjo EPM (Erosion Potential Method) modela (Gavrilović, 1988). Na podlagi laboratorijskih meritev izhlapevanja živega srebra iz tal je bil izdelan Hg emisijski model. Rezultati so pokazali, da na porečju Idrijce erozija kontaminiranih tal in površinski odtok ostajata glavni izvor živega srebra za vodno okolje. Na podlagi izračunanih vnosov in ponorov v/iz porečja je moč sklepati, da brez ustreznih remediacijskih ukrepov ni možno pričakovati zmanjšanja obremenjenosti tega okolja z živim srebrom.

Ključne besede: živo srebro, snovni tok, modeliranje, porečje Idrijce

Abbreviations

Hg	=	mercury
Hg^0	=	chemical symbol used to denote mercury in its elemental or uncharged form
Hg^{2+}	=	chemical symbol used to denote mercury in its positively charged or reactive state
Hg(p)	=	symbol used to denote mercury attached onto or absorbed into a particle
THg	=	total mercury (sum of all Hg species)
PHg	=	particulate Hg in water and precipitation, operationally-defined (> 0.45 µm)
DHg	=	dissolved Hg in water and precipitation, operationally-defined (< 0.45 µm)
RHg	=	reactive mercury in water and precipitation, operationally-defined ($SnCl_2$ reducible)
DGM	=	dissolved gaseous mercury in water and precipitation
MeHg	=	methyl mercury, mercury containing the CH_3 species
TGM	=	total gaseous mercury in ambient air
GEM	=	gaseous elemental mercury in ambient air
RGM	=	reactive gaseous mercury in ambient air; operational term for gaseous Hg^{2+} compounds
TPM	=	total particulate mercury in ambient air; mercury attached to atmospheric particles
MEF	=	mercury emission flux from soil to atmosphere
Kd	=	distribution coefficient; ratio between Hg bound to suspended solids and dissolved Hg
TSS	=	total suspended solids in water
Ea	=	activation energy

1 Introduction

1.1 General introduction

Mercury (Hg) is a potent toxic substance, the toxicity of which is elicited at very low concentrations. As a chemical element, mercury cannot be created or destroyed and the same amount has existed on the planet since the earth was formed. Mercury, however, can cycle in the environment as part of both natural and human (anthropogenic) activities. The natural mercury sources include volcanoes, soils, forests, lakes and open oceans, while the anthropogenic sources are mainly from combustion and waste incineration (Pirrone et al., 1996; Pacyna et al., 2001; Pirrone et al., 2003). Due to these activities, mercury is redistributed in the atmospheric, terrestrial and aquatic ecosystems through a complex combination of transport and transformation processes. During this cycle, mercury's chemical compounds, mostly organic, can bioaccumulate and biomagnificate in living organisms to levels that can result in a variety of ecological and human health impacts. Both the measured data and the modeling results indicate that the amount of mercury mobilized and released into the biosphere has increased by a factor of 2-3 since the beginning of the industrial age (EPA, 1997; EU Position Paper, 2001; UNEP, 2002).

Mercury's adverse effects on health and environment were recognized quite early. Since the first major reported pollution incident in Minamata Bay in Japan in the 1950's, many research activities on mercury have taken place and mercury was recognized as a pollutant of global concern requiring global solutions. Nowadays, mercury related research activities are oriented towards better understanding of processes of atmospheric emissions, transport and deposition mechanisms to terrestrial and aquatic receptors, chemical transformations of mercury to more toxic species i.e., methylmercury, studies on the bioaccumulation of mercury in the aquatic food web as well as exposure and risk assessments. Although mercury may be considered as one of the best documented hazardous substances utilized by man, there is still a great need to improve our knowledge of certain specific aspects involved in the cycling of mercury on local, regional and global scales. Knowledge of the concentrations, transport, transformation, and dynamics of mercury in all environmental compartments is needed to predict its potential harmful impacts, as well to be able to suggest suitable remediation actions.

Due to the increasing concern regarding the global increase of environmental levels of mercury, especially the high toxicity and biomagnificative character of methylmercury (MeHg), mercury strategies were developed that envisages a number of actions to protect humans health and the environment on both the European level and worldwide. Within the European Union (EU), the EU mercury strategy was developed, a comprehensive plan addressing mercury pollution regionally, as well as globally. In the EU mercury strategy, restrictions in the use of mercury were proposed as well as an export ban for mercury from the EU. An important feature of the EU strategy is also support for and promotion of international actions such as the reduction of global mercury supply, trade and demand. Worldwide, in the frame of the United Nation Environment Programme (UNEP), global mercury strategies were proposed. One of the priority tasks outlined by the UNEP in addressing the global challenges to reduce risks from releases of mercury is also the remediation of existing contaminated sites affecting public and environmental health. From the increasing concerns regarding the global increase of environmental levels of mercury point of view, especially the high toxicity and biomagnificative character of methylmercury (MeHg), strong contributors of Hg such as contaminated sites are of paramount importance. E.g., mining operations in areas rich in cinnabar ore can be strong sources of mercury for many years, even after mining has been discontinued. There are different ways of transport of mercury away from these sources, causing Hg dispersion on regional and global scale, respectively. One way is by riverine flow as a result of erosion of Hg contaminated soils and sediments, which can carry Hg in dissolved and particulate phases for hundreds of kilometers to the marine ecosystems. On the other hand, due to its volatile nature, significant amounts of elemental mercury (Hg^0) from such areas are emitted to the atmosphere. Elemental mercury has a long residence time in the atmosphere. Therefore, it can be spread over long distances and contribute to the global mercury cycle of mobilization, deposition and remobilization. The ratio between different mercury phases (dissolved, particulate and gaseous) if significant for several reasons: the physical state as well as

chemical form of Hg affects its behavior and its environmental fate, as well as influencing health affects and risk assessment. The deposition of mercury away from such local sources can result in the remobilization of Hg that is available for methylation. Hence, secondary sources of toxic forms of Hg can be produced at great distances from the original source.

In the present study, one such contaminated site, namely the Idrija mercury mine area, was chosen as a study site. The Idrija mercury mine is the second largest Hg mine in the world which operated for more then 500 years. Although the production of mercury (Hg) at the Idrija mercury mine stopped in 1994, centuries of mining and ore processing operations left behind intense pollution of nearly all environmental compartments. Mercury pollution in the Idrija region is relatively good documented. In the last decades, many studies were performed in this area. However, most of the studies focused on mercury within individual environmental compartments and processes, respectively. In this work, an integrated approach was used, taking all the environmental compartments and major processes into account. An attempt was made towards the establishing of sources and sinks, fate and distribution of mercury in the Idrijca River catchment. Two approaches that go hand in hand were used. By measurements of mercury and its species/forms in soils, sediments, water and air, recent sources and levels of mercury were established. These data were than used for development and calibration of a mass-balance model of mercury at the Idrijca River catchment scale.

This doctoral thesis is divided into seven chapters. In the first chapter, problem of mercury pollution in the Idrija mercury mine region, Slovenia, is outlined and put in a wider, regional and global context. Mercury's global cycle, its physical and chemical forms, and principal factors influencing mercury biogeochemistry in the environment are given as well. In chapter 2, the purpose of the thesis is defined that serve as a general background of the thesis, in order to understand the approach used. Chapter 3 and 4 introduce the reader to the study area, sampling design and strategies, as well as to the analytical methods used during the experimental work. In chapter 5, results of the experimental work are presented and relationships between local conditions and site specific mercury levels/forms in various environmental compartments of the Idrijca River catchment are discussed. Based on these results, a mass-balance model of mercury was developed. The modeling design, approach and methods used in the compiling of data, as well as the results of the model are presented in chapter 6. In chapter 7, conclusions and recommendations for the future work on mercury problem at Idrija region are given.

Some of the results presented herein have already been published elsewhere, or are in the process of being published. Two published manuscripts are inserted as a supplementary material in Appendix C.

1.2 Mercury in the environment

Mercury in the environment can exist in a large number of different physical and chemical forms with a wide range of properties. It can be found in three oxidation states: Hg^0, Hg^+ and Hg^{2+}. The main forms of mercury that can be found in nature are as follows:

- Hg^0: the reduced form of mercury. It is very volatile and electrically neutral. Because of its volatility it is the dominant form in the atmosphere.
- Hg^{2+}: the oxidized form in all non-methylated bivalent mercury compounds. In the lithosphere it is primarily present as the very insoluble mineral cinnabar (HgS). In aqueous solutions Hg^{2+} can be dissolved or bounded onto particles. It can be in both organic and inorganic forms. In nature Hg^{2+} is the dominant form.
- CH_3Hg^+ (monomethylmercury - MeHg): those are all MeHg mercury compounds that can be dissolved or bounded onto particles. Those compounds are dominant mercury compounds in fish. Organo-mercury compounds are more volatile and more easily bioaccumulated than their inorganic precursors.
- $(CH_3)_2Hg$ (dimethyl mercury - DMM): a volatile and unstable form. It originates from biologic methylation at high pH or from MeHg under anaerobic conditions. It can be found in the marine environment, while in freshwater systems it is usually under the limit of detection (<LOD).

1.2.1 Global mercury cycle

Conversion between the different physical and chemical mercury forms provides the basis for mercury's distribution pattern in local and global cycles and for its biological enrichment and effects. Natural transformations and environmental pathways of mercury are very complex and are greatly affected by local conditions. Here, only a general mercury biogeochemical cycle is given (Fig. 1). Cycling of mercury

between different forms and the transformation/transport process involved within and among the individual environmental compartments are described into more detail in chapter 5, where the results of the study are presented and relationships between local conditions and site specific mercury levels/forms in these compartments are discussed.

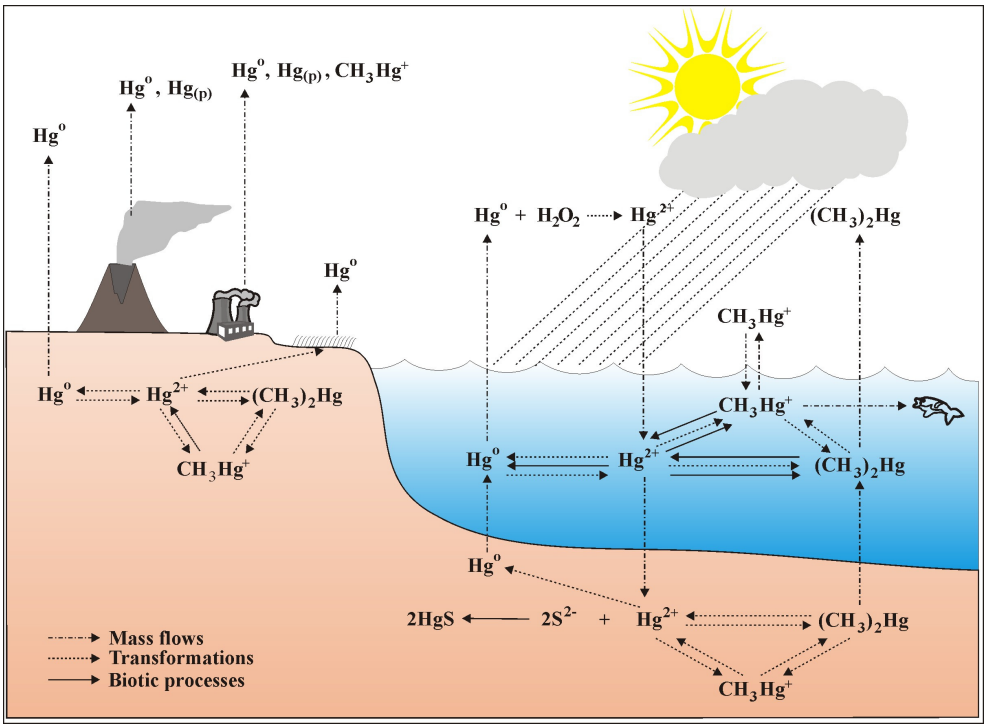

Figure 1: *Global mercury cycle.*

Fig. 1 provides a conceptional and simplified illustration of the environmental compartments, sources and transport processes which play a significant role in the mercury cycle considering the main Hg species. There are two main types of reactions in the mercury cycle that convert mercury through its various forms: oxidation-reduction and methylation-demethylation. In oxidation-reduction reactions, mercury is either oxidized to a higher valence state (e.g. from relatively inert Hg^0 to the more reactive Hg^{2+}) through the loss of electrons, or mercury is reduced, the reverse of being oxidized, to a lower valence state. In the environment, mercury is transformed into methylmercury when the oxidized or mercuric species (Hg^{2+}) gains a methyl group (CH_3). The methylation of Hg^{2+} is primarily a natural, biological process resulting in the production of highly toxic and bioaccumulative methylmercury compounds ($MeHg^+$) that build up in living tissue and increase in concentration up the food chain, from microorganisms like plankton, to fishes and humans. Changes in speciation from inorganic to methylated forms are the first step in the aquatic bioaccumulation processes. These processes are considered to occur in both the water column and sediments.

The global mercury cycle is rather complex due to the volatility of elemental mercury (Hg^0), which allows mercury to travel in a multi-step sequence of emission to the atmosphere, transportation, deposition and re-emission. Mercury vapour is released into the atmosphere from a number of natural sources and through anthropogenic emissions (mainly from combustion of fossil fuels). As a result, mercury from point source emissions may remain localized in the environment, or may be transported regionally and even globally. Following release to the atmosphere and depending on its physical/chemical form, mercury can be either deposited in the vicinity of the emission source, or subjected to long-range atmospheric transport via air masses. Because the uptake of Hg^0 in cloud water is relatively slow, this process may be responsible for the deposition of mercury far from its source and may be important when considering global mercury pollution. Gaseous Hg^{2+} and particulate mercury (Hg(p), mercury adsorbed onto particulate matter in air) emissions generally undergo direct wet or dry deposition to the earth's surface locally. A part of deposited mercury is re-emitted to the atmosphere as Hg^0 by exchange at the air/water and air/land boundary. In addition to atmospheric pathways, mercury can be transported through river systems in their sediment loads, or in aqueous solution, as a consequence of soil erosion and leaching. Where mercury is carried on particles, the distance traveled is limited by sedimentation. Transport of contaminants via particles tends to halt due to the sedimentation at riverine lakes, reservoirs and bottom sediment of oceans. These sediments

are thought to be ultimate sink where mercury is deposited in the form of highly insoluble HgS.

Lamborg et al. (2002) estimated that on the global scale anthropogenic emissions contribute into the atmosphere about 2600 tons of mercury per year, while natural emissions from terrestrial surfaces contribute about 1000 tons. Wet and dry atmospheric deposition was estimated at ~4200 tons per year and mercury evasion from the oceans at ~800 tons per year.

1.2.2 Mercury transport and fate in the river catchment

It is increasingly becoming known that mercury transport and speciation in the terrestrial environment play major roles in methylmercury bioaccumulation potential in surface water (Gabriel and Williamson, 2004). River catchments can be considered as a non-point source of mercury to aquatic environment. The significance of the non-point contribution of Hg from terrestrial catchments to aquatic systems depends on biogeochemical processes in the catchment, its storage in ecosystem components, its transfer among components, and its loss either as a gas or in solution (Grigal, 2001). At the catchment scale, mercury transport and its transformations become rather complex. The following key processes schematically illustrated in Fig. 2 must be taken into account:

(a) mercury input from atmospheric deposition,

(b) mercury assimilation and accumulation in forest canopy and release from forest litter,

(c) mercury input from bedrock weathering,

(d) mercury transformation in soils,

(e) mercury evaporation from soils,

(f) mercury transport through erosion and runoff, and

(g) mercury transport and transformations within the stream channels.

Mercury fate in the catchments, especially its outputs depends very much on the catchment characteristics. Catchment characteristics such as the size and topography, land cover and land use, control the retention of Hg in terrestrial compartment and transport of Hg to sites of methylation via complex hydrologic, chemical, and biologic processes (Munthe et al., 2007).

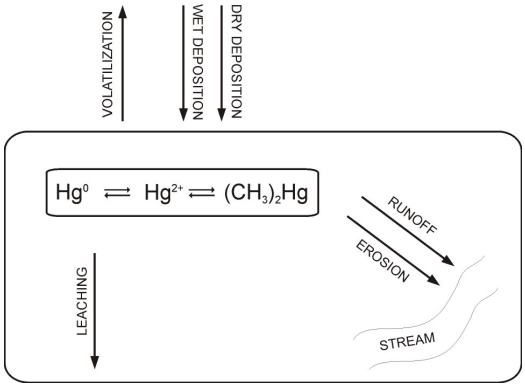

Figure 2: *Mercury transport and fate in the river catchment.*

1.2.3 Principal factors influencing Hg biogeochemistry

Mercury distribution, speciation and its concentrations in the ecosystems depends upon several environmental factors such as pH, Eh, temperature, dissolved organic matter (DOM) etc. In the following sections the most important factors are described in more detail.

1.2.3.1 pH

The pH or alkalinity influences both the availability and transformations of mercury within individual environmental compartment. In systems with particulate and dissolved complexes that contain Hg^{2+} ions, the mercury concentration associated with solids or in solution depends upon the proportion between complexation and adsorption. The pH can change this proportion.

In soils, pH is an important factor controlling Hg^{2+} adsorption-desorbtion processes. As with all metals, mercury adsorption generally decreases with decreasing pH, due to H^+ ions removing and replacing metal ions (Gabriel and Williamson, 2004). Acidic environments (pH<5.4) were found to be favorable for Hg^{2+}

desorption, and thus, soil acidification can increase the release of Hg from the soil, and subsequently to the surrounding environment (Jing et al., 2007). Moreover, there is more Hg^{2+} available for formation of methylmercury, which is also more favored in acidic conditions (Boszke et al., 2002).

In the aquatic environments, pH influences the occurrence and the migration of different mercury species. In water of low pH, the dominant are the soluble mercury compounds, such as $HgCl_2$ and CH_3Hg^{2+}, whereas in mild alkaline conditions Hg° and $(CH_3)_2Hg$ dominate. Therefore, in the water of higher pH a greater amount of mercury is transformed to the elementary mercury and a smaller amount of Hg^{2+} is available for methylation (Boszke et al., 2002). Acidic waters also cause a higher uptake of Hg from the atmosphere into water, thus increasing the amount of Hg^{2+} that is available for further chemical reactions.

1.2.3.2 Redox potential (Eh)

Similar as pH, redox conditions influence mercury speciation and availability in different environmental compartments. In soils, mercury is strongly bound, in part, due to the S-functional groups that are frequently associated with organic molecules (Schuster, 1991). The dominant factor controlling the formation of sulfide-mercury species is redox potential. Redox potential dictates whether sulfur is in a reduced or oxidized form.

In the aquatic environmens, redox potential influence the methylation-demethylation processes. Methylation of mercury is fastest in slightly anaerobic environments. Methylation is slower in the presence of oxygen and vice versa - demethylation is faster in the presence of oxygen. Both of these trends result in higher rates of net methylation in low oxygen environments (low Eh). Hence, in the water of oxidative properties the dominant compounds are $HgCl_4^{2-}$ and $HgOH^+$, while in reductive conditions it is CH_3HgS^- and HgS_2^-, and in variable conditions most often CH_3HgCl and CH_3Hg^{2+} are found (Boszke et al., 2002).

1.2.3.3 Temperature

The transformations of mercury, in particular the processes of methylation and demethylation, are temperature dependent. The rate of mercury methylation in the bottom sediments is higher at high temperatures, which is related to an enhanced activity of micro-organisms in such conditions. In the summertime (because of higher temperatures, lower oxygen content and increased primary production), the methylation of mercury is usually higher. The optimum temperature of mercury methylation is reported to be between 33 and 45 °C (Guimaraes et al., 1998).

Temperature also affects the kinetics of the mercury sorption from the soil components and the bottom sediments. It has been found that the concentration of inorganic fraction of mercury Hg^{2+} in the solution increases with increasing temperature, probably due to an increase in the concentration of dissolved organic carbon (DOC). Even more important, increased soil temperature results in the increased volatilization of mercury from the surfaces.

1.2.3.4 Organic matter (particulate and dissolved)

Strong interactions between mercury and organic matter found in soil and aquatic environments are attributed to the binding of mercury with sulfur-containing functional groups in organic matter. The formation of organic Hg^{2+} complexes in soils and sediments is known to be the dominating process of mercury binding (Schuster, 1991; Yin et al., 1997). This complexing behaviour greatly limits the mobility of mercury in soil as most of the mercury in soil is fixed in the bulk organic matter and could therefore be only mobilized through elution in runoff by being attached to suspended soil or humus.

Dissolved organic matter (DOM) interacts very strongly with mercury, affecting its speciation, solubility, mobility, and toxicity in the aquatic environment. DOM has the potential to promote methylmercury formation in some environments by stimulating microbial growth or to inhibit methylation by reducing the amount of inorganic mercury available for methylation through complexation (Ravichandran, 2004).

2 Aims and Hypothesis

Mercury pollution in the Idrijca River catchment, a result of five centuries of mining and ore processing operations in this area, was studied in order to better understand the cycling of mercury at the catchment scale, gaining an understanding of its chemical and transport processes, and to place this knowledge in the context of the global mercury cycle.

The main aim of the thesis was synthesis of the knowledge of environmental mercury behavior in the Idrijca River catchment, its physico-chemical properties and transport/multi-media partitioning/accumulation characteristics, based on the paradigm of *biogeochemical cycles* and *chemical mass balance budgets*.

To meet this aim, the following specific issues were addressed. Mercury mobility and accessibility to transformation and transport processes was studied to determine the main mercury sources and sinks at the catchment scale. Sources of mercury in the Idrijca River catchment were identified by measurements of its concentrations in all environmental compartments including water, soils, river sediments and air. Transformation mechanisms involved in the cycling of mercury were studied based on the results of mercury speciation analysis. The main focus was on the partitioning of mercury between dissolved, particulate and gaseous phases. Transport of different forms of mercury within and between the environmental compartments was investigated in order to establish mercury cycle/mass balance at the catchment scale. The processes that were taken into account include erosion of contaminated soils, surface runoff, riverine transport, atmospheric deposition and mercury emission from the surfaces. The final purpose of the thesis is the contribution to a science-based and cost-effective remediation planning in the Idrija mercury mine area in the future.

In Fig. 3, outline of the study is given, showing the environmental compartments and processes of mercury transformation and transport within the individual environmental compartments that were taken into account.

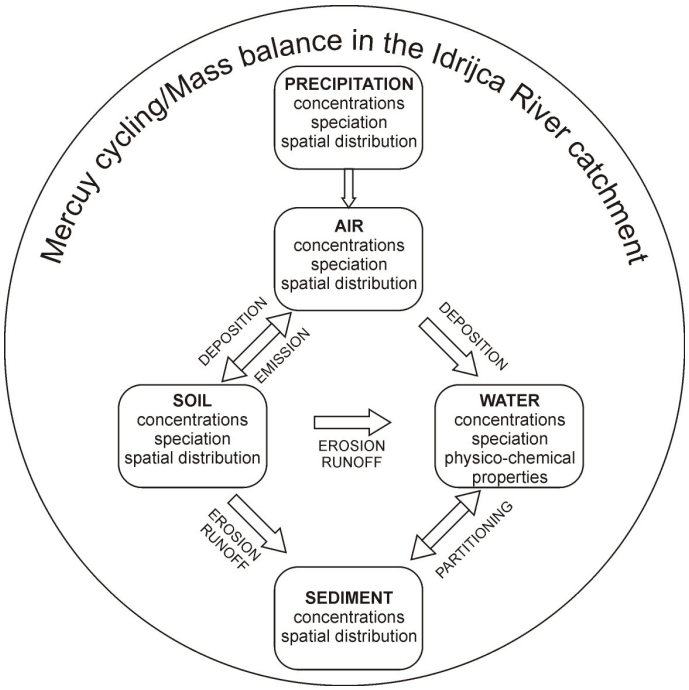

Figure 3: *Outline of the study.*

3 Study area

3.1 Geographical data

The study area (Idrijca River catchment) covers the area of the transitional zone between the Alps, the Dinaric Mountains and the Adriatic Sea (Fig. 4). The Idrijca River draining the area is approximately 60 km long and it originates on the Vojskarsko plateau (924 m. a. s. l.). Along the valley the Idrijca River flows through the town of Idrija where the mercury mine is located and merges with the Soča River about 40 km downstream from the town of Idrija. The direction of the flow of the Idrijca River is mainly influenced by the tectonics. Idrijca is supplied with waters from the karst springs (siphonic Wild lake, Podroteja) and several tributaries (right Belca, Zala, Cerknica and Bača, left Nikova, Kanomljica and Trebušica). The first 50 km of the channel are cut mostly into the carbonate rocks. The consequence of this is a tight valley with narrow bottom and steep slopes (V shaped valley – Vintgar type). Only the last 10 km of the valley, where the bedrock is softer, it becomes wider. Both Idrijca and its tributaries have a torrential character. The whole area is geomorphologic very heterogeneous, with a wide range of altitudes from 170 to more than 2000 m a. s. l.

In the Idrijca River catchment forests cover as much as 80 % of the surface. Due to the unfavorable relief, the land was never suitable for agriculture. Therefore, the rest 20 % is mostly natural grassland with some pastures, while urban areas present less than 1 %. Beech (*Fagus sylvatica*) is the dominant tree species in the region.

The town of Idrija, where the mercury mine is located, lies 20 km from the Idrijca River spring, on the alluvial plains at the confluence of the Nikova and the Idrijca (Fig. 4). The location can be taken as marking the dividing line between the Alps to the north and the Karst plateau to the south, which then leads on to the mountains of the Balkan Peninsula.

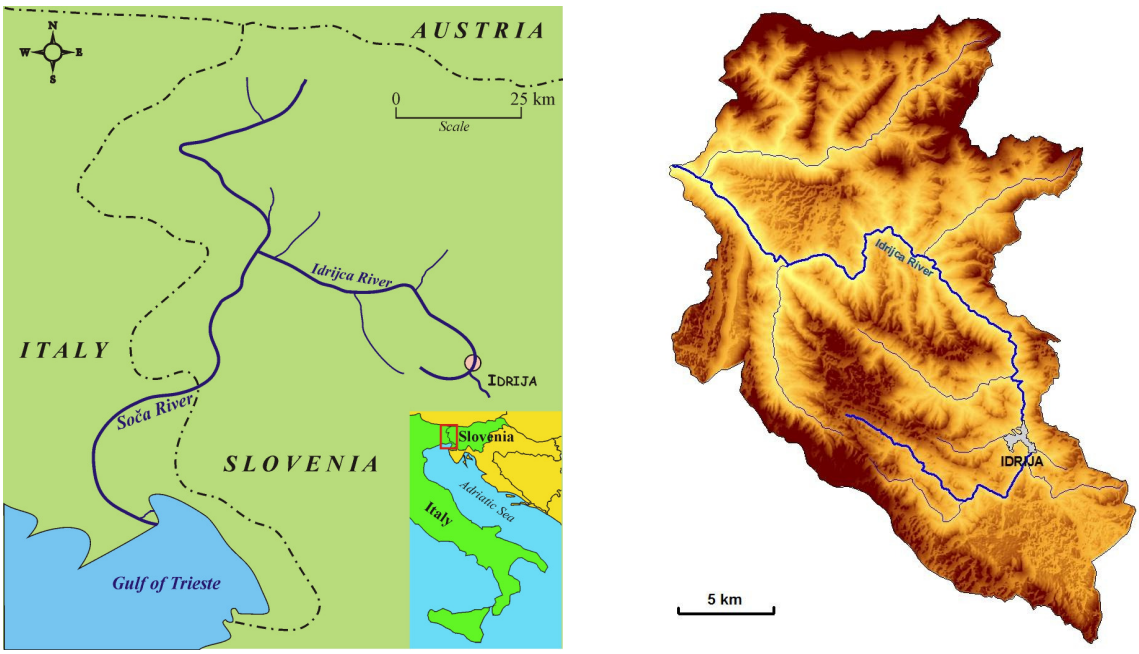

Figure 4: *Location of the Idrijca River catchment (left) and its topography (right).*

3.2 Geology

The upper part of the catchment is composed of massive and stratus Triassic limestone and dolomite, which alternates with massive dolomite and conglomerates, which are composed of dolomite. The central flow of the Idrijca is composed of Permian green grey conglomerate sandstone, mica quarz sandstone, and red sandstone with conglomerate on the right bank of the river. The left bank of the River Idrijca in its central flow is composed of Triassic dolomite, which alternates with sandstones, mudstones and marl. The lower flow, before the confluence with the River Soča, is composed of Triassic stratus and massive dolomite and Cretaceous limestone breccia with marls (Buser, 1987). The surroundings of Idrijca have a complicated tectonic structure with a typical fold structure rupture, with faults in different directions. The main fault lines run in the NW–SE direction. The greatest is the Idrijca fault, which ruptures the whole area of Slovenia and is also one of the largest in Europe.

The Idrija mercury ore deposit is located directly below the town of Idrija between the Idrijca River and its tributary, the Nikova stream. The ore deposit extends in the directions north-west and south-east. It is 1500 m long and 300-600 m wide. The depth of the ore-bearing zone is about 450 m (Likar et al., 2006). According to Mlakar and Drovenik (1971) in Čar (1998), the Idrija ore deposit is composed of Carboniferous, Permian, Scythian, Anisian and Ladinian rocks enriched with cinnabar. Native mercury can be found in Carboniferous clastic rocks, Scythian siltstone and marlstone with lenses of oolitic limestone, as well as in various lithological components of the Skonca beds and tuffites of the Ladinian age. The deposit was formed during two phases. Mercury mineralization of Anisian and older rocks is of epigenetic origin, while the mineralization of Ladinian strata is primarily of syngenetic and partly of epigenetic origin.

3.3 Pedology

According to the Slovenian soil classification, soil groups are distinguished on the basis of presence of water, soil permeability and salt presence. Further division is made on the basis of parent material (Vrščaj and Lobnik, 1999). Because of its exceptional diversity and distinct variation over short distances, the bedrock is the most important pedogenetic factor. Through mechanical and chemical weathering, mineral elements enter the soil and have a decisive influence on its basic characteristics. Soil are further formed under the influence of factors such as the relief, climate, vegetation and the time during which the soil forming and modifying processes have acted. A fully developed soil profile has four distinct horizons: an uppermost with organic litter, the A-horizon of mull, the B-horizon of mineral soil and the C-horizon that contacts the bedrock.

In the Idrijca River catchment, the following main soil types are found:

- *Rendzinas* on carbonaceous parent rocks are the prevailing soils covering more 68 % of the area. These soils have almost no C and B-horizons, so the organic horizon more or less directly contacts the bedrock. They are further divided into subtypes depending on the degree of mineralisation of the organic litter and the parent rock.
- *Cambisol* cover 27 % of the study area. For these soils a yellowish to reddish B-horizons that is coloured by hydrates of iron and contain a lot of clay, is typical. Based on the parent material three groups can be found in the study area: *Dystric Cambisol* (brown soils on non-carbonaceous parent rocks), *Eutric Cambisol* (brown soils on dolomite and limestone) and *Chromic Cambisol* (yellowish brown soils on hard carbonates).
- *Leptosols* cover less than 4 % of the area. These soils are poorly developed with a very shallow profile depth (indicating little influence of soil-forming processes), and contain large amounts of gravel.
- *Fluvisols* presenting approximately 2 % of the area are found along the watercourses at sites that are flooded periodically by surface waters or rising groundwater.

For details on the soils in our study area, see map in Appendix B.

3.4 Climate

In general, the study area has a warm humid temperate climate. It is characteristic of such climate that the average temperatures of the coldest month do not drop below -3 °C and that at least four months have an average temperature above 10 °C. Relative to precipitation, all seasons receive approximately the same amount of rain with no distinctive dry or wet periods (Ogrin, 2004). However, there are significant differences within the catchment. The transit character of this area between the Alps, Dinaric mountains

and the Mediterranean influence the climate the most. Northern parts of the catchment have an alpine climate. As the mountains (Julian Alps) block air circulation from the northern Adriatic Sea to the north, annual precipitation here is very high and ranges between 2400 and 3200 mm year^{-1}. To the south and southwest of the Alpine-Dinaric barrier, whose relief opens toward the Adriatic Sea, climate becomes submediterranean. The precipitation regime in submediterranean is with high precipitation in the fall and at the end of spring or beginning of the summer and low precipitation in the winter and summer (Ogrin, 2004). At the catchment scale, average air temperature for the months representative of the seasonal meteorological variation in the domain are: 0-2 °C in January, 6-10 °C in April, 16-22 °C in July, and 8-12 °C in October. High peaks and steep mountain slopes prevent air circulation in the valley. The most common winds follow the geography of the valley. In its upper part the most common wind direction is S–N and in the lower parts the prevailing wind direction is E–W. In Fig. 5, the average monthly precipitation for the period 1971-2001, collected at two selected gauging stations within the Idrijca River catchment (Idrija and Kneške Ravne, respectively) is shown. It can be seen from Fig. 5 that precipitation in the area is very variable, both spatially and from year to year (error bars on the plots showing standard variations of monthly averages).

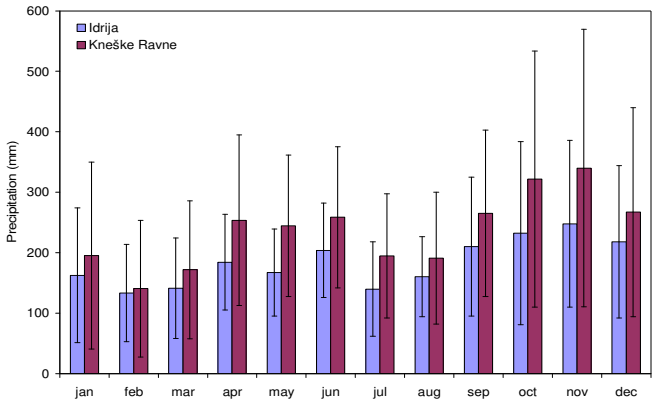

Figure 5: *Average monthly precipitation at two gauging stations in the Idrijca River catchment (source: ARSO).*

3.5 Hydrology

The hydrology of the Idrijca River system is relatively complex due to many tributaries, the karstic terrain and highly complex system of surface and groundwater flows (Širca et al., 1999). Idrijca River and its tributaries are a runoff fed streams, where discharge is primarily a function of rainfall. Rivers and streams in the catchment have a nival-pluvial flow regime, i.e. their discharge curves display two high and two low extremes (Kolbezen, 1998). Monthly discharges from two gouging stations in the catchment are given in Fig. 6. Gauging station Hotešček is located at the Idrijca River, just before the Bača River inflow, while station Bača pri Modreju is located at the outflow of the Bača River.

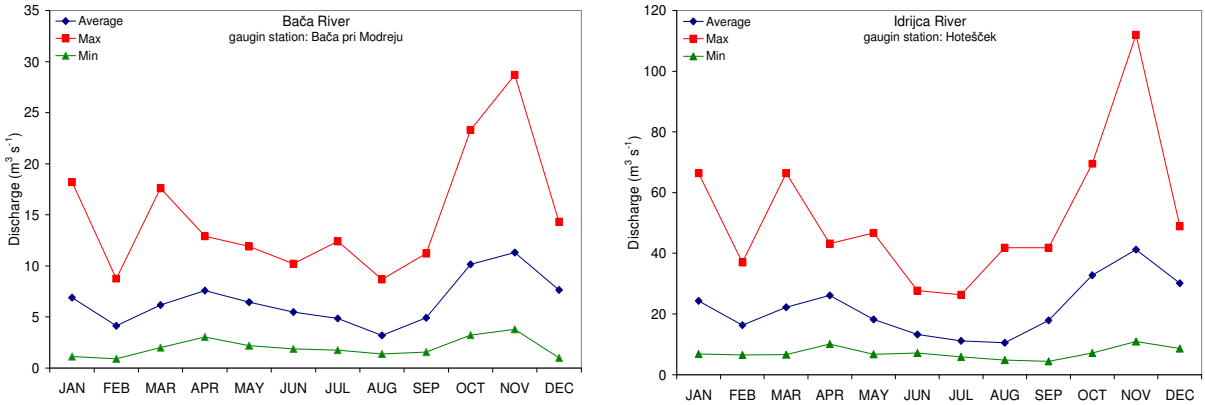

Figure 6: *Maximum, average and minimum monthly discharges (m^3s^{-1}) of the Idrijca and Bača River for the period 1991-2004* (source: Environmental Agency of Republic Slovenia).

At Hotešček, the mean annual discharges are 24.7 $m^3 s^{-1}$ for a period between 1961 and 1990, and 22.0 $m^3 s^{-1}$ for a period between 1991 and 2004 (source: Environmental Agency, Ministry of the Environment, Spatial Planning and Energy). At Bača pri Modreju, the mean annual discharges are 7.1 $m^3 s^{-1}$ for a period between 1961 and 1990, and 6.6 $m^3 s^{-1}$ for a period between 1991 and 2004. There are typically two water-discharge extremes during the year: the longer spring maximum from March to June (due to snowmelt) and the shorter but more intensive autumn maximum in October and November. The lowest daily discharges usually occur in August. The analysis of hydrological data for the period of 45 years for the Idrijca River as well for the Bača River showed a general decrease in the average minimum low discharges and, on the other hand, the increase in the annual extremes of high discharges (Ulaga, 2002). The global climate change and changes in land use are probably the main reasons for such trends.

3.6 Environmental impacts of the Idrija mercury mine

Due to the mercury containing rocks that lie directly on the surface, the Idrija ore deposit holds a special place among mercury deposits in the world. From the mineralogical aspect the ore deposit is classified as a monomineral deposit, as most of the mercury appears in the form of cinnabar (HgS~70 %) and only to a relatively smaller extent in the form of native mercury (Hg^0~30 %). From the very beginning of mining activities, the effects of primary *geogenic* mercury and secondary *anthropogenic* mercury pollution began to accumulate (Čar and Dizdarevič, 2002). However, weathering and natural emissions from the ore deposits has been a low intensity processes in comparison with the anthropogenic intervention.

According to official data, during the operating period of the mine (since 1490) over 12 million tons of mercury ore had been extracted, which amounts to 107.500 tons of commercial mercury produced. Taking into account the losses during mining and inefficient smelting, the total amount of mercury mined is estimated to be at least 153.000 tons (Mlakar, 1974; Miklavčič, 1999; Dizdarevič, 2001). It has been estimated that the difference of 45.500 tons of mercury were emitted into the environment during the operating period of the mine, which ceased production in 1994 (Dizdarevič, 2001). Mining and ore processing operations left behind intense pollution of all environmental compartments. During the ore smelting high concentrations of mercury in the air were measured, locally reaching even 4000 ng m^{-3}, and the total evasion to the atmosphere exceeded 20 kg day^{-1} of mercury in 1968-1972 (Dizdarevič, 2001). Consequently, mercury was deposited not only in the vicinity of the mine but also in the wider Idrija region. Since strong temperature inversions are common and strong winds are rare in the Idrija area, it can be assumed that a big part of the degassed Hg was redeposited within the Idrijca River catchment. Moreover, significantly quantity of mercury bound to smelting remains which were deposited along the river banks of the Idrijca River, has been washed away and, mostly in its particulate form, transported downwards the Idrijca and Soča River system all the way to the Gulf of Trieste.

Due to the growing ecological awareness in the 70's, when mercury production reached its final peak, the first extensive research on Hg cycling in the town of Idrija and its vicinity started (Byrne and Kosta, 1970; Kosta et al., 1974). Since then, the environmental impact of mercury mining in the Idrija region has been intensively studied. Hg cycling in different environmental compartments was investigated in the town of Idrija and its surroundings, along with its impacts on humans and their health (e.g. Biester et al., 1999, 2000; Falnoga et al., 2000; Gnamuš et al., 2000; Gosar et al., 1997, 2002, 2006; Hines et al., 2000; Horvat et al., 2002; Bonzongo et al., 2002; Kobal et al., 2004; Kocman et al., 2004; Kotnik et al., 2005; Žibret et al., 2006; Žižek et al., 2008). Moreover, an assessment of the extent of mercury contamination including mathematical modeling in the Gulf of Trieste, esturay were Idrijca and Soča are draining Hg contaminated sediments was performed (Horvat et al., 1999; Širca et al., 1999; Covelli et al., 1999; Rajar et al., 2000; Faganeli et al., 2003).

There are some common outcomes of all these studies that can be summarized as follows. Although more then 10 years after the closure of the mine, the Idrija mining district continues to emit high levels of Hg into the Idrijca River with extremely high concentrations of Hg and MeHg present throughout the system. Hg carried downstream is available to be transformed in both the Soča River system and the marine environment in the Gulf of Trieste. Nowadays, the major terrestrial mercury sources are natural rocks containing mercury, deposits of residues from combustion, weathering and erosion of contaminated soils as well as redeposition of contaminated river sediments. It is generally accepted that the formation and bioaccumulation of methylmercury is the most critical point of environmental quality in this mercury contaminated site. The reduction of all mercury forms (especially methlmercury) in all environmental compartments can, therefore, be defined as the priority objective with regard to the mercury contamination problem in the wider Idrija area and the Gulf of Trieste.

4 Experimental

4.1 Introduction

Natural transformations and environmental pathways of mercury are very complex and are greatly affected by local environmental conditions. To assess the environmental fate and the impacts of anthropogenic mercury emissions, a range of biogeochemical interactions affecting mercury in its different physical states and chemical forms must be examined. Sampling campaigns and experimental work for this research was organized as shown in Table 1.

Table 1: *Sampling media and the experiments performed.*

Media	Experiment	Purpose
water	Hg speciation	to determine the amount and chemical forms of Hg in the Idrijca River and its major tributaries to investigate the influence of changing hydrological conditions on chemistry and transport of mercury in river water
	general geochemical analysis	to determine the chemical water parameters that impact the chemistry of mercury in river water
soil	Hg speciation Hg fractionation	to establish spatial and vertical distribution of different forms of mercury in soils at the Idrijca River catchment scale, taking different origin and different vegetation cover types into account
	isotopic composition ($\delta^{13}C$, $\delta^{15}N$)	to identify terrestrial sources of total (THg) and methylmercury (MeHg) and to better understand the processes controlling transfers of Hg compounds from terrestrial to aquatic environment to identify the parameters that influence the binding, mobility and potential bioavailability of different mercury forms the most to characterize the soils in terms of organic matter composition
	flux chamber	to investigate the influence of different environmental parameters including temperature, moisture and solar radiation on the volatilization of mercury from soil to the atmosphere
sediment	total Hg in different size fractions	to determine the amount and spatial distribution of mercury in the sediments of the Idrijca River and its major tributaries to estimate the mercury pool available for further aquatic transport and transformation processes
air	Hg^0 mapping	to assess spatial distribution and major sources of Hg^0 to the atmosphere in the area between the towns of Idrija and Spodnja Idrija to investigate the influence of seasonal variations and changed weather conditions on Hg^0 distribution in air
	Hg speciation	to better understand the fate and environmental behavior of mercury in the atmosphere
precipitation	Hg speciation	to determine the rates of atmospheric mercury deposition, both wet and due to the throughfall, taking seasonal and spatial variations into account to characterize the nature of mercury deposition and its connection to atmospheric mercury sources in the Idrijca River catchment
	isotopic composition ($\delta^{18}O$, $\delta^{2}H$)	to study the meteorological transport history of the air masses

4.2 Sample collection and sample preparation

Sampling campaigns and *in situ* measurements of air, precipitation, soil, river sediment and water samples were carried out at different locations in the Idrijca River catchment in the 2004-2007 period. In Fig. 7 sampling locations and the type of samples obtained are shown. A short summary of sampling locations including location name, description and media sampled is presented in Table 2.

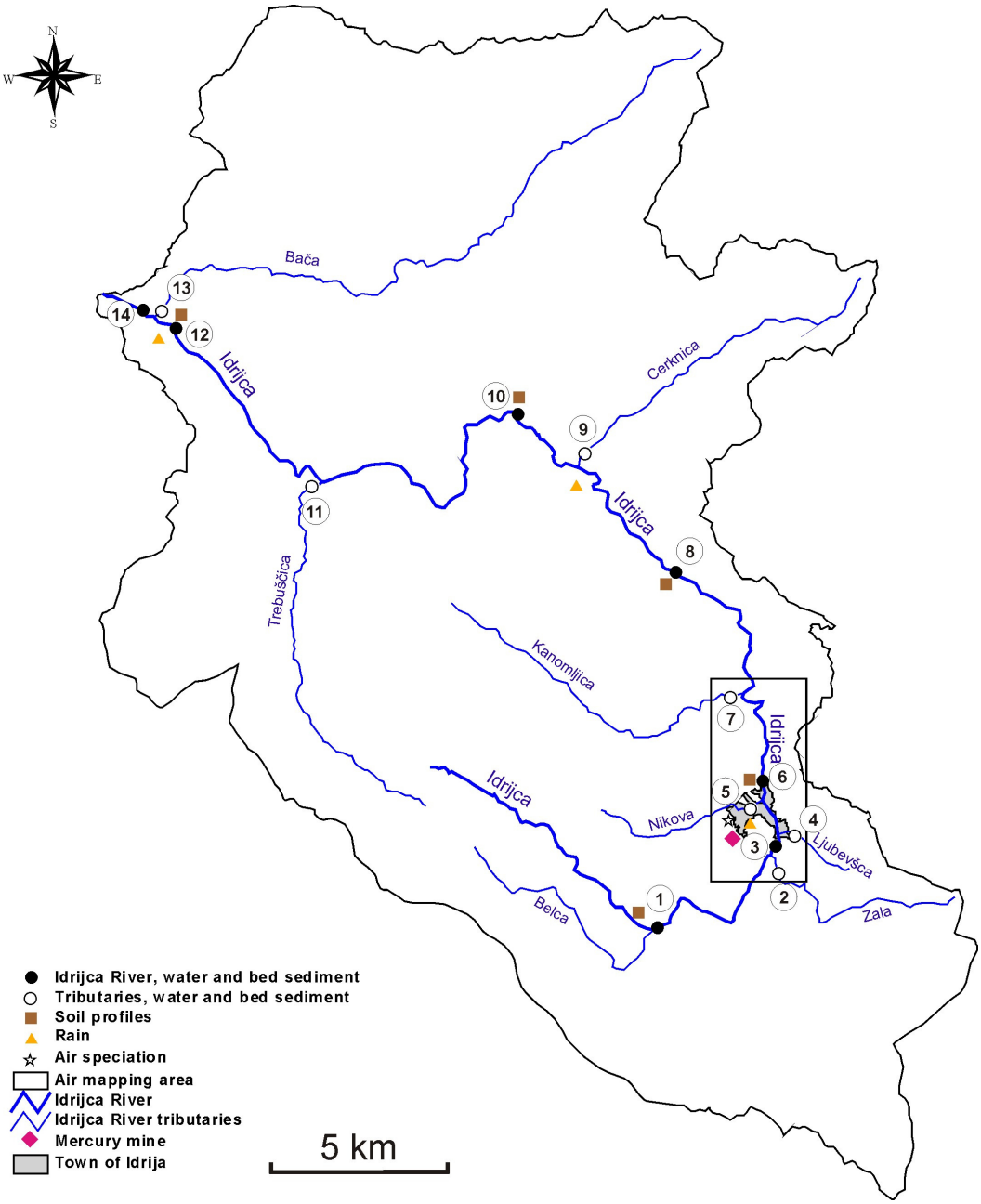

Figure 7: *Sampling locations in the Idrijca River catchment and the type of media sampled.*

Table 2: *Description of the sampling locations, abbreviations and type of sample.*

No.	Abbr.	Full Name	Location description	Experiment/Media sampled
1	*BE*	Belca	confluence of Belca and Idrijca Rivers	water bed sediment soil profiles
2	*ZA*	Zala	right hand site Idrijca R. tributary	water bed sediment
3	*PO*	Podroteja	Idrijca River, 1 km upstream from the town of Idrija	water bed sediment
4	*LJ*	Ljubevšca	right hand site Idrijca R. tributary in the town of Idrija	water bed sediment
5	*NI*	Nikova	left hand site Idrijca R. tributary in the town of Idrija	water bed sediment
6	*ID*	Idrija	Idrijca River in the town of Idrija, after the mine drainage	water bed sediment precipitation speciation in air soil profiles flux chamber
7	*KA*	Kanomljica	left hand site Idrijca R. tributary, 5 km downstream	water bed sediment
8	*TR*	Travnik	Idrijca River, 10 km downstream	water bed sediment soil profiles flux chamber
9	*CE*	Cerknica	right hand site Idrijca R. tributary, 16 km downstream	water bed sediment rain
10	*RE*	Reka	Idrijca River, 20 km downstream	water bed sediment soil profiles flux chamber
11	*TR*	Trebuščica	left hand site Idrijca R. tributary, 30 km downstream	water bed sediment
12	*HO*	Hotešček	Idrijca River, before Bača River inflow	water bed sediment rain
13	*BA*	Bača	right hand site Idrijca R. tributary, 38 km downstream	water bed sediment
14	*IS*	Idrijca bef. Soča	Idrijca River, before the outflow in Soča River	water bed sediment

4.2.1 Surface waters

Surface water sampling locations were selected based on their distance from the Idrija mercury mine area and relationship to the confluences of major and minor streams, at points before and after the confluence. Water samples were obtained from 14 locations altogether, 7 from the Idrijca River and 7 from its major tributaries, respectively (Fig. 7, Table 2). Sampling was performed during different seasons in fall 2006 and spring 2007, according to the discharge regimes of the Idrijca and its tributaries. Additional water samples for mercury analysis were collected at station Hotešček during high water discharges to investigate the influence of changed hydrological conditions on mercury speciation.

Temperature, conductivity, dissolved oxygen (DO) and pH measurements were performed in situ during

sampling. For mercury analysis samples were collected directly into acid-cleaned 1L Teflon® bottles. Unacidified samples were stored in coolers during transport to the laboratory. Dissolved Hg species were determined within 24 hours of collection. Further filtration, preparation and analytical procedures are described in Section 4.3.

Sample aliquots collected for other chemical analysis were passed through a 0.45 µm filter into polythene/glass bottles and kept refrigerated until analysed. Samples for major cation (pre-treated with HNO_3), anion and alkalinity analyses were preserved in HDPE bottles. Samples for DOC analyses were acidified and sampled in glass bottles of volume 30 ml. Samples for stable carbon isotope analysis of particulate organic carbon ($\delta^{13}C_{POC}$) were collected in LDPE bottles.

4.2.2 Soil

Soil profile samples were taken from 5 locations (Fig. 7, Table 2) by means of a stainless steel auger at a depth of 0-30 cm. Three soil types were studied at each sampling site according to their characteristics and location in the catchment: forest soil, meadow soil and alluvial soil. At each location 3 soil profiles were taken from the river site towards the hill site as shown in Fig. 8. In the laboratory each soil profile was sectioned according to specific soil pedologic horizons. Samples were then divided in separate PVC ziplock bags for mercury and isotopic composition analysis, respectively and stored at -20 °C before analyzed.

For the flux chamber experiment, approximately 1 m^2 of top 2 cm soil sample was collected from 3 locations (Fig. 7, Table 2) by means of PVC cutter. At each of the three locations (Idrija, Travnik and Reka) two types of soils, meadow and forest soil, respectively, was sampled. At location Travnik also soil sample from the alluvial plain was obtained.

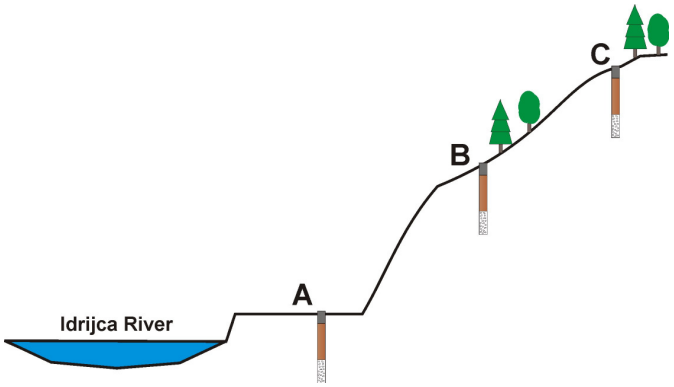

Figure 8: *Schematic cross section of the Idrijca River and the locations of soil profiles.* (A – alluvial plain, B – hill slope, C - hill slope).

4.2.3 River sediment

Stream sediments were sampled in fall 2006. Samples were obtained from 10 locations altogether, 4 from the Idrijca River and 6 from its major tributaries (Fig. 6, Table 2). A composite stream sediment sample was taken from each locations within a distance of 50 m, stored into 1L polyethylene containers and transported to the laboratory. After removal of gravel, stones and plant residues, grain-size distribution was determined by wet sieving and fractions for geochemical analysis were prepared (< 0.063 and < 2 mm for Idrijca River sediments and < 2 mm for tributary sediments). Samples were dried at 30° C for three days (until constant weight) in dark, ground and homogenized in an agate mortar, transferred into polypropylene containers and kept until the analysis at 4° C in dark.

4.2.4 Suspended river sediment

Suspended river sediment was sampled once in January 2007, during a flood wave of the Idrijca River at location Hotešček, before the Bača River inflow. Net drift sampler (diameter of 20 cm) shown in Fig. 9 was used. Sampler was positioned cca. 10 cm above the river bed and was exposed for 1 h. Before analyzed for mercury, suspended sediment was sieved/separated in three fractions: < 0.063 mm, 0.063-2 mm and organic material fraction.

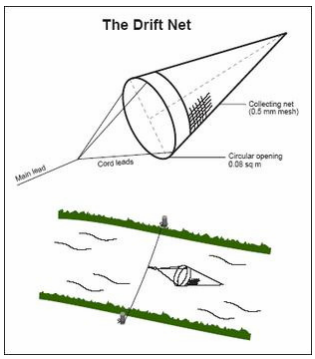

Figure 9: *Schematic of the drift net sampler.*

4.2.5 Precipitation

Rainwater samples were collected in the town of Idrija from October 2006 to September 2007. Two sampling vessels were installed in the town of Idrija, one on the open air and another in the forest where throughfall samples were collected. All the samples were collected on the precipitation event basis. Additional precipitation collectors were installed downstream along the Idrijca River, in Jagršče and Bača pri Modreju (locations 9 and 12, respectively on Fig. 7). At these two locations, samples from two individual precipitation events that occurred on February and March 2007 were obtained. For both precipitation events, at location Jagršče, also throughfall samples were collected.

Precipitation samples were colleted by means of Bergerhoff samplers, which are wide mouthed glass pot open at all times. In this way, mercury deposited by both dry and wet deposition is collected. Collecting pots were placed in the protective basket and were supported by an aluminium carrier so that the top of the pots was approximately 1.5 above the ground (Fig. 10).

All samples, replacement sample bottles and other labware were handled with care in order to avoid contamination during sample bottle replacement, transport and storage. All parts of precipitation collectors that were in contact with the sample, sample vessels, sample containers and labware were cleaned extensively before use according to the procedures described in Kotnik et al. (2008). Samples were stored in the acid pre-cleaned Teflon® bottles, double bagged, in the dark refrigerator at 5°C.

Snow was collected after two snowfall events in February 2006 and March 2007, respectively. Snow samples were taken by scooping snow directly from the ground into a 1L Teflon® bottles a few hours after a new snowfall. The snow was stored and transported frozen. Further processing of both the rain and snow samples was then the same as for the other water samples.

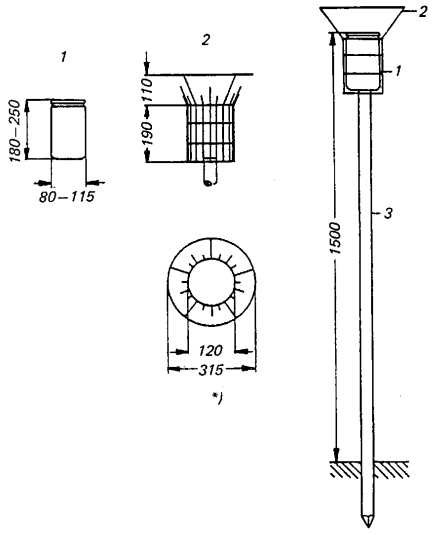

Figure 10: *Schematic of Bergerhoff sampler.* (all dimensions in mm, 1-collecting pot, 2-protective basket, 3-post).

4.2.6 Air (air mapping and speciation)

Measurements of total elemental mercury in air were performed during three sampling campaigns over the area between the towns of Idrija and Spodnja Idrija. Measurements (air mapping) were conducted in August 2006, October 2006 and July 2007. Lumex 915^{+} absorbtion spectrometer installed in a car together with GPS instument was used. Both values (Hg concentration and geographical coordinates) were recorded by a portable computer through appropriate software. Air was pumped through the analytical cell continuously at a rate of 18 L min^{-1}. Concentrations were measured every second. During each campaign, elemental mercury in air was measured at more than 100 locations between 11 am and 3 pm.

In September 2006, measurements of mercury speciation in air over the town of Idrija were performed during a 4-days sampling campaign. Different mercury species in air were collected by pumping the air through three different traps: a trap containing quartz micro-fibre filter, quartz glass tube containing gold powder and quartz glass annular denuder impregnated with KCl. Samples were collected continuously with 12-h time resolution. Details about the procedure are given in more detail in analytical section of this chapter.

4.3 Analytical methods

In the following sections only a short summary of the methods is presented. In order to better assure a review of the analytical methods, these methods are summarized in Table 3.

Table 3: *Overview of the analytical methods.*

Parameter	Matrix	Preparation	Method	Reference
THg	soil, sediments	Drying, milling, homogenization, acid digestion	CV AAS	Horvat et al. (1991), Horvat and Lupšina (1991), Horvat (1996)
TMeHg	Soil, sediments	Drying, milling, homogenization, acid digestion, solvent extraction	CV AFS	Horvat et al. (1993a, 1993b), Liang et al. (1994)
Hg_{ws}	soil	Extraction with Milli-Q	CV AAS	Bloom et al. (2003)
THg	water, rain, snow	HCl, BrCl, irradiation by UV light	CV AAS	Horvat et al. (1991), Horvat and Lupšina (1991), Horvat (1996)
RHg	water, rain, snow	None	CV AAS	Horvat et al. (1991), Horvat and Lupšina (1991), Horvat (1996)
DHg	water, rain, snow	Filtration (0.45 µm), HCl	CV AAS	Horvat et al. (1991), Horvat and Lupšina (1991), Horvat (1996)
PHg	water, rain, snow	Substraction of DHg from PHg	CV AAS	Horvat et al. (1991), Horvat and Lupšina (1991), Horvat (1996)
Hg^0	water, rain, snow	N_2 flow, trapping on gold traps	CV AFS	Kotnik et al. (2007), Horvat et al. (2003)
TMeHg	water, rain, snow	Solvent extraction	CV AFS	Horvat et al. (1993a, 1993b), Liang et al. (1994)
DMeHg	water, rain, snow	Filtration (0.45 µm), solvent extraction	CV AFS	Horvat et al. (1993a, 1993b), Liang et al. (1994)
PMeHg	water, rain, snow	Substraction of DMeHg from TMeHg	CV AFS	Horvat et al. (1993a, 1993b), Liang et al. (1994)
Hg^0	air	none	Lumex 915^+	Sholupov and Ganeyev, 1995
TRM	air	Trapped on KCl impregnated denuder	CV AFS	Lindberg et al. (2002)
TPM	air	Trapped on quartz filter	CV AFS	Lindberg et al. (2002)
TGM	air	Trapped on gold traps	CV AFS	Lindberg et al. (2002)
Hg evaporation	soil/air boundary	Flux chamber	Lumex 915^+	Bahlmann et al. (2006), Ferrara et al. (1998)
Cation chemistry	water	Filtration (0.45 µm)	ICP-OES	Kanduč et al., 2007
Anion chemistry	water	Filtration (0.45 µm)	Dionex ICS-2500 IC	Kanduč et al., 2007
DOC	water	pre-treated with concentrated HCl	Shimadzu TOC-5000A	Kanduč et al., 2007
$\delta^{13}C$	soil	pre-treatment with 1 M HCl, drying at 60°C	Isotope Ratio MS	Kanduč et al., 2007
$\delta^{15}N$	soil	drying at 60°C	Isotope Ratio MS	Kanduč et al., 2007
$\delta^{18}O$	rain	water-CO_2 equilibration	Isotope Ratio MS	Epstein and Mayeda, 1953
$\delta^{2}H$	rain	Cr reduction	Isotope Ratio MS	Morrison et al., 2001

4.3.1 Mercury analysis and speciation

4.3.1.1 Total mercury (THg) in soils and sediments

Total Hg concentrations in soil and sediment samples were determined by cold vapor atomic absorption spectrometry (CVAAS). Before analyzed, samples were dried at 30º C for three days (until constant weight) in dark, ground and homogenized in an agate mortar. After overnight decomposition with a mixture of acids in a closed Teflon® vials at 125 °C, mercury was reduced with $SnCl_2$, amalgamated on a gold trap and flushed by air from the heated trap into the measuring cell of a LCD Milton Roy mercury detector (Horvat et al., 1991).

4.3.1.2 Methylmercury (MeHg) in soils

The determination of methylmercury in sediment samples was carried out based on dithizone extraction and ECD-gas chromatography. The sediment samples (ca. 0.5 g) were shaken with 10 ml of 1 M potassium hydroxide in ethanol for 10 min using a mechanical shaker. The treated sediment was acidified with hydrochloric acid and was bubbled with nitrogen gas for 5 min. The sample was then mixed with 2 ml of 20% hydroxylamine hydrochloride and 2 ml of 20% EDTA and shaken with 5 ml of purified 0.05% dithizone in toluene. The toluene layer was transferred into a 10-ml test tube and washed twice with 3 ml of 1 M sodium hydroxide. The toluene layer was transferred into another test tube and the methylmercury contained in the organic layer was back-extracted with 2 ml of a 5- ppm sodium sulfide solution. After the toluene layer was removed, the aqueous layer was washed with 2 ml of toluene and acidified with 3–4 drops of 1 M hydrochloric acid. The excess of sulfide ions was removed by nitrogen gas bubbling for 5 min and then methylmercury was re-extracted into 0.2 ml of purified 0.05% dithizone in toluene. The toluene layer was washed with 1 M sodium hydroxide and with distilled water, and then subjected to ECD gas chromatography (Model G3800, YANACO Co., Ltd., Japan) for the quantification of methylmecury.

4.3.1.3 Water soluble mercury fraction (Hg_{ws}) in soils

For the determination of concentration of water soluble mercury in soils, the first step of the sequential extraction procedure proposed by Bloom et al. (2003) was used. Milli-Q water was used to extract water soluble fraction of mercury from soil. Extractions were carried out using 0.5 g of fresh soil sample. The sample weight to extractant volume ratio was of 1 to 100. 50 mL of Milli-Q was added to the sample and subjected to end-over-end shaking at 250 rpm for 18 ± 4 h. The vials were then centrifuged at 3800 rpm for 10 min, and the supernatant liquid decanted for filtration through a membrane filter of 0.45 mm pore size. The extract was then placed in a clean Teflon® bottle and oxidized by adding 1 mL of 0.2 M BrCl. Total Hg in the oxidized fraction extract was then determined using $SnCl_2$ reduction, trap gold amalgamation and CVAAS.

4.3.1.4 Total (THg), reactive (RHg), dissolved (DHg), particulate (PHg) and dissolved gaseous mercury (DGM) in precipitation and river water

Total Hg (THg) was determined by acidification of 100 ml of sample with 0.5 ml suprapur concentrated HCl. The oxidation of all Hg compounds was achieved by adding 1 ml solution of BrCl and exposure of the sample to UV light for 3 h. Prior to measurement 60 µl of $NH_2OH{\cdot}HCl$ was added to remove the excess of bromine and chlorine. Oxidized Hg in the sample was then reduced by 10 ml of 5% $SnCl_2$ solution in 0.5 M H_2SO_4 in a reduction cell. Reduced Hg^0 was swept from the sample by N_2, trapped on a gold trap and released by heating to an LDC Milton Roy CV AAS mercury analyzer. The limit of detection was 0.05 ng L^{-1} calculated on the basis of three standard deviations of the reagent blank. The method used is described in detail elsewhere (Horvat et al., 1987, 1991).

Dissolved Hg (DHg) was measured after about 0.5 L of water sample was filtered through Nalgene filtration units (cellulose nitrate membrane, 0.45µm), acidified with HCl 30% Suprapur to make a 1% HCl solution, and stored in the refrigerator until analyses were possible. Dissolved Hg was then measured in the same way as total Hg.

Particulate Hg (PHg) in water was determined by the subtraction of DHg from THg.

Reactive Hg (RHg) was determined immediately after sampling. An aliquot of 50-100 ml of sample was transferred to an acid precleaned reduction vessel containing 5 ml of 5% $SnCl_2$ solution in 0.5 M H_2SO_4 to reduce free inorganic Hg^{2+} to Hg^0. Reduced Hg^0 was swept from the solution by aeration with Hg-free N_2 and amalgamated on a gold trap. Hg was released from the gold trap by heating and measured on a Milton Roy cold vapour atomic absorption spectrometer (CVAAS) instrument.

Dissolved gaseous Hg (DGM) was determined by transferring 0.1-0.2 L of sample to a glass bubbler

immediately after sampling. The sample was purged by a flow of 300–400 ml min^{-1} of N_2. Volatile Hg species were purged for 10 min and collected on a sampling gold trap which was then transferred to a double amalgamation CVAFS analyzer system. Hg on the sampling gold trap was then released by heating (~500 °C) for 1 min in a flow of Ar to a permanent gold trap, released again (heating for 1 min, ~500 °C) and detected by a CVAFS analyzer (Tekran 2500). The system was calibrated by gas phase Hg (Hg^0) kept at 4 °C (Tekran, model 2505 mercury vapour calibration unit). An aliquot of 10–25 µl was transferred with a gas-tight syringe into the measurement train through a septum. The amount of Hg injected was calculated from gas law and a correction for the difference in temperature of the gas phase and the syringe was also applied. The detection limit was 0.005 ng L^{-1} based on three standard deviations of the blank. The method is described in more detail in Horvat et al. (2003). It should be noted that DGM concentrations reported in this study correspond to all volatile Hg species present in aquous samples—elemental Hg (Hg^0) and dimethyl Hg ($(CH_3)_2Hg$).

Monomethyl mercury (MeHg) was determined following the procedure described in Horvat et al. (1993, 2003) and Liang et al. (1994, 1996). The water sample (70 ml) was put into an acid precleaned Teflon bottle (125 ml) together with 5 ml of concentrated HCl and 30 ml of CH_2Cl_2. MeHgCl was extracted into the organic solvent by shaking overnight and then back extracted into 40 ml of MilliQ water by evaporation of CH_2Cl_2. The whole sample was transferred to a Teflon reaction vessel and buffered with acetate buffer to pH 4.9 and 50 µl of 1% $NaBEt_4$ solution was added. After 15 min ethylated MeHg was purged onto a Tenax trap for 15 min with N_2 and thermally desorbed (~200 °C) onto an isothermal GC column at 80 °C. Hg species were converted into Hg^0 by pyrolitic decomposition (~600 °C) under a flow of Ar and measured by a cold vapour atomic fluorescence spectrometer (CV AFS) (Brooks Rand). The limit of detection calculated on the basis of three times the standard deviation of the blank was about 0.03 ng L^{-1}. Spike recovery was made for each batch of analysis and ranged from 80 to 90%. The results were corrected for the recovery factors for each batch. As in the case of total Hg, MeHg was measured in filtered and non-filtered samples.

4.3.1.5 Mercury analysis and speciation in air

4.3.1.5.1 Determination of elemental mercury in air

Measurements of elemental mercury in air were performed using a portable Zeeman Mercury Analyzer RA-915$^+$. The analyzer operation is based on differential atomic absorption spectrometry using high-frequency modulation of light polarization. The detection limit of the instrument for ambient air, industrial and natural gases is 2 ng m^{-3} at a flow rate through the instrument of 20 L min^{-1}. The accuracy of the method is 20 % (Sholupov and Ganeyev, 1995).

4.3.1.5.2 Mercury speciation in air

Gaseous elemental mercury (GEM), total particulate mercury (TPM) and divalent gaseous mercury (RGM) were measured by collecting of Hg in three different ways. Procedures descriptions presented here were adopted from Wänberg et al. (2007).

Divalent gaseous mercury (RGM) was collected by drawing sample air through a quartz glass annular denuder whose inner surface is coated by KCl. Divalent gaseous Hg compounds (i.e., $HgX_2(g)$ where $X=Cl^-$, Br^-, . . .) adsorbs onto the KCl crystal surface, whereas elemental mercury and small particles do not. The denuder inlet is equipped with an impactor with a 2.5µm cut-off. During sampling the denuder is maintained at 50°C (to protect the KCl coating from humidity) in an electrically heated housing. The denuder package is placed at an open outdoor place with the intake 1.5–2 above the ground. Directly after sampling the denuders were brought to a field laboratory for analysis. In the analysis step the denuders were purged with N_2 or Ar and electrically heated to 500°C. During heating (15 min) the divalent mercury decomposes forming gaseous Hg^0 which is concentrated by collection on an Au-trap. In the final step the Au-trap is thermally desorbed in a stream of argon and the Hg^0 vapour is detected by CVAFS.

For the particulate mercury (TPM), a quartz micro-fibre filter of 7mm diameter is housed in a quartz glass tube of 140 mm length. The filter is supported by a screen grid made from pure nickel. The sampling device serves as both particulate trap and pyrolyzer for airborne particulate species. After sampling, the Hg content is analyzed via pyrolysis where the trap is heated to 800–900 °C in a stream of argon. In this step, all mercury is decomposed to Hg^0 and subsequently transferred to the gas phase. To improve the sensitivity the mercury vapor is first concentrated on an Au-trap which then is thermally desorbed and Hg^0 is detected with CVAFS. To avoid disturbances from other matter (e.g., PAH) that also may give rise to fluorescence a pyrolysis oven was placed in-between the TPM-trap and Au-trap in the gas line.

Gaseous elemental mercury (GEM) was measure by drawing the air through a quartz glass tube (14 cm

long, inner diameter 0.4cm) containing a gold surface. Elemental mercury in the air is quantitatively adsorbed through amalgamation with the gold. The Au-traps were then analyzed by CVAFS after double amalgamation and thermal desorption. Air was pumped through all three mercury traps at a flow rate 600-800 mL min^{-1}. Schematic of experimental set up is shown sown in Fig. 11.

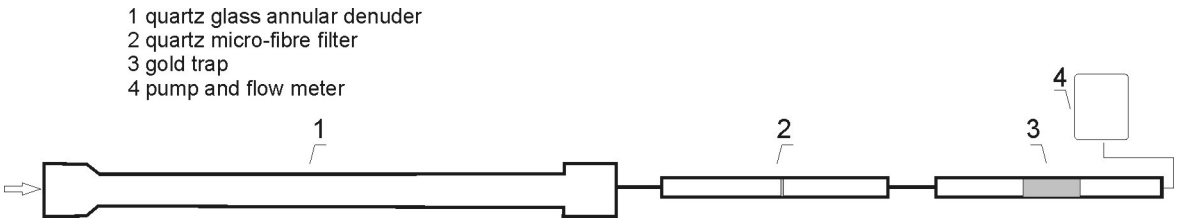

Figure 11: *Experimental set up for the mercury speciation in air.*

4.3.1.6 Mercury flux from soil to the atmosphere

4.3.1.6.1 In situ measurements

In situ measurements of mercury fluxes from soil to the atmosphere were performed using the flux chamber technique (Schroeder et al., 1989; Xiao et al., 1991; Kim and Lindberg, 1995; Ferrara et al., 1998). The increase of mercury concentration inside the chamber was measured as a function of time. The flux chamber was constructed from a 5-mm-thick Plexiglas, which allows a low chamber blank and good penetration of solar radiation. Dimensions of the flux chamber were 25 x 25 x 25 cm with a removable bottom plate. All fittings and tubing were made from Teflon® and were acid pre-cleaned. A Teflon® tube for sampling the external air was fixed on the upper part of the chamber. The external and internal air was measured at a constant flow rate of 18 L min^{-1} by a portable Zeeman Mercury Analyzer RA-915$^+$. Three inlet ports allowed ambient air to enter the chamber. The lower edges of the chamber were sealed using surrounding soil to limit the infiltration of outside air. The chamber blank was 1-2 ng m^{-3}. The external air concentration was measured every 15 min, while the internal chamber concentration was measured and recorded every second. The average concentration for the 15 min period was then calculated. The rate of mercury exchange was calculated using the following equation (Ferrara and Mazzolai, 1998; Ferrara et al., 2000; Poissant and Casimir, 1998):

$$F = \frac{(C_i - C_e) \cdot Q}{A} \tag{1}$$

where F is the Hg flux (ng m^{-2} h^{-1}), C_i and C_e are the chamber internal and external Hg concentrations in ng m^{-3}, Q is the flow rate through the chamber (m^3 h^{-1}) and A is the chamber surface area (m^2). A similar approach using the flux chamber technique is described in more detail by Ferrara and Mazzolai (1998) and Ferrara et al. (1998).

4.3.1.6.2 Laboratory flux chamber experiment

For the determination of mercury fluxes from soil under controlled environmental conditions, laboratory flux measurement system (LFMS) developed and designed by Bahalmann et al. (2006) was used (Fig. 12). The LFMS is constructed of a cylindrical flux chamber with a diameter of 50 cm corresponding to a surface area of ~ 2000 cm^2 and a variable height between 10 and 40 cm, resulting in a chamber volume between 20 and 80 L. All system parts coming in contact with samples are made of or coated with Teflon®. The bottom and the side of the chamber are made of Teflon® coated stainless steel and the top is made of FEP-sheet (0.25 mm thick). Inlet and outlet ports are on opposite sides of the chamber in a height of 8 cm over the sample surface. For continuous mixing of incoming air a fan, which is adjustable between 300 and 2000 r.p.m. is installed in the centre of the flux chamber. The use of the fan avoids stagnation zones and uncontrolled induction of vertical components of airflow. Further on, the fan controls the flushing air velocity.

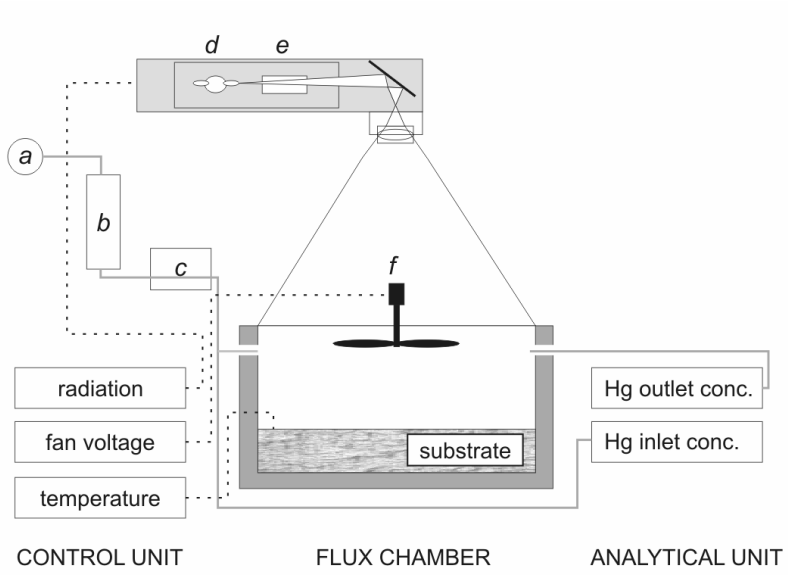

Figure 12: *Experimental set up of the laboratory flux chamber system.* a: gas supply (ambient air), b: charcoal filter, c: mass flow controller, d: XE-Arc light source, e: water filter, f: fan (Bahlmann et al., 2006)

Ambient air is pulled through the chamber at predefined flow rates between 0.5 and 30 L min^{-1} using high capacity mass flow controllers and membrane pumps. Hg is removed from the incoming ambient air by means of an activated carbon scrubber. To investigate the influence of solar radiation on mercury exchange processes a solar simulator was used with a 2000W Xenon short arc lamp as light source. The Xenon arc lamp provides a continuous light spectrum with a constant intensity of 320 W m^{-2}. The spectrum is quite similar to the AMO-0 spectrum in the visible UV region. About 65% of the out coming IR-radiation was adsorbed by a water filter (thickness: 10 cm). This significantly reduces the heating of the substrate. The temperature was continuously measured in the soil at 0.5 cm depth using highly precise Pt-100 sensors. The soil temperature at 0.5 cm depth is referred to as SST-0.5 in this work. The concentrations of Hg were measured simultaneously at the inlet and the outlet of the chamber by Zeeman Mercury Analyzer RA-915$^+$ and fluxes were then calculated using Eq. (1).

4.3.2 Surface water geo-chemical characteristics

4.3.2.1 General water quality parameters

Temperature, conductivity, dissolved oxygen (DO), and pH measurements were performed in the field by standardized methods. The precision of dissolved oxygen saturation and conductivity measurements was ± 5 %. Because pH is sensitive to CO_2 degassing and warming, water samples were collected in a large volume, air-tight container and pH was measured at least twice to verify electrode stability. The field pH was determined on the NBS scale using two buffer calibrations with a reproducibility of ± 0.02 pH unit.

4.3.2.2 Cations, anions, DOC and alkalinity

Analysis of cations, anions and dissolved organic carbon in river water samples were performed at the University of Michigan, USA.

Major (Ca, Mg, Na and K) and minor (Sr, Mn, Fe, Al, and Si) cations were measured by inductively coupled plasma optical emission spectroscopy (ICP-OES) with a Jobin Yvon Horiba instrument. The precision of the method was ± 2% for major and ± 5% for minor elements.

Major anions (SO_4^{2-}, NO_3^-, Cl^-, F^- and Br^-) were analyzed on a Dionex ICS-2500 IC (ion chromatograph) apparatus with an analytical precision of ±2%.

Dissolved organic carbon (DOC) concentrations were measured using high-temperature platinum-catalyzed combustion followed by infrared detection of CO_2 (Shimadzu TOC-5000A) with a precision of ± 2 %.

Total alkalinity was measured within 24 h of sample collection by the Gran titration procedure (Gieskes, 1974) with a precision of ± 1%.

4.3.2.3 Particulate organic carbon ($\delta^{13}C_{POC}$) isotopic composition

The carbon stable isotope composition of particulate organic carbon ($\delta^{13}C_{POC}$) was determined with a Europa Scientific 20-20 continuous flow IRMS ANCA - SL preparation module. For POC, 1 l of the water sample was filtered through a Whatman GF/F glass fibre filter (0.7 μm). Filters were treated with 1M HCl to remove carbonate material and then dried at 60°C and stored until analyses. Approximately 1 mg of particulate matter was scraped from the filter for analysis. Also, the isotopic composition of carbon of bulk particulate matter (organic and inorganic) with no acid pre-treatment was measured. Precision was ± 0.2‰

4.3.2.4 SEM/EDXS mineral composition of suspended matter

Samples of the river water suspended matter were examined to determine their qualitative and quantitative composition using a JEOL JSM 5800 with electron micro analyser scanning electron microscope/energy dispersive X-ray spectroscopy microscopy (SEM/EDXS) at the Department of Ceramics at the Jožef Stefan Institute. Water samples were first filtered through a Whatman GF/F (pore size 0.7 μm) glass fibre filters. Filters were then dried at 105 °C for 24 hours and impregnated with graphite before analysed.

4.3.3 Stable isotopic composition ($\delta^{13}C$ and $\delta^{15}N$) of soils

The isotopic composition of carbon ($\delta^{13}C$) and nitrogen ($\delta^{15}N$) in soils was determined using a Europa 20–20 continuous flow IRMS ANCA–SL preparation module. Approximately 8 mg of acid pretreatable soil was weighed in a tin capsule for carbon analysis and 30 mg of bulk sample for nitrogen analysis. The isotopic composition of nitrogen and carbon was determined after combustion of the capsules in a hot furnace (temperature 1000°C). Generated products were reduced in a Cu tube (600°C), where excess O_2 was absorbed. H_2O was trapped on a drying column composed of $MgClO_4$. Gases were separated on a chromatographic column and ionized. NBS 22 (oil), IAEA-CH 7 and IAEAN-1 (ammonium sulphate) reference materials were used as reference materials. Precision was ± 0.2‰ and ± 0.3‰ for $\delta^{13}C$ and $\delta^{15}N$, respectively.

4.3.4 Stable isotopic composition ($\delta^{2}H$ and $\delta^{18}O$) of precipitation

The stable isotopic composition of water samples was measured on a dual inlet Finnigan DELTA^{plus} and continuous flow Finnigan DELTA^{plus} XP mass spectrometer with the HEKAtech high-temperature oven at the Institute of Water Resource Management in Graz, Austria. The oxygen isotopic composition ($\delta^{18}O$) was measured by means of the water-CO_2 equilibration technique (Epstein and Mayeda, 1953), and the isotopic composition of hydrogen ($\delta^{2}H$) was performed using H_2 generated by reduction of water over hot chromium (Morrison et al., 2001). Results are expressed in δ-notation, as per mil (‰) deviation of the isotope ratio from the international standard V-SMOW. Measurement reproducibility of duplicates was better than ±0.1‰ for $\delta^{18}O$ and ±1‰ for $\delta^{2}H$.

4.3.5 Data quality assurance

All samples, controls and CRMs were prepared in duplicate or triplicate and every measurement for each replicate was repeated 2-3 times.

For the determination of THg in solid samples, one certified reference material (CRM) and one reference material (RM) were also used to assess accuracy: CRM BCR 580, Estuarine sediment, obtained from the Institute for Reference Materials and Measurements (IRMM) and RM IAEA 405, Trace elements and methylmercury in estuarine sediment, obtained from the International Atomic Energy Agency (IAEA).

Due to the lack of suitable reference materials (RMs) for mercury fractionation studies SOIL-1, an internal material, was used for QA/QC of water soluble mercury faction in soils. The preparation of this material is described in more detail Kocman et al. (2006) in Appendix C.

5 Results and discussion

The results presented and discussed here are organized in four major subsections, according to the main environmental compartments within and between mercury is cycling: water, river sediments, soils and air. In the beginning of each subsection, mercury forms and mercury transformation processes in the individual environmental compartment, known from the literature, are presented. Further, relationships between local conditions and site specific mercury levels/forms in these compartments are discussed.

5.1 Water

Once in aquatic ecosystem, mercury cycles between gaseous, dissolved and particulate forms (Fig. 13). Mercury cycling pathways in aquatic environments are very complex. The various forms of mercury can be converted from one to the next through the processes of methylation/demethylation and reduction/oxidation. The most important process is the conversion to methylmercury (CH_3Hg^+), the most toxic mercury form. The latter undergoes strong bioaccumulation in living organisms and biomagnification in the food-chains.

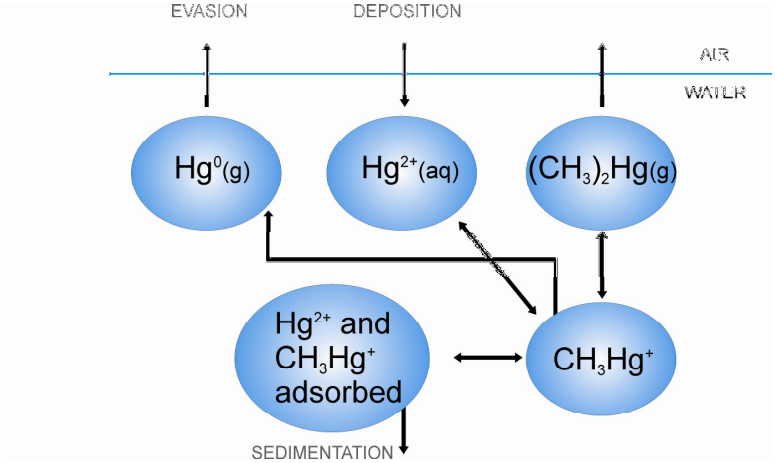

Figure 13: *Mercury cycle in aquatic environment.*

Multiple forms of Hg that can be found in aquatic environment depend on the physical and chemical characteristics of water, which control its behavior. Therefore, not only mercury but also general hydro-geochemical characteristics of the Idrijca River and its tributaries were investigated. Surface water sampling locations were selected based on their relationship to confluences of major and minor streams, typically sampled before and after the confluence. Sampling was performed at 14 locations (Fig. 7) in different seasons (autumn = November 2006 and spring = May 2007), according to the discharge regimes of the Idrijca (7 sampling locations) and its tributaries (7 sampling locations). Considering the long-term discharge regime of the River Idrijca, it should be mentioned that sampling was performed in low (autumn, 2006) and mean (spring, 2007) discharges. The results of the general geochemical analysis are presented in section 5.1.1, while the results of the mercury analysis are presented in section 5.1.2.

5.1.1 The hydro-geochemical characteristics of the Idrijca River system

The hydrogeochemical characteristics of the Idrijca River and its tributaries were studied to obtain information on different natural processes that provide chemical elements to the dissolved and particulate load and influence the chemistry of mercury in aquatic environment. Chemical characteristics of the surface water are the result of natural mechanisms such as (1) precipitation, (2) weathering of bedrock, (3) evaporation and (4) mineral phase precipitation (Chen et al., 2002). Beside natural mechanisms, water

chemistry is influenced also by anthropogenic inputs. In the present study the major solute (HCO_3^-, Ca^{2+}, Mg^{2+}, DOC, SO_4^{2-}, Cl^-…) dynamics of the Idrijca River system through time and space was studied. Temperature, conductivity, dissolved oxygen (DO), and pH measurements were performed in the field. Moreover, isotopic composition of organic carbon on filters was determined. Graphical presentation of the results is shown in the following figures (Fig. 14–19). Results in numeric form are summarized in Appendix A.

5.1.1.1 Major solute chemical composition and weathering intensity

Measurements of major ions in the Idrijca River catchment revealed that, according to the classification of Gibbs (1970), Idrijca River and its tributaries are a typical HCO_3^- - Ca^{2+} - Mg^{2+} rivers (Fig. 14). Concentrations varied seasonally according to discharge, with higher concentrations observed in autumn at lower discharge and lower concentrations during the spring sampling season. Results of the chemical composition of the surface water samples in both the Idrijca River and its tributaries suggest that water chemistry is predominantly influenced by the process of the bedrock weathering. In the Idrijca River catchment carbonate and clastic sedimentary rocks are exposed on the surface. Ca^{2+} and Mg^{2+} are result of the carbonate and silicates weathering. Na^+ and K^+ are result of the silicates and evaporites weathering, while SO_4^{2-} and Cl^- are result of the evaporites weathering (Stumm, 1992).

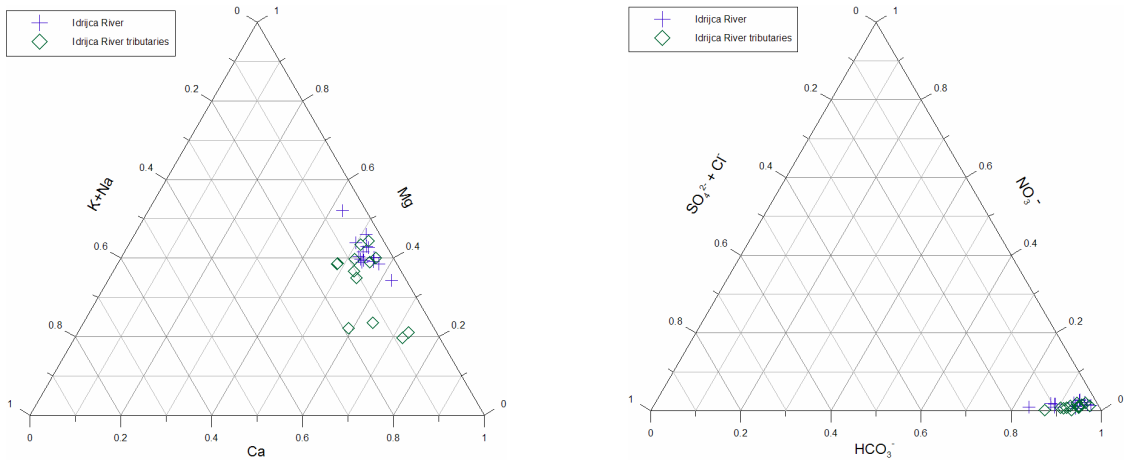

Figure 14: *Major ion chemistry of the Idrijca River and its tributaries.* (cations–left, anions–right)

Chemical composition of waters in the Idrijca River catchment as a result of bedrock weathering is further supported by the stehiometric ratio 2:1 between HCO_3^- and the sum of calcium and magnesium ions (Ca^{2+} + Mg^{2+}). It can be seen from Fig. 15 that water samples from both Idrijca River and its tributaries follow this ratio, which is typical for carbonate and clastic rock weathering. Differences in HCO_3^- concentrations in carbonate-bearing catchments are related to the geological composition of the watershed, relief, mean annual temperature, the depth of the weathering zone, the soil thickness and residence time in the system. Weathering rates increase in thicker soils like shales due to the higher residence time of shallow groundwaters in contact with minerals in comparison to watersheds composed of carbonate minerals. The results for Ca^{2+} + Mg^{2+} ranging from 1.5 to 2.5 and alkalinity concentrations ranging from 3.1 to 5.1 mM in the Idrijca watershed indicate that dissolution of carbonates alone has significant role in the upper part of the River Idrijca (location 1), and also in the lower part at location 13 (Bača tributary), which coincides with the geological composition of the watershed.

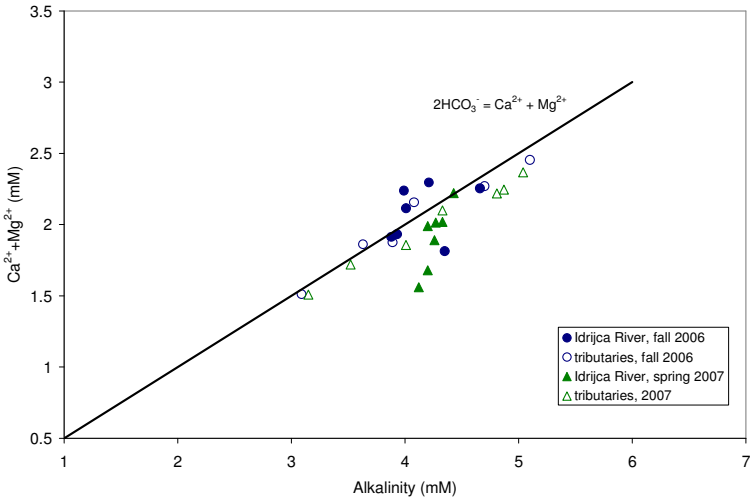

Figure 15: *River water geochemical parameters*. Sum of calcium and magnesium (Ca^{2+} + Mg^{2+}) vs. alkalinity in the Idrijca River catchment. Line indicating (Ca^{2+} + Mg^{2+}) alkalinity ratio = 1:2.

For the weathering of carbonates a Mg^{2+}/Ca^{2+} molar ratio around 0.5 is characteristic (Meybeck, 1996). Deviation from this ratio arises from additional mineralization of water due to erosion of mechanically less resistant clastics rocks. The Mg^{2+}/Ca^{2+} ratio also indicates the relative contributions of calcite and dolomite which contribute to the chemical composition of water. Dolomite weathering gives a Mg^{2+}/Ca^{2+} molar ratio around 1, while dolomite and calcite weathering gives a ratio around 0.5. In the case of weathering of calcite as the dominant mineral, the Mg^{2+}/Ca^{2+} ratio can be below 0.2. In the Idrijca River catchment the Mg^{2+}/Ca^{2+} ratio was found to be between 0.3 and 1 (Fig. 16). Most of the samples indicate that weathering of dolomite is dominant over the entire Idrijca River, especially in the upper and central flow of the river, where weathering of dolomite prevails. A Mg^{2+}/Ca^{2} ratio around 0.33, which is typical for weathering of calcite with magnesium, is characteristic only in the lowland tributaries of the River Idrijca composed mainly of calcite (Cerknica – location 9 and Bača - location 13).

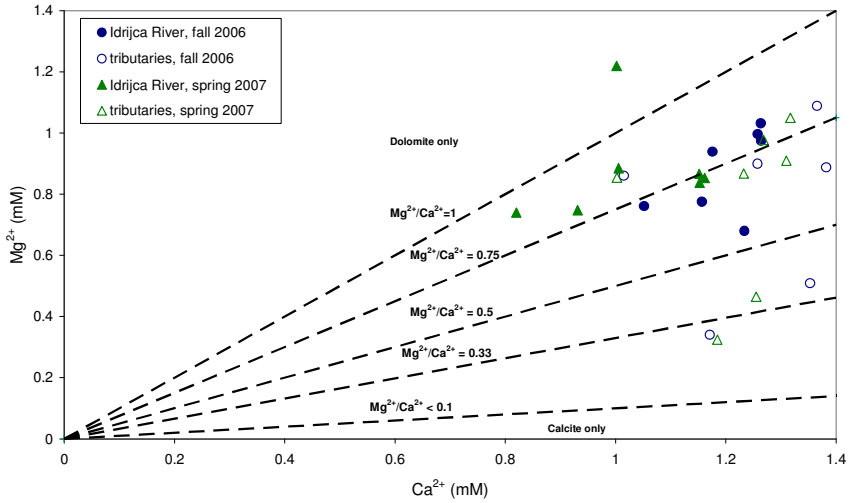

Figure 16: *River water geochemical parameters*. Ca^{2+}/Mg^{2+} ratios in different sampling seasons, Lines indicating relative contributions of calcite and dolomite to the chemical composition of water.

The major control on carbonate weathering intensity is runoff, (e.g., Holland 1978; Amiotte Suchet and Probst 1993). Carbonate weathering intensity normalized to drainage area quantifies HCO_3^- produced from mineral weathering. In Slovenian catchments total alkalinity comprises carbonate alkalinity (Kanduč et. al., 2007) and therefore total alkalinity is assumed as HCO_3^-. Figure 17 compares carbonate weathering intensities as a function of specific runoff for the Idrijca catchment, combining new data from this study with published official data for the Sava River (EIONET 2005) and data from Berner and Berner (1996) for world rivers. It was callculated from available data (mean long term discharge, alkalinity, drainage area)

that the River Idrijca at the location Hotešček has a very high carbonate weathering intensity of around 227 mmol km^{-2} s^{-1} (Fig. 17). Compared to other rivers, in the Idrijca River catchment linked factors such as lithology, steep terrain and specific climate result in the increased weathering intensity.

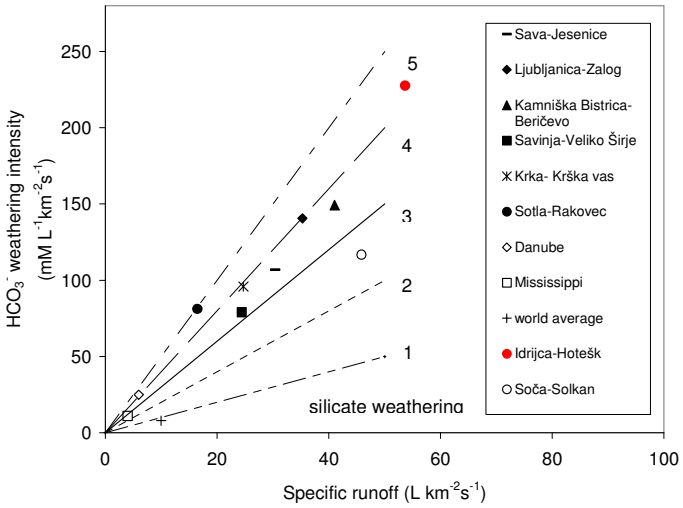

Figure 17: *Carbonate weathering intensity versus specific runoff indicating high carbonate weathering intensity in the Idrijca River catchment.*

In Fig. 18 concentrations of selected ionic species (Cl^-, SO_4^{2-}, NO_3^-) and dissolved organic carbon (DOC) in the Idrijca River and are shown. These parameters were selected due to their influence on the biogeochemical characteristics and behavior of mercury in aquatic environment.

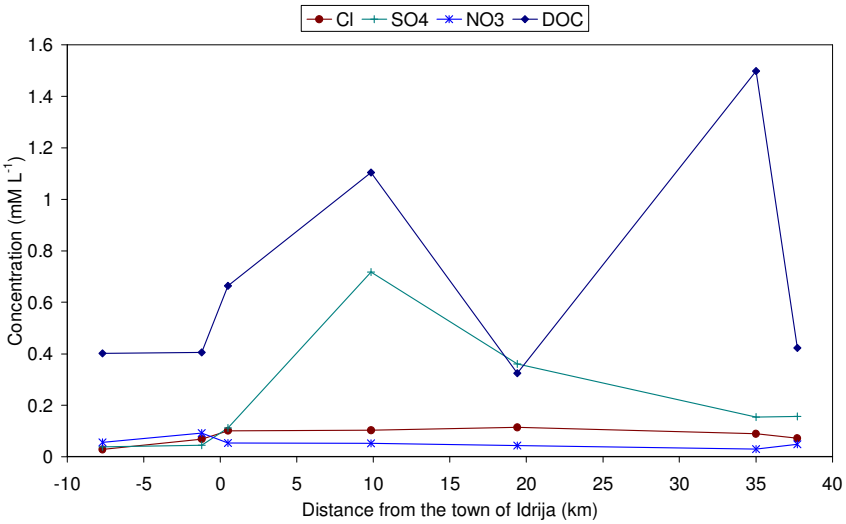

Figure 18: *Concentrations of selected ionic species (Cl^-, SO_4^{2-}, NO_3^-) and dissolved organic carbon (DOC) in the Idrijca River*

As most of the catchment is covered with forest and due to the absence of significant anthropogenic sources, concentrations of Cl^-, SO_4^{2-} and NO_3^- were low in both the Idrijca River and its tributaries. Measured concentrations are in the range typical for unpolluted rivers (Roy, 1999).

Dissolved organic carbon (DOC) concentrations reached up to 1.83 mM during both sampling seasons. During fall sampling DOC concentrations reached up to 1.57 mM and in the spring sampling season ranged from 0.23 to 1.83 mM, which is typical of unpolluted rivers (Tao 1998). Higher DOC concentrations were observed in some tributaries of River Idrijca (see data in Appendix A). This can be related to a higher organic matter input and consequent decomposition in the terrestrial environment, which increases DOC leached from soils, especially in the spring sampling season. DOC may also be photochemically degraded downstream towards the mouth of the river, however similar concentrations of DOC were observed at the source as at the mouth of the River Idrijca, which contradict this assumption.

5.1.1.2 Characteristics of suspended matter

The results of the qualitative composition of grains obtained from SEM/EDXS microscopy indicate that the organic component is dominating (Fig. 19) in the river suspended material. Inorganic component is composed of terrigenic components like silica, alumosilicate minerals (clay minerals), Fe and Al oxides, hydroxides and carbonates as remnants of carbonate and clasitc rock weathering products in the Idrijca River catchment.

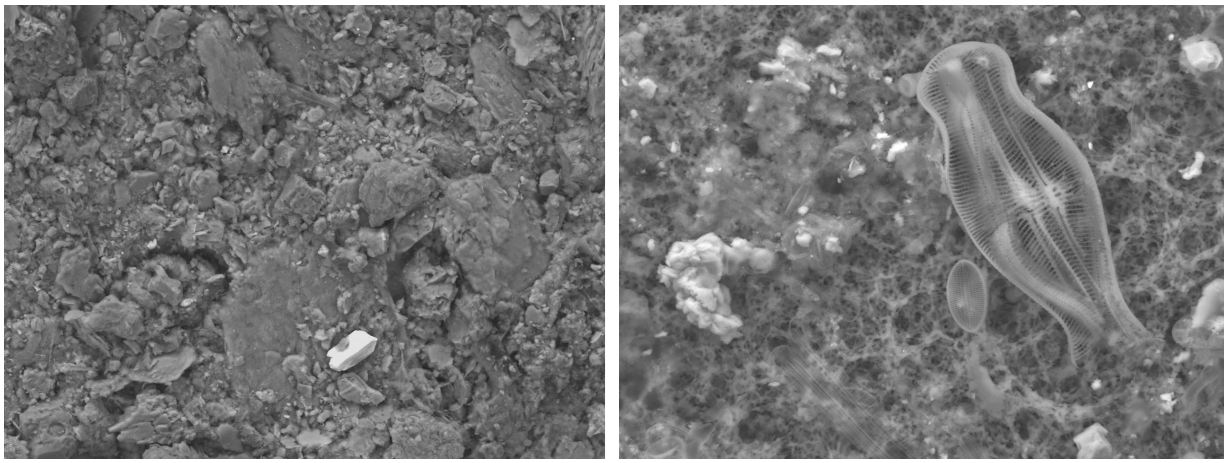

Figure 19: *SEM/EDXS microscopy of suspended matter in the Idrijca River from location 12 (Hotešček).* Marked grains represent alumosilicate particle (A) and frustules of a diatom impregnated with silica (B), material of organic origin is dominating (dark colored parts on both pictures).

Due to the known Hg affinity to organic material, the abundance and the nature of this material is of extreme importance, as it can influence the behavior (e.g. binding, partitioning, transformations…) of Hg in the aquatic environment. Suspended organic matter (SOM) in rivers is mostly derived from soil and plant material. In this study, the isotopic composition of carbon ($\delta^{13}C_{POC}$) in suspended river sediment was used to ascertain the relative contribution of terrestrial vegetation and soil matter in the river ecosystem.

$\delta^{13}C_{POC}$ values in the Idrijca catchment have an average value of -27.6‰ (Appendix A) and are similar to those obtained from the soil profiles (average -26.6‰), indicating that POC is mostly derived from soil organic material, rather than from plant material, macrophytes or phytoplankton in the river, which have more negative $\delta^{13}C$ values (Ittekkot 1988; Hedges 1992). The characteristic $\delta^{13}C$ value of plant material in Slovenian watersheds is -31.6‰ (Kanduč et al., 2007). According to a simple mixing model, the proportion of soil and plant litter can be calculated in POC (particulate organic carbon) using the following equation:

$$\delta^{13}C_{POC} = D \cdot \delta^{13}C_{plant} + (1 - D) \cdot \delta^{13}C_{soil} \quad (2)$$

where, D is the proportion of plant material in suspended matter, [%]; (1 - D) is the proportion of soil material in suspended matter, [%];$\delta^{13}C_{plant}$ is the isotopic composition of carbon in plant litter assumed to be -31.6‰, [‰];$\delta^{13}C_{soil}$ is the isotopic composition of carbon in soil matter, average measured value of -26.6‰, [‰], $\delta^{13}C_{POC}$ - isotopic composition of carbon in particulate organic carbon (POC), average measured value of -27.6‰, [‰].

Isotopic composition of POC revealed terrestrial origin of suspended organic matter as a result both soil and plant litter weathering and erosion, respectively. According to Eq. 2 the percentage of soil matter in particulate organic matter prevails and is estimated to be 80%, while plant litter presents only 20%. The results of carbon isotopic composition along with its influence on the mercury partitioning in both water and soils, are discussed into more detail in the following sections.

5.1.2 Mercury in the Idrijca River system

Mercury concentrations were measured in surface water samples obtained from 7 locations in the Idrijca River to determine the amount and spatial distribution of Hg. To determine the loads of Hg to the Idrijca River, samples were also taken from 7 major tributaries of the Idrijca River. As mercury toxicity depends mostly on its form/reactivity that control mercury transformation processes, beside total Hg concentrations (THg), also different Hg forms were measured in these samples: dissolved mercury (DHg), particulate mercury (PHg), reactive mercury (RHg), dissolved gaseous mercury (DGM) and methylmercury (MeHg). To investigate seasonal variations in Hg distribution and speciation, three sampling campaigns under different hydrologic conditions were performed. The first sampling campaign was performed in fall 2006 after a long period of dry weather when water discharges were low. The second campaign was performed in spring 2007 during the rainy season when water discharges were moderate. Additional samples were obtained in spring 2007 from four locations in the Idrijca River during high water discharges. The results obtained are presented graphically in Fig. 20-22 and summarized in numerical form in Appendix A.

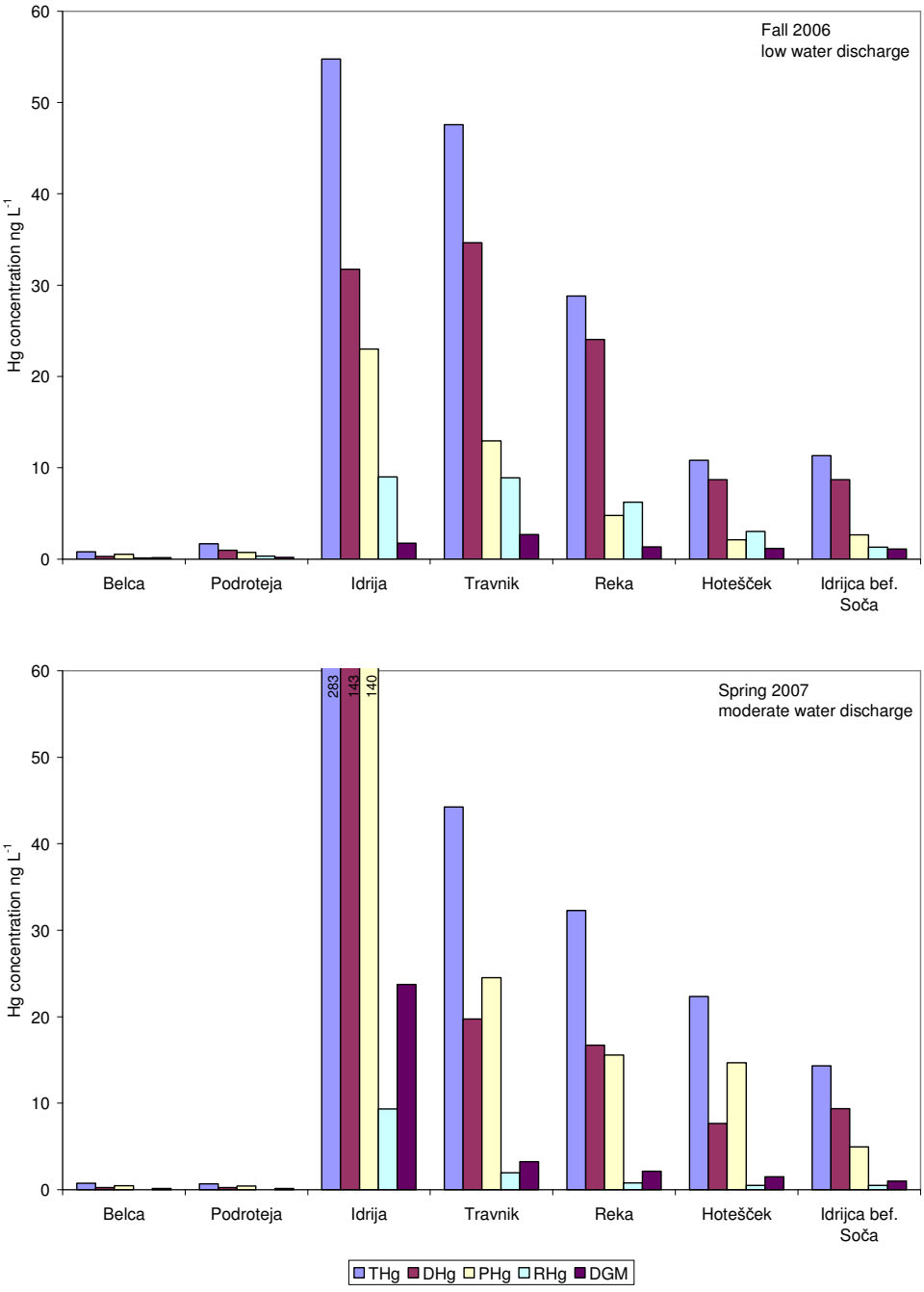

Figure 20: *Distribution of different mercury species in Idrijca River.* (A-Fall 2006, B-Spring 2007).

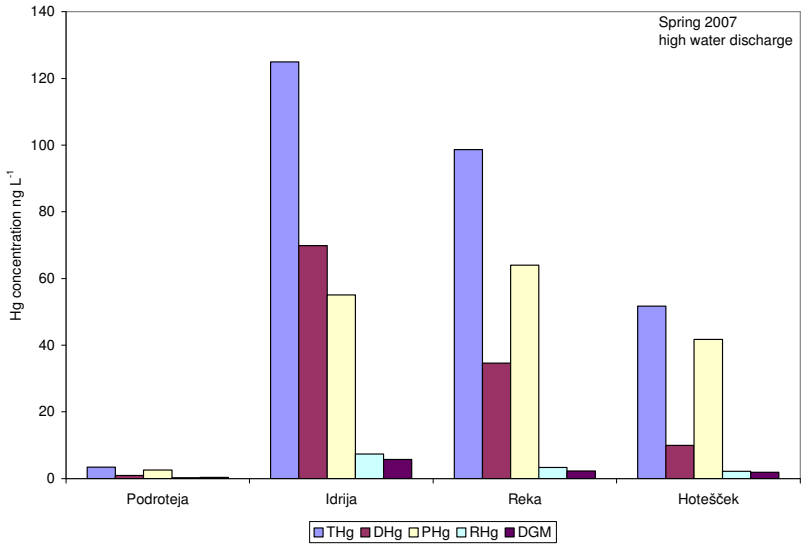

Figure 21: *Distribution of different mercury species in Idrijca River during high water levels.* Spring 2007.

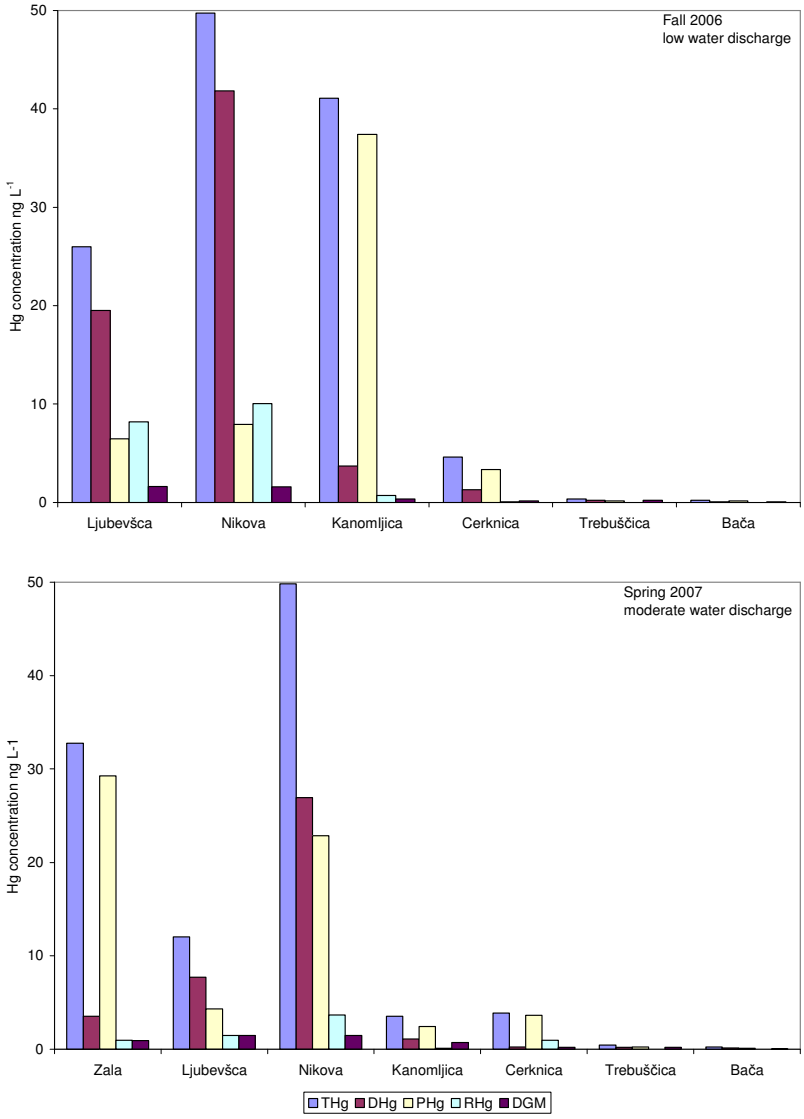

Figure 22: *Distribution of different mercury species in the Idrijca tributaries.* (A-fall 2006, B-spring 2007).

5.1.2.1 Mercury speciation in river water

In general, the results of mercury analysis in river water in this study showed similar picture as that observed during previous sampling campaigns in 1998 and 2000 (Hines et al., 2000; Horvat et al., 2002; Bonzongo et al., 2002). Although more than 10 years after the closing of the Idrija mercury mine, the trends observed remain similar, as follows.

5.1.2.1.1 Total Hg concentrations in non-filtered river water

Total Hg concentrations in the Idrijca River increased over 100-fold just downstream of the mining district and remained elevated for a factor of more than 10 until the inflow in the Soča River, compared to values obtained in the upper part of the Idrijca River. The highest mercury concentrations were observed in the town of Idrija at site where water draining out of the mine is collected and released in the Idrijca River (up to 300 ng L^{-1}). This is also the reason for a big difference in Hg concentrations observed at location Idrija among both sampling campaigns. In fall 2006 at this location sample was obtained just before the mine drainage release, while in spring 2007 sample was obtained after the release. Afterwards, Hg concentrations gradually decreased downstream reaching 10-15 ng L^{-1} of total Hg just before the confluence with Soča River. This is still high and close to 12 ng L^{-1}, a concentration that the EPA indicates may result in chronic effects to aquatic life (US Environmental Protection Agency, 1992).

Measurements of Hg concentrations in seven tributaries of the Idrijca River revealed a similar picture (Fig. 22). Clear decrease of Hg concentrations with the increasing distance of the individual tributary drainage area from the mining district was observed. During both sampling campaigns the highest concentrations were measured in the Nikova, a stream draining the town of Idrija and the Pront hill where native mercury-bearing carboniferous clastic rocks can be found. There was a clear decrease of Hg concentrations observed with the increasing distance of the tributary inflow from the town of Idrija. Hence, the lowest Hg concentrations (< 1 ng L^{-1}) were measured in the samples collected in the Trebuščica and Bača tributary, respectively. Hg loads from these two tributaries are insignificant compared to others. Hg concentrations at these two remote sites are comparable to concentrations measured in water from non-polluted sites (e.g. Peckenham et al. 2003).

5.1.2.1.2 Total dissolved and particulate mercury in river water

Although important, total Hg concentrations alone do not reveal the information about the mercury behavior. The behavior of Hg in aquatic system depends on the partitioning, t.i. the distribution between aqueous and particulate phases of different Hg species. Partitioning is controlled by natural processes such as erosion, weathering, atmospheric deposition, anthropogenic input and the exchange of Hg between different compartments of an aquatic system (Hissler and Probst, 2006).

It should be noted that this operationally defined "dissolved" fraction includes both the "truly dissolved" Hg species as well as Hg species that are associated with colloids.

Analyses of filtered water samples revealed that between 34 and 83% of total Hg passed through a 45 µm filter in Idrijca River samples and between 6 and 84% in tributaries samples. The percentages of dissolved Hg (DHg) in tributaries are slightly lower (average 43%) as compared to Idrijca River (56%). This may be the result of soil erosion processes in torrential tributary streams, which leads to relative increase of particulate bound Hg. The percentage of particulate phase Hg was also higher during higher water discharges. PHg is mostly related to suspended material in water (TSS) which concentrations are controlled by changing hydrological conditions (see chapter 5.1.2.4). In the suspended phase, it is supposed that the mercury species bound to the organic material are dominant. This was confirmed by a relationship between the PHg concentration and isotopic composition of the particulate organic carbon (POC) ($\delta^{13}C_{POC}$). Isotopic composition of POC revealed terrestrial origin of suspended organic matter as a result of soil and plant litter weathering and erosion, respectively. More positive $\delta^{13}C_{POC}$ values indicate the presence of soil organic matter in POC, while more negative $\delta^{13}C_{POC}$ values indicate that plant litter is a dominant source of POC. Degradation of plant litter is one of the major sources of humic substances in river water. Humic substances are known to have a large ion-exchange capacity. The results suggest that with the increasing amount of humic substances contained in suspended organic material, Hg is more strongly bound to particulate phase (Fig. 23).

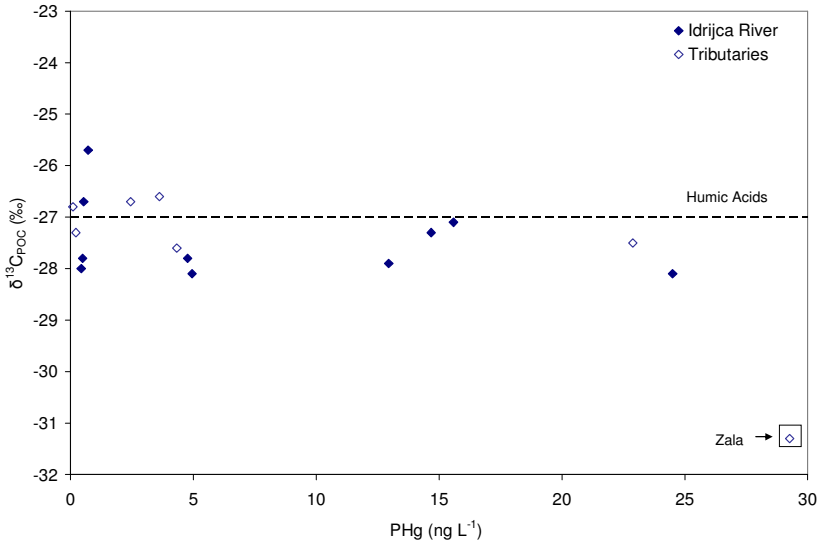

Figure 23: *Isotopic composition of $\delta^{13}C_{POC}$ vs. Hg bound to particulates.*

However, at the mercury mine polluted sites such as Idrija region, a significant part of the Hg particulate phase in water can be due to the cinnabar particles present. Results of the SEM/EDXS microscopy of suspended matter confirmed this assumption. In Fig. 24 a grain of a cinnabar on the filter from the location Hotešček on the Idrijca River can be seen. Although Hotešček is located almost 40 km downstream from the town of Idrija, erosion of soils and the resuspension of riverbed sediments containing cinnabar obviously still effect composition and partitioning of Hg in water. The results of the qualitative composition of grains obtained from SEM/EDXS microscopy indicate that the organic component is dominating, supporting the assumption of Hg affinity to binding with organic matter as discussed above.

In terms of mercury partitioning, even more important than the presence of cinnabar particles is their size. The size of the cinnabar grains observed is approximately 1 µm. Taking the size of both the cinnabar particles and organic matter into account, the results indicate the importance of the colloidal suspended sediment fraction in the Hg partitioning in the river systems. Similar was observed by other authors. Babiarz et al. (2001) demonstrated by their experiment that the colloidal phase plays an important role in regulating the freshwater partitioning of both inorganic Hg and MeHg. Guo and Santschi (2007) reported percentages of colloidal Hg mercury in different water system can reach up to 88%. Colloidal size and its surface properties are extremely important to understanding of environmental function since colloidal aggregation and the sorption of mercury depend on the nature of the colloid-colloid and colloid-water interfaces.

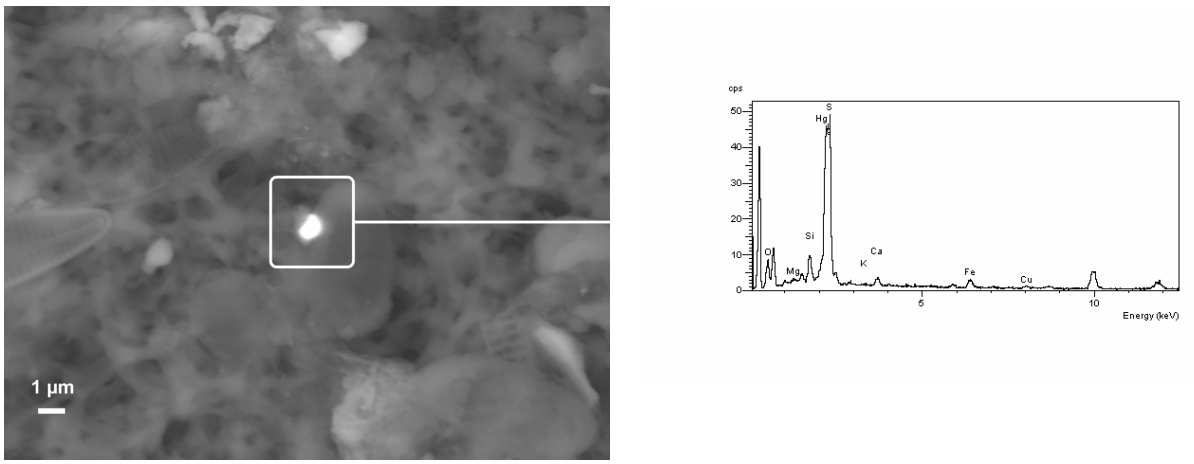

Figure 24: *SEM/EDXS microscopy of suspended matter in the Idrijca River from location 12 (Hotešček).* Marked grain represents a qualitative spectrum (belonging graph) of the cinnabar particle, low content of suspended matter is observed, material of organic origin is dominating (dark colored parts).

5.1.2.1.3 Reactive mercury in river water

To better understand the partitioning of Hg in river environment, also the easily-reducible fraction of mercury (dissolved and suspended phases) undergoing reduction upon treatment by a solution of $SnCl_2$, so-called reactive mercury (RHg), was determined. It should be noted that "total" reactive mercury in a water sample represents all Hg species that are readily available for reduction with $SnCl_2$ solution and volatile Hg species. The methods to measure reactive Hg are not standardized (or agreed), and therefore difference may occur in various studies due to differences in the protocols employed. In this study reactive mercury was measured immediately after sampling from 50-100 ml of non-filtered and non-acidified water sample. Dissolved gaseous Hg and easily reducible fractions of Hg ware therefore purged from the sample and measured as reactive Hg. The results in this study are corrected for the presence of DGM by subtracting its value from the ''total reactive'' mercury measured by the analytical procedure described. As the measurements were performed 3-6 hours after the sampling, the influence of storage time or any other pretreatment of the samples could not affect the data. Reactive mercury is a methodologically defined parameter, but it can be useful in interpretation of data.

RHg in river water samples (corrected for DGM) represents a portion of inorganic Hg that consists mostly of the Hg fraction weakly bound to inorganic (e.g. $Hg(OH)_2$, $HgCl_2$) and organic complexes (Horvat et al., 2001). Among the inorganic anions, Hg^{2+} forms the strongest covalent compound with chloride ions. The Hg^{2+} can also hydrolyse to $Hg(OH)_2$. Well-aerated waters containing traces of stable organic ligands speciate mercury between different chloro- and hydroxy-mercury complexes as a function of pH and Cl concentrations (Boszke et al., 2002). The data from the Idrija suggest a general increase of RHg with increasing Cl concentrations (Fig. 24). Therefore, it could be assumed that this part of RHg corresponds to Hg mainly complexed with Cl, as Hg associated with dissolved organic matter is known to be strongly bound and can not be released in such conditions (Ravichandran, 2004). However, comparison of the Cl ranges and pH conditions (between 7.5 and 8.5) in the Idrijca river system with the dominance diagram of hydroxo- and chloro-complexes (Fig. 25) indicates that hydroxo-complexes would most probably dominate.

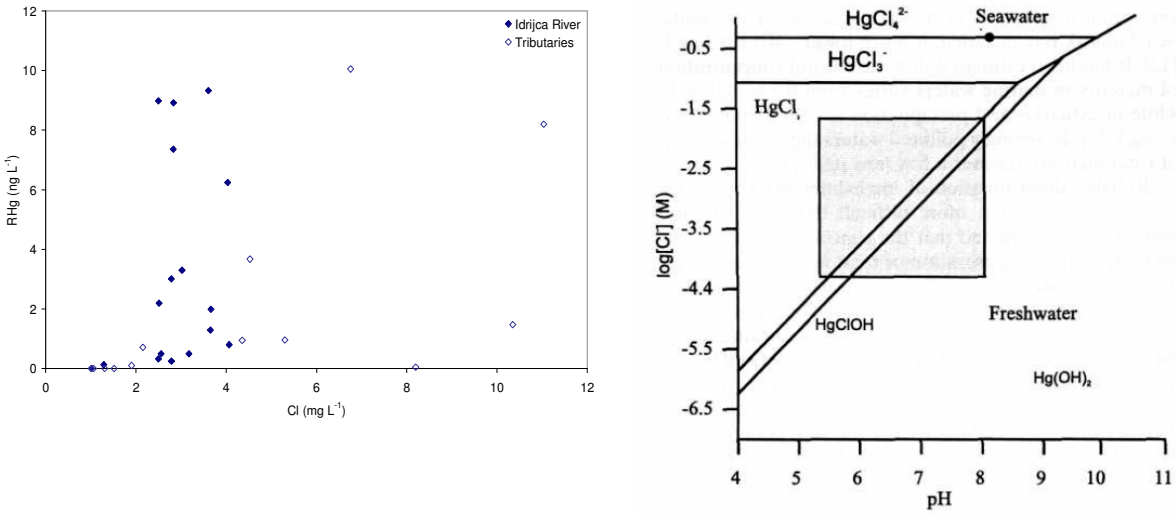

Figure 25: *Reactive Hg vs. Cl concentrations in the Idrijca River and its tributaries (left) and dominance diagram of hydroxo- and chloro-complexes of Hg(II) as a function of pH and chloride concentrations (right).* (Morel et al. 1998).

Reactive Hg concentrations in water samples increased from < 0.05 ng L^{-1} in the Idrijca River upstream of the mining area and in the remote tributaries to a maximum of 10 ng L^{-1} within the town of Idrija. In the Idrijca River, RHg then decreased downstream the Idrijca reaching concentrations around 1 ng L^{-1} just before the inflow in the Soča River.

The concentrations of RHg is in good correlation with the concentrations of DHg (R^2=0.82), although the concentrations of reactive Hg are lower on average by about a factor of 10. This may suggest that one portion of dissolved Hg is the one responsible for further transformations of Hg in water. Somewhat weaker but steel significant correlation (R^2=0.60) between reactive Hg and Hg bound to particulates indicates weaker reactivity of Hg bound to particles. Moreover, significantly higher RHg concentrations were observed during low water discharges in both Idrijca River and its tributaries, suggesting that RHg is formed within the water column under such conditions.

5.1.2.1.4 Dissolved gaseous mercury (DGM) in river water

The formation and volatilization of dissolved gaseous mercury (DGM) is an important mechanism by which freshwaters may naturally reduce their mercury burden. The measured DGM concentrations represent all volatile Hg species in water samples. As dimethyl Hg in surface waters is usually under the limit of detection, it is assumed that the values for DGM represent only dissolved Hg^0. DGM concentrations in the Idrijca River vary from concentrations below 0.15 ng L^{-1} in the upstream parts of the catchment up to 24 ng L^{-1} near the mine drainage, while in the tributaries DGM concentrations range between 0.03 and 1.6 ng L^{-1}. These results are difficult to compare with other river systems, as the few studies that investigated Hg exchange between rivers and the atmosphere mostly deal with the estuarine section of the rivers. However, DGM concentrations measured in the Idrijca River tributaries are comparable with those reported for Hg impacted rivers (O'Driscoll et al., 2007) and estuaries (Cardona-Marek et al., 2007), while DGM concentrations in the Idrijca River are up to 20 fold higher. In the Idrija mercury mine region, a big part of DGM can originate from the native mercury bearing rocks, mine drainage and mine residuals. E.g., one of the highest DGM concentrations in the tributaries was measured in the Nikova stream which is draining the hill Pront area, where the outcropping bedrocks contain native Hg. On the other hand, DGM in surface water may also results from the reduction of divalent Hg either photolytically and/or microbiologically. DGM may also be oxidized to divalent Hg in surface waters, particularly in the presence of chloride ions (Yamamoto, 1996), which would result in an increase of reactive Hg.

The correlation between DGM and percentage of mercury as reactive mercury (relative to DHg) in the Idrijca River is presented in Fig. 26. Data obtained at location Idrija in spring 2007 were omitted from the plot as very high DGM concentrations at this site are due to the mine drainage and are not a result of natural processes. A reverse relationship was observed between DGM and percentage of mercury as reactive Hg, although not statistically significant. Based on this relationship it can be assumed that reduction of Hg^{2+} prevails in this specific environment.

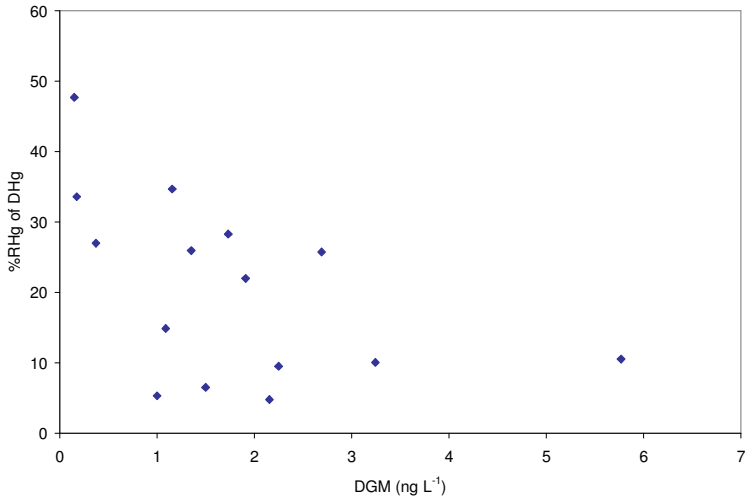

Figure 26: *Correlation between DGM and percentage of mercury as reactive mercury (relative to DHg) in the Idrijca River.*

5.1.2.1.5 Methylmercury (MeHg) in river water

Results of the MeHg measured in water samples of the Idrijca River for the spring 2007 sampling campaign are presented in Fig. 27. Methylmercury was measured in filtered and non-filtered samples at six locations in the Idricja River.

MeHg concentrations in both filtered ($MeHg_{diss}$) and non-filtered samples ($MeHg_{tot}$) revealed a slightly different picture compared to the total Hg. Although a similar trend was observed, the concentrations of MeHg in the Idrijca River increased by only a factor of 2-4 below the mine and reached its maximum cca. 10 km downstream from the mine at location Travnik (0.53 ng L^{-1}). Concentrations then decreased downstream and reached 0.21 ng L^{-1} before the inflow in Soča River. Similar trend was observed previously (Hines et al. 2000; Horvat et al. 2002; Bonzongo et al. 2002).

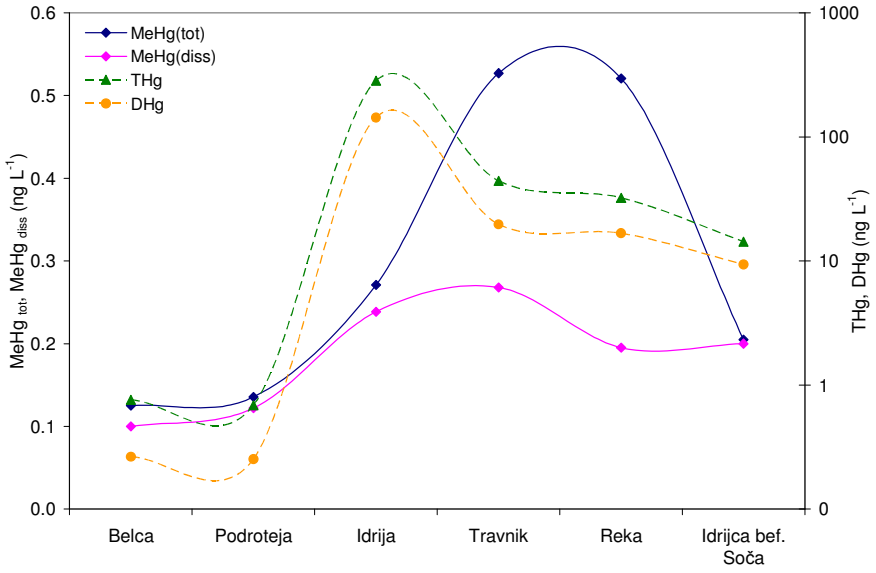

Figure 27: *$MeHg_{tot}$ and $MeHg_{diss}$ concentrations and comparison with THg and DHg concentrations in the Idrijca River.*

Dissolved methylmercury (DMeHg) represents from 40 up to 98% of total methylmercury ($MeHg_{tot}$). The percentage of $MeHg_{diss}$ was lower at two most MeHg abounded sites, Travnik and Reka, respectively. The ratio of MeHg to Hg in filtered and non-filtered samples was found to be increased upstream from the mine, where $MeHg_{tot}$ was up to 20% of THg and $MeHg_{diss}$ up to 48% of DHg. Along the Idrijca downstream from the mine MeHg remained less than 1.5% until the Idrijca merges with the Soča.

While the distribution coefficient (*Kd*) was in the range of 10^5-10^7 for the total Hg, *Kd* was in the range of 10^3-10^6 for methylmercury. This indicates stronger binding of inorganic Hg forms to suspended particles compared to MeHg. Large differences in *Kd* are due to variability in the concentration of TSS. There is a negative correlation between *Kd* and MeHg (Fig. 28, A), which is consistent with the other studies performed in Idrija region and other stream waters impacted by Hg mining activities (e.g. Gray et al., 2000), where it was observed that with increasing content of TSS, MeHg decreases.

Further, fate and relationship between MeHg and surface water chemical parameters, such as dissolved organic carbon (DOC) and sulphate (SO_4) was investigated. The dissolved fraction of MeHg showed a general increase with increasing DOC concentrations downstream from the mine (Fig. 28, B). The Hg-DOC affinity is well known and was observed in many aquatic systems. Mercury methylation is mainly a microbially mediated process, with abiotic methylation likely to be important in organic-rich lakes (Ullrich et al., 2001). In microbial methylation, complexation with DOC generally limits the amount of inorganic mercury available for uptake by methylating bacteria because DOC molecules are generally too large to cross the cell membranes of the bacteria. However, in sulfate-limited environments (such as Idrijca River) where microbes may be utilizing organic matter as energy source, DOC may have a stimulating effect on microbial growth and thus enhance methylation rates in the water column and sediments (Ravichandran et al., 2004 and authors within).

Finnaly, relationship between percent MeHg and sulphate concentrations for filtered and non-filltered samples was investigated. In both cases, with the exception of most Hg polluted site in Idrija, the percentage of MeHg decreses with increasing sulphate concentrations (Fig. 28, C). This can be explained by the role of sulphate-reducing bacterias (SRB) in Hg methylation. The methylation of mercury by SRB implies that the product of sulfate reduction, sulfide, is likely to limit methylation by formation of insoluble mercuric sulfide. It was therefore hypothesized that methylation occurs at a range of sulfate concentrations below which SRB respiration is inhibited and above which excessive sulfide is produced. On the other hand, in oxic conditions and environments with high mercury concentrations such as in Idrijca River, reductive demethylation can be favored (Barkay and Wagner-Dobler, 2005). This can than explain relative low MeHg concetations in Idrijca River. However, it must be noted that the number of MeHg data presented here is rather limited.

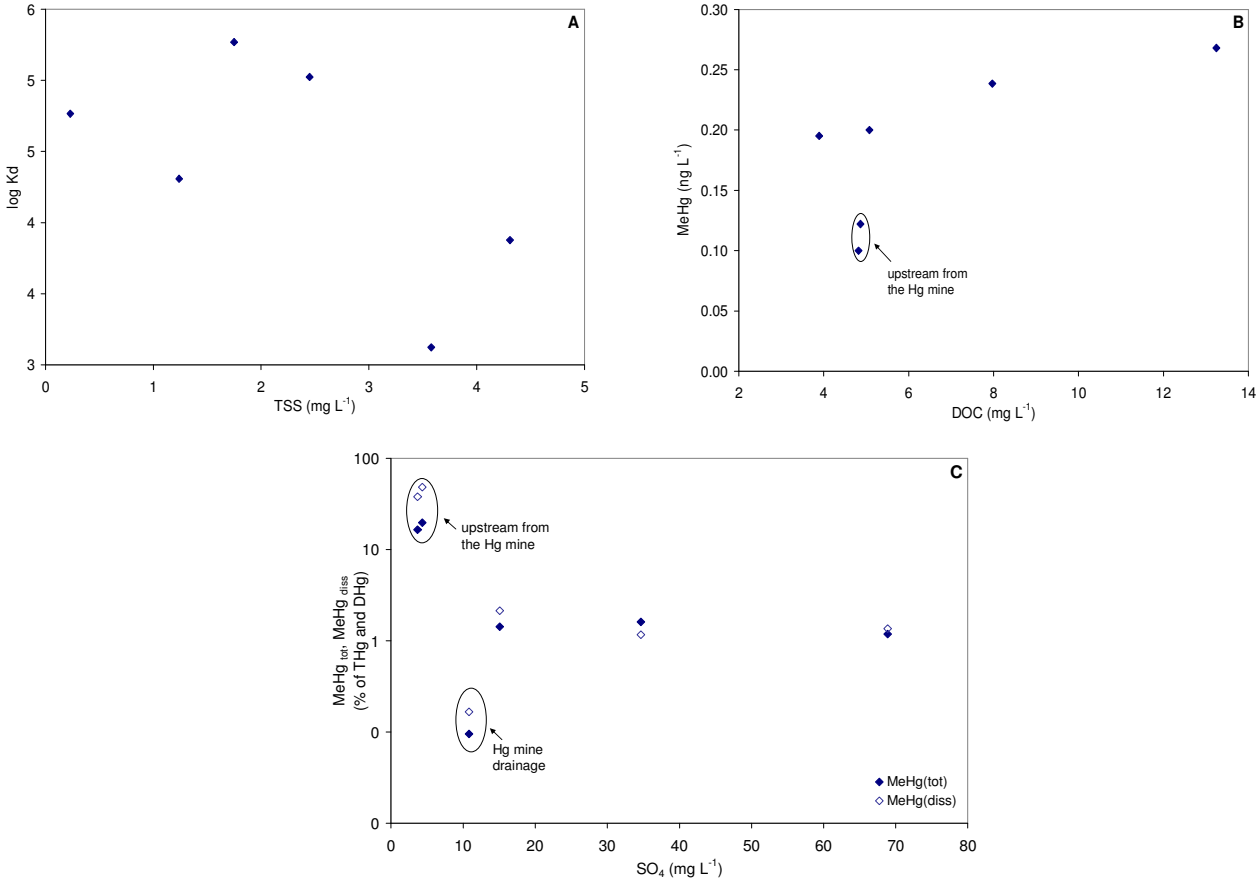

Figure 28: *Relationship between (A) MeHg and coefficient of distribution, (B) $MeHg_{diss}$ and DOC and (C) MeHg/THg ratios and sulfate concentrations in Idrijca River.*

5.1.2.2 Mercury partitioning between dissolved and particulate phases

Partitioning of mercury between dissolved and particulate phases can also be described by the distribution coefficient (K_d), defined as the ratio between Hg bound to suspended solids (TSS) and dissolved Hg (L kg^{-1}). When the distance between pollutes sites in the town of Idrija and downstream sampling sites increases, exchange between the dissolved and particulate phases increases, resulting in the relative increase of dissolved Hg species. This is most obvious in the case of reactive and dissolved gaseous mercury (DGM) which relative percentages increase downstream. This process is controlled by the physico-chemical conditions of the river water such as pH, red-ox conditions, temperature and complexation with a variety of organic and inorganic ligands (Boszke et al., 2002; Hissler and Probst, 2006). The ligands may be considered as belonging to four "carrier" groups: suspended mineral particles (TSS), particulate organic carbon (POC), dissolved organic carbon (DOC) and inorganic complexes and ions (ICI) (Meili, 1997).

The distribution coefficient K_d was in the range between 10^5–10^7 for THg. It must be noted that in the calculation of the distribution coefficient, dissolved Hg was corrected for DGM. Relatively large difference in K_d values are most probably due to variability of TSS concentrations. There is a negative correlation between K_d and TSS (Fig. 29), particularly in the parts of the catchment that were not directly influenced by the mercury mine (Idrijca River tributaries and locations upstream from the mine). At these sites K_d is controlled by DHg, while at sites directly influenced by the mine, K_d is more effected by the particulate bound Hg. The pattern observed is consistent with previous studies in Idrijca River (Hines et al., 2000; Horvat et al., 2002; Bonzongo et al., 2002) and other studies performed in stream waters impacted by mercury pollution (e.g. Gray et al., 2000; Hissler and Probst, 2006).

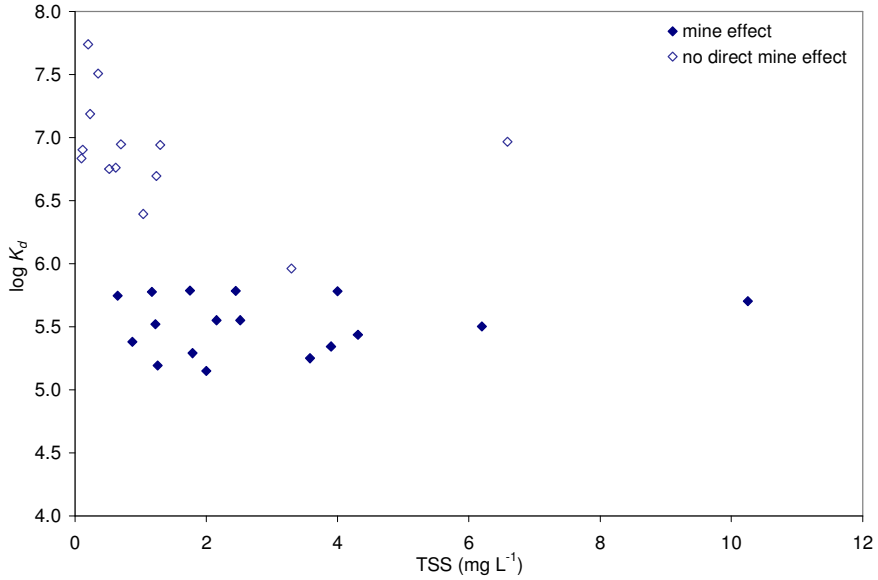

Figure 29: *Relationships between Hg partitioning coefficient (log K_d) and total suspended solids concentration (TSS).*

The pH of water determines the solubility and biological availability of chemical constituents including mercury. In general, increase of pH leads to cation adsorbtion and anion desorption that increases the quantity of inorganic and organic ligands in solution. In presence of a wide range of anionic ligands, Hg^{2+} can produce charged and neutral chemical compounds, the nature of which would then control Hg bioavailability (Bonzongo et al., 2002). These processes seem to influence also Hg partitioning in the Idrijca River catchment. K_d decreases when pH increases, particularly for pH higher than 8 (Fig. 30). This trend is more evident during higher water levels, when pH is higher due to the weathering and erosion process of the carbonate-rich bedrock. Under such conditions, complexation of dissolved Hg by organic and inorganic ligands is increased.

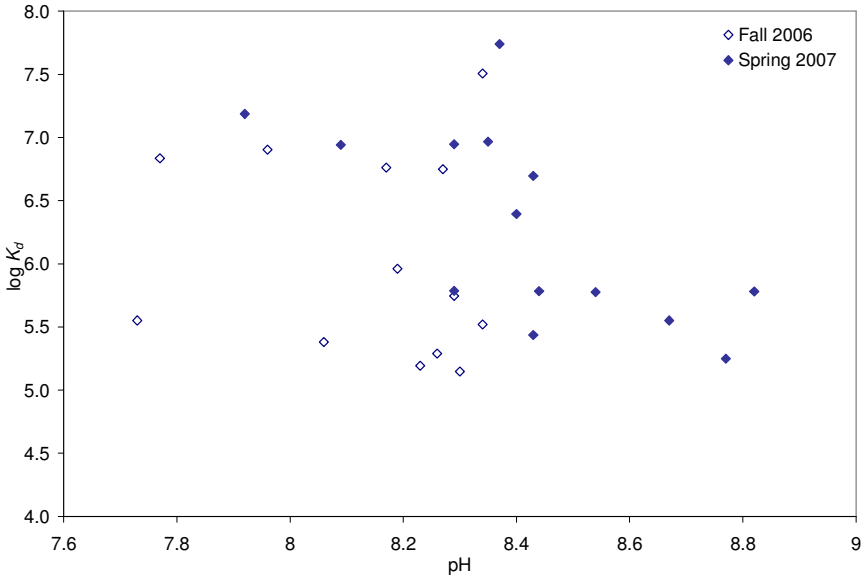

Figure 30: *Relationships between Hg partitioning coefficient (log K_d) and pH.*

The relative importance of each ligand for Hg complexation will depend on the concentration of the Hg and the ligand, and the binding strength for the Hg–ligand complex (Ravichandran, 2004). Among the inorganic ligands, hydroxide, chloride, and sulfide are considered important in controlling the speciation of mercury in aquatic environments (Schuster, 1991; Ravichandran, 2004). In the absence of organic chelators

hydroxide complexes ($Hg(OH)_2$, $HgOH^+$) and chloride complexes ($HgCl_2$, $HgCl_4^{2-}$) are the dominant Hg species in freshwater systems (Dyrssen and Wedborg, 1991). Although decreasing Hg adsorbtion on aqueous particulates was observed with the increasing Cl concentration (Fig. 31), at pH conditions and chloride concentration range observed, Cl is unlikely to compete with the hydroxide, as discussed in section 5.1.2.1.3. Mercury–chloride complexes are thought to be important at low pH and/or high chloride concentrations. Moreover, the stability constants for Hg-chloride complexes reported in the literature (authors within Ravichandran, 2004) are much lower than those for Hg-DOC complexes (10^7-10^{14} compared to 10^{20}-10^{28}). Therefore, DOC would most probably constitute the main ligand for Hg complexation, especially during higher water discharges due to the increased input of terrestrial organic matter (Fig. 32).

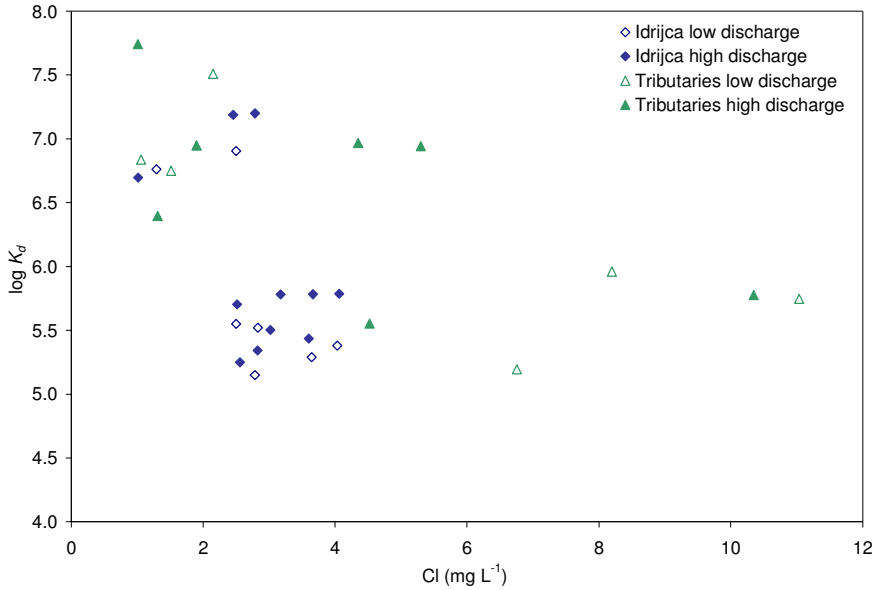

Figure 31: *Relationships between Hg partitioning coefficient (log K_d) and Cl concentration.*

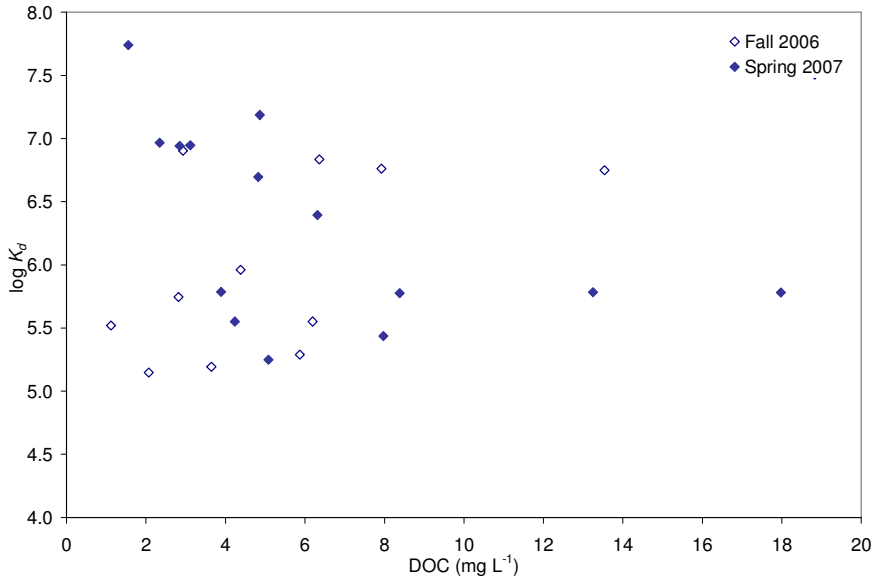

Figure 32: *Relationships between Hg partitioning coefficient (log K_d) and dissolved organic carbon (DOC) concentration.*

5.1.2.3 Hydrologic conditions and Hg speciation/partitioning in river water

The influence of changing hydrological conditions on Hg speciation/partitioning was investigated at location Hotešček where additional samples apart from those presented in previous sections were obtained during higher water discharges. Location Hotešček was chosen due to its position (before the relatively unpolluted Bača River inflow) and because of the gauging station where water discharge is measured continuously. Based on the measured Hg concentrations and water discharges mercury loads during different hydrological conditions can then be calculated.

As it can be seen from Fig. 33, mercury concentrations at location Hotešček during different hydrological conditions vary significantly. Total mercury concentrations measured range from 10 up to 700 ng L^{-1}. However, the observed differences are mostly due to variation of mercury bound in/to particulate phase (PHg). During high water discharges, relative contribution of PHg arises from bellow 20 up to more than 99 %. On the other hand, concentrations of other mercury species remained rather constant and were within the same order of magnitude (RSD =15-30%). As there is no correlation between the Hg bound to particulates and other Hg species, the differences of DHg, RHg and DGM measured under different hydrologic conditions are most probably due to the variable physico-chemical conditions discussed above.

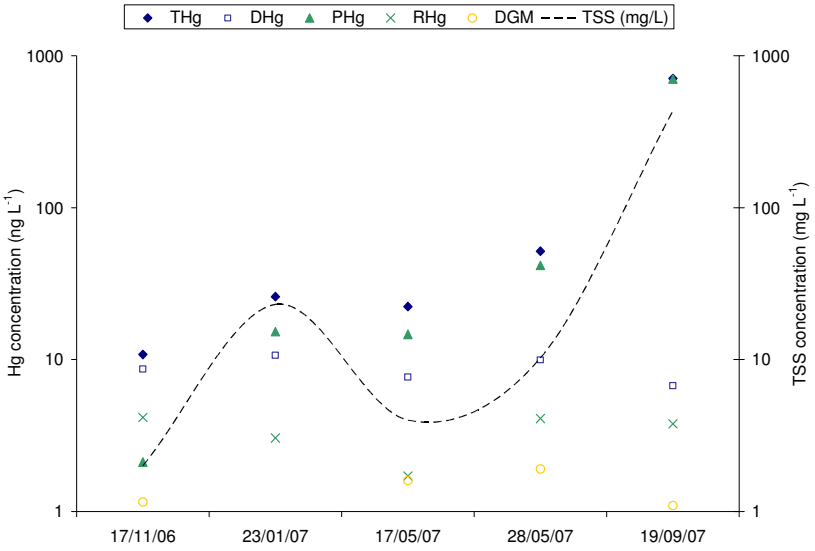

Figure 33: *Mercury speciation in water at location Hotešček under different hydrological conditions.*

The results of mercury speciation in water samples obtained under different hydrological conditions indicate the importance of resuspension of Hg from the river bed, erosion and transport of Hg-contaminated particles in the mass flow and mass budget of the mercury at the catchment scale. Total Hg concentrations were highly correlated with total suspended sediment (TSS) concentrations, and filtration experiments confirmed the strong association of Hg with suspended sediments.

Consequently, the longitudinal profiles of the evolution of *Kd* between different sampling locations were quite different during different hydrologic periods. In Fig. 34, spatial evolution of Hg distribution coefficient along the Idrijca River is shown. During the low water discgarge, *Kd* progressively decreased from upstream to downstream, whereas during moderate and high water discharges, *Kd* increased after the town of Idrija . At station Idrija, *Kd* was comparable during all three periods, demonstrating at this station, the distribution of Hg is greatly influenced by the drainage from the mining sites.

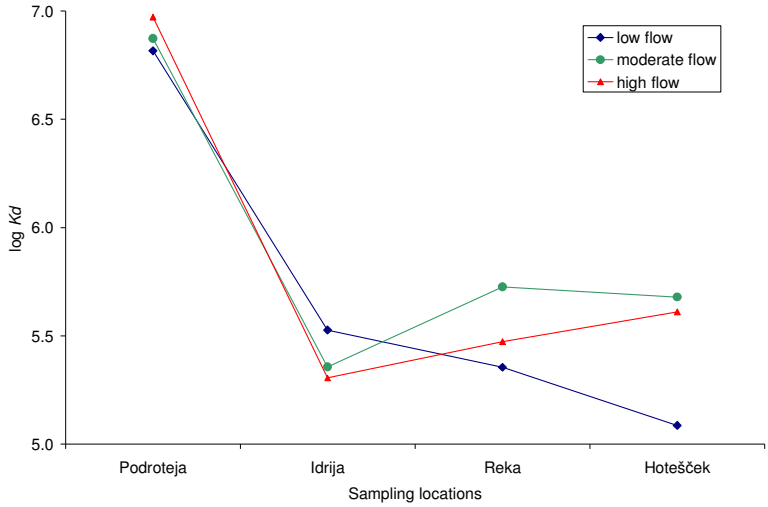

Figure 34: *Spatial evolution of Hg distribution coefficient (log K_d) along the Idrijca River.*

5.1.2.4 Mercury in the suspended solids (TSS)

The results of mercury speciation in water samples obtained under different hydrological conditions indicated the importance of resuspension of Hg from the river bed on the transport of Hg-contaminated particles, its mass flow and mass budget. To study these processes in more detail, sampling of the suspended sediment material was performed during the 23/01/2007 flood wave at location Hotešček, using the net drift samplers. Suspended sediment obtained was sieved/separated in three fractions and analyzed for total mercury: <0.063 mm fraction, 0.063-2 mm fraction and organic material fraction (OM).

While the river bed sediment is being resuspended during the rising stages of the river, deposition of suspended sediment occurs during the falling river stages. Therefore, the time of the sampling is of crucial importance. In Fig. 35, a hydrograph for the 23/01/2007 flood wave and the time of sampling is shown. Long term average discharges (1971-2001) at station Hotešček are given for comparison with the flood wave.

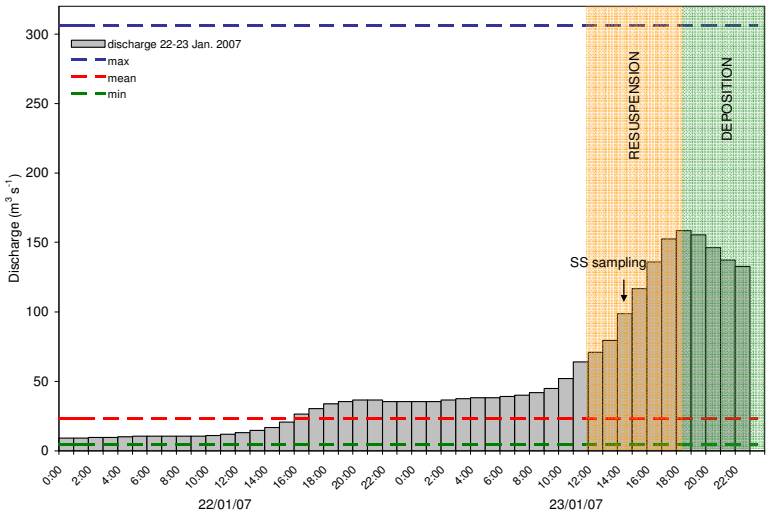

Figure 35: *Hourly discharges of the 22-23 January 2007 flood wave and average yearly minimum, mean and maximum discharges for a period 1971-2000 (dashed lines), location Hotešček.*

The results of the suspended sediment analysis are shown in Fig. 35. Grain size distribution revealed 0.063-2 mm fraction as the most abounded, presenting 52 % of total suspended sediment, while other two fractions (<0.063 mm and OM) present 24 % each. Fine particles were found to be 4-7 times more concentrated in Hg than the coarse ones and OM (52 µg g^{-1} compared to 13 and 7 µg g^{-1}, respectively). In contrast to the stream sediment samples, majority of Hg in suspended sediment (65 %) was found to be related to fine <0.063 mm fraction.

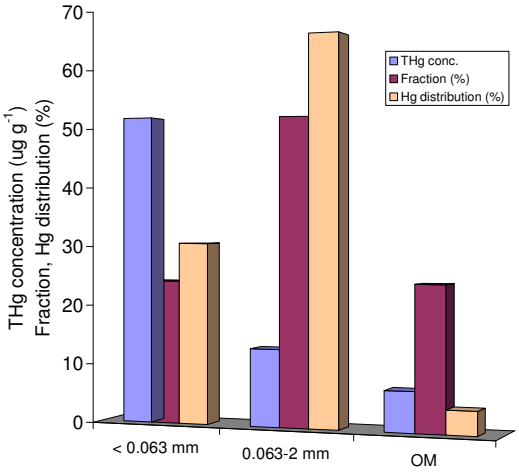

Figure 36: *Percentages of <0.063 mm, 0.063–2 mm and organic material (OM) in suspended sediment, THg concentrations and distribution in different fractions.*

5.2 River Sediment

The concentration of mercury in river sediments is a very good indicator of water pollution with mercury. On one hand, river sediments are compartments where mercury accumulates as a result of simple sedimentation and transport processes and on the other, mercury is released from the sediments becoming available for further biogeochemical transformations (Boszke et al., 2003). Mercury transformation processes in sediment include reduction and methylation/demethylation. The production of methylmercury in the freshwater column and in sediments is thought to be primarily a biological process although chemical methylation by organics has also been observed (Celo et al., 2006). In general, a fraction of Hg^{2+} is methylated to MeHg by a variety of bacteria (aerobes and anaerobes), while other bacteria demethylate MeHg first to Hg^{2+} as an intermediate and finally to Hg^0 (Fig. 37). The rates of these processes depend significantly on the specific environmental conditions in a given water system.

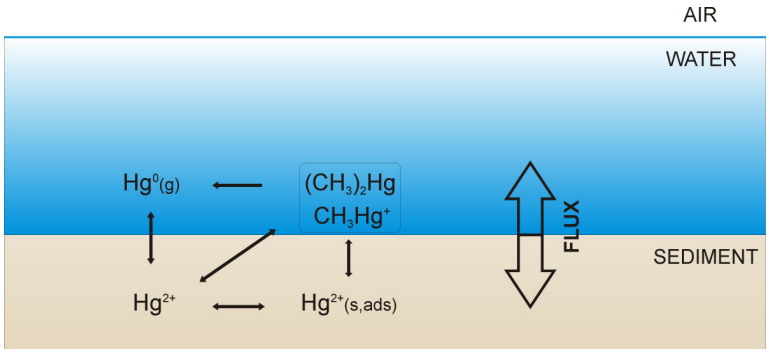

Figure 37: *Hg transformation in river sediment.*

Previous studies in the Idrija region (e.g. Hines et al., 2000, 2006; Horvat et al., 2002) showed that the river sediments present the major source of methylmercury in the aquatic environment. However, there are still a lot of gaps in the understanding of the mechanisms that govern methylation processes. At the moment a lot of work is carried out at the Jožef Stefan Institute within the Department of Environmental Sciences, towards better understanding of these processes in the Idrijca River. E.g., new methodologies for determination of the mercury methylation potential by the use of radiotracers were developed (Žižek et al., 2008). Due to the complexness of the problem, detailed study of the methylation processes was out of the scope of the present work. Therefore, in the present study, only total Hg concentrations in sediments were determined. In the Idrijca River sediments, mercury concentrations were measured to determine its amount, spatial distribution and consequently, its pool available for further transport and transformation processes. Moreover, mercury in the major Idrijca River tributaries was also measured to determine the Hg loads to the Idrijca River as a result of soil weathering and erosion processes.

5.2.1 Mercury in the sediments of the Idrijca River

Concentrations of total Hg in Idrijca River stream sediments at four locations are presented in Fig. 38. Two sediment fractions were analyzed: the silt and clay size fraction with the diameter less than 0.063 mm and a coarser-grained fraction between 0.063 and 2 mm. Percentages of fine and coarse sediment fractions and the relative abundance of mercury in these two fractions were also calculated.

Analysis of both silt/clay and coarser fraction in the Idrijca River revealed Hg concentrations from less than 0.1 μg g^{-1} in the upper part of the catchment to more than 4000 μg g^{-1} just downstream of the mercury mine. This maximum was followed by a rapid decrease downstream until it reached a rather constant but still high concentrations of approximately 30-50 μg g^{-1} before the confluence with the Soča River. The distribution of Hg between both size fractions is not uniform along the Idrijca River. With the exception of the most polluted site in Idrija, fine particles (<63 μm) were up to 12 times more concentrated in Hg than the coarse ones (63 μm to 2 mm), where total Hg concentrations ranged from 0.2 to 54 μg g^{-1} and 0.03 to 33 μg g^{-1}, respectively. However, the abundance of the coarse fraction indicates that 60-98 % of the total Hg is bound to coarse grained particles. Therefore, the coarse fraction could represent the principal reservoir for Hg trapping in the riverbed. In terms of riverine transport, mercury transport associated with the finer particles is dominating during average hydrological conditions, while mercury concentrated in coarse ones is remobilized during extreme hydrological events.

The concentration of mercury in river sediments does not depend simply on the distance from pollution sources but also on hydrological conditions. Idrijca is a fast flowing river which at higher levels partially erodes its own river bed and the flood plains along the stream channel. This indicates that the sources and transport of Hg are strongly influenced by inhomogeneities along the river system that include particles of cinnabar originating from the mine. During the samples preparation and its characterization, cinnabar coatings were observed on some opaque minerals. Gosar et al. (1997) reported 1% of cinnabar grains resulting in 10% of the Hg content in some of the Idrijca river sediments. The dominance of cinnabar Hg fraction (more than 80%) in coarse grained flood plain samples was also confirmed by the results of the sequential extraction procedure (Kocman et al., 2004, Appendix C). In contrast, non-cinnabar fractions were found to be enriched in areas where fine grained material is deposited. Hence, weathering and erosion process seems to be the main source of Hg for the Idrijca River. This is also supported by the geochemical composition of water (see section 5.1.1.), especially composition of particulate organic matter (POM) which play an important role in the binding and transport of Hg within the river systems (Schafer et al., 2006). Also the results of the isotopic composition of POC revealed its terrestrial origin due to weathering and erosion processes. Moreover, during the analytical work sample homogeneity for THg determination was difficult to achieve due to the nugget effect caused by the cinnabar particles. This is explained in more detail in Kocman et al., 2006 (Appendix C).

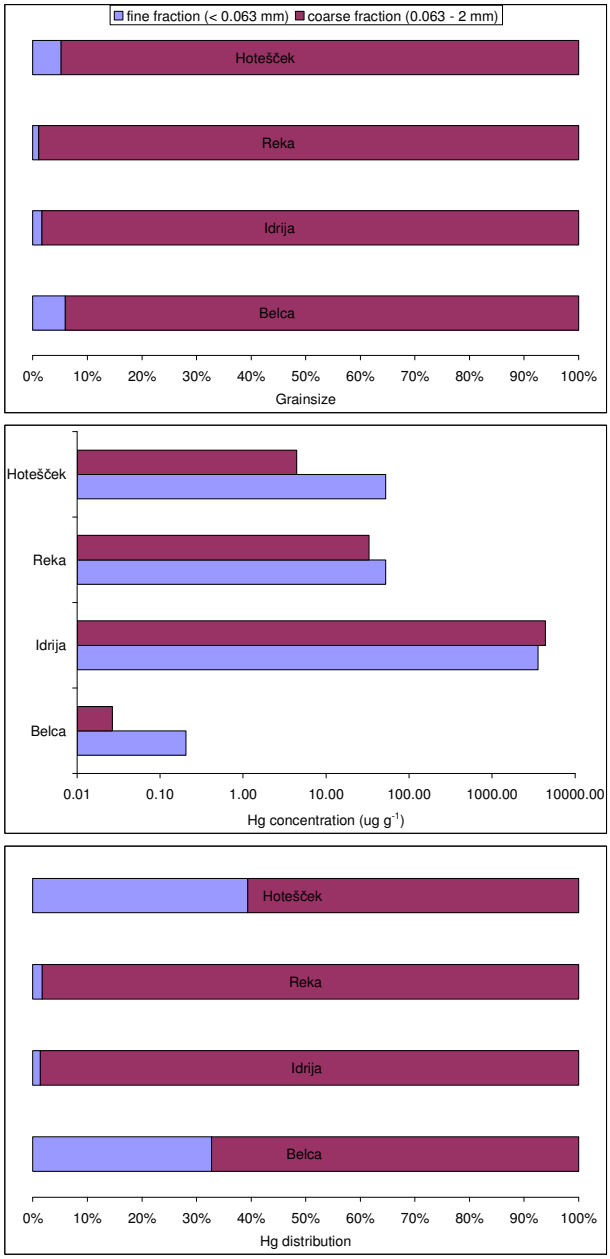

Figure 38: *Percentages of fine and coarse sediment fractions (A), THg concentrations (B) and abundance of Hg in each fraction (C) at four sampling stations of the Idrijca River.*

5.2.2 Mercury in the sediments of the Idrijca River tributaries

Most of the Idrjica's tributaries have a torrential characteristic constantly transporting fine particles downstream. During the sampling, sufficient amount of fine grained sample that would be representative was difficult to obtain. Therefore, only mercury in a composite fraction with diameter below 2 mm was measured at these sites. Results of total mercury measured in the sediments of the Idrijca tributaries are graphically presented in Fig. 39.

The highest THg concentrations (up to 4 µg g^{-1}) were measured in the sediments of the tributaries draining parts of the catchment near the mercury mine. With the increasing distance of the individual tributary inflow from the town of Idrija, Hg concentrations decrease rapidly, resulting in less than 0.02 µg g^{-1} Hg in the Bača River. These results suggest that atmospheric deposition, especially in the centuries of the ore smelting operations, was the main source of Hg in catchment soils and consequently, due to the processes of weathering and erosion, also in the river sediment.

It must be noted, however, that relatively low THg concentrations measured in the sediments of the Idrijca River tributaries are most probably due to the coarser grains prevailing in the samples analyzed. As the atmospheric deposition is the main source of mercury in the catchments that are drained by the Idrijca

River tributaries, mercury in the surrounding soils (the source of the river sediment) is mostly bound to clay and silt size particles. Therefore, it would be realistic to expect much higher concentrations of mercury in river sediments associated with fine grained particles. Consistent with this assumption, Frančišković-Bilinski et al. (2005) reported much higher concentrations in the sediments of the Bača River in size fraction <63 µm compared to results presented here (2.6 compared to 0.02 µg g^{-1}).

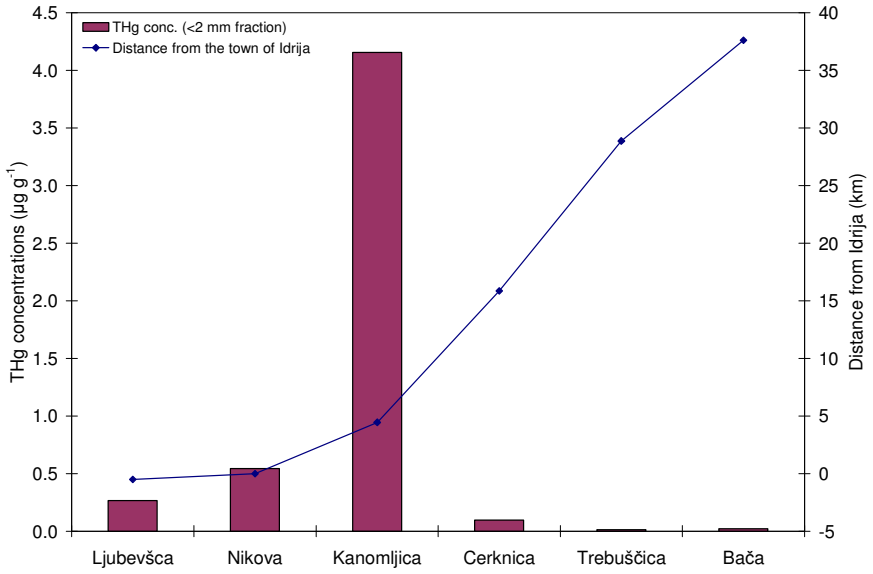

Figure 39: *Mercury in the sediments of the Idrijca River tributaries.*

5.3 Soil

Mercury in soil appears as different chemical species with different solubility, sorption qualities and toxicity, depending on the biogeochemical characteristics of the soil. The key parameters governing the Hg speciation in soils are their redox potential, pH, and content of various ligands. The mobility of mercury in soil is then controlled by adsorbtion and desorbtion processes depending on complexation by ligands in aqueous solution and soil mineral phase. Hg has a strong tendency to build complexes with Cl^-, OH^-, S^{2-} and S-containing functional groups of organic ligands. Under naturally occurring conditions of Eh and pH the solubility of Hg in soil is mainly determined by $Hg(OH)_2$, Hg^0 and HgS (Schuster, 1991). At redox potentials >0.4 V, in acid soils, $HgCl_2$ is the dominating Hg species, whereas $Hg(OH)_2$ dominates at pH >7. In reducing soil conditions, i.e. at low redox potentials, almost insoluble HgS is precipitated. Hg vapour is stable only at very low redox potentials in the presence of sulphides (S^{2-}) (Bringmark, 1997). See Figure 40 below.

The main Hg transformation processes in soil include reduction/oxidation and methylation/demethylation. The net mercury methylation rate (the net result of methylation and demethylation) for most soils appears to be quite low; with much of the measured methyl mercury in soils potentially resulting from wet deposition. There are four dissipation processes that remove mercury from the surface soils: volatilization (diffusion of gas phase out of the soil surface), runoff of dissolved phase from the soil surface, leaching of the dissolved phase through the soil horizon and erosion of particulate phase from the soil surface.

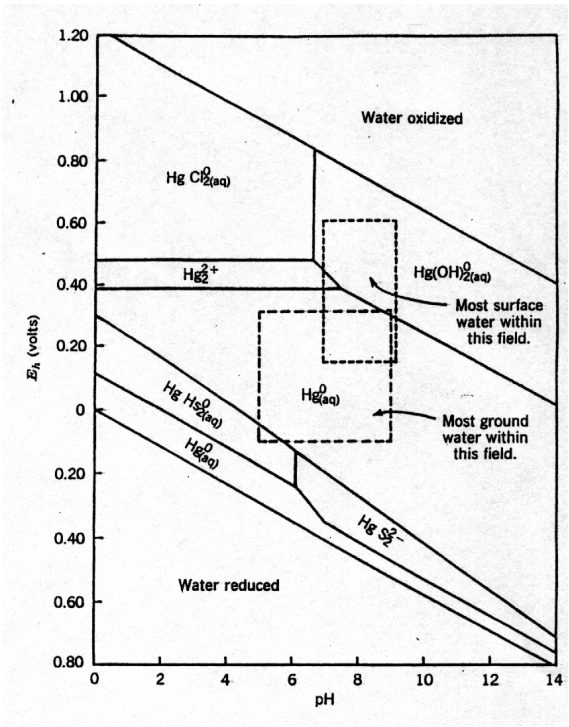

Figure 40: *Stability fields of mercury species in water (soil water) at various redox potentials (Eh) and pH values, when chloride and sulphur concentrations of 1 mM each were used in the calculations (Source: Schnoor, 1996).*

In the present study, spatial and vertical distribution of mercury in soils from the upstream to the downstream part of the Idrijca catchment and from the river side toward the hill slope was investigated. Three soil profiles (0-30 cm) distributed from the river side towards hill side (A-C) were studied at each of the four sampling sites according to their characteristics and location in the catchment. Each of the soil profiles was sectioned according to specific soil pedologic horizons. Thus, the collected soil samples had different thicknesses corresponding to each soil profile..

In order to investigate the binding, mobility and potential bioavailability of mercury in these soils, concentrations of three mercury fractions/forms were determined: total mercury (THg), methylmercury (MeHg) and water soluble mercury (Hg_{ws}). To better characterize the soils in terms of organic matter composition which is known to strongly influence the mercury biogeochemistry in soils, stable carbon and nitrogen isotope analysis ($\delta^{13}C$ and $\delta^{15}N$) in these soils were also performed.

5.3.1 Soil composition and characteristics

According to Slovenian soil classification, the soils sampled can be divided into two groups: soils from locations Belca and Travnik were classified as *Eutric Cambisol*, while soils from locations Idrija and Reka were classified as *Rendzic Leptosol*. Both groups were developed on the carbonate bedrock. Soils from the first group are thicker with well developed B-horizon. Soils from the second group are poorly developed with almost no C and B-horizons, organic horizon contacts the bedrock and contain a lot of gravel. Moreover, there is also a difference among the soil profiles within the individual sampling location. In general, soils obtained at the hill slopes have more clayey texture, while soils obtained at the alluvial plains have more loamy texture.

In Fig. 41 the results of stable carbon and nitrogen isotope ($\delta^{13}C$ and $\delta^{15}N$) analysis from all soil profiles and locations are presented. The $\delta^{13}C$ value varied from -29.3 to -22.5 ‰, with an average of -26.6 ‰ ± 1.2 ‰, and the soils are enriched in the heavy isotope in deeper horizon of the soil profile. A similar pattern was observed in $\delta^{15}N$ values versus depth. The arrows in Fig. 41 indicate that decomposition of organic matter enriches soil with the ^{13}C and ^{15}N isotopes, probably due to microbial processing, which can be responsible for these shifts. Isotopically depleted materials may be used by microorganisms, while the leftover and isotopically enriched materials may end up in the SOM (soil organic matter). Soil represents degraded organic matter originating from plant litter (assumed $\delta^{13}C$ value of -31.6 ‰); therefore degradation of organic matter from different locations on slopes surrounding the catchment can be estimated. At locations Idrija, Reka and Travnik degraded plant litter in surface humic soil horizon prevails,

while at locations Belca top humic horizon is composed of plant litter, which are related to lower $\delta^{13}C$ values. Deeper horizons are composed of degraded organic matter with more positive $\delta^{13}C$ values (minimum measured $\delta^{13}C$ value was -22.5‰). Degraded organic material originates from C3 plant material. The results showed that the vertical differentiation of soil organic matter (SOM) $\delta^{13}C$ is controlled by the development of soil profile, and closely correlated with the composition of SOM and its turnover processes. The fractionation of carbon isotope happened during both the transformation of vegetation debris into topsoil organic matter (OM) and its regeneration after the topsoil buried, which resulted in a significant increase of SOM $\delta^{13}C$ with the depth.

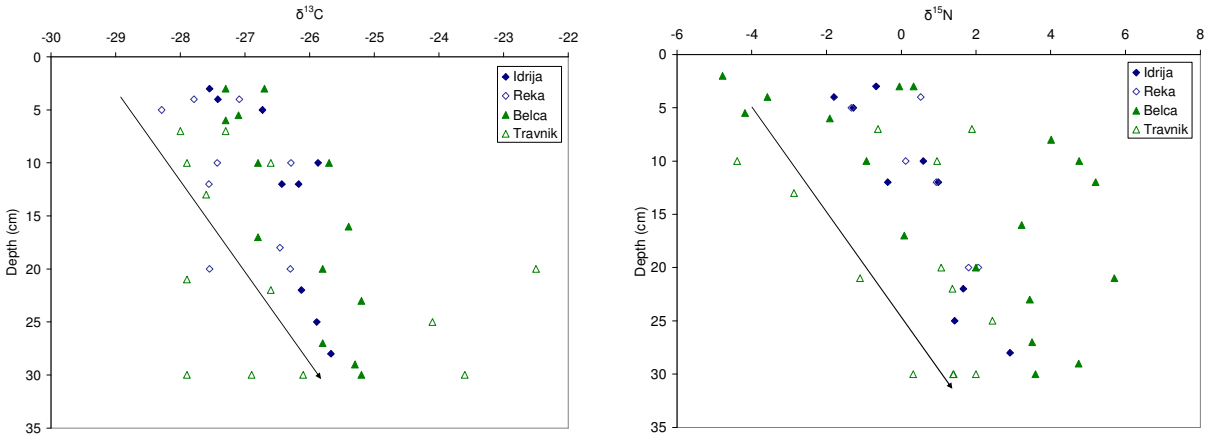

Figure 41: *$\delta^{13}C$ and $\delta^{15}N$ versus depth in soil profiles of the Idrijca catchment.* Arrows indicate degradation of organic matter.

5.3.2 Spatial distribution of mercury in soil profiles

Two soil categories (alluvial soil and hillslope forest soil) were investigated to assess the distribution of mercury in the soil profiles from the upstream to the downstream part of the Idrijca catchment and from the river side toward the hill slope. Mercury species and fractions were studied in the different pedologic horizons. The results of the measurements of different mercury species and fractions in soil profiles are graphically presented in Fig. 42-43 and summarized in Appendix A. In the 12 profiles, total mercury (THg) concentrations ranged from 0.30 to 1100 mg kg^{-1}, methylmercury (MeHg) concentrations ranged from 0.27 to 10 µg kg^{-1} and water soluble mercury (Hg_{ws}) concentrations from 0.94 to 3492 µg kg^{-1}. The results reveled significant differences in Hg distribution among both, the sampling locations and within individual sampling location (alluvial (A) and hill slope soils (B,C), respectively). In the following sections, results are discussed individually for each of the sampling locations.

5.3.2.1 Total mercury (THg)

In the mercury polluted areas such as Idrija, Hg in soils can be a result of atmospheric deposition, direct input by mine residuals and calcines or deposition of contaminated suspended particulate matter during high water discharges or flooding. Significantly differences in both the amount and distribution of Hg in soils suggest different origin of mercury from site to site.

The lowest THg concentrations were measured in the soil profiles of location Belca. Due to its position, prevailing wind directions and relative distance from the most polluted sites in Idrija (cca. 8 km upstream of the mine), it can be assumed that only the atmospheric deposition took place at this location. Therefore, THg concentrations at this site can be considered as a local background. In both hill slope profiles (B and C) THg concentrations gradually decreased with depth, which is consistent with a known Hg affinity to organic matter, which also decrease with the depth. In the alluvial soil profile (A), THg concentrations decreased more rapidly (below 2 cm) with the depth. At this site, alluvial plain is steel active, resulting in poorly developed soil horizons. With the exception of a thin (2 cm) upper humic layer, the profile is dominated by loamy texture and less organic matter. The later can also be the reason for the lowest Hg concentrations at location Belca in this profile at depths above 2 cm. On the hill slope, profile B is enriched with Hg throughout the soil profile when compared to profile C. Most probably, this is a result of the hill slope denudation processes which lead to enrichment of Hg in the talus soil.

RIVER SIDE HILL SIDE

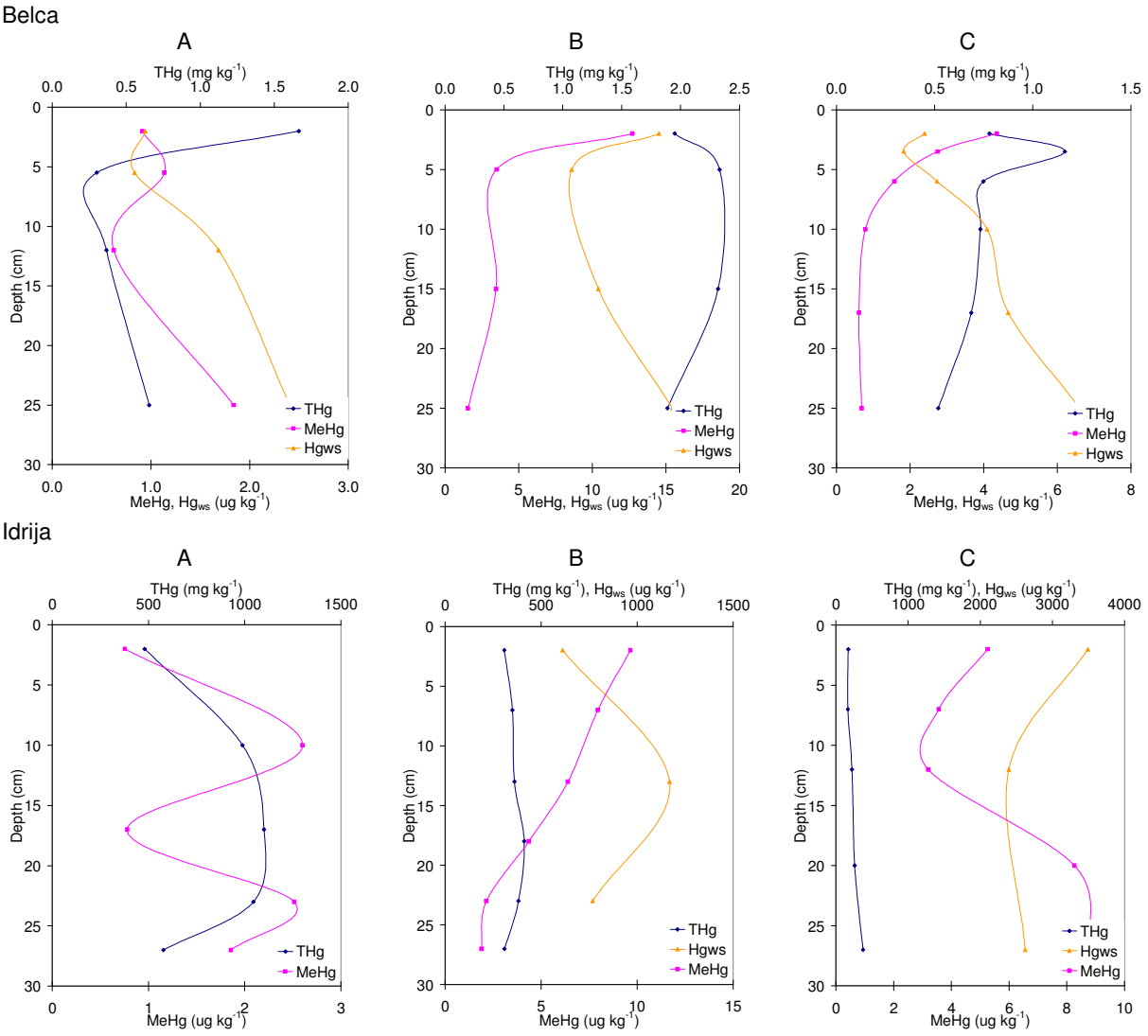

Figure 42: *Vertical and horizontal distribution of total, methylmercury and water soluble mercury in soil profiles, locations Belca and Idrija. A-alluvial soil, B and C – hill slope soil*

As expected, the highest THg concentrations were measured in the Idrija soil profiles. In contrast to location Belca, there was no evident trend in THg vertical distribution observed. While the heterogeneity in vertical distribution of THg in alluvial soil can be linked to random deposition of contaminated suspended particulate matter during high flow or flooding of the Idrijca River, rather uniform distribution of THg in both hill slope profiles can be explained by the vicinity of the pollution source. Site in the town of Idrija where the soil profiles were taken is only 100-meters air distance from the Hg ore facilities and was under direct influence of smelting residuals for centuries. Most probably the capacity of the organic matter in the topsoil layer to retain Hg deposited was excided and Hg was leached during precipitation in the deeper soil layers. Nowadays, after the end of smelting operations, Hg is more significantly removed from the upper soil layers due to erosion, surface runoff and volatile Hg emission, resulting in the Hg distribution observed. This assumption is further supported by horizontal distribution of Hg within this location, as B profile was found to be enriched in Hg compared to profile C.

RIVER SIDE HILL SIDE

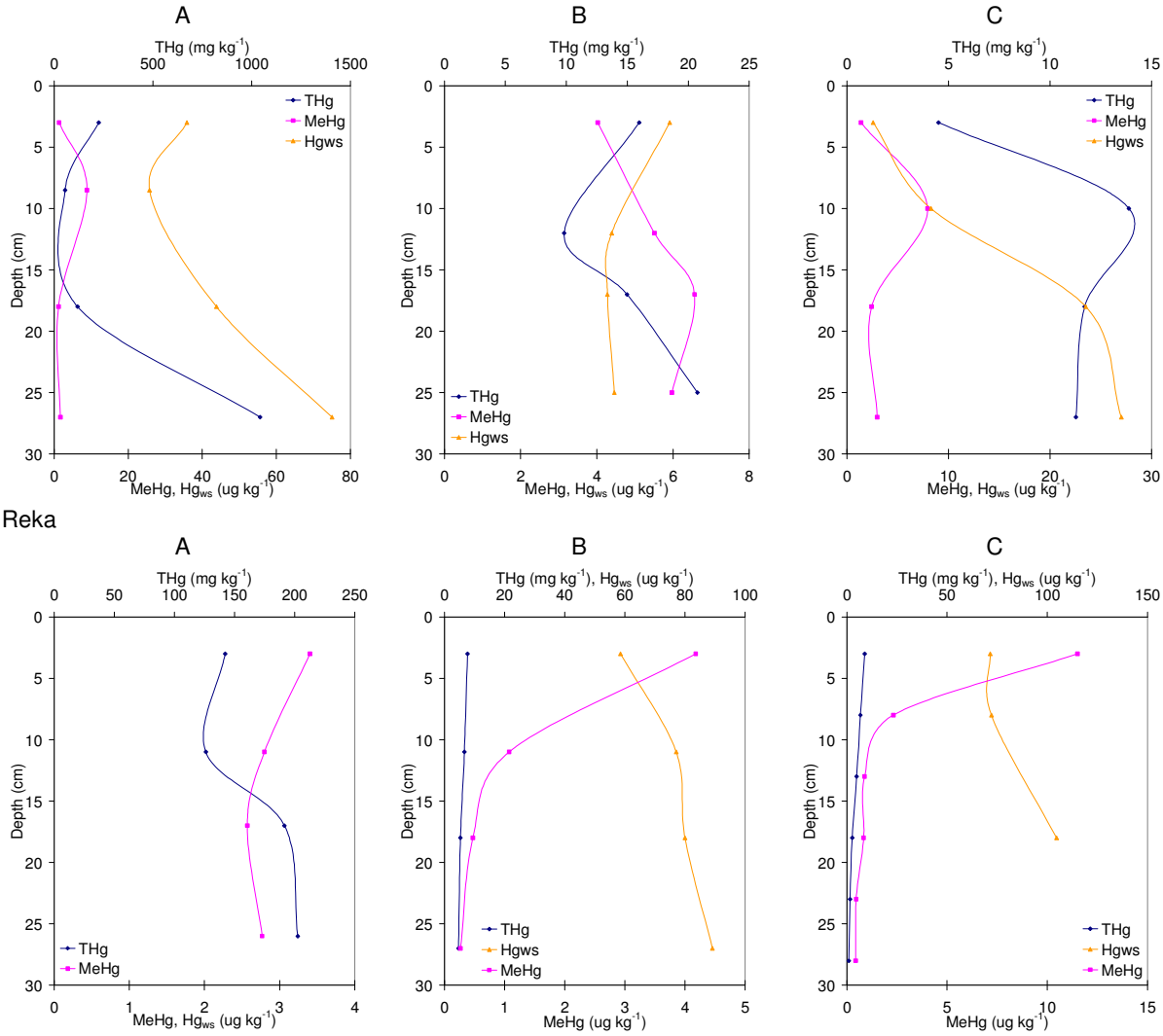

Figure 43: *Vertical and horizontal distribution of total, methylmercury and water soluble mercury in soil profiles, locations Travnik and Reka. A-alluvial soil, B and C – hill slope soil*

THg concentrations in the soil profiles from the two locations downstream from the mine (Travnik and Reka, respectively) are of the same order of magnitude. However, its vertical distribution, especially in the hill slope profiles, differs significantly. At location Travnik, heterogeneity in the vertical distribution of THg was observed, while at location Reka THg was distributed more uniformly, showing a decrease with the depth. One of the reasons for this difference might be a different soil texture. At location Travnik hill slope soils are well developed with a relatively thick (up to 15 cm) humic layer followed by clayey layer. On the other hand, hill slope soils from location Reka are poorly developed with a thin humic layer followed by loamy layer. In soils with a loamy texture, mercury can more easily migrate to the deeper layers. Similar was observed by other authors (Biester et al., 2002). Heterogeneity in vertical distribution of THg in the hill slope profiles from location Travnik compared to location Reka can also be explained by the so-called "nugget effect", a term which describes particles of small size with a high amount of Hg (most probably cinnabar particles). It is known from the previous studies (Kocman et al., 2006) that it is very difficult to assure sufficient homogeneity for mercury determination in soils reach in cinnabar. Cinnabar particles present in soils from location Travnik could be the reason for the observed heterogeneity. Fractionation studies were not performed on samples analyzed within this study. However, it is known that the cinnabar bound mercury in relatively enriched (compared to non-cinnabar) in soils closer to the pollution sources in the town of Idrija (location Travnik in this case), while at locations more distant from the pollution sources (location Reka in this case), soils are enriched in non-cinnabar mercury forms (Gosar et al., 2006).

In general, taking all sampling locations into account, the distribution of THg along the vertical profiles

on the hill slopes suggests a predominant influence of atmospheric deposition on the accumulation of Hg. A clear and significant decrease of THg concentrations with the distance from the mercury mine was observed. With the exception of Idrija site, higher THg concentrations were generally observed in the organic rich 5-15 cm topsoil layer which is consistent with the observations of other authors (e.g. Biestler et al., 2002; Remy et al., 2003; Hissler and Probst, 2006). At all four locations, B profiles were enriched in Hg compared to C profiles, particularly in the topsoil layer. This can be linked to denudation processes (weathering and erosion), which removed the upper soil layer and lead to enrichment of both, Hg and organic matter, in the downwards slopes. This typical behavior indicates, on one hand, that retention of Hg is strongly related to coupling to organic matter. On the other hand, this implies that Hg is effectively transported to deeper soil layers as soluble and insoluble complexes. At all three sites downstream from the mine, THg in soil profiles remained above the local background of the surface soils (0.5-2 mg kg^{-1}) even at depths above 25 cm. The most gradual decrease of Hg concentrations was observed at Reka site. At this site, soils have more loamy texture compared to others, and Hg can more easily migrate to deeper soil layers. These results indicate the importance of not only the organic matter in the vertical distribution of Hg in soils, but also the soil texture. In alluvial soils, again, a clear decrease of THg concentrations was observed with the distance from the mining area. However, THg distribution in alluvial soil profiles revealed more random distribution along the soil profiles. This heterogeneity is a consequence of random deposition of contaminated suspended particulate matter during high flow or flooding of the Idrijca River. As observed by Žibret et al. (2006), distribution and content of mercury in the alluvial soil does not depend solely on the distance from the source but also on the position of soil within the alluvial plain (floodplain or terraces) which determines it activeness. In the present study, alluvial soil was obtained from the active (frequent floods) floodplain at locations Belca and Idrija, while at locations Travnik and Reka alluvial soils were obtained from the 1st terrace. At later two locations, an increase of THg concentrations with depth was observed, which can be explained with less efficient mining and roasting technologies used in the past during the formation of these sediments. Nevertheless, it is questionable if the sequence shows sedimentation in chronological order due to erosion and re-deposition of sediments typical of alluvial plains. However, other cores taken from the same sites show a similar course of Hg enrichment (Gosar et al., 1997; Horvat et al., 2002; Kocman et al., 2004; Žibret et al., 2006).

5.3.2.2 Methylmercury (MeHg)

In contrast to total Hg concentrations, MeHg concentrations measured in soils from all four locations were of the same order of magnitude. However, its distribution among and within individual location differ significantly. Differences in MeHg distribution were observed when locations with low THg content were compared to locations with higher THg content and when both soil types were compared (alluvial and hill slope soil, respectively). Therefore, in terms of MeHg distribution, 12 soil profiles analyzed can be divided in two categories, based on the THg content and the type of soil.

At both locations with the lowest THg content, Belca and Reka, respectively, the distribution of MeHg along the hill slope soil profiles showed higher concentrations in the surficial horizon, which decreased with depth. On the other hand, in the hill slope profiles from locations Idrija and Travnik, MeHg was found to be distributed much more heterogeneously. One of the reasons for this heterogeneity can be different mercury binding in soils from these locations. As disused in the previous section, soils from these two sites are enriched with cinnabar compared to soils from locations Belca and Reka, respectively. Methylation of Hg can be inhibited when bioavailability of Hg^{2+} is low. The presence of rather insoluble and non-reactive cinnabar, especially its uneven distribution along the soil profiles, would alter the mobility and potential bioavailability of mercury, resulting in MeHg distribution observed. These assumptions were further supported by an estimate of MeHg relative abundance, calculated as MeHg/THg ratio. The MeHg/THg ratios were low in more contaminated soil samples, while the relative abundance of MeHg was high in soils collected from less contaminated areas. However, even when the MeHg/THg ratio was low in areas highly contaminated with Hg, MeHg concentrations were elevated (up to 10 µg kg^{-1}). Thus, not only total Hg concentrations, but also reactivity of Hg should be taken into account to assess its potential bioavailability.

In the alluvial soils, MeHg was found to be distributed very heterogeneously along the profiles of both more frequently active floodplains (Belca and Idrija, respectively). On the other hand, in the alluvial soil profiles obtained from the terraces at locations Travnik and Reka, MeHg was distributed much more uniform. These differences can be explained by much more stable conditions in the soils from the terraces compared to those from the floodplains. Namely, terraces are sites where floods occur very rarely or have occurred in the past. On the floodplain the soil profile is not well developed because of recent deposition, while on terraces there was enough time for both chemical and biological transformations to occur.

The most important issue related to the MeHg contamination is the question of the MeHg origin. Was MeHg released directly from the mercury mine area or produced by in situ methylation? Measured

methylmercury concentrations in soils are the result of the methylation rate (the net result of both the methylation and demethylation processes). In order to determine environmental conditions and parameters influencing the presence of MeHg, relationships between soil characteristics and Hg species concentrations/ratios were investigated. In it known that Hg species have a great affinity for soil organic matter, especially for humic substances (e.g. Schuster, 1991; Yin et al., 1997). Therefore, relationship between MeHg and soil organic carbon isotopic composition ($\delta^{13}C$) was investigated.

Based on the $\delta^{13}C$ values the origin and the nature of organic matter can be assessed. MeHg concentrations showed a fairly close relationship to organic content in the soil samples; generally MeHg was found to be negatively correlated with the $\delta^{13}C$ values, suggesting MeHg production is enhanced in humic substances reach environment (more negative $\delta^{13}C$ values) compared to soil mineral phase (more positive $\delta^{13}C$ values) (Fig. 44, A). More negative $\delta^{13}C$ values are characteristic for environments of a high humification state of organic matter and significant bacterial activity. Thus, the nature (e.g. evolution, bacterial activity) of organic matter rather than its quantity may have a significant influence on complexation and formation of MeHg. Similar was observed at other mercury polluted sites (e.g. Remy et al., 2006).

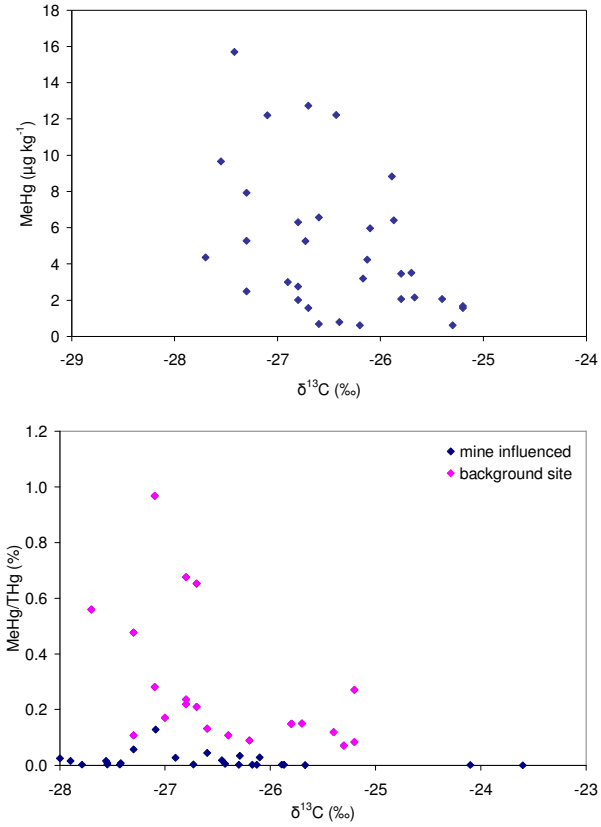

Figure 44: *Relationship between the nature of organic matter and (above) methylmercury concentrations, (below) MeHg/THg ratio in soils.*

On the other hand, soil organic matter seems to influence MeHg/THg ratios only at background sites (Fig. 44, B). An inverse relationship appears to exist between the THg concentration and the proportion of MeHg found. That is, when low concentrations of THg are found, the proportion of MeHg is high and visa-versa. The MeHg/THg ratios were low in most Hg polluted and alluvial soil samples, however, MeHg was relatively high. In contrast, in soils collected from areas uncontaminated by Hg, the relative abundance of MeHg was high (up to 1 %). Even when the MeHg/THg ratio was low in areas highly contaminated with Hg, MeHg concentrations were elevated. Low MeHg/THg ratios can be due to low Hg methylation and/or MeHg demethylation processes (Remy et al., 2006). As demonstrated by Ullrich et al. (2001), high or low concentrations of anorganic Hg may depress MeHg production or may favor demethylation. Demethylation process can be enchanced in Hg reach environment (Gilmour and Henry, 1991), especially with respect to the induction of the *mer* operon genes present in many Hg-resistent bacteria. In the Idrija region, MeHg production seems to be more efficient in low THg contaminated soils in which demethylation processes are minimized.

5.3.2.3 Water soluble Hg (Hg_{ws})

The fraction called water-soluble mercury (Hg_{ws}) includes mercury species present in pore water. Water soluble fraction is recognized as very important from an environmental risk point of view due to its easy availability in environmental weathering conditions (Bloom et al., 2003). Even small percentages should be treated with caution because they represent in fact very significant Hg concentrations. Mercury species extracted by water may be easily transported by natural processes and serve as the substrate for mercury methylation processes (Stein et al. 1996; Ullrich et al. 2001; Boszke et al. 2003). Therefore, in present study, water soluble Hg fraction was used as a parameter that can reveal potential bioavailability. Moreover, water soluble Hg fraction is likely the most labile and able to migrate in interstitial soil solutions (Kot and Matyushkina, 2002), and even moves downward into deeper soil layer or groundwater.

The contribution of water-soluble species in the total concentration of mercury in the soil samples examined was relatively low. However, their absolute concentration was much higher in contaminated than in the samples less contaminated with mercury. On average, mercury concentrations in soil leachates ranged from 6-40 µg kg^{-1} in less contaminated hill slope soils from location Belca and Reka and from 50-1230 µg kg^{-1} in soils from locations Idrija and Travnik. Independent of the THg and MeHg distribution, with the exception of most contaminated Idrija soils, Hg_{ws} concentrations seem to increase along the soil profile. In soil profiles from both less contaminated locations (Belca and Reka, respectively), an inverse relationship appears to exist between the THg concentration and the proportion of Hg_{ws} found. That is, when low concentrations of THg are found, the proportion of Hg_{ws} is high and visa-versa. In contrast - most probably due to the presence of insoluble cinnabar in these samples - there was no correlation between THg and Hg_{ws} observed in the soils from more contaminated locations Idrija and Travnik, respectively. Once again, as with the distribution of THg and MeHg, these results indicate the strong influence of Hg binding in soils on its mobility and potential bioavailability.

As methylmercury is a water soluble Hg species and due to the fact that measured MeHg and Hg_{ws} concentrations are of the same order of magnitude, one would expect rather good correlation between MeHg and Hg_{ws}, at least at locations less contaminated by Hg. However, no such correlation was observed. Several explanations for this are possible. Either MeHg measured in soils is bound so tightly to the organic matter in the soil that it is not available for leaching, or conditions in the leachates are not favorable for methylation to occur. The first assumption is more likely as it is consistent with the known fact that measured methylmercury in soil is the net result of both the methylation and demethylation processes and has affinity towards binding with the organic matter.

In contrast to MeHg, water soluble Hg fraction was found to be positively correlated with the $\delta^{13}C$ values (Fig. 45). As suggested by Biester et al. (2002), in soils, Hg bound in soluble organic complexes in the topsoil layer (more negative $\delta^{13}C$ values) is carried to deeper soil layers, where these positively charged metal cations of organic complexes are adsorbed to the negatively charged surfaces of clay minerals (more positive $\delta^{13}C$ values). Most probably, during the leaching experiment, this is the Hg fraction obtained. Moreover, the results indicate the importance of the soil composition on the Hg_{ws} content. Although total Hg concentrations in soils from location Reka are in the same range as those of location Travnik, and the organic matter is showing the same pattern, water soluble Hg in Travnik soils is significantly lower than in soils of Reka due to the higher clay content in Travnik soils, which favours the formation of less soluble organo-mineral complexes. Therefore, retention of Hg in soils is not determined solely by the amount of organic matter but also its texture.

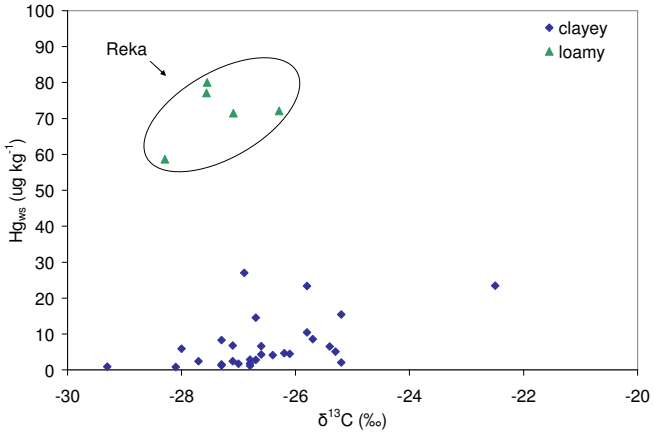

Figure 45: *Relationship between the nature of OM and concentrations of water soluble Hg (Hg_{ws}) in soils.*

5.3.2.3.1 Fractionation of water soluble mercury (Hg_{ws}) in aqueous soil phase

Water soluble mercury species in soil leachates can be distinguished to easily reducible reactive Hg and non-reactive Hg species. In terms of potential bioavailability, reactivity of mercury in aqueous soil phase is of paramount importance. During the mercury fractionation studies in Idrija soils very strong positive correlations ($R^2 > 0.9$) were observed between the water soluble mercury fraction and other fractions including weak-acids soluble, organo-chelated and elemental mercury fraction (see Table 3 in Kocman et al., 2004 in Appendix C). These correlations suggest that in the water phase, mercury may not be present in the form of water-soluble ionic species but rather as the species bound to organic matter, which agrees with the results of other authors (e.g. Biester et al. 2002; Renneberg and Dudas 2001; Wallschläger et al. 1996). Furthermore, these correlations also suggest that part of elemental mercury may be oxidized to divalent mercury - species soluble in water, and next converted by biotic transformations to organomercury species.

To better understand these processes, an additional experiment was performed on the seven soil samples that were obtained from the same locations as the soil profiles discussed in section 5.3.2. 100 g of each of the seven soil samples investigated was placed in a 1 L glass bottles. Samples were diluted with 900 mL of Milli-Q water and left to stay overnight. Supernatant water was then filtered through 45 µm filters and different mercury species (DHg, RHg and DGM) were measured according to the procedures described in chapter 4. The results are given in Table 4. Total mercury concentrations and organic matter content (OM) in soils as well as dissolved organic carbon (DOC) in aqueous solution are given as additional variables.

In terms of total Hg, samples analyzed varied over a wide range of concentrations (between 4 and 417 $\mu g\ g^{-1}$ THg). In all the samples, measured total dissolved mercury concentrations (DHg) in soil solution were very high, ranging from 92 up to almost 5000 $ng\ L^{-1}$ in the Idrija forest soil. In general, with the exception of alluvial soil from location Travnik, there is a positive correlation between the DHg in soil solution and THg soil concentrations. Relatively low DHg concentrations in the most mercury abounded alluvial soil sample from location Travnik can be explained by the dominance of unsoluble cinnabar particles in this sample. In contrast to DHg, concentrations of easily reducible reactive mercury (RHg) were of the same order of magnitude for all the samples. Consequently, at most polluted sites (location Idrija and alluvial plain at Travnik) reactive Hg present less than 6 % of total water soluble Hg, while at other sites reactive Hg can reach up to 55 %. Therefore, although at polluted sites total water soluble Hg fractions can be very high, concentrations of easily reducible and therefore potentially bioavailable Hg are relatively low. Moreover, although for an order of the magnitude lower, dissolved gaseous mercury (DGM) in soil solution revealed the same pattern as reactive Hg.

These results suggest that majority of mercury in soil water phase is present as species bound to organic matter or suspended mineral particles rather than water-soluble ionic species or in dissolved gaseous form. However, it must be noted that as in the case of river water samples, mercury fractions measured in the soil water phase are operationally-defined. Therefore, it is not possible to estimate what is the contribution of mercury bound either to organic or inorganic ligands that passed the 0.45 µm pore size filter used in the experiment and could alter the mercury ratios in the soil water phase discussed here.

Table 4: *Fractionation of water soluble mercury in aqueous soil phase.*

Sample	Description	THg soil ($\mu g\ g^{-1}$)	DHg ($ng\ L^{-1}$)	RHg ($ng\ L^{-1}$)	DGM ($ng\ L^{-1}$)	OM (%)	DOC ($mg\ L^{-1}$)
Idrija A	forest	251 ± 4.2	4927	146	5.5	16	12
Idrija B	meadow	100 ± 2.2	985	43	4.3	10	6
Travnik A	forest	19 ± 0.4	137	31	9.9	22	22
Travnik B	meadow	23 ± 0.7	260	67	4.1	18	17
Travnik C	alluvial plain	417 ± 78	492	27	4.2	8	-
Reka A	forest	9 ± 0.6	206	44	2.8	19	15
Reka B	meadow	4 ± 0.1	92	50	4.7	16	25

Ratio between Hg^{2+} and Hg^0 in aqueous soil phase is also important as it would influence the evaporation rates of mercury from soils. It is known from the literature (Schluter, 2000 and authors within) that evaporation rate would decrease with increasing soil organic matter and clay content. Especially organic matter is known to have high sorption capacity and/or affinity for inorganic Hg^{2+}. However, not solely the soil organic matter content but quantity of dissolved organic matter (DOM) in soil solution, specifically DOM-mercury complexes, affect the mercury evaporation rate. The content of mercury in soil solution can be highly correlated with the content of DOC. In the presence of DOC reduction of Hg^{2+} can be substantially enhanced (Ravichandran, 2004). Consistent with this, two trends were observed. Although

not statistically significant, with the exception of sample Travnik A, the data suggest an increase between the RHg and DGM ratio with the increase of the soil organic matter content (Fig. 46, above). In contrast, with the exception of sample Idrija B, ratio between RHg and DGM tends to decrease with the increasing DOC concentrations (Fig. 46, below).

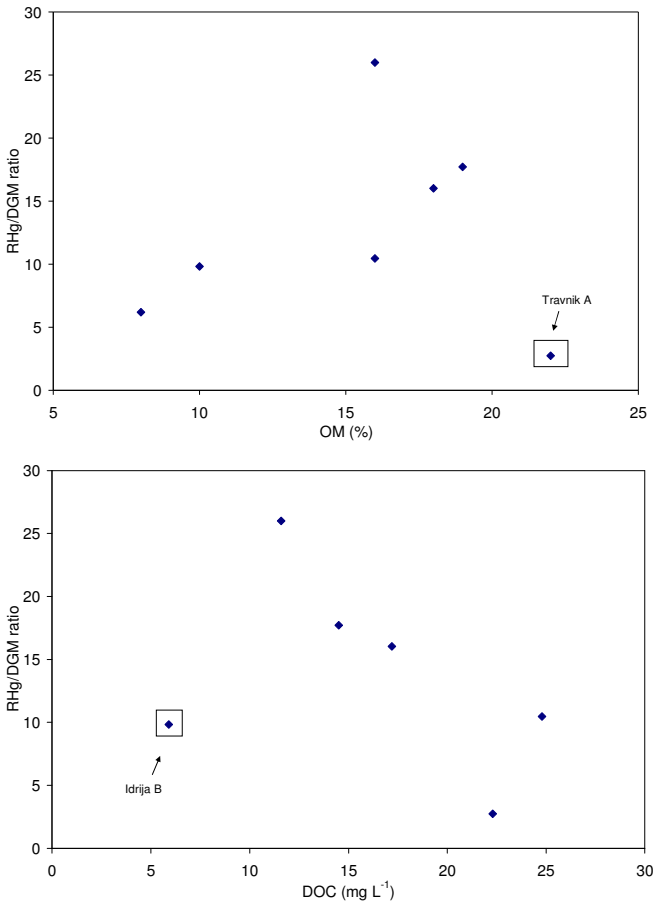

Figure 46: *Relationship between the RHg/DGM ratio and organic matter content (above), DOC in soil solution (below).*

5.4 Atmosphere

In the atmosphere, mercury exists primarily in inorganic form with two oxidation states: Hg^0 and Hg^{2+}. Hg^0 constitutes the majority of mercury in the atmosphere (>90%, Schroeder et al., 1991) and is the predominant form in the gaseous phase. Hg^{2+}, on the other hand, can be found in both the gaseous and the particulate phase bound in aerosols. In atmospheric water Hg^{2+} tends to be either dissolved or adsorbed onto particles in droplets (Fig. 47). With the exception of industrialized areas, particulate mercury is a minor constituent of the atmosphere (Lin and Pehkonen, 1999).

Before being deposited back to the ground, atmospheric mercury can undergo various physical and chemical transformations which are controlled by the properties of different mercury species in the atmosphere. Gaseous elemental mercury (Hg^0) is relatively inert to chemical reactions with other atmospheric constituents. Its residence time is believed to be in the order of 1 year (Schroeder and Munthe, 1998). Therefore, once released to the atmosphere, it can be dispersed and transported over long distances before being deposited to terrestrial and aquatic ecosystems. Hg^{2+} is an oxidation product of Hg^0. Compared to Hg^0, Hg^{2+} has a much shorter lifetime in the atmosphere (from several days to a few weeks, Slemr et al., 1981; Lindqvist and Rodhe, 1985). Hg^{2+} is a highly surface reactive species and deposits much faster than Hg^0 through both dry and wet processes (Lindberg and Stratton, 1998). The presence of water seems to accelerate Hg^0 oxidation. Schroeder et al. (1991) proposed several possible reactions between mercury and a variety of atmospheric oxidants and reductants by using their thermodynamic data. They suggested that O_3 and Cl_2 may be important oxidants of Hg^0, while SO_2 and CO may be important reductants of Hg^{2+}.

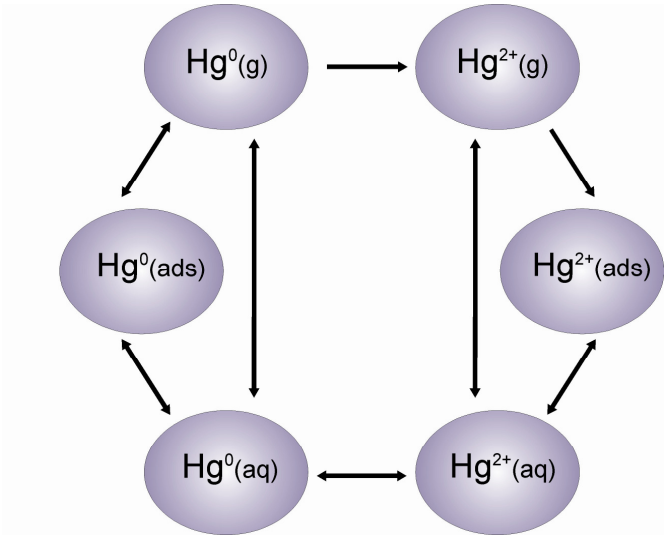

Figure 47: *Mercury cycle in the atmosphere.*

In the present study, the following actions were undertaken in order to study mercury distribution and its cycling in the atmosphere of the Idrija region. Mapping of air Hg^0 concentrations was performed using a portable Lumex 915^+ absorption spectrometer to assess spatial distribution and major sources of mercury to the atmosphere in the area between the towns of Idrija and Spodnja Idrija. The influence of seasonal variations and changed weather conditions on Hg^0 distribution in air was also investigated. Moreover, analyses of mercury speciation in the air over Idrija were performed during a 4-days sampling campaign to better understand the fate and transformation of mercury in the atmosphere of this specific mercury polluted site. As the speciation and chemical transformations of mercury in the atmosphere strongly influence its deposition mechanism, speciation results were then compared to results of mercury speciation in the wet and throughfall deposition (rain and snow), presented in section 5.5. Furthermore, laboratory measurements of emission of Hg^0 from the soil surfaces were performed to determine the magnitude and factors influencing mercury exchange between the surface and the atmosphere (section 5.6).

5.4.1 Mapping of air Hg concentrations

Mapping of air Hg^0 concentrations was performed during three measurement campaigns in 2006 and 2007, using a portable Lumex 915^+ absorption spectrometer installed in a car together with GPS measurements. Hg concentrations within individual campaign were measured at more than 100 locations in Idrija and its surroundings. Both values (Hg concentration and geographical coordinates) were recorded by a portable computer through appropriate software. The concentration values recorded at individual points were further smoothed into geochemical map using the advantages of geographical information system (GIS). The geochemical map of distribution in the atmosphere above Idrija was then drawn (Fig. 48).

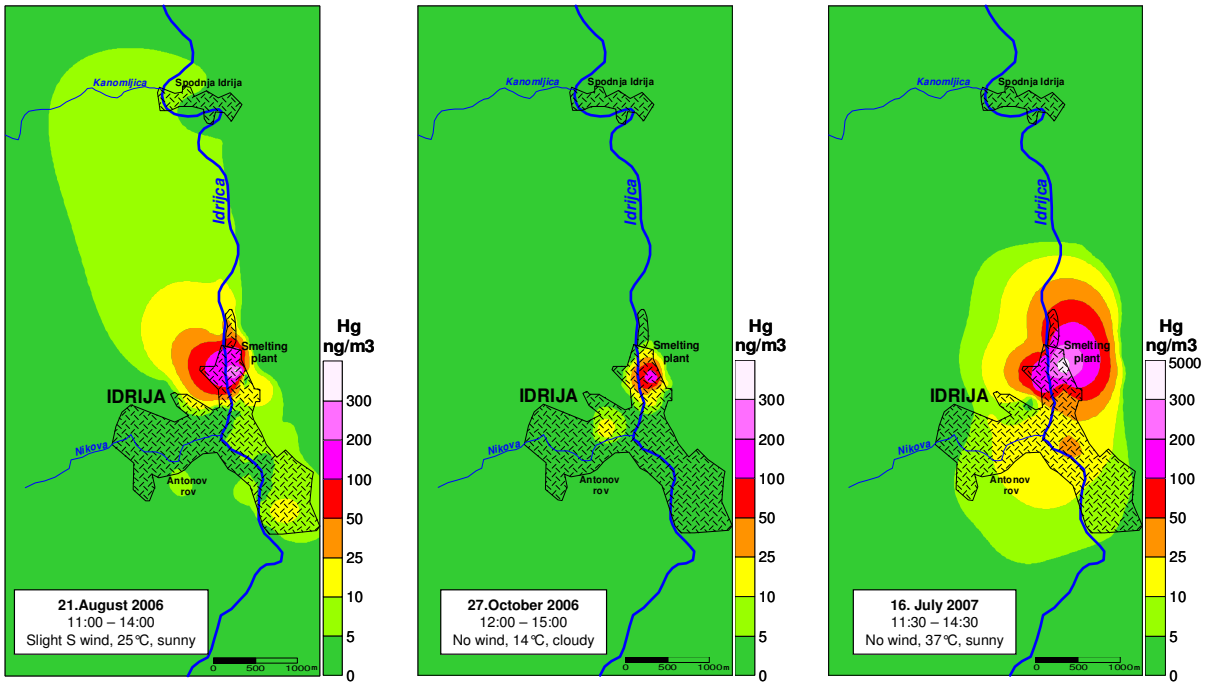

Figure 48: *Air Hg^0 concentration maps in Idrija and its surroundings.*

The Hg concentrations measured in the air in Idrija and surroundings were relatively low (mostly below 10 ng m^{-3}). However, Hg concentrations near the former smelting complex completely dominate the map. It seems that the area around the former smelting plant remains the main source of Hg in air over the Idrija Valley.

Mercury in air is mostly a result of Hg volatilization from the soil surfaces containing mercury. This process is known to be influenced by different factors such as the amount of Hg in the substrate, solar radiation, soil moisture content, wind direction and velocity (e.g. Schlüter, 2000). The results suggest that in the Idrija area, spatial and vertical distribution of atmospheric Hg in the valley depends mostly on wind condition, while temperature influences the Hg volatilization from soils. Consistent with this, the lowest concentrations were measured on October 27th 2006, on cloudy and relatively cold day. During both summer campaigns, significantly higher concentrations were measured. On August 21st 2006 slight south wind resulted in somewhat elevated air concentrations between the old smelter and Spodnja Idrija, indicating the importance of wind direction in atmospheric Hg distribution. During extremely hot summer day on July 16th 2007 that followed after a summer storm event, near the former smelting plant Hg concentrations increased enormously (above 5000 ng m^{-3}), indicating the importance of both temperature and soil moisture on mercury emissions.

A similar detailed mapping was performed in 1994 (Gosar et al., 1997) and in 2003 (Kotnik et al., 2005). Comparison of the results obtained in 1994 and 2003 shows a similar spatial distribution that strongly depends on the geography of the valley. In November 2003, in the town of Idrija mercury emission measurements were also performed by Grönlund et al. (2005), using the differential lidar technique. Grönlund et al. (2005) observed the same spatial pattern of Hg^0 distribution; strongly elevated concentrations of the order of a few hundred ng m^{-3} associated with the smelter which then rapidly fall off away from the smelter. During that study, an attempt was also made to quantify the total mercury flux from the most contaminated area. In their study, Grönlund et al. (2005) calculated an average flux from the area of the former smelter to approximately 2-4 g h^{-1}.

At locations with major sources of Hg vapors (smelter, mine ventilation shaft), measured Hg concentrations presented here are of the same order of magnitude than those measured in 1994 and 2003. On the other hand, at other locations, concentrations are of an order of magnitude lower than those in 1994 and are comparable to those in 2003. This would suggest a slow decrease of Hg air concentrations with time. However, it is difficult to compare the results of different studies due to the variable conditions during the measurement campaigns. Therefore, Hg concentrations in air in the town of Idrija that have been continuously monitored since the beginning of 1999 by the Idrija Mercury Mine Research Unit were summarized in Fig. 49. After the Hg mine and the smeltery closure, Hg concentrations in air have been continuously monitored at several locations in Idrija and its surroundings. The Hg concentration is measured once per month at two locations in the town and near the two Hg mine ventilation shafts. Since 1999 Hg concentrations exceeded 100 ng m^{-3}, and even in two cases 1000 ng m^{-3}, but only near the Inzaghi shaft. The general trend at all four locations is the same. Concentrations were only slightly higher near the ventilation shafts than in the town, due to closing-down work in the mine. A significant decrease of average concentrations near the shafts was observed in 2002 and 2003. At all four locations higher concentration levels were observed in summer, most probably due to higher soil and air temperatures, and stronger solar radiation, and consequently higher emission rates of Hg from polluted soils.

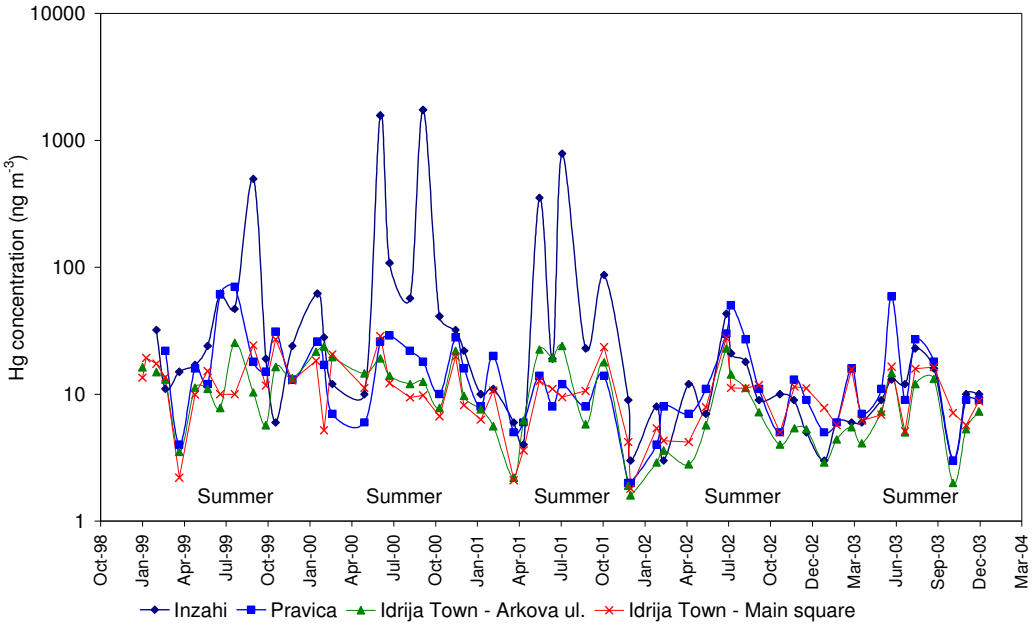

Figure 49: *Hg concentrations in air near Hg mine ventilation shafts and in Idrija Town.*

Nowadays, beside the smelter complex, the main sources of Hg in air in Idrija are two still active mine ventilation shafts, evaporation of Hg from the heavily polluted sites, mineralized rock dumps of primary or partially exploited ore, outcrops of the ore deposit, and ore residues. However, high Hg contents of the air are not only due to anthropogenic sources, but may also partly be natural, as in the hill Pront area, where the outcropping bedrocks contain native Hg.

5.4.2 Mercury speciation in air

Measurements of three different mercury species in air were performed during the 4-days measuring campaign in the town of Idrija in late summer 2006. Measured gaseous elemental mercury (GEM), divalent ("reactive") gaseous mercury (RGM), and particulate mercury (TPM) concentrations were 7.9-12.6 ng m^{-3} (average 9.6 ng m^{-3}), 10-24 pg m^{-3} (average 19 pg m^{-3}), and 15-68 pg m^{-3} (average 47 pg m^{-3}), respectively. TRM and RGM represented <1 % of the total mercury (on average 0.2 and 0.5 %, respectively). Concentrations of all three species in the atmosphere of this mercury polluted site are 2-3 fold higher compared to concentrations measured at background sites (e.g. Wängberg et al., 2007).

The results of speciation analysis are graphically presented in Fig. 50. GEM was sampled with 3-h time resolution during daylight hours and with 12-h time resolution during night hours, while both TPM and RGM were sampled with 12-h time resolution in order to investigate diurnal trends. The results in Fig. 49

are given as two 12 h average samples per 24 h period for all three species, starting 8:30 and 20:30 CET (Central European Time).

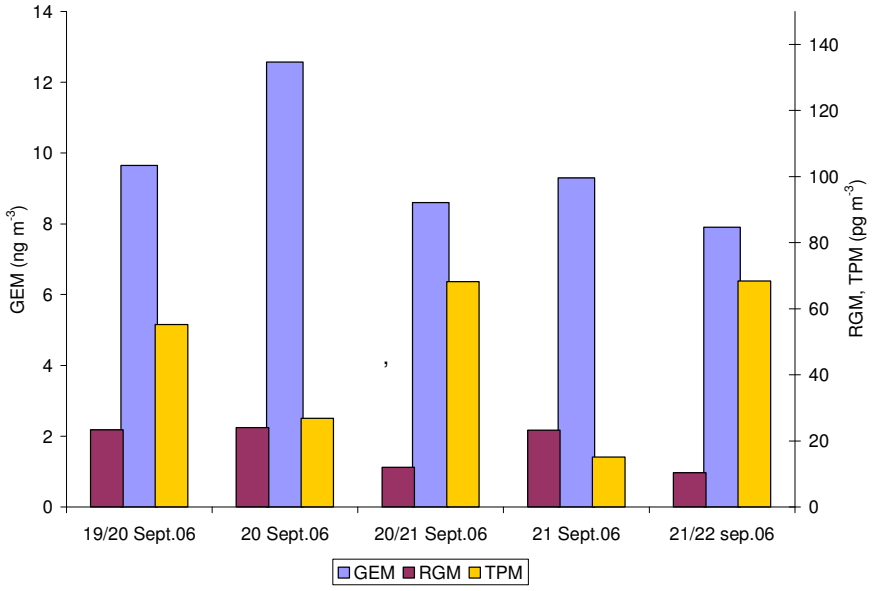

Figure 50: *Hg speciation in the Idrija air, diurnal trends.*

Knowledge of the speciation of atmospheric Hg is crucial for predicting its deposition rates and understanding its biogeochemical cycle in both air and terrestrial/aquatic ecosystems. The three species of mercury have significantly different atmospheric behavior. Hg^0 is relatively inert to chemical reactions with other atmospheric constituents. Due to its long residence time (~ 1 year), Hg^0 can be transported for long distances before being deposited to terrestrial and aquatic receptors. TPM and RGM species dominate the deposition of mercury, both wet and dry. Although Hg^0 is the dominant form of atmospheric Hg, even trace amounts of RGM and TPM species may control the overall deposition of Hg. Due to its high solubility and surface reactive properties, RGM can be removed from the atmosphere through both dry and wet deposition at rates much faster than GEM (Lin and Pehkonen, 1999).

Although measurements of different Hg species in air were performed for relatively short period (4-days), some patterns were observed that support the observations of other authors and are in agreement with a general knowledge of mercury atmospheric behavior. With the exception of the first measurement (night from September 19th to 20th), concentrations of GEM and RGM exhibited some diurnal trends. Average GEM concentrations were 1.2-1.5 times higher during the day when compared to night, indicating the importance of ambient photoreduction of divalent mercury forms (i.e. $HgCl_2$ and $Hg(OH)_2$) and at this mercury polluted site especially increased volatilization of Hg^0 from the soil due to the increased temperature and solar radiation during the daytime hours. Moreover, significantly higher RGM concentrations were observed during the day than during night, indicating a pertinent oxidation of Hg^0 to Hg^{2+} by reaction with elevated ozone (O_3) concentrations during the light hours of the day when compared to night. On the other hand, higher TPM concentrations were measured during the night hours. This trend could be explained by the increased adorbtion of Hg^{2+} onto particles in the water droplets which are present in the atmosphere due to the night dew. However, at mercury polluted site such as Idrija, mercury bound to/in particulates in air (TPM) is most likely the result of local mercury sources and fine particulate matter ejected from contaminated surface due to the eolian erosion. This assumption can be supported by the fact that particulate mercury trapped onto filters during the sampling procedure was very hard to remove using standard operating conditions described by Lu et al. (1998). During the analytical procedure, particulate bound mercury trapped onto filters is decomposed by pyrolysis. The trap is heated externally at 900 °C for 15 min. As not all mercury was released after 15 minutes, the decomposition time had to be increased to 30 min in order to completely decompose all mercury from the particulates. This unusual behavior that was not observed elsewhere although the same analytical setup was used (e.g. Wängberg et al., 2007), is suggesting that mercury in the particulate phase in the Idrija air must be very firmly "matrix" bound. Most probably, it is in the form of cinnabar particles that were resuspended from the contaminated surfaces in the area. The later was further supported by the results of the SEM/EDXS analysis of the particular matter in the rain water that confirmed the presence of cinnabar particles (see section 5.5). Moreover, cinnabar particles in air were also observed at another mercury mine site in Almaden, Spain (Mareno et al., 2005).

Somewhat higher concentrations of both GEM and RGM on the night from September 19th to 20th compared to other nights can be explained by the fact that it drizzled throughout the day on September 19th. On the one hand, increased soil moisture would increase the volatilization of Hg^0 resulting in elevated GEM concentrations. On the other hand, as reported by Lin and Pehkonen (1999), the presence of water can accelerate Hg^0 oxidation. The later could then explain higher RGM concentrations measured under such conditions. During the next three days of the experiment, meteorological conditions were very constant (worm with no rain) which resulted in trend observed and disused above.

As GEM was sampled with 3-hours time resolution during the daylight hours, it was possible to investigate its daylight trend into a more detail. In Fig. 51 3-hours averages measured during the day, 12-hours averages measured during the nigh and air temperature are shown. Comparison of the GEM values obtained within 3-hour intervals during the daylight hours revealed the highest concentrations in early and late afternoon hours. This is in a good agreement with the elevated soil/air evaporation rates observed at this site (Kotnik et al., 2005) during evening and early night hours between 7 pm and 1 am. During this part of the day soil temperatures are the highest. Higher evaporation rates during this period are also related with the moisture content in topsoil, which increased after sunset due to the evening dew. Both temperature and moisture are known factors controlling mercury evaporation from soils. In general, all GEM concentrations measured are in a good agreement with the concentrations measured at the same site during the air mapping (section 5.4.1.) as well as with the results reported by other authors (Gosar et al., 1997; Kotnik et al., 2005; Grönlund et al., 2005).

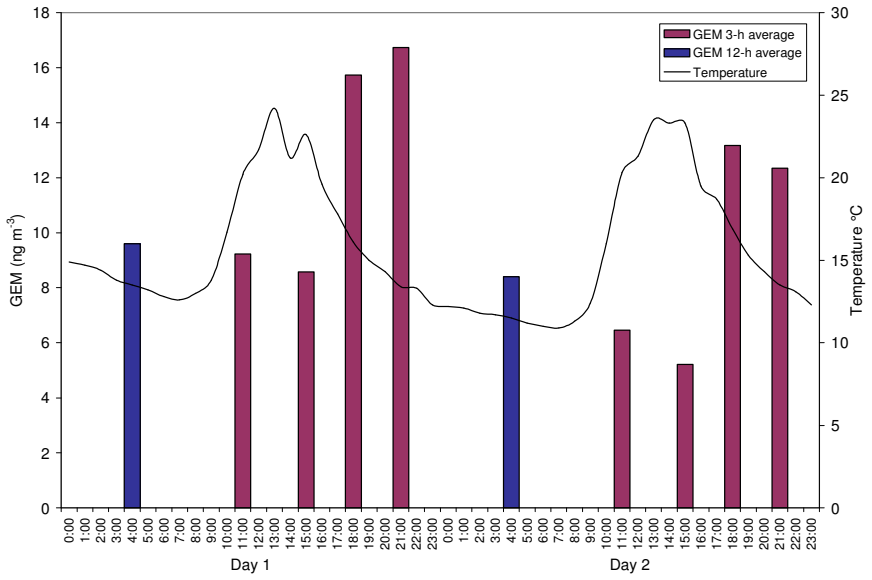

Figure 51: *GEM concentrations in air over Idrija, 3-hour averages.*

5.5 Precipitation

In this section, the results of mercury speciation analyses in precipitation is presented and discussed in order to characterize the nature of mercury deposition and its connection to atmospheric mercury sources in the Idrijca River catchment. Samples were collected on the precipitation event basis in the sampling vessels open at all times. Therefore, based on the amount of sample collected and the time during vessels were exposed, it was possible to calculate mercury deposition rates.

Precipitation samples were collected in the town of Idrija from October 2nd, 2006 to September 19th, 2007 in order to follow the amount and temporal variations in mercury atmospheric deposition over the year. Two sampling vessels (wide mouthed jars open at all times) were installed in the town of Idrija, one placed out on the open air and another in the deciduous beech forest where throughfall samples were collected. To investigate the spatial distribution of Hg deposition at the catchments scale, additional precipitation collectors were installed downstream along the Idrijca River, in Jagršče and Bača pri Modreju (locations 9 and 12, respectively in Fig. 7). At these two additional locations, samples from two individual precipitation events that occurred on February 25th and March 8th 2007 were obtained. For both precipitation events, at location Jagršče, also throughfall samples were collected. Additionally, mercury was also measured in the snow samples collected after two snow events that occurred in the town of Idrija in February 2006 and 2007, respectively.

5.5.1 Mercury in the precipitation in the town of Idrija

5.5.1.1 Mercury speciation

Precipitation concentrations of total mercury in rainwater in the town of Idrija sampled from October 2, 2006 to September 19, 2007 (n= 17), fluctuated between 3.15 and 28.54 ng L^{-1} (Fig. 52) with an average concentration of 10.53 ng L^{-1}. The volume-weighted mean (VWM) concentration was 9.22 ng L^{-1}. The results of speciation analysis reveled relatively heterogeneous distribution of different mercury forms measured after an individual precipitation event (Fig. 52 and Table 5). Due to the low amount of sample collected, concentrations of dissolved gaseous mercury (DGM) were measured only in 5 samples out of 17. Therefore, in contrast to the Hg speciation results in river water, results for reactive mercury (RHg) in precipitation samples were not corrected for DGM.

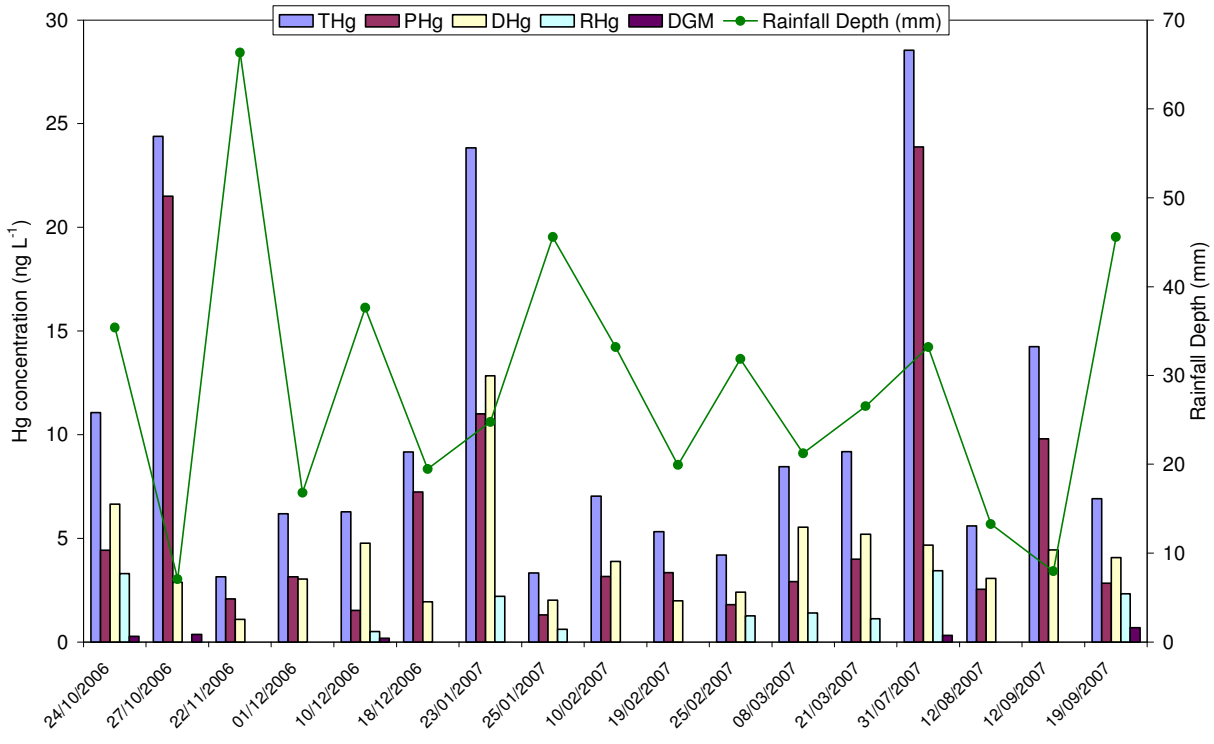

Figure 52: *Concentrations of different mercury species in rainwater in the town of Idrija.*

Table 5: *Mean mercury concentrations, ranges and percentages of different mercury species.*

Species	THg	PHg	DHg	RHg*	DGM
mean	10.53	6.36	4.18	1.79	0.37
range	3.15-28.5	1.51-23.9	1.09-12.8	0.50-3.4	0.18-0.69
VWM	9.22	5.21	4.01	1.70	0.47
% of THg (range)		40-88	12-76	8-34	1-10
% of THg (mean)		54	46	10	4

* not corrected for DGM

Comparison of mercury concentrations measured in the rain collected after an individual precipitation event vary significantly. In this study, sampling vessels open at all times were used. Therefore, it is rather difficult to determine the relative contribution of dry and wet mercury atmospheric deposition, respectively. However, based on the speciation results, some conclusions can be drawn, as follows.

As it can be seen from Fig. 52, elevated total Hg concentrations are mostly related to elevated concentrations of mercury bound to particulate phase (PHg), which can be a result of both dry deposition and wash-out of particle bound mercury. On average, PHg represents more than 50% of total Hg, the rest being in the dissolved phase. There was no correlation found between particulate and dissolved phases in the precipitation samples. Several explanations for the absence of the correlation are possible. Either the wet scavenging operates on both phases with the different proportion of efficiency, or particulate phase Hg is predominantly a result of dry deposition. Nevertheless, a decreasing trend in mercury content (expressed in log concentrations) in both dissolved (<0.45 μm) and particulate (>0.45 μm) phases with increasing amount of precipitation (Fig. 53) suggest that both forms are removed from the atmospheric reservoir by precipitation. However, as discussed also by Poissant and Pilote (1998), it is not clear whether the mercury binding to particles in precipitation is due to scavenging of particle-phase mercury or to Hg oxidation followed by sorption mechanisms.

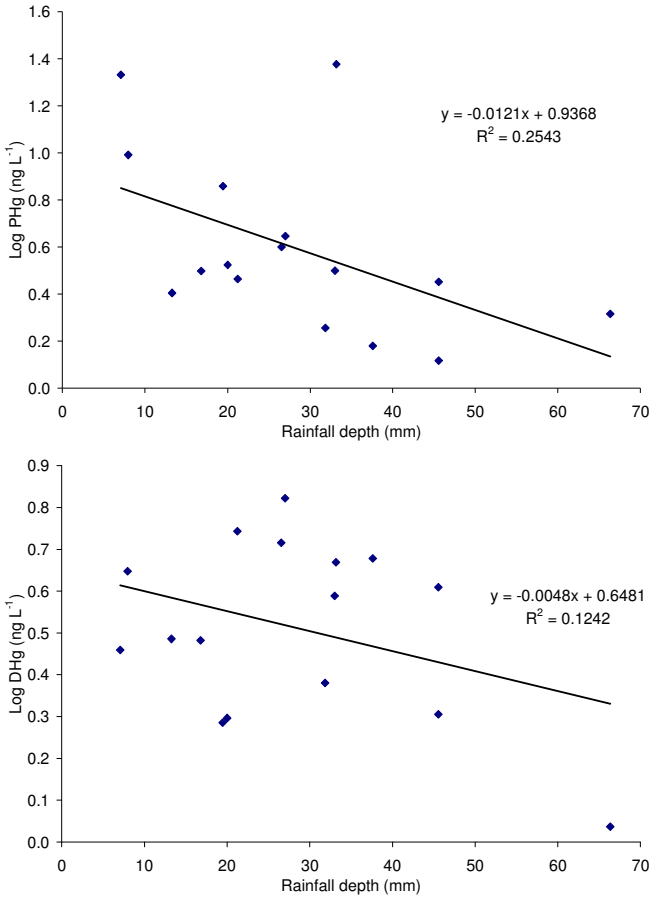

Figure 53: *Relationship between amount of precipitation, expressed as rainfall depth in mm and the logarithm of dissolved mercury concentration (below) and the logarithm particulate phase mercury concentration (above).*

On the other hand, knowing that the dominant form of mercury in the atmosphere is gaseous elemental mercury (~99%), the concentrations of truly dissolved mercury in rainwater could also be predicted by Henry's law, using the linear relationship between elemental mercury solubility and temperature (Sanemasa, 1975):

$$\log H = -1003 \cdot \left[\frac{1}{T(Kelvin)} \right] + 2.886 \tag{3}$$

In this case H is a Henry's Law constant, a thermodynamic parameter related to the amount of mercury expected to be in equilibrium in both phases (atmosphere and rainwater) at a given temperature. From both Henry's Law constant and measured atmospheric Hg^0 concentrations (C_{atm}) it is possible to determine the rainwater mercury concentration ($C_{rainwater}$) expected in equilibrium according to:

$$H = \frac{C_{atm}}{C_{rainwater\,/\,equilibrium}} \tag{4}$$

Taking average Hg^0 air concentration of 10 ng m^{-3} measured at the sampling site and annual average air temperature of 283 K, the concentration of the dissolved mercury should be around 0.05 ng L^{-1}. Hence, this suggests that only a small part of the total dissolved phase mercury is truly dissolved elemental mercury, whereas most of the 'dissolved' mercury in precipitation, namely the 'operationally-defined dissolved phase' (<0.45 μm) is in colloidal particle form or in molecular complexes. This is further supported by measured DGM concentrations which on average represent less than 10 % of measured total dissolved phase (<45 μm). Although DGM concentrations were relatively low, which is consistent with known low Hg^0 solubility, it must be noted that DGM measured in precipitation samples can also be a result of the aqueous phase Hg^{2+} reduction in the sampling vessel itself. No correlation between the DGM and reactive Hg concentrations (RHg) was observed to support this assumption. However, the number of samples in which both DGM and RHg was measured is rather limited (only 5), as usually there was not enough of sample collected to perform all the analysis.

Relatively insoluble Hg^0 in air must be oxidized to a much more soluble Hg^{2+} form to be stripped from the atmosphere by precipitation. Hg^0 solubility is known to be greatly enhanced by the presence of oxidants such as O_3 in rain (Munthe, 1991) and is rapidly transformed into more soluble vapor species in an oxidizing atmosphere saturated with water vapor (i.e. during precipitation) (Lindberg, 1998). The oxidation seems to take place either within the aqueous aerosol, or in the gas phase with the Hg^{2+} then being absorbed by the droplets and particulates, respectively. A positive correlation between reactive Hg and Hg bound to particulates (R^2=0.47) indicates the importance of gas-particle partitioning in mercury deposition. Furthermore, this correlation suggests that mercury binding to particles in rainwater is due to Hg^0 oxidation followed by sorption mechanisms. The absence of correlation between the dissolved and reactive Hg, on the other hand, suggest that most of dissolved phase mercury in rainwater is firmly bound in colloidal particles or in molecular complexes.

However, all the assumptions discussed here must be called into question due to the fact that the results of the SEM/EDXS microscopy revealed the presence of cinnabar particles on rainwater filters (Fig. 54). The presence of cinnabar particles is most probably the result of the eolian erosion of cinnabar containing soils and sediments in the area. It is known that at sites with mercury mining history, aerosols containing cinnabar can be found in the atmosphere. Gosar et al. (2006) reported elevated concentrations of cinnabar in the attic dust of houses in the town of Idrija compared to sites more distant from the pollution source. Mercury-bearing airborne particles were also observed at another mercury mine polluted site in Almaden, Spain (Moreno et al., 2005). The presence of a single cinnabar particle in the sampling vessel would significantly effect the concentration of Hg in precipitation measured. Due to the variable weather conditions (e.g. wind, soil moisture content, snow cover…) aerosols are not uniformly distributed in the atmosphere, both spatially and temporally. This would then lead to differences in mercury deposition which can explain the variations in concentrations of mercury measured in precipitation collected after an individual precipitation event.

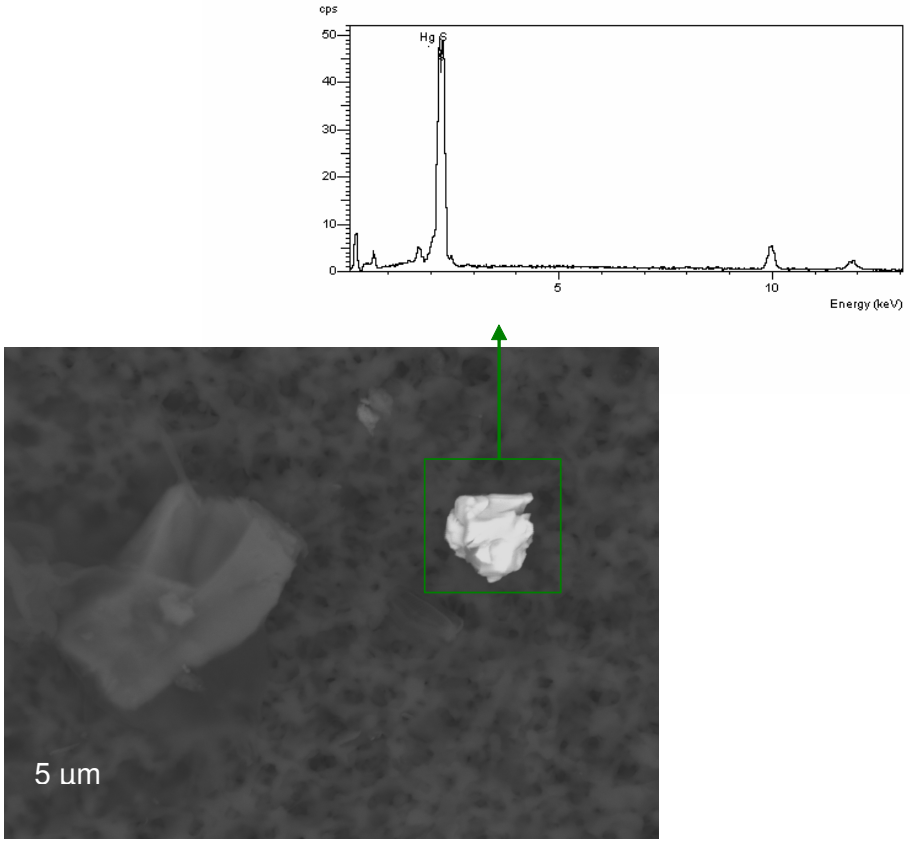

Figure 54: *SEM/EDXS microscopy of suspended matter in the rain water from location Idrija.* Marked grain represents a qualitative spectrum (belonging graph) of the cinnabar particle, low content of particulates is observed, filter fibers represent the uncovered area of the filter.

Concentrations of total mercury (THg) measured in snow collected after two snow events (February 2006 and 2007, respectively) from several locations in the town of Idrija are comparable with those of rain (Fig 55). However, compared with rain, snow has higher content of particulate mercury (on average 75 % compared do 54 % in rain). Both snow events differ in terms of Hg bound to particulate phase, while concentrations of dissolved Hg fractions are comparable.

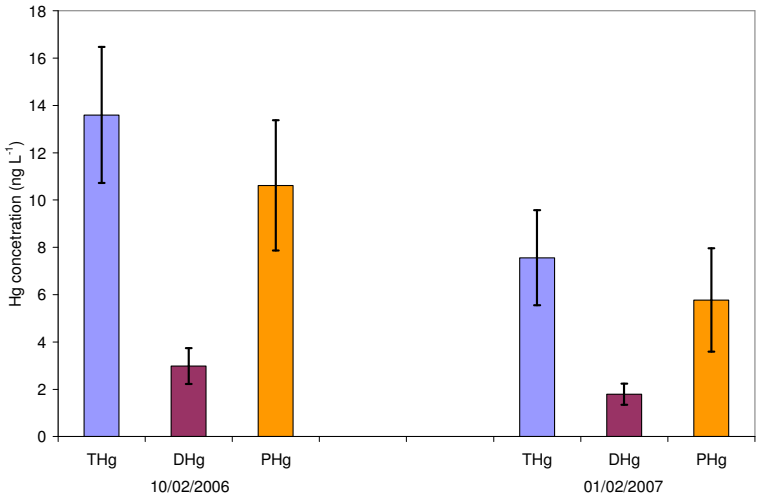

Figure 55: *Mercury concentrations in snow of Idrija.* Error bars showing standard deviations of parallel determinations.

5.5.1.2 Mercury deposition

As it can be seen in both Fig. 52 and Table 5, THg as well as concentrations of different mercury species measured in the samples obtained after an individual precipitation event very a lot. It is known (e.g. Keeler et al., 2005) that Hg concentrations in precipitation depend on several factors such as seasonal variations, diurnal variations, duration, frequency and the amount of precipitation. At the mercury contaminated site these differences can be also due to the cinnabar particles present in the atmosphere. To harmonize the influence of the amount of precipitation and the time during which the sampling vessels were exposed, mercury deposition was calculated according to recommendations of the European Committee for Standardization using the following equation:

$$Dep_{Hg} = \frac{M_{Hg}}{A_{samp} \cdot n} \tag{5}$$

where:
Dep_{Hg} = mercury deposition (ng m^{-2} day^{-1})
M_{Hg} = mass of Hg per sample (ng $sample^{-1}$)
A_{samp} = sampler collecting area (m^2)
n = number of days sampling vessels were exposed (day)

The atmospheric loading of Hg to the Idrija town calculated by equation 5 is shown in the event deposition plot (Fig. 56). Event THg deposition varied from 11-84 ng m^{-2} day^{-1} with the average event deposition being 37 ng m^{-2} day^{-1}. These rates are comparable with the deposition rates obtained at industrial site in Šoštanj, Slovenia (Kotnik et al., 2008). Variations in the event based deposition (Fig. 56) are much lower compared to results expressed in ng L^{-1}. This is due to the differences in the amount of sample collected within an individual precipitation event and due to the differences in the exposure time. In the calculation of Hg deposition the influence of both parameters is taken into account. However, the amount of the sample collected can only explain approximately 15% of the variance in the Hg concentration (correlation coefficient between the amount of sample collected and THg concentrations R^2=0.15), suggesting the predominant influence of the exposure time on the variations observed. Moreover, this is also a clear indication of the importance of dry mercury deposition in total atmospheric deposition in the area investigated. Furthermore, seasonal variability in atmospheric Hg deposition was investigated. It is widely known that the concentrations of oxidants such as ozone, OH radicals and acids that oxidize gaseous Hg^0 to gaseous Hg^{2+} are higher during warmer months and would lead to elevated concentrations of more soluble and reactive Hg^{2+} that deposits much faster than Hg^0 (Keeler et al., 2005). The expected seasonal variability in atmospheric Hg deposition was not observed. This might be due to the unusually warm 2006/2007 season, low number of samples collected during summer months and the non-customary frequency of rain events throughout the sampling period.

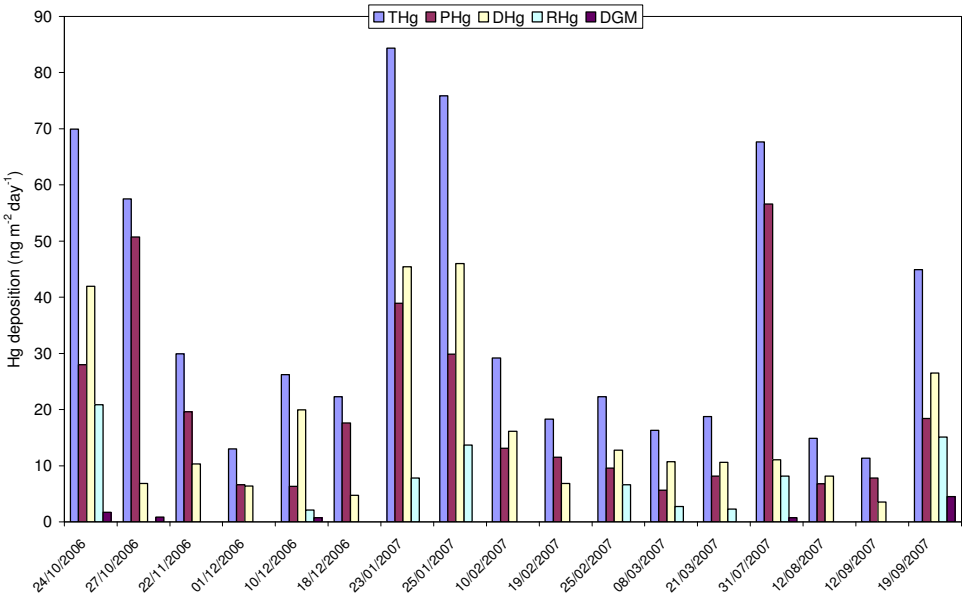

Figure 56: *Deposition of different mercury species in rainwater in the town of Idrija.*

5.5.2 Mercury in the throughfall in the town of Idrija

Sampling vessel for collection of throughfall samples in the town of Idrija was installed in the deciduous beech forest. In order to diminish the influence of spatial variations in mercury deposition and to be able to compare the throughfall with the precipitation, throughfall samples were collected in direct vicinity (cca. 20 m) of the location where precipitation samples were collected. During the mapping of Hg in air, concentrations ranging between 5 and 10 ng m^{-3} were measured at this location. Hg concentrations in surrounding soils range between 10 and 20 mg kg^{-1} (Gnamuš et al., 2000; Gosar et al., 2006).

5.5.2.1 Mercury speciation

Concentrations of total Hg (dissolved and particulate phase) in throughfall during the growing season ranged from 14.3 to 125.2 ng L^{-1}. The volume-weighted mean (VWM) is 40.7 ng/L. The results of mercury speciation in throughfall collected after an individual precipitation event are shown in Fig. 57 and summarized in Table 6.

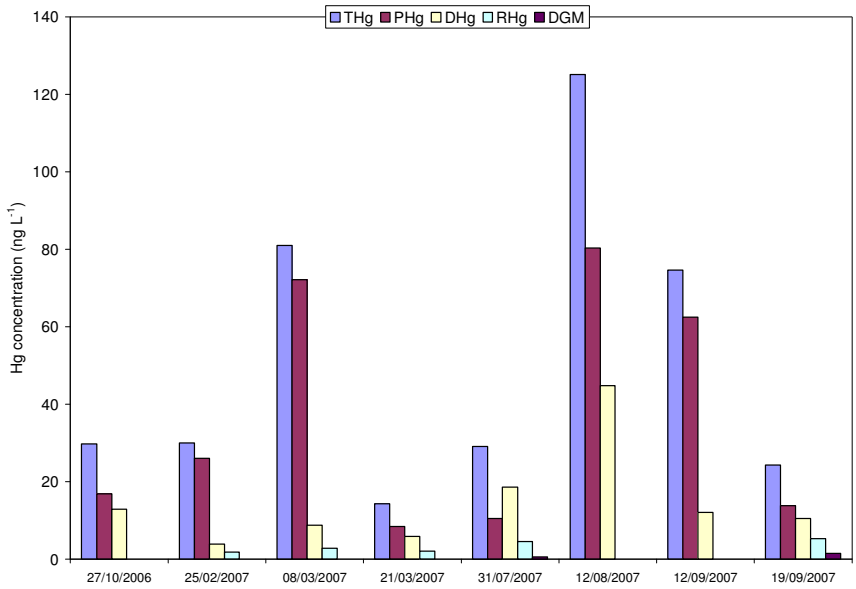

Figure 57: *Concentrations of different mercury species in the throughfall in the town of Idrija.*

Table 6: *Mean mercury concentrations, ranges and percentages of different mercury species in throughfall.*

Species	THg	PHg	DHg	RHg	DGM
Mean	51.0	36.3	14.7	3.3	1.0
Range	14.3-125	8.5-80	3.9-45	1.8-5.3	0.6-1.5
VWM	40.7	28.1	12.6	3.6	1.1
% of THg (range)		36-89	11-64	3-22	2-6
% of THg (mean)		68	32	12	4

Throughfall concentrations of mercury were significantly higher than the associated event precipitation concentrations. Concentrations of both, particulate and dissolved phase mercury in throughfall significantly exceeded those in rainwater. It is known from the literature that wet deposition cannot account for all mercury reaching the forest floor via throughfall and litterfall (e.g.; Guentzel et al., 1998; Schweisig and Matzner, 2000; Rea et al., 2001). Mercury may be deposited to a forest canopy in both gaseous and aerosol forms (Schroeder and Munthe, 1998). Gaseous Hg forms include elemental gaseous Hg (Hg^0) and reactive gaseous Hg (Hg^{2+}). Some authors (e.g. Rea et al., 2001) reported that the majority of the dry deposition flux is in a gaseous form, which may then undergo many reactions and transformations on the leaf surface. Any resulting water soluble Hg compounds may wash-off the leaf surface in throughfall. Elevated concentrations of total dissolved mercury (DHg) measured in all throughfall samples confirmed these assumptions. Moreover, also the concentrations of truly dissolved gaseous mercury (DGM) were significantly higher in the throughfall compared to precipitation. It must be noted, however, that DGM was measured in two throughfall samples only.

Positive correlation between PHg and DHg concentrations (R^2=0.32) on the other hand, a trend that was not observed in rainwater samples, suggests that wash-off of Hg deposited and accumulated on the canopy by dry deposition represents a significant part of mercury deposited on the forest floor. Furthermore, a decreasing trend of both particulate and dissolved Hg phases in the throughfall with increasing rainfall depth was observed. The first trend indicates that dry deposited Hg is rather quickly and efficiently removed from the canopy. The second trend, on the other hand, indicates that major part of the dissolved phase Hg is related to wash-off and dissolution of previously dry deposited mercury. These assumptions are further supported by the concentrations of reactive mercury species (RHg) and the presence of organic matterial, both parameters being relatively elevated in the throughfall compared to precipitation samples. Namely, both "operationally-defined" mercury phases measured, reactive and dissolved, respectively, have a tendency to bind with organic complexes. As shown by the results of the SEM/EDXS microscopy, organic material is prevailing form of the particulate matter in the throughfall samples (Fig. 58). Furthermore, SEM/EDXS microscopy of particulate matter in the throughfall revealed the presence of cinnabar particles with a 5 µm diameter. As discussed in section 5.5.1, due to its insolubility, cinnabar particles can alter the partitioning between particulate and dissolved mercury phases.

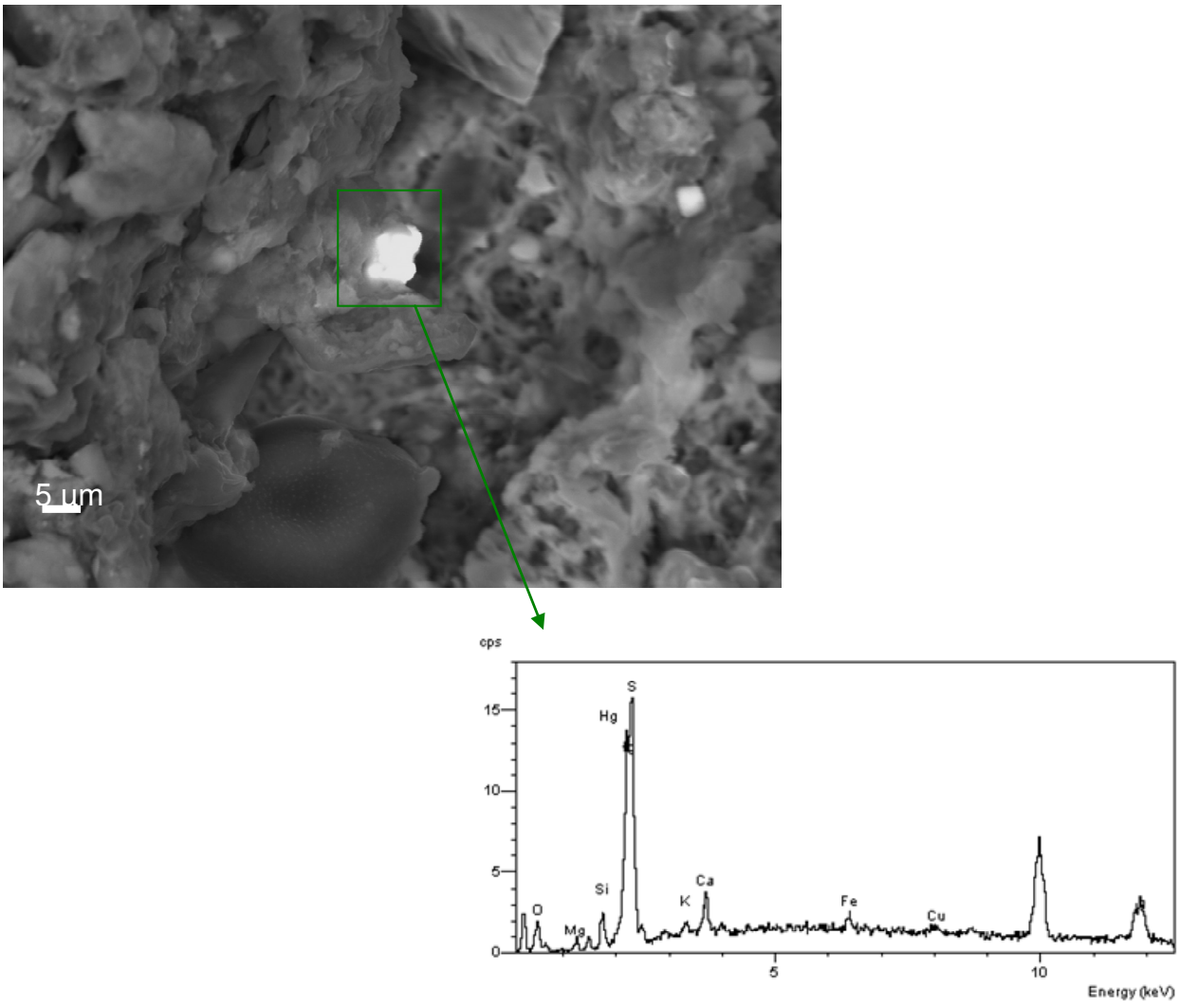

Figure 58: *SEM/EDXS microscopy of suspended matter in the throughfall from location Idrija.* Marked grain represents a qualitative spectrum (belonging graph) of the cinnabar particle surrounded with the material of organic nature (dark part), high content of suspended matter is observed.

5.5.2.2 Mercury deposition

Mercury deposition by the throughfall in the town of Idrija calculated by equation 5 is shown in the event deposition plot (Fig. 59). Event THg deposition varied from 30 to 160 ng m^{-2} day^{-1} with the average event deposition being 130 ng m^{-2} day^{-1}. Variations in the mercury throughfall deposition are much higher than the variations in the deposition due to the precipitation. Some of these differences can be explained by various amount of sample collected after the precipitation event. However, mercury partitioning and its deposition by throughfall are not only governed by the amount of rainfall. Factors such as duration of the dry period between two precipitation events, duration of the growing season (associated with the Leaf Area Index), wind conditions and ground surface moisture content that control the eolian erosion, are also important. However, based on the fact that particulate bound Hg present the majority of the total Hg concentrations in these samples (on average 68 %), the results suggests that at specific mine polluted site such as Idrija, dry deposition is mostly governed by the deposition of Hg containing aerosols.

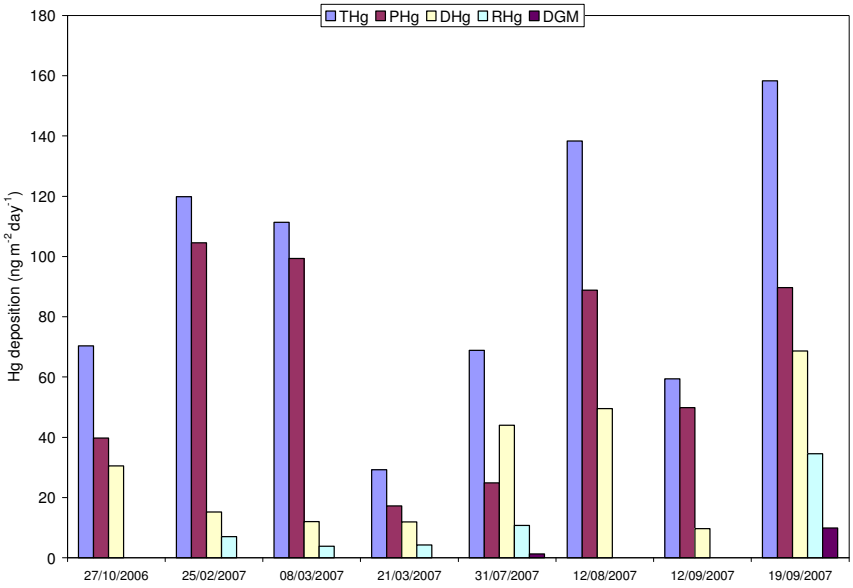

Figure 59: *Deposition of different mercury species in the throughfall in the town of Idrija.*

It must be noted, however, that throughfall is not only wash-off of dry deposition but also inputs from precipitation and foliar leaching must be taken into account. Dry deposited Hg^0 and Hg^{2+} may be taken up through the leaf stomata and fixed in the foliage (Mosbaek et al., 1988). It was demonstrated by Rea et al. (2000) that during the washing experiment, wash-off of dry deposited Hg occurred rapidly, while foliar leaching occurred continuously. Gaseous Hg may react on the leaf surface and be re-emitted as Hg^0 which may account for some fraction of the emission of Hg^0 from forest canopies. It is known that in the Idrija region, vegetation can uptake mercury from the soils and air (Gnamuš et al., 2000). However, these processed were not investigated within the present work.

5.5.3 Spatial and meteorological variations

To investigate the spatial distribution of Hg deposition at the catchments scale, additional rain collectors were installed in Jagršče and Bača pri Modreju (locations 9 and 12, respectively on Fig. 7). Samples from two individual precipitation events that occurred on February 25th and March 8th 2007 were obtained. For these two events also concentrations of methylmercury (MeHg) as well as the stable isotopic composition of hydrogen and oxygen (δ^2H and $\delta^{18}O$) in rainwater was measured.

The stable isotopes oxygen-18 ($\delta^{18}O$) and deuterium (δ^2H) offer a broad range of possibilities for studying processes within the water cycle also in studies related to atmospheric circulation and climatic investigations (Araguas-Araguas et al., 2000) including meteorological transport history of the air masses that can influence the Hg concentrations in precipitation (Keeler et al., 2005). The results of the isotopic composition presented in Fig. 60 show a good correlation between δ^2H and $\delta^{18}O$ obtained for each station for both precipitation events. Also the local meteoric water lines are close to the Global Meteoric Water Line. However, there is a significant difference in isotopic composition of hydrogen and oxygen in both precipitation events. Based on the more extensive database and long-term patterns observed in isotopic composition reported for Slovenia and Croatia (Vreča et al., 2006), lower values of both δ^2H and $\delta^{18}O$

measured in 25.02.2007 event are suggesting the maritime origin of air masses. On the other hand, higher values measured in 08.03.2007 event are suggesting the continental origin of air masses. These assumptions were further confirmed by the observation of radar precipitation images (ARSO, 2007) showing that precipitation reached the catchment from the continental west during the 25/02/2007 event, while air masses were approaching from the Mediterranean south during the 08/03/2007 event.

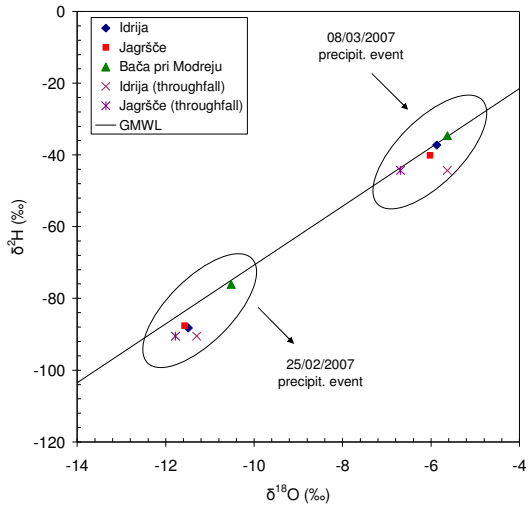

Figure 60: *The relation between δ^2H and $\delta^{18}O$ of two precipitation events; GMWL, Global Meteoric Water Line.*

When these two meteorological different precipitation events were compared in terms of mercury concentrations, the following observations were made. There was no significant spatial variation in Hg concentrations within the individual precipitation event (Fig. 61, A). Minor differences among the sampling sites can not be explained with the distance from the pollution source in the town of Idrija, suggesting that Hg atmospheric deposition at the catchment scale is more governed by the regional meteorological conditions. Significantly higher Hg concentrations measured during the 08/03/2007 support this assumption. Maritime air masses of the 08/03/2007 event are moist and contain considerable amounts of water vapor and halogens. In such conditions Hg solubility and reactivity (e.g. reduction of Hg0) is greatly enhanced (Munthe, 1991). Moreover, these air masses are originating over the Mediterranean which is a known source of atmospheric mercury (e.g. Ferrara et al., 2000; Kotnik et al., 2007). However, on contrary to these observations, in terms of calculated mercury deposition rates, there was no significant difference among both precipitation events. Moreover, there are significant spatial variations in Hg deposition rates between the sampling sites (Fig. 61, B) that again can not be explained by the distance from the local pollution sources. These results would than suggest that Hg atmospheric deposition rates in the Idrija region is more influenced by the factors such as amount of precipitation, duration of period of dry weather and local meteorological conditions. This is further supported by the results of mercury measurements in the throughfall at locations Idrija and Jagršče, respectively (Fig. 62). Mercury concentrations and deposition rates vary significantly at both sites and are mostly influenced by the amount of Hg in the particulate phase.

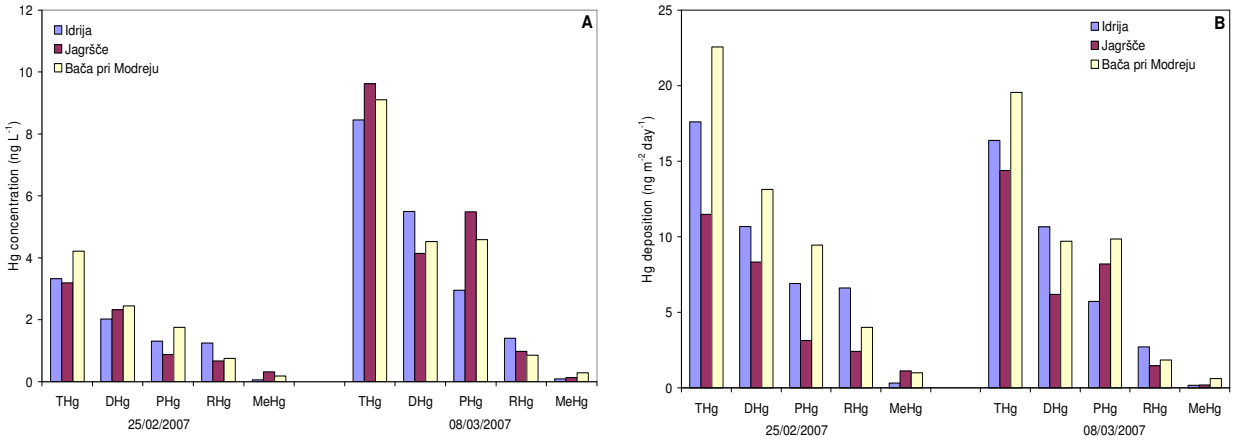

Figure 61: *Spatial variations in concentration (A) and (B) deposition rates of different Hg species during two meteorologically different precipitation events.*

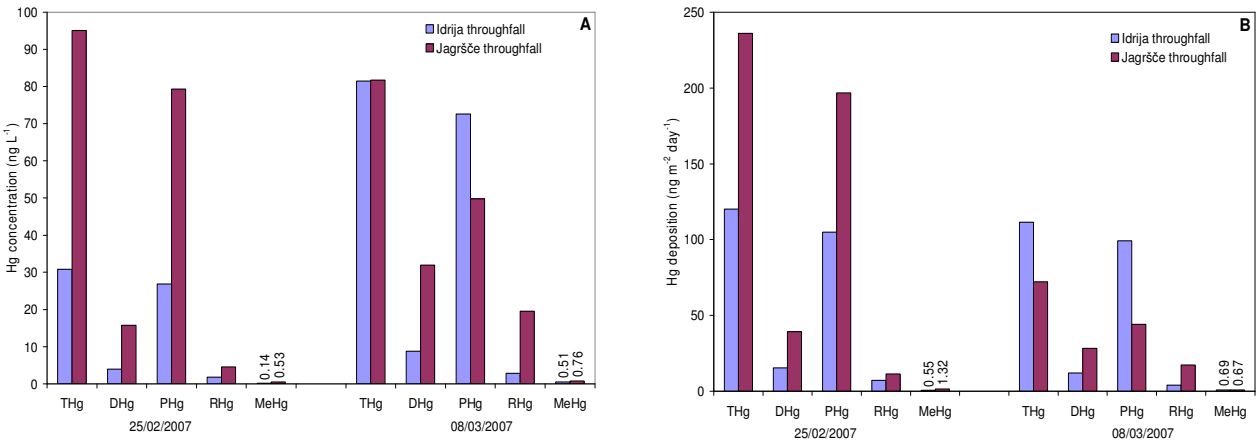

Figure 62: *Spatial variations in concentration (A) and (B) deposition of different Hg species in throughfall at locations Idrija and Jagršče during two meteorologically different precipitation events.*

Methylmercury (MeHg) concentrations for both precipitation events were in the range of 0.06 to 0.32 ng L^{-1}. In the throughfall samples MeHg concentrations were significantly higher (between 0.14 and 0.76 ng L^{-1}). These values are in the range of other published values (e.g. Hall et al., 2005). On average MeHg presents 1.4 % of THg and can reach up to 10 %, which is comparable to results of Bloom and Watras (1989) for continental regions.

Up to now, sources of methylmercury in both wet and dry deposition are very much unknown. Possible explanations are volatilization of gaseous MeHg, evasion and demethylation of dimethylmercury, and methylation of Hg0. Hammerschmidt et al. (2007) observed a positive relation between the MeHg and operationally defined reactive Hg species (RHg) in precipitation. They suggested that MeHg may be formed in the atmosphere through a reaction involving labile Hg^{2+} complexes. Similar, Hall et al. (2005) observed a decrease of MeHg with the increasing sample volume due to the wash-out effect and suggested that particle-bound MeHg was present in the atmosphere prior to the rain event. Consistent with, positive correlations between MeHg and concentrations of dissolved (DHg) and reactive (RHg) mercury phases, respectively, were observed (Fig. 63). Data of both precipitation and throughfall measurements are included in the plot.

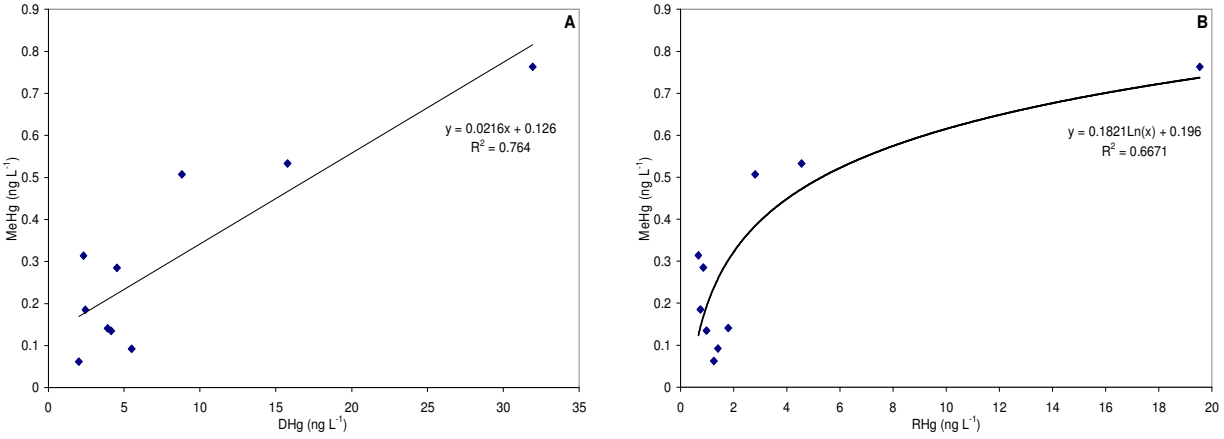

Figure 63: *Relation between concentrations of methylmercury (MeHg) and (A) dissolved (DHg) and (B) reactive (RHg) mercury.*

5.6 Mercury evaporation from soil

Evaporation from soil is an important pathway of the mercury flux in the environment. However, estimations of the quantitative significance of evaporation relative to other pathways are very uncertain (Schlüter, 2000). In the Idrija mercury mine area, some efforts have been made in the past to better understand the mechanisms of mercury evaporation from soil to the atmosphere and to quantify the contributions from major sources. Kotnik et al. (2005) measured mercury evaporation from topsoil using the ‘‘flux chamber’’ technique at two heavily polluted locations in Idrija and downstream the Idrijca River at Bača pri Modreju. In their study, the influence of weather conditions, soil and air temperature, air and soil Hg concentration and soil type on the measured results was observed. Grönlund et al. (2005) estimated average mercury flux from the most polluted sites in the town of Idrija to approximately 2-4 g h^{-1}, using differential absorption lidar techniques. However, results of their study were influenced by rainfall and associated low temperatures which decreased the mercury evaporation from the ground. Furthermore, the simulation of mercury evaporation from different soil types from the Idrija region was performed complemented by the selective sequential extraction procedure in order to assess the potential for mercury volatilization (Kocman et al., 2004 in Appendix C). In that study the effect of soil temperature, soil moisture as well as specific mercury binding in soil on its volatilization was observed.

The results of all previous studies revealed that still too little is known about the amounts and species of mercury evaporating from soils in the Idrija region as well as the factors causing and affecting this process. For scaling-up and modelling of mercury evaporation from soils a comprehensive assessment of the processes controlling the evaporation of mercury from soils is imperative. Therefore, in the present study, mercury evaporation from soil was studied in more detail. Laboratory flux measurement system (LFMS) designed by Bahlmann et al. (2006) was used to directly measure mercury emission flux (MEF) under controlled simulated environmental conditions including soil temperature, soil moisture and solar radiation. The final aim of the evaporation experiment was the quantification of the mercury soil-air fluxes at the catchment scale on the yearly basis. Therefore, all soil samples were investigated together with vegetation cover, representing the actual situation in nature. In this way, also the comparison of the results obtained under laboratory condition with the *in situ* Hg flux measurements was possible.

5.6.1 Sample material: characteristics and total mercury content

Altogether, seven soil samples were collected from three locations in the Idrijca River catchment (Idrija, Travnik and Reka, respectively). Soil samples were selected with respect to total mercury concentration, land cover and soil texture. For this reason, at all three locations two types of soil were obtained (forest and meadow soil, respectively), while at location Travnik also an alluvial soil sample was taken. In order to characterize these samples, beside the total mercury concentrations, the texture and the organic matter content (OM) were determined as additional variables. Table 7 gives an overview over the sample characteristics.

Table 7: *Characteristics of the samples investigated.*

Sample	Type/Land Cover	Texture	OM (%)	THg (µg/g)
Idrija A	forest	clayey	16	251 ± 4.2
Idrija B	meadow	clayey	10	100 ± 2.2
Travnik A	forest	clayey	22	19 ± 0.4
Travnik B	meadow	clayey	18	23 ± 0.7
Travnik C	alluvial plain	loamy	8	417 ± 78
Reka A	forest	loamy	19	9 ± 0.6
Reka B	meadow	loamy	16	4 ± 0.1

The total mercury concentrations of the samples investigated covered a range from 4 to 417 µg g^{-1}. With the exception of location Travnik, higher THg concentrations were measured in the forest soil samples compared to meadow soils. This can be explained by the organic matter content which is higher in the forest soil and has a high adsorption capacity for mercury. At location Travnik high organic matter content was measured in both forest and meadow soil samples. As a result of deposition and accumulation of contaminated suspended particulate matter during high flow or flooding of the Idrijca River, the highest THg concentrations were measured in the alluvial plain soil from location Travnik.

In terms of texture, samples can be divided into two groups. Forest and meadow soil samples from locations Idrija and Travnik have a clayey texture, while alluvial soil and soils from location Reka have loamy texture with relatively equal mixture of sand and silt particles.

5.6.2 Laboratory flux measurement system (LFMS)

Based on the recommendations of the designer of the laboratory flux measurement system (LFMS), the standard operation conditions chosen for the experiments were as follows: a flushing flow rate of 12 L min^{-1}, a fan voltage of 6 V, a soil surface temperature of 20-25 °C, a soil layer of 2 cm thickness and no light exposure (Bahlmann et al., 2006). Simultaneous measurements of Hg^0 were made at the outlet of the chamber using a Lumex RA-915$^+$ Zeeman portable mercury spectrometer (Sholupov and Ganeyev, 1995). This system utilized atomic absorption in a column of chamber air which was constantly replenished by a pump maintaining an air flow of 12 L min^{-1} through the system. By using Zeeman modulation techniques the system is particularly sensitive and real time measurements can be performed rather than relying on the customary gold amalgamation technique for pre-concentration before atomic absorption spectrometer measurements. Spectra were collected and recorded by the computer as 10 s averages. Baseline correction time (period of time during which the level corresponding to the zero mercury vapor concentration in the analytical cell) was set to be 20 s and was measured every 5 min. The calibration and function of the instrument was checked prior to every measurement by measuring known Hg vapor concentration in the test cell installed in the instrument. Relative deviation of the measured value of the Hg vapor concentration in the test cell from the tabulated value was within 5 %. The detection limit is 1 ng m^{-3} (Sholupov and Ganeyev, 1995) which corresponds to a mercury flux of 3.6 ng m^{-2} h^{-1}.

In the beginning of the experiment, LFMS had to be calibrated. In the calibration phase, operational conditions including stability of a flushing flow rate, turbulent mixing, measurements of Hg^0 in the incoming air and the baseline correction time were controlled. Due to the moderate total mercury concentrations (19 µg g^{-1}) compared to other samples, forest soil sample from location Travnik (Travnik A) was chosen and investigated during this phase. Under the defined standard conditions the observed mercury flux for sample Travnik A was 54 ng m^{-2} h^{-1} and remained constant within ±10 % for the next 100 h. This temporal stability under constant environmental conditions indicates that a constant amount of mercury available for volatilization must be provided. Therefore, stability of fluxes over time depends also on the amount of mercury available to vaporize. When assuming the volatile fraction to consist primarily of Hg^0, permanence of fluxes can be estimated based on the amount of Hg^0 in soil and the actual measured flux. However, there is no direct reference method and/or appropriate reference materials for measurements of volatile mercury fraction in soils. Hence, available pool of volatile mercury in soil is difficult to determine. Some efforts have been made before to determine the volatile mercury pool in the soils from the Idrija region (Kocman et al., 2004). For this purpose a simple mercury volatilization simulation experiment was applied. A sample was heated to 70 °C for several hours in the evaporation vessel connected to a gold sand trap which was then analyzed by cold vapor atomic fluorescence spectrometer (CVAFS). The procedure together with the results of the volatilization simulation experiment is described into more detail in Kocman et al. (2004) in Appendix C. Taking the results of the volatilization simulation experiment into account, the total amount of Hg^0 per m^2 and cm at Idrija forest site is 300 µg when assuming a soil density of 1.5 g cm^{-3}. This is about 1 x 10^3 times higher than the observed flux of 150 ng m^{-2} h^{-1} at 20 ºC and thus could theoretically maintain this flux for more then a year. In this calculation Hg deposition and soil moisture variations were not taken into account. Also the yearly average temperatures are much lower then 20 ºC. Moreover, only a part of all volatile Hg was obtained during the volatilization simulation experiment. Therefore, this period is most probably even longer.

After the calibration phase, when stable operational conditions were achieved, samples were processed. Over each of the selected seven soil samples the effect of the soil surface temperature, soil moisture and solar radiation on the mercury emission flux (MEF) was investigated. Altogether, mercury emission fluxes were measured over each sample for 8-16 hours. During this time, environmental conditions were regulated. In the beginning of the experiment, to investigate the temperature effect, samples were cooled down to about -4 °C and then allowed to heat to room temperature. Simultaneously, mercury emission flux and soil surface temperature were measured. When the fluxes and soil temperature became constant (after approx. 6 h) samples were radiated with a UV light of a constant intensity (320 W m^{-2}) for 1 hour. After 1 hour of radiation, UV light was turned off and MEF was measured until the levels before the radiation were achieved, which last approximately one hour. Samples were then left to be overnight at the room temperature without the flow flushing through the system. Next day, before the measurements continued, air flow was released through the system and the fan was turned on for about half hour to avoid stagnation zones and uncontrolled induction of vertical components of airflow. Mercury fluxes were then measured

under standard conditions. After approx. 2 hours, precipitation was simulated by sample rewetting using 300 mL of Milli-Q water. The amount of water used corresponds to a 1.5 mm precipitation event. Later on, when the fluxes became constant (usually within next 4 hours) samples were radiated for additional hour. Moisture content was measured in the uppermost 5 mm of the sample. An aliquot of the sample was obtained and moisture measured three times during the experiment for each sample: after samples heated to the room temperature and fluxes became constant, just before the precipitation simulation, and at the end of the experiment.

Results of the LFMS experiment are graphically presented in Figures 64-70. On each plot MEFs, temperatures and periods of UV light exposure are shown. Time values marked on the *x* axis correspond to the effective experimental time in hours.

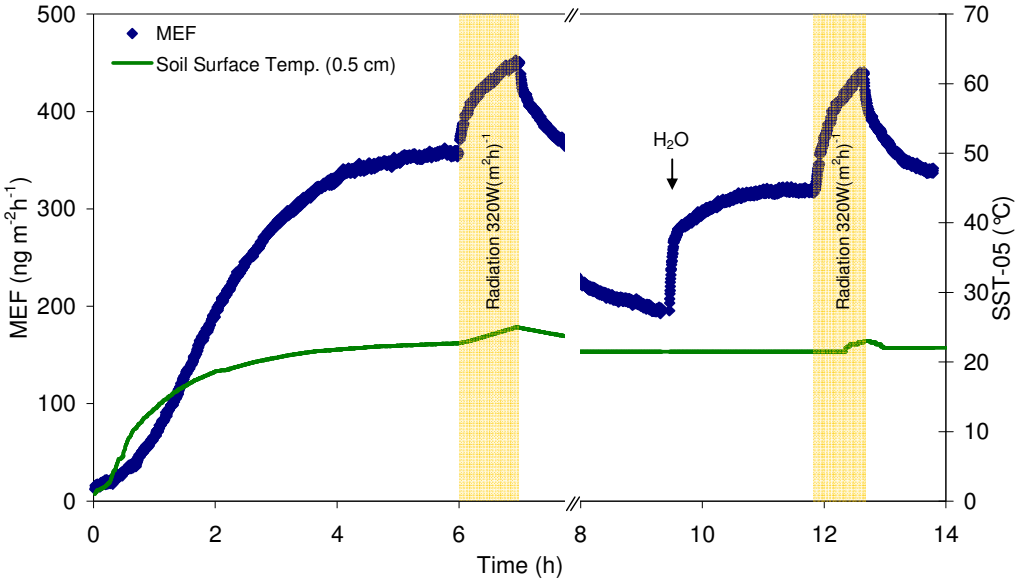

Figure 64: *Mercury emission flux (MEF) measured under different simulated conditions (temperature, precipitation and UV light induced), location Idrija A (forest soil).*

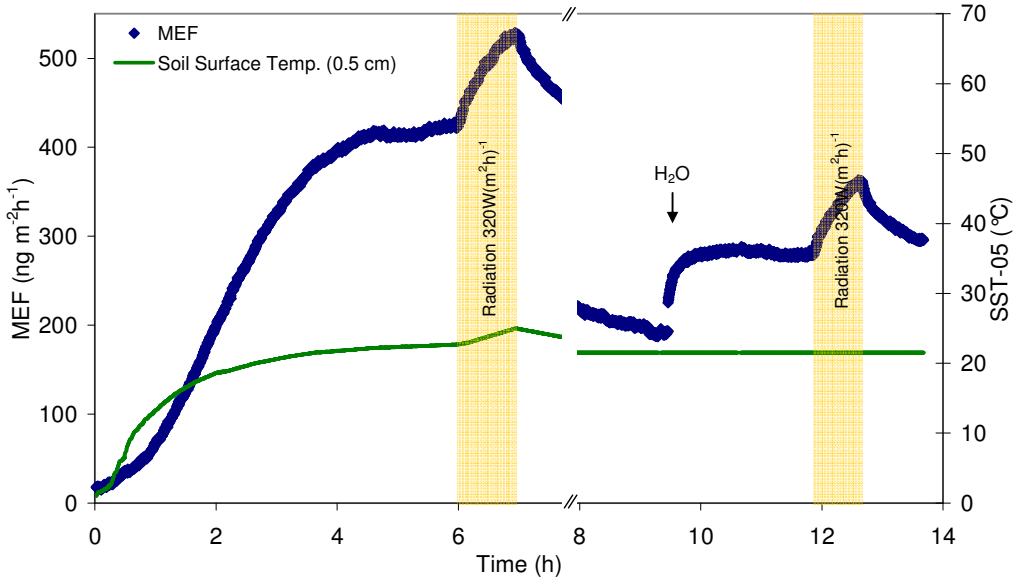

Figure 65: *Mercury emission flux (MEF) measured under different simulated conditions (temperature, precipitation and UV light induced), location Idrija B (meadow soil).*

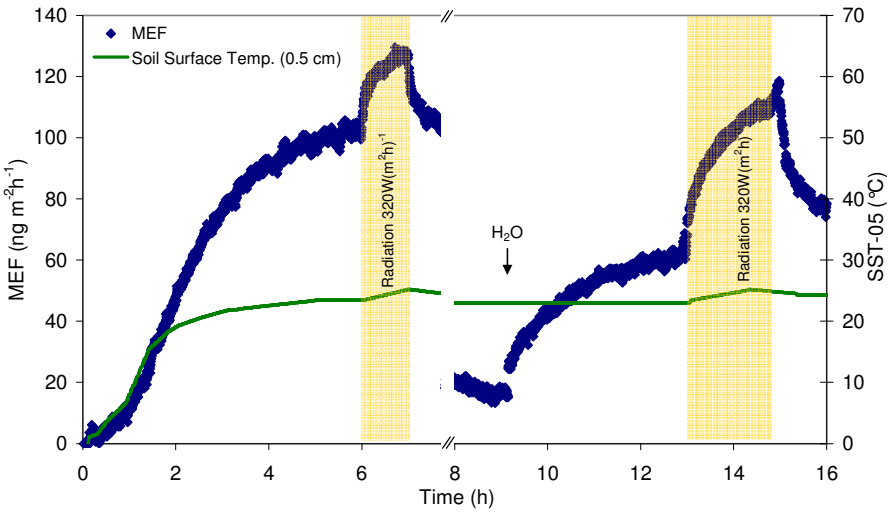

Figure 66: *Mercury emission flux (MEF) measured under different simulated conditions (temperature, precipitation and UV light induced), location Travnik A (forest soil).*

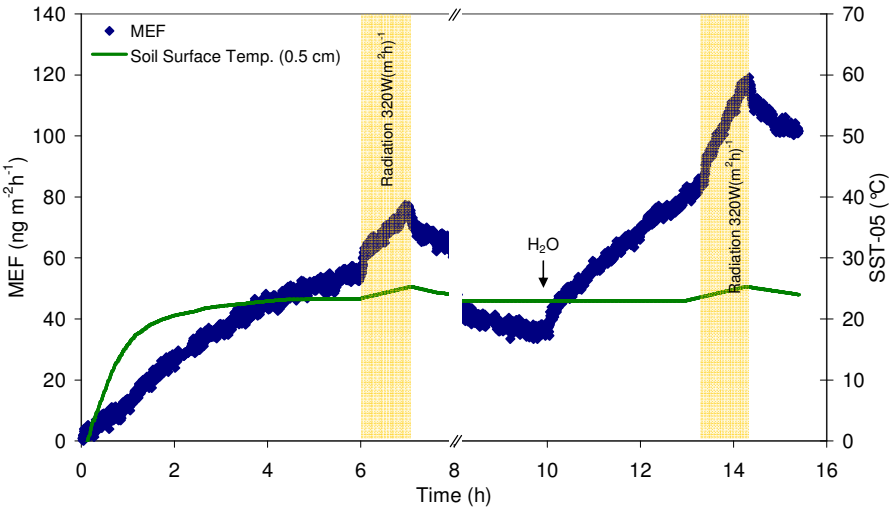

Figure 67: *Mercury emission flux (MEF) measured under different simulated conditions (temperature, precipitation and UV light induced), location Travnik B (meadow soil).*

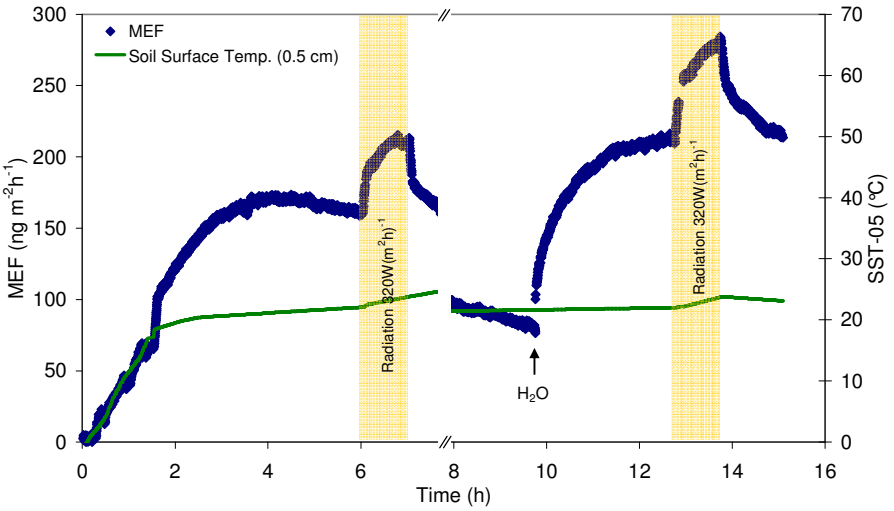

Figure 68: *Mercury emission flux (MEF) measured under different simulated conditions (temperature, precipitation and UV light induced), location Travnik C (alluvial soil).*

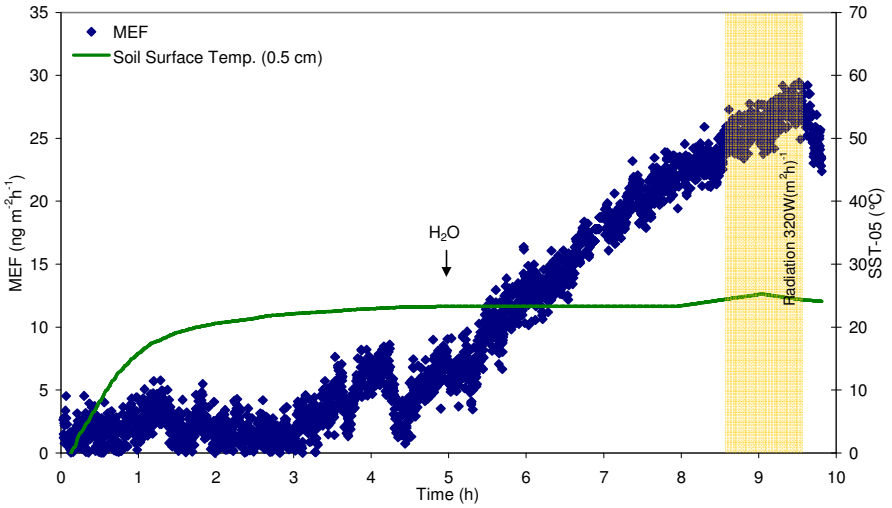

Figure 69: *Mercury emission flux (MEF) measured under different simulated conditions (temperature, precipitation and UV light induced), location Reka A (forest soil).*

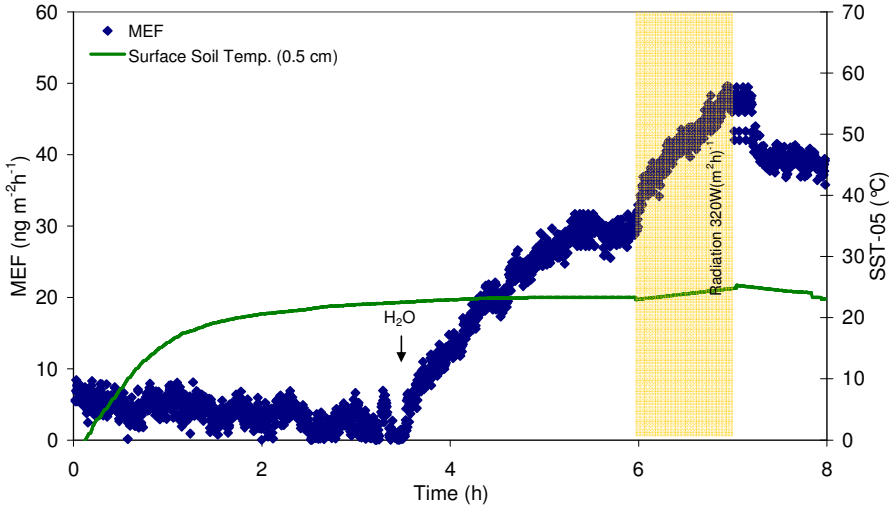

Figure 70: *Mercury emission flux (MEF) measured under different simulated conditions (temperature, precipitation and UV light induced), location Reka B (meadow soil).*

5.6.2.1 Effect of soil temperature

The effect of soil temperature on MEF was investigated in the temperature range between 0 and 25 ºC. Temperature was measured at the depth of 5 mm. Following observations presented in Carpi and Linberg (1998), this is the soil layer thickness over which reduction of non-volatile Hg species to volatile ones occurs. For all soils a strong correlation between the soil surface temperature and the MEF with correlation coefficients between 0.798 and 0.8512 was observed. At temperatures below 0 ºC no mercury flux was measured or the fluxes were below the limit of detection (3.6 ng m^{-2} h^{-1}), respectively. As it can be seen from Fig. 64-68, in the 0-10 ºC range Hg emission can be described by a linear function whereas the Hg emission rate increases logarithmically from 10 to 25 ºC.

Thermally controlled emission of mercury from soils is governed by the interfacial equilibrium of Hg^0 between the soil matrix and the soil gas. As suggested by Schluter (1996), vapor pressure of highly volatile Hg^0 is increased and sorption by soil is decreased due to increasing thermal motion. Increased temperature also causes an increase in reaction rates and microbiological activity resulting in a more intensive formation of volatile mercury species. Similar temperature affects were observed by other authors (e.g. Zhang et al., 2001; Bahlmann et al., 2006).

One way to understand the processes driving the thermally enhanced emissions is to calculate the activation energy associated with Hg flux. The activation energy (E_a) is the energy necessary for the system to absorb in order to initiate a Hg flux increase, or Hg emission, or release from soils to occur. Assuming

that the transfer of Hg^0 from soil to atmosphere is governed by pseudo first order reaction, the temperature dependence of Hg fluxes over the soil surface can be described by Arrhenius equation,

$$k = A \cdot e^{-\frac{E_a}{R \cdot T}} \tag{6}$$

where

k … flux of Hg,
R … gas constant,
T … temperature in degrees Kelvin,
A … preexponential frequency factor and
E_a … activation energy.

Hg flux plotted as a function of temperature was used to calculate the activation energy (*Ea*) for the observed Hg flux. To a first approximation, A is found to be independent of temperature for many reactions, so that a plot of *ln k* (here, Ln MEF) versus 1/T gives a straight line of slope *–Ea/R* and intercept equal to Ln A. In Fig. 70 correlations between the reciprocal absolute temperature of the surface soil (0.5 cm depth) and the Ln MEF for samples investigated are shown.

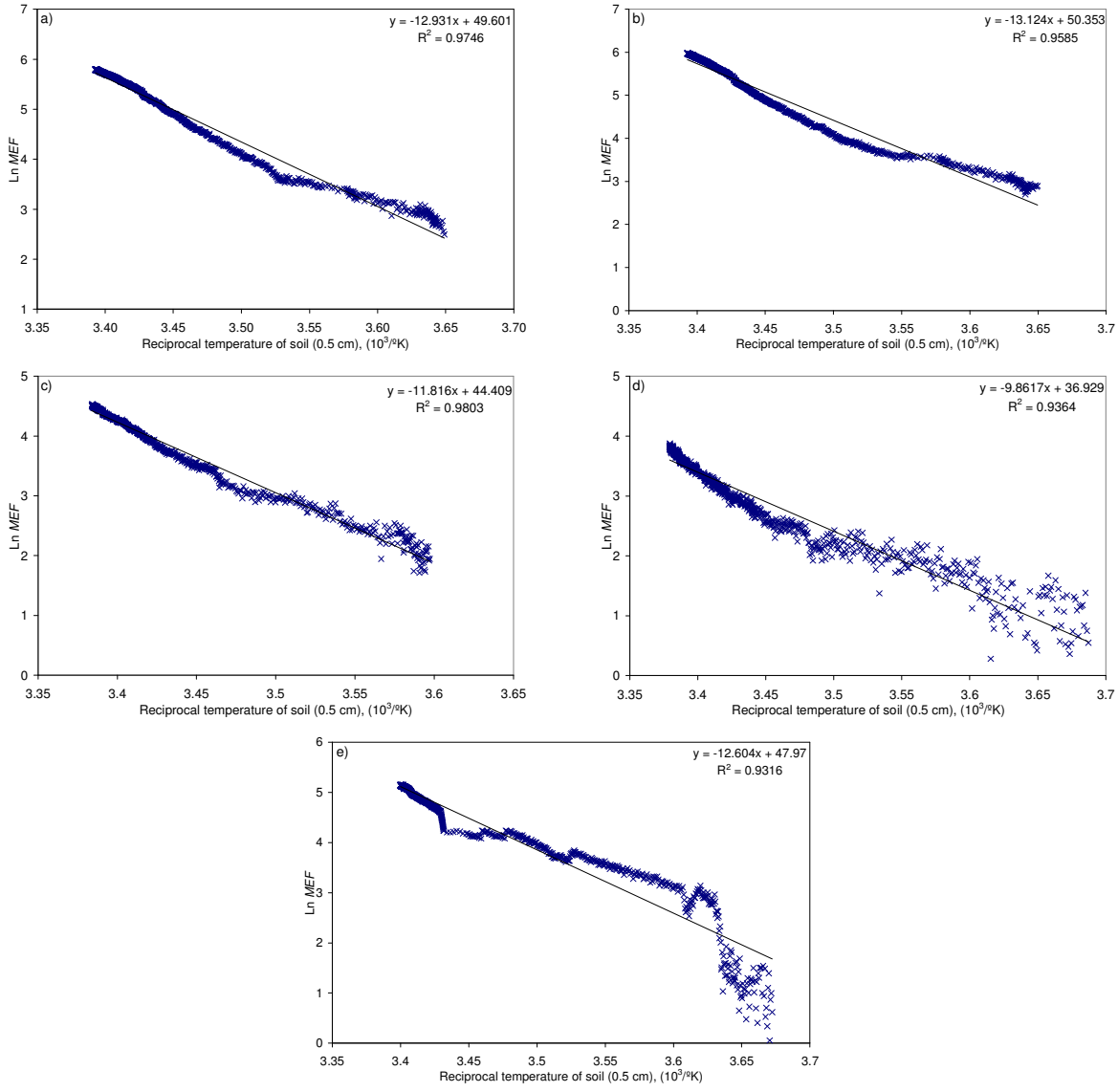

Figure 71: *Temperature dependence of mercury flux over the soil surface, Arrhenius plots for samples a) Idrija A, b) Idrija B, c) Travnik A, d)Travnik B and e) Travnik C.*

Callculated activations energies (Ea) and belonging preexponential frequency factors (given as *LnA*) are given in Table 8. These activation energies are in a good agreement with published data for mercury contaminated soils (Schluter, 2000) where HgS is predominantly mercury form and are somewhat higher than values reported for background soils (e.g. Bahlmann et al., 2006; Gustin et al., 1997; Poissant and Casimir, 1998). Since the enthalpy of vaporization of elemental Hg is much lower than the measured Ea (58 kJ mol^{-1} compared to 82-109 kJ mol^{-1}), it is evident that Hg emissions from soils can not solely be explained by the direct emission of elemental Hg from the soil surface.

Table 8: *Calculated activation energies and frequency factors.*

Sample	Ea (kJ mol^{-1})	Ln(A)
Idrija A	108	49.60
Idrija B	109	50.35
Travnik A	98	44.41
Travnik B	82	36.93
Travnik C	105	47.97

In contrast to previously published results (e.g. Schluter, 2000; Bahlmann et al., 2006), the apparent *Ea* for the emission of mercury from soils did not show any decrease with increasing total mercury concentrations in soils, although total Hg concentrations in soils investigated varied over a wide range of values (from 4 to 417 µg g-1). On contrary, as shown in Fig. 72 the results indicate that *Ea* increases logarithmically with increasing mercury concentration in soil.

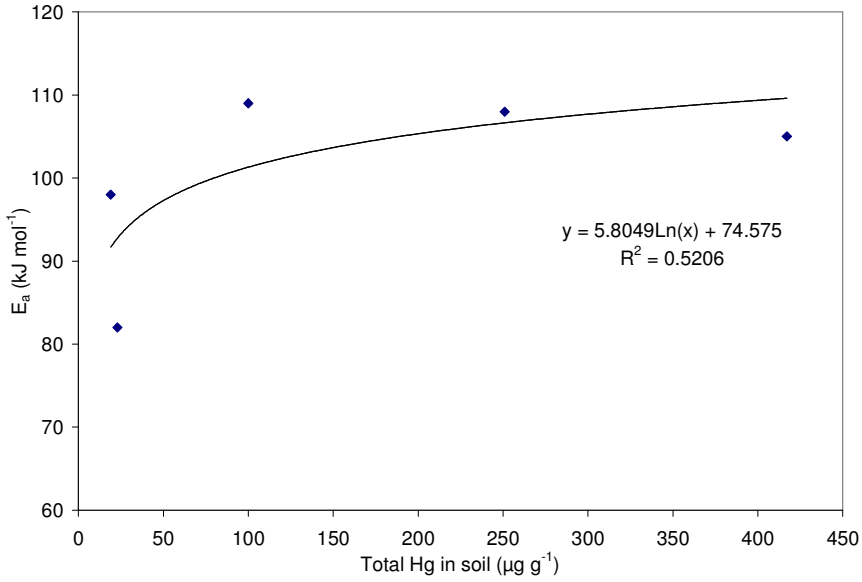

Figure 72: *Lin–ln relation between the apparent activation energy (E_a) of MEFs and total mercury concentration in soils.*

Significantly higher activation energies were obtained for mercury contaminated soils from location Idrija and alluvial soil compared to less contaminated samples from location Travnik. These results indicate the importance of not only amount but also the mercury species and their binding in soils. It is known that increasing availability of mercury in soils to the abiotic and biotic processes would increase the formation of volatile mercury species. As reported by Schlüter (2000) in his review of the mercury evaporation in soil, mercury evaporation occurs most easily in soils rich in Hg^0, followed by soils dominated by inorganic Hg2+, which is bound to soil components and probably relatively easily available for transformation to volatile mercury species. The highest activation energy of mercury evaporation is usually found in soils whose mercury content is dominated by the extremely unsoluble, and therefore for transformation probably relatively unavailable, HgS. Consistent with this, the highest activation energy of mercury evaporation was found in Idrija soils whose mercury content is dominated by the extremely unsoluble HgS (Kocman et al., 2004 in Appendix C). On contrary, dominating inorganic Hg^{2+} bound to soils at Travnik sampling site (Travnik A and B, respectively) as a consequence of atmospheric deposition resulted in lower activation energies.

5.6.2.2 Effect of solar radiation

Immediately after the soils were radiated with 320 W/m^2 MEFs increased by 25-60 % compared to fluxes obtained under dark conditions. A steep decrease of MEFs followed approximately 10 min after the end of radiation. Fluxes became more constant within the next hour. However, they were still higher as before the radiation phase. Based on the decreasing rates Bahlmann et al. (2006) calculated a mean half-life of 20 h for the light-induced flux over dry soils and a mean half-life time of 63 h for the light-induced fluxes over wet soils. One of the reasons for the elevated MEFs could be also temperature which increased and remain elevated from 1 to 2 ºC during the 1 h radiation in the upper 0.5 cm soil layer. To check this effect, measured fluxes under light radiation were compared to the calculated fluxes using the temperature dependency of MEF:

$$Ln(MEF) = Ln(A) - \frac{E_a}{R \cdot T} \tag{7}$$

where E_a is the apparent activation energy, A is the frequency factor, T is the absolute temperature and R is the gas constant. The modeled fluxes using the temperature dependency underestimated substantially measured fluxes during radiation phases (Table 9). Hence, the observed increase of the soil surface temperature only accounts for a minor fraction of the observed increase of the MEFs. The results show that the light-induced flux is independent of the soil temperature. This reveals evidence of a photolytical reduction of divalent mercury species at the soil surface as previously reported by other authors (e.g. Carpi and Lindberg, 1998; Gillis and Miller, 2000; Zhang et al., 2001). Although high, observed light-induced offset was much smaller than reported by other authors. This is due to the fact that other authors measured fluxes over bare soil, while here MEFs measured over soil covered with a vegetation cover are reported. Obviously, a part of the energy induced by the radiation is subtracted by the canopy. However, it must be noted that during the experiment, radiation was stopped after 1 h, before the light-induced offset became constant and reached its maximum, respectively.

Table 9: *Measured vs. calculated fluxes.*

Sample	MEF measured	MEF calculated	Difference (%)
Idrija A	452	328	38
Idrija B	526	463	14
Travnik A	129	105	23
Travnik B	77	46	67
Travnik C	211	187	15

5.6.2.3 Effect of soil moisture

Usually, each sample was processed within two days. During the night hours, the experiment was stopped for about 12 hours and the sample was left at the room temperature without the flow flushing through the system. After 12 h when samples were further investigated, a significant decrease of MEFs was observed. MEFs measured under standard operation conditions became 1.5-2.3 fold lower. This decrease can be explained by the change of the soil surface moisture which decreased between 4 and 9 % within last 12 h. There is a good agreement between the magnitude of the MEF decrease and the change of surface soil moisture among individual samples. Even more important, after defrosting when samples heated to the room temperature, soil water started to slowly diffuse from the surface to the deeper soil layers. Consequently soil moisture tension in the upper surface layer became weaker. As demonstrated by Bahlmann et al. (2004), MEFs over soils can be in a big part controlled by soil moisture tension, not only by the soil moisture level. During the experiment, rather rapid decrease of both soil moisture and soil moisture tension is enhanced by a fan installed for continuous mixing of incoming air, which is not a case under natural conditions.

Soils rewetting (precipitation simulation) resulted in a sharp and rapid spike of the MEFs for all samples. MEFs increased 1-3 folds within first 20 min. This sharp spike immediately after the rain event is consistent with the physical displacement of interstitial soil air by the infiltrating water. The enhanced emissions are thought to be due to the more polar water molecules out-competing the Hg for binding sites on the soil facilitating its release (Gustin, 2003). Afterwards, fluxes were slowly increasing until became constant within next 3-4 hours. However, different samples revealed different picture. For example, although very deficient in terms of total Hg concentrations compared to other samples, two samples collected at Reka site revealed the strongest response to simulated precipitation. Moreover, MEF measured

from these two samples before rewetting under standard operation conditions were below or close to the detection limit of the Lumex 915+ instrument. The series of experiments conducted and the knowledge of very various general meteorological conditions at different sampling sites suggest that the flux of Hg^0 from soil is a function of not only the precipitation but also of the soil moisture content prior to the rain event. At higher initial soil moisture levels there is a much lower enhancement in MEF compared to drier initial soil moisture levels.

To further investigate this effect, the surface soil moistures before a precipitation simulation and the enhancement of the MEF due to the precipitation were correlated using a precipitation enhancement factor, *f*, defined as:

$$f = \frac{MEF_{aft} - MEF_{bf}}{MEF_{bf}} \tag{8}$$

where MEF_{aft} is the mercury flux value calculated for the 20 min period immediately after the simulated precipitation and MEF_{bf} is the mercury flux value determined just before the simulated precipitation. A plot of the resulting precipitation enhancement factor versus the surface soil moisture before the rain event is given is Fig. 72. The figure clearly indicates a declining trend in the precipitation enhancement factor with increasing surface soil moisture. The data thus indicate that, although there is a spike in Hg^0 emissions during the rain event due to physical displacement, the enhancement of the Hg flux after the rain event is mach lower if the surface soil moisture is greater than approximately 15%.

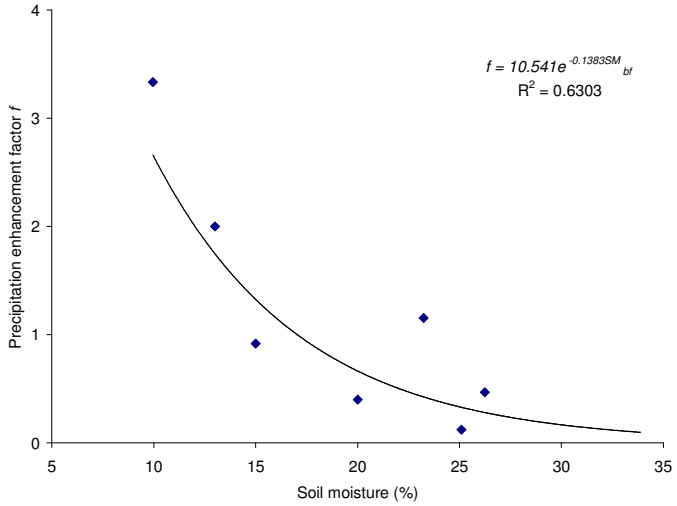

Figure 73: *Precipitation enhancement factor versus surface soil moisture before a simulated precipitation.*

These observations imply that the process responsible for the enhancement of Hg^0 emissions from the soil is connected to the mercury aqueous soil phase. As most of the mercury in the soil exists in the reactive form as Hg^{2+} (McKay et al., 1995), the mercury must undergo both ionic and phase changes to gaseous Hg prior to being emitted to the atmosphere. Two pathways, where the aqueous phase may have the potential to either limit or enhance the emission of Hg^0 from the soil surface, are the mobility of Hg^{2+} by dissolution from soil particles into the soil aqueous phase and by enhanced aqueous redox reactions that transforms Hg^{2+} in the soil solution to Hg^0 (Lindberg et al., 1999). As demonstrated during the soil leaching experiments (see section 5.3.2.3.1) these processes are most probably controlled by both the organic matter content (OM) in soil as well as concentrations of dissolved organic matter (DOM) in the aqueous soil phase.

6 Modeling of mercury cycling in the Idrijca River catchment

In this chapter mercury cycling in the Idrijca River catchment based on its mass balance budgets is presented and discussed. This section describes the models and modeling scenarios used to predict the environmental fate of mercury. Measured mercury concentrations in environmental media were used when available to parameterize these models. Integrating models and the results of field measurements presented in the previous chapter the mass balance of mercury was determined. With this approach, accounting for mercury entering and leaving the catchment, its mass flows were identified which otherwise might have been unknown or difficult to measure. The main aims of modeling were as follows:

– relating the processes, reservoirs and fluxes/loads of the mercury cycle to estimate main sources and sinks of mercury at the catchment scale,
– to estimate reservoir masses, flux rates, and turnover times,
– to assess the impact of anthropogenic mercury sources on its cycle,
– to simulate future trends of mercury contamination at the catchment scale.

6.1 Modeling framework

An analysis at the catchment scale could be conducted at various levels of complexity, ranging from simplistic gross estimates to dynamic models. When choosing what model to use for a particular area and a certain problem, several factors must be considered, e.g. the modeling purpose, the model representation, data requirements and availability, and the ease of parameter estimates. Taking these factors into account, in the present study a scoping-level analysis of the mercury mass balance model, based on an annual mass balance of water, sediment loading from the catchment and annual atmospheric deposition were used.

The modeling domain is the area of the Idrijca River catchment. Four reservoirs (atmosphere, land, water, sediment) are conceptualized within this domain, related through four transfer processes. A schematic of the modeling approach that illustrates the major transport and transformation processes considered in this study is given in Figure 74. The following mercury terms were taken into account: inputs due to the deposition of particle-bound mercury through dry fall, deposition through wet fall and litterfall. Hg output terms include gaseous flux from soil to air by volatilization, vertical hydrologic transport through soil by percolation, and horizontal hydrologic transport from surficial soil by runoff water and runoff erosion particles. While it is recognized that the land and water reservoirs have biota sub-reservoirs (e.g., land: forest, water: fish), these were not quantified in the present model due to insufficient data. These processes have not been studied since the problems are rather complex and are out of the scope of the present study. Details are provided in the following sections.

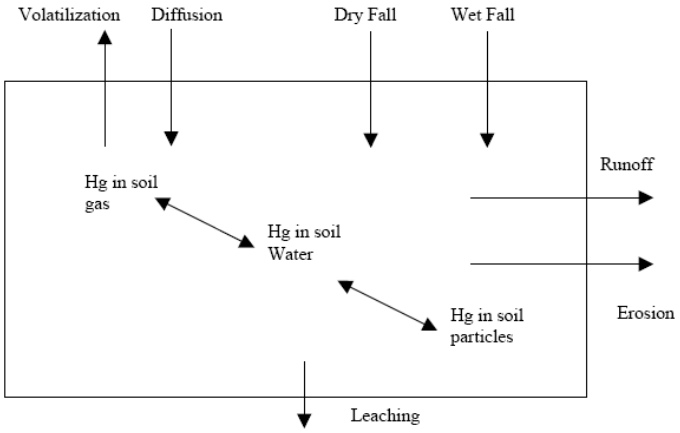

Figure 74: *Overview of the major processes in the mercury soil mass balance model (source: US EPA, 1997)*

6.2 Theoretical basis and assumptions of the mercury mass balance model

With the aim of establishing mercury mass balance, its transport and geochemical cycling in the Idrijca River catchment on a yearly basis, combined modeling approaches were used and adjusted for site specific conditions. To account for the spatial heterogeneity of the catchment, advantages of the geographical information system (GIS) were used and incorporated into models. A schematic of the modeling approach that illustrates the major modules and the GIS databases used is given in Figure 75 and described here as follows:

- The net precipitation and throughfall Hg measurements were used to calculate a long-term atmospheric deposition rates.
- For the calculation of mercury terrestrial loads to the water system approach adopted from the Watershed Characterization System (WCS) which was derived from IEM-2M, the U.S. EPA mercury fate spreadsheet documented in the Mercury Report to Congress (U.S. EPA, 1997), was used. The complexity of this loading function model falls between that of a detailed simulation model, which attempts a mechanistic, time-dependent representation of pollutant load generation and transport, and simple export coefficient models, which do not represent temporal variability. It provides a mechanistic, simplified simulation of precipitation-driven runoff and sediment delivery. Solids load and runoff are used to estimate mercury delivery to the receiving waterbody from the catchment. This estimate is based on mercury concentrations in wet and dry deposition and processed by soils in the watershed and ultimately delivered to the receiving waterbody by runoff, erosion and direct deposition.
- Analytical equations for determining the annual volume of detached soil due to surface erosion and an area-based sediment delivery ratio proposed by Gavrilović (1972, 1976, 1988) were used.
- Hydrology module for the calculation of mercury load from surface runoff: The hydrology module includes a the long-term average yearly water balance, including precipitation, surface runoff, evaporation and infiltration. Spatial water mass balance at the catchment scale was established using the advantages of geographical information system (GIS).
- Based on the results of the laboratory flux chamber experiment Hg model was build within the geographical information system (GIS) environment to scale-up annual Hg emissions to the atmosphere at the catchment scale.

Key assumptions in the mercury mass balance model are:

- The study area (Idrijca River catchment) can be subdivided into smaller subcatchments (hydrographic units) which have homogeneous characteristics with respect to the mercury behaviour.
- Soil mercury concentrations within a hydrographic subunit are uniform and can be estimated by the following key parameters: dry and wet contaminant deposition rates, a set of soil transformation rates, a soil bulk density, and a soil mixing depth.
- The partition of mercury components among soil water and soil particle phases can be described by partition coefficient.
- Dissolved Hg is lost from the surficial soil layers through infiltration and runoff. Particulate Hg is lost through water runoff erosion. Infiltration carries an insignificant loading of mercury to the shallow groundwater due to the high sorption to soil solids.
- Subwatershed Hg loadings in runoff water and runoff erosion particles are delivered to the catchment tributary system.
- Because atmospheric mercury deposition is primarily Hg^{2+}, and because concentrations of Hg^0 and MeHg are much less than Hg^{2+} in soil, soil mercury is treated as a single total mercury component.
- A fraction of the soil Hg is reduced and volatilized back to the atmosphere. Reduction of Hg^{2+} is much slower than volatilization of Hg^0. This 2-step loss process is represented as a single step controlled by the reduction rate constant. Mercury reduction loss is assumed to be equal to the volatilization loss.
- The total runoff of an area is a simple sum of the runoff of hydrographic subunits, and there is no mercury loss when it is transported from a source to the outlet through the runoff.
- The sediment transport can be described using an area-based delivery ratio formula.

The nature of this methodology is quasi-steady with respect to time and homogeneous with respect to space. While it tracks the buildup of soil and water concentrations over the years given a steady

depositional load and long-term average hydrological behavior, it does not respond to unsteady loading or meteorological events.

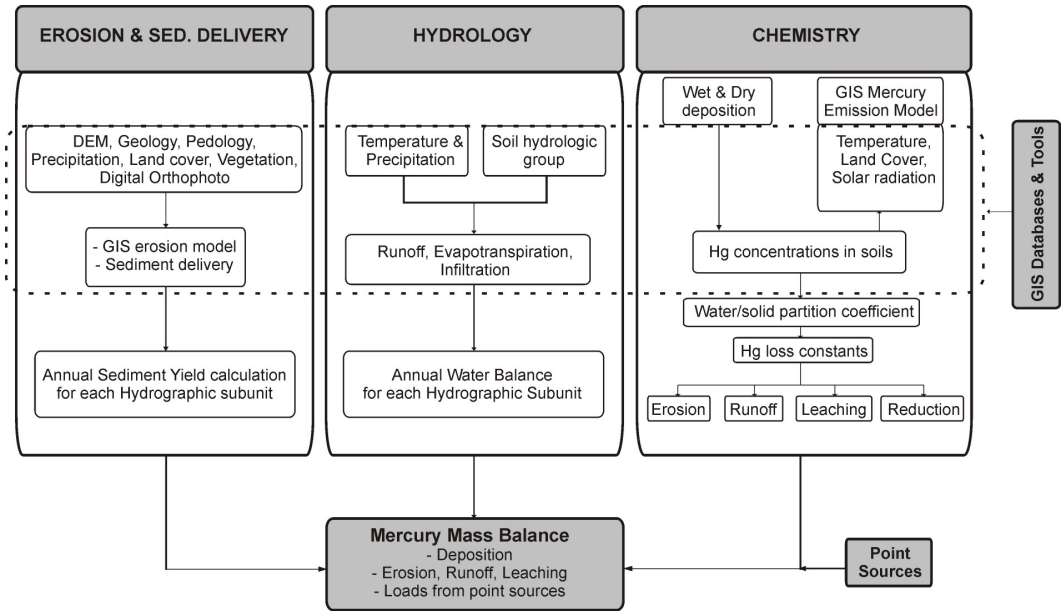

Figure 75: *Overview of the Mercury Mass Balance Model*

For modeling purposes, the Idrijca River catchment was delineated into 64 smaller subcatchments (hydrographic units). In this way, it was possible to calculate mercury loads to the Idrijca River at various points along its length. Division of the study area allowed more accurate estimation of the sediment trapping within the catchment. Moreover, in terms of mercury spatial distribution and transformations in soils, individual hydrographic units have more uniform characteristics. The division was based on the catchment delineation thematic GIS map obtained from the Environmental Information and Observation Network (EIONET) for Slovenia. Figure 76 shows the modeling hydrographic subunits, coding system and major hydrography of the Idrijca River catchment.

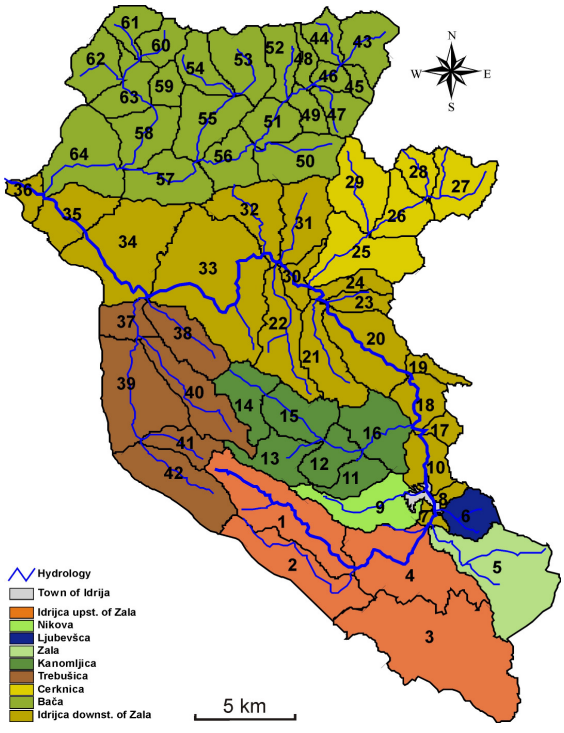

Figure 76: *Hydrographic subunits, coding system and major hydrography of the Idrijca River catchment*

6.3 Processes in the model: mathematical description and parameterization

6.3.1 Loads to catchments soils

In the total atmospheric loading term (L_{atm}) in the mass balance calculation the sum of the wetfall, dryfall and throughfall was taken into account. In the present study dry deposition of mercury was not measured directly. However, since during sampling the sampling vessels open at all times were used, for the sum of wetfall and dryfall, deposition rates were calculated from the mercury concentrations in precipitation. For the throughfall, net throughfall deposition (total throughfall deposition minus precipitation deposition) was calculated based on the mercury concentrations in throughfall samples. Deposition rates (ng m^{-2} day^{-1}) were calculated on an event basis by dividing the deposition (ng m^{-2}) by the number of days sampling vessels were exposed. The following equation was then used to represent total annual atmospheric deposition:

$$L_{atm} = D_{d+w} \cdot A_H + D_{tf} \cdot A_f \tag{9}$$

where:

L_{atm}... annual atmospheric loading (g yr^{-1})
D_{d+w} ... annual dry and wet deposition rate (g m^{-2} yr^{-1})
D_{tf} ... annual throughfall deposition rate (g m^{-2} yr^{-1})
A_H ... area of the hydrographic subunit (m^2)
A_f ... area of the hydrographic subunit covered by forest (m^2)

6.3.2 Transport and transformation processes in catchment soils

In the mass balance model, two mercury soil phases were taken into account: dissolved (Hg in soil water) and particulate (Hg bound in/to soil particles) phase, respectively. The total concentration of both mercury phases in soil is assumed to reach equilibrium described by the soil water partition coefficient.

The total transport loss of mercury from the soil is the sum of the loss rates due to leaching, runoff, erosion, and volatilization. In the governing mass balance equations, these loss rates are expressed as the product of a loss rate constant, the total dissolved and particulate phase concentration, and the soil volume.

Soil mercury water and solid fraction at equilibrium:

Fraction of mercury in the dissolved and particulate phase, respectively, depends on the amount of water that a given volume of soil can hold and mercury concentrations in soil and soil water. It is described by the following two equations:

$$f_{ws} = \frac{\Theta_w}{\Theta_w + K_{ds} \cdot BD} \tag{10}$$

$$f_{ps} = \frac{K_{ds} \cdot BD}{\Theta_w + K_{ds} \cdot BD} \tag{11}$$

where:

f_{ws} ... soil mercury water fraction
f_{ps} ... soil mercury solid fraction
θ_w ... soil volumetric water content (ml cm^{-3})
K_{ds} ... soil water partition coefficient (ml g^{-1})
BD ... soil bulk density (g cm^{-3})

Amount of water that a given volume of soil can hold depends on the type of the soil. These values were derived from the hydrologic soil group classification and can range from 0.15 to 0.42 ml cm^{-3} for soils with low and high runoff potential, respectively. Based on the knowledge of characteristics and spatial distribution of soils in the study area, a uniform value of 0.25 ml cm^{-3} was used.

The partition coefficient (K_{ds}) is the ratio of the mercury concentration sorbed onto soil particles to that dissolved in soil water at equilibrium. The adsorptive properties of mercury can depend on a variety of environmental factors: pH of soil, amount of organic matter in the soil or water, percent of sand, silt or clay in soil, other chemicals present and even the magnitude of the chemical concentration in the water itself. Because of the complicated nature of the sorptive process, and because of the varying amounts of relatively inorganic mineral fractions, reported values for the partition coefficient can vary over many orders of magnitude. For the upper soil layer values for K_{ds} were reported to range between 24.000 and 270.000 L kg^{-1}, with a mean value of about 60.000 L kg^{-1} (Lyon, 1997). Site specific partition coefficients used in this study were calculated from the measured data on Hg concentrations in soils and soil water soluble fraction. Two different values were used: 250.000 L kg^{-1} for most mercury contaminated soils between the town of Idrija and Spodnja Idrija, and 100.000 L kg^{-1} for the rest of the catchment.

Leaching loss rate constant:

The leaching loss rate constant is a function of the leaching volume and the dissolved mercury fraction and is calculated by the equation (12). The first term times the soil volume is the annual percolation volume, while the second term times the total concentration is the aqueous concentration in percolating water.

$$ks_L = \left(\frac{I}{z_d} \right) \cdot \frac{f_{ws}}{\Theta_w} \tag{12}$$

where:

ks_L ... leaching loss rate constant (yr^{-1})
I ... infiltration (cm yr^{-1})
z_d ... watershed soil incorporation depth or mixing depth (cm).

Infiltration is a part of precipitation that remains from precipitation after evapotranspiration and surface runoff is subtracted. For calculation of the leaching loss rate constant, digital infiltration map provided by the Geological Survey of Slovenia was used. In this map infiltration (mm $year^{-1}$) was estimated based on the infiltration coefficients by the Kennessy methodology, using slope, land cover and lithostratigraphical maps. For each hydrographic subunit an average value for yearly amount of infiltration was calculated using the advantages of the GIS. Based on the observations of Hg vertical distribution in soil (section 5.3) soil mixing depth (z_d) was set to 20 cm.

Runoff loss rate constant:

The runoff loss constant is a function of the runoff volume and the dissolved mercury fraction and is calculated by equation (13). The first term times the soil volume is the annual runoff volume, while the second term times the total concentration is the aqueous concentration in the runoff.

$$ks_{Ro} = \left(\frac{R_o}{z_d} \right) \cdot \frac{f_{ws}}{\Theta_w} \tag{13}$$

where:

ks_{Ro} ... runoff loss rate constant (yr^{-1})
R_o ... runoff (cm).

For calculation of the runoff loss rate constant, digital infiltration map provided by the Geological Survey of Slovenia was used. In this map, the amount of surface runoff was calculated as a product of effective precipitation (difference between precipitation and evapotranspiration) and surface runoff coefficient that was derived with Kennessy methodology, using slope, land cover and lithostratigraphical maps. The evapotranspiration was estimated with Turc's formula, where the distribution of average yearly precipitation and temperature for the period from 1961 to 1990 were used. For each hydrographic subunit an average value for yearly amount of runoff was calculated using the advantages of the GIS.

Reduction loss rate constant:

Following observations presented and discussed in section 5.6, it can be assumed that the net flux of Hg° from the soil surface to the atmosphere is driven by the reduction of Hg^{2+}. Reduction rate constants were derived from evasion flux measurements over soil. Following the procedure described by Tsiros and Ambrose (1999), an equation was developed for the reduction rate constant calculation:

$$MEF = K_r \cdot C_{Hg} \cdot BD \cdot z_r \cdot \Theta_w \tag{14}$$

where:

MEF ... net mercury emission flux (µg m^{-2} $year^{-1}$)
K_r ... reduction rate constant normalized to soil water content
C_{Hg} ... concentration of mercury in soil (µg kg^{-1})
z_r ... soil layer thickness over which reduction occurs (mm)

There is evidence that reduction in soil is mediated by sunlight, is proportional to soil water content, and occurs most rapidly within the upper 5 mm of the soil surface (Carpi and Lindberg, 1997). As a result, the input reduction rate constant is normalized to a reference depth of 5 mm and 100% water content. To derive the reduction rate constant ks_{red} used in the model, K_r must be multiplied by the soil water content and averaged over the entire soil depth. First, the observed fluxes were modified to represent annual averages (see GIS Mercury Emission Model in section 6.6).

$$ks_{red} = K_{rs} \cdot \Theta_w \cdot \left(\frac{z_r}{z_d} \right) \cdot 365 \tag{15}$$

where:

ks_{red} ... reduction loss rate constant (yr^{-1})
K_{rs} ... soil base reduction rate (day^{-1})
z_r ... soil reduction depth (cm).

Erosion loss rate constant:

The erosion loss constant is a function of the erosion mass and the particulate mercury fraction. The first term times the soil volume is the annual erosion mass, while the second term times the total concentration is the sorbed concentration on the eroding particles.

$$ks_E = \left(\frac{Xe \cdot SDR \cdot ef}{z_d} \right) \cdot \frac{f_{ps} \cdot 10^7}{BD} \tag{16}$$

where:

ks_E ... erosion loss rate constant (yr^{-1})
Xe ... erosion (kg km^{-2} yr^{-1})
SDR ... sediment delivery ratio
ef ... mercury enrichment factor.

The enrichment factor accounts for the fact that eroding soils tend to be lighter in texture, more mercury abundant in surface area, and higher in organic carbon. All these characteristics lead to concentrations in eroded soils that tend to be higher than those in *in situ* soils. Mullins et al. (1993) described the following equation for calculating enrichment factor that was used in the present study:

$$ef = 2 + 0.2 \cdot \ln\left(\frac{Xe}{A_H} \right) \tag{17}$$

Calculated values for enrichment factors range between 2.02 and 2.57 for individual hydrographic subunit. These values are close to the correction factor of 1.8 calculated by Žibret and Gosar (2006) that was used to represent the difference between the Hg concentration in the fraction, smaller than 0.063 mm and the concentration in the bulk overbank alluvial plain sediments of the Idrijca River.

Annual soil erosion (*Xe* in kg km^{-2} yr^{-1}) and sediment delivery ratios (*SDR*) were estimated by the Erosion Potential Method (EPM). The application of the EPM model is described into more detail in section 6.5.

Resultant soil concentration:

Based on the loss rate constants from leaching, runoff, reduction and erosion, the resultant soil concentration can be calculated by the equation (18), as suggested by the Dai and Manguerra (2000).

$$C_s = \left[C_0 \cdot e^{-ks_{total} \cdot T}\right] + \frac{D \cdot \left[1 - e^{-ks_{total} \cdot T}\right] \cdot 10^5}{z_d \cdot BD \cdot ks_{total}} \tag{18}$$

where

C_s ... soil mercury concentration at equilibrium (ng g^{-1}),
C_0 ... initial soil mercury concentration (ng g^{-1}),
ks_{total} ... soil mercury loss rate (yr^{-1}) from leaching, runoff, and erosion,
z_d ... watershed soil incorporation depth or mixing depth (cm),
BD ... soil bulk density (g cm^{-3}),
T ... deposition period (yr^{-1}),
D ... annual atmospheric mercury deposition rate (g m^{-2} yr^{-1})

6.3.3 Loads to catchment tributary system

In the mass balance calculation, the total mercury load (L_{total}) to the Idrijca River catchments tributary system is the sum of loadings including dissolved Hg lost from the surficial soil layers through surface runoff and particulate bound Hg lost through water runoff erosion:

$$L_{total} = L_{runoff} + L_{erosion} \tag{19}$$

where

L_{total} ... total load to the tributary system
L_{runoff} ... surface runoff load
$L_{erosion}$ ... erosion load

Load due to surface runoff:

During periodic runoff events, dissolved mercury is transported to surface waters as given by the following equation:

$$L_{runoff} = ks_{Ro} \cdot V_s \cdot C_s \cdot BD \tag{20}$$

where

L_{runoff} ... mercury surface runoff load (g year^{-1})
ks_{Ro} ... soil runoff rate constant (year^{-1})
V_s ... soil layer volume (m^3)
C_s ... soil mercury concentration

Load due to soil erosion:

During periodic erosion events, particulate bound mercury in the soil is transported to surface waters as described by the following equation:

$$L_{erosion} = ks_E \cdot V_s \cdot C_s \cdot BD \tag{21}$$

where

L_{runoff} ... mercury surface runoff load (g year^{-1})
ks_{Ro} ... soil runoff rate constant (year^{-1})
V_s ... soil layer volume (m^3)
C_s ... soil mercury concentration

6.3.4 Output flux from the catchment

Output flux from the Idrijca River catchment due to the riverine transport was calculated for different mercury compounds. Fluxes were calculated for different parts of the catchment where data on both water discharges and mercury concentrations in water were available. Calculated fluxes were used for validation of the modeling results. In the Idrijca River catchment, water discharges are measured at five gauging stations: in Podroteja and Hotešček at the Idrijca River, in Cerkno at the Cerknica River, in Dolenja Trebuša at the Trebušica River and in Bača pri Modreju at the Bača River. The flux of mercury at these stations was calculated by the following equation:

$$F_{out} = C_w \cdot \Phi \tag{22}$$

where

F_{out} … mercury flux from the catchment (ng day^{-1})
C_w … concentration of mercury in river water (ng m^{-3})
Φ … water discharge (m^3 day^{-1})

6.4 Mercury data: mercury in soil spatial distribution

For development of soil mercury mass balance equations, including atmospheric deposition, transformation and transport processes, a good knowledge about spatial distribution of mercury in the surface soil is needed. Spatial distribution of mercury concentrations in soil at the catchment scale was assessed based on the point source data obtained in the present study and from the data reported in the literature (Hess et al., 1993; Palnikaš et al., 1995; Gnamuš et al., 2000; Kocman et al., 2004; Gosar et al., 2006; Žibret and Gosar, 2006). Here, a short literature overview is given, as follows.

The spatial distribution of mercury in soil on an 8×14 km area with Idrija at the center was studied by Hess (1993) in a regular 1 km grid (127 sample sites). Mercury concentrations above 10 mg kg^{-1} were detected in soils in valleys and at foot of slopes, and lower values in higher parts and at margins of the sampled area.

Palinkaš et al. (1995) reported results of Hg pollution in the vicinity of the Idrija mercury mine. Soils were sampled at 52 locations distributed in an irregular grid. The maximum value (87.6 mg kg^{-1}) was determined in the mining area. The mean mercury concentration in the soils was 15 mg kg^{-1}. The distribution of mercury along four vertical profiles suggested a predominant influence of atmospheric deposition on the accumulation of Hg.

Kocman et al. (2004, Appendix C) separated Hg phases in contaminated soil in the Idrija Hg-mine region by a selective sequential extraction procedure complemented by volatilization of elemental mercury. Fractionation measurements indicated cinnabar as the predominant Hg fraction, followed by Hg^0. Accumulation of cinnabar predominantly occurred in coarse grained flood plain sediments, where on average it constituted more than 80% of total Hg. In contrast, non-cinnabar fractions were found to be enriched in areas where fine grained material was deposited, reaching up to 60% of total Hg. In that study, 41 to 51 mg kg^{-1} were found in soil samples taken in the area which is not under the direct influence of mining activity, and 322 to 345 mg kg^{-1} in samples taken nearby the smeltery. High amounts of mercury (60 to 415 mg kg^{-1}) were also detected in samples from the alluvial plains downstream of Idrija.

On the basis of the investigated soil and attic dust samples in the 160 km^2 area around Idrija, Gosar et al. (2006) established that mercury concentrations in soil exceed the critical values for soil (10 mg kg^{-1}) on 19 km^2. The estimated weighted mercury average for the studied area was 1.3 mg kg^{-1} (0.26-973 mg kg^{-1}) for soil and 9.7 mg kg^{-1} (0.58-1055 mg kg^{-1}) for attic dust. Gosar et al. (2006) estimated that potential health risk could occur in the area between the towns of Idrija and Spodnja Idrija, where the total content of Hg is very high. In this area authors estimated median for soil at 47 mg kg^{-1} and for attic dust at 129 mg kg^{-1}. Spatial distribution of mercury in soil and attic dust correlate well and depends very much upon the morphology of the terrain. High values occur in the Idrijca river valley and at base of slopes, while lower values prevail at higher elevations and tend to decrease with distance from Idrija (Gosar et al., 2006).

Gnamuš et al. (2000) investigated Hg distribution in soils and plants growing in the Idrija area. For the purpose of their study analytical data from similarly contaminated sampling areas were grouped into distinctive contaminated zones. The areas in the Idrija region consisted of the immediate vicinity of the mine-smelter complex, then four areas around the town of Idrija (grouped as Zone A), and 3 others at greater distance in the wider Idrija area (grouped as Zone B). Thus the mine-smelter area and Zone A were characterized by heavy deposition of mercury vapor and airborne particles from mercury sources. In continuation of the study the abundance of mercury in soil close to smelter (mean 1256 mg kg^{-1}, n=14) and in plants growing thereon (mean 42 mg kg^{-1}) were determined. In the closer surroundings of Idrija, the average Hg concentrations in soil amounted to 288 mg kg^{-1} (n=96) and in plants up to 14 mg kg^{-1} (n=48), while in the wider surroundings the average Hg concentrations in soil amounted to 2.44 mg kg^{-1} (n=72).

Žibret et al. (2006) determined the quantity of accumulated material in the alluvial plain sediments downstream from the Idrija mercury mine. It has been established that the floodplains along the Idrijca River are strongly enriched with mercury. The concentrations on the surface of the active floodplain vary between 200 and 500 Hg mg kg^{-1}. Hg content gradually decreases with the distance from the river and height above the river channel to approximately 50 mg kg^{-1} on the surface of the first terrace and 5 mg kg^{-1} on the surface of the second terrace.. The total amount of accumulated mercury in the alluvial plain sediments of the Idrijca River from the town of Idrija to the town of Bača pri Modreju was calculated to be 2029 tons.

Based on all these studies performed in the last decades it can be stated that spatial distribution of mercury in soil in the Idrijca River catchment is relatively well documented. Some similar patterns can be derived from these studies. The highest mercury concentrations in soil are in the close vicinity of the Idrija mercury mine, between the towns of Idrija and Spodnja Idrija. Area near the former smelting facilities in the town of Idrija is the most polluted one. Obviously, Hg enriched particles settled down in the immediate vicinity of the smokestack of the smelter. Upstream and downstream from the mining area, Hg concentrations in soil decrease relatively sharply. In the more distant parts of the catchment, atmospheric deposition was the major source of mercury in the soil. The distribution of mercury that was transported by air along the Idrijca River valley depends mostly on the distance from the source of pollution, shape of the valley and local winds blowing along the valley.

For the purpose of the mercury soil mass balance calculation, an uniform mercury concentration must be applied to each of the hydrographic subunits. In the mercury pollutes sites such as Idrijca River catchment, Hg has a very complex distribution with values ranging from less than 1 μg g^{-1} up to few hundreds of μg g^{-1}. Hence, interpolation of its spatial distribution is a difficult task. In general, at the catchment scale, sources of mercury in soils can be separated into three groups: Hg from the regional atmospheric deposition from the smelter stack, Hg in the vicinity of the mine due to the mercury-rich parent material and mining activities, and Hg in alluvial soils due to the transport and accumulation of mercury contaminated sediments in the Idrijca River and its deposition during flooding. The knowledge of these different sources was taken into account before the spatial interpolation of Hg point data. For the part of the catchment that can be assumed to correspond to the regional atmospheric deposition only (upstream from the town of Idrija and downstream from the town of Spodnja Idrija), a continuous surface map of mercury distribution was created from the point data, using the inverse distance method within the geographical information system (GIS). Local extreme values/areas were treated separately. Thus, the data points with a higher concentration than 25 μg g^{-1} were omitted from the interpolation. Higher concentrations at these can be the result of different anthropogenic and natural sources: unsmelted ore wastes, primary ore smelting residues, ore residue dumps, outcropping of mineralized rocks (e.g. Pront-area, where ore-bearing rocks containing native mercury and cinnabar crop out), locations of old ignition facilities, places where the smelting residues were used for road construction or other building purposes. These sites are located mainly between the towns of Idrija and Spodnja Idrija or close by. For this part of the catchment map of the spatial mercury distribution in soils was generated separately based on the measurements performed within the present study and the data from the literature discussed above.

6.5 Erosion model

When choosing what model to use for a particular area and a certain problem, several factors must be considered, e.g. the modelling purpose, the model representation, data requirements and availability, and the ease of parameter estimates. Taking these factors into account, in the present study erosion of particulate phase mercury from the soil surface was estimated by the Erosion Potential Method (EPM) or Gavrilović's method (Gavrilović, 1972, 1976, 1988).

6.5.1 Erosion Potential Method

The Erosion Potential Method (EPM) is a parametric distributed model which has been widely used for the annual prediction of soil erosion rates and sediment yield on the basin scale in Slovenia and Croatia in the last 35 years (e.g. Nyberg and Prevodnik, 1999; Kodrič, 1999; Mrak, 1999; Petkovšek, 2000; Globevnik et al., 2003; Mikoš et al., 2006). The EPM has been developed for management practices in erosion protection, mainly in forest management and torrent control. This method was also applied in basins of the Italian and Swiss Alps (Bazzoffi, 1985; Beyer-Portner, 1998; Fanetti and Vezzoli, 2007; Tazioli, 2007).

The base of the EPM model is the concept that the effective sediment transported by the stream (G_y) is related to the sediment yield produced by the soil erosion (W_s; $m^3\ a^{-1}$) and to the sediment deposited in the watershed (SDR, sediment retention coefficient), according to the following relation:

$$G_y = W_s \cdot SDR \tag{23}$$

The calculation of the sediment production (W_s) involves empirical coefficients (erodibility coefficient, soil protection coefficient and erosion coefficient) and a matrix of physical characteristics (annual precipitation, temperature, average slope, and surface area). Using field investigations on the Morava River (Serbia), and laboratory experimental work, Gavrilović (1976) prepared detailed tables for the determination of parameters. Basins with strong spatially variability of these parameters should be divided in sub-basins that present homogeneous characteristics.

The EPM equation applied to estimate the annual volume of detached soil due to surface erosion is the following relation:

$$W_s = P \cdot \pi \cdot F_w \cdot K_t \cdot \sqrt{K_z^3} \tag{24}$$

where

W_s ... average annual sediment production [$m^3\ a^{-1}$]
P ... mean annual precipitation [$mm\ a^{-1}$]
K_t ... temperature factor as a function of the annual mean temperature [dimensionless]
K_z ... catchment erosion coefficient [$\mu m\ a^{-1}$]
F_w ... drainage area [km^2]

The equation for K_t is as follows:

$$K_t = \sqrt{(0.1 + \frac{T}{10})} \tag{25}$$

where T is the average yearly temperature [°C]. The erosion coefficient K_z can be estimated using corresponding tables or calculated from:

$$K_z = K_y \cdot K_x \cdot (K_o + \sqrt{F_{sl}}) \tag{26}$$

where

F_{sl} ... average slope of the basin (%)
K_y ... soil erodibility coefficient (soil resistance to erosion)
K_x ... soil protection coefficient (existing vegetative status)
K_o ... erosion and stream network development coefficient (observed erosion processes)

The original Gavrilović equation has been questioned by Pintar et al. (1986). The core of the criticism as summerized by Nyberg and Prevodnik (1999) is the following:

- More than 90 % of the sediment production is due to reworking of old sediment deposits, not a function of the direct weathering of the bedrock. Thus, the geomaterial coefficient (K_y) is mainly a function of the sediment type, its granularity and composition.
- The values of the coefficient of vegetation protection (K_x) is not merely a function of the density

of forest, shrub and undergrowth cover, but also of the vegetation association.

– Sediment production from stream banks, deep erosion on small areas and surficial erosion on large areas must be treated separately, i.e. in the parameterization for the mean catchment slope (F_{sl}), catchment area (F_w) and the visually estimated factor of the extent of erosion processes (K_o).
– The input parameters π, the temperature coefficient (T) as a function of the yearly mean temperature and the precipitation coefficient (P) as a function of the mean annual precipitation, are not relevant. Instead, temperature differences and precipitation intensities are important for sediment production, as they are relevant for raindrop splashing and surface runoff. A useful parameter for raindrop splashing and their runoff is the maximum daily precipitation (mm d^{-1}).

Using these critics, the original Gavrilović equation was revised for Slovenian conditions into the shape,

$$W_s = 20 \cdot P_{\max} \cdot \sqrt{K_z^3} \cdot F_w \tag{27}$$

where

P_{max} ... maximum daily precipitation [mm d^{-1}]

For the determination of the sediment delivery ratio (SDR), Gavrilović (1976) suggested the following equation:

$$SDR = \frac{(O \cdot D)^{0.5}}{0.25 \cdot (L + D)} \tag{28}$$

where

O ... perimeter of the basin (or sub unit) (km)
D ... average height distance of the basin (or sub unit), expressed in (km)
L ... length of the basin (km).

Average height distance is calculated as:

$$D = \frac{\sum_{i=1}^{n} f_i \cdot h_i}{F_w} - H_{\min} \tag{29}$$

where

f_i … represents area between two contour lines (km^2),
h_i … average altitude between the contour lines (m), and
H_{min} …the minimal altitude of the basin (m).

The Gavrilović model uses a scoring approach for only three descriptive variables (soil cover, soil resistance, type and extent of erosion), whereas the other variables are quantitative descriptors of the catchments conditions. Gavrilović prepared the tables with the scores for soil cover, soil resistance and the type and extent of erosion. The values used for the factors are presented in Table 10.

Table 10: *Descriptive factors used in the EPM model.*

Coefficient of soil cover	K_y
Mixed and dense forest	0.05–0.20
Thin forest with grove	0.05–0.20
Coniferous forest with little grove, scarce bushes, bushy prairie	0.20–0.40
Damaged forest and bushes, pasture	0.40–0.60
Damaged pasture and cultivated land	0.60–0.80
Areas without vegetal cover	0.80–1.00
Coefficient of soil resistance	K_x
Hard rock, erosion resistant	0.2–0.6
Rock with moderate erosion resistance	0.6–1.0
Weak rock, schistose, stabilised	1.0–1.3
Sediments, moraines, clay and other rock with little resistance	1.3–1.8
Fine sediments and soils without erosion resistance	1.8–2.0
Coefficient of type and extent of erosion	K_o
Little erosion on watershed	0.1–0.2
Erosion in waterways on 20–50% of the catchment area	0.3–0.5
Erosion in rivers, gullies and alluvial deposits, karstic erosion	0.6–0.7
50–80% of catchment area affected by surface erosion and landslides	0.8–0.9
Whole watershed affected by erosion	1.0

6.5.2 GIS application, data description and data sources

An important resent evolution of the EPM model is its application by the use of spatially distributed input data (topography, geology, soil and land use) in a Geographic Information System (GIS) environment. The GIS technique makes more objective estimation of the spatial distribution of the basin factors and could provide a means for accurately predicting total sediment transport. The GIS application is based on calibrated values of the four basic factors that control the erosion rate: climate, vegetation/land cover, relief and soil/bedrock. The GIS technique permits to identify and quantitatively classify the sub-areas with similar erosion potential in the catchment.

In the present study, the EPM was applied by the use of spatially distributed input data on elevation, geology, soils, and land use in a GIS environment. This makes a representative estimation of the factors easier and more objective, though constrained by the quality of the input data. The following description of the GIS data used in the erosion model is based on data description supplied by official data holders and on literature reviews.

Elevation data

The national surveying and mapping authority of Slovenia has produced a digital elevation model with the cell size 25 m (DMR 25). Database represents a regular 2D grid of points to which altitude has been added. Positional accuracy of points is ± 1 m, altitude accuracy is 1.5 m for open flat terrain, 3 m for rough terrain and ± 6.5 m for mountain terrain.

Geology

Geological data were obtained from the digital geological map of Slovenia provided by the Geological Survey of Slovenia. Geological map in scale 1:100.000 is a basic document and groundwork for the understanding of the geology of Slovenia. Described are lithology of rocks, their relationships, age and other geological phenomena. It was produced on the basis of geological mapping and numerous analyses in

the period 1962 – 1998 in the frame of a comprehensive project "Basic geological map of Yugoslavia". The map consists of 22 authorized sheets in scale 1:100.000. Geological margins and tectonic units are captured as lines, while lithostratigraphic units are captured as polygons. The lithology and age of a unit are attributes, structural elements and other geological phenomena (fossils, mineral resources, hydrogeological phenomena etc.) are captured as points. Four sheets that cover the Idrijca River catchment were used: Postojna, Tolmin, Nova Gorica and Kranj.

Pedology

Soil data from the National Soil Survey Programme in Slovenia was available at the Biotechnical Faculty of the University of Ljubljana. A digital soil map in the scale 1: 25 000, was obtained as an ESRI shape file, containing soil polygons, pedocartographic units (PCU), with defined compositions in percentage of different soil types, pedosystematic units (PSU). The exact positions of the different soil types within the soil polygons are not known. The map was created based on field surveys, where the presence of different soil types was predicted from the topography, vegetation (indicator species) and bore hole samples. Various cuts in the slopes (roads, stone and gravel pits) were inspected. It is very difficult to estimate the positional accuracy of the polygon borders on the map. Associated with the map were two dBase files, containing data on estimated average soil depths, pH in the first and second soil horizons and content of organic and coarse materials in the first and second soil horizons.

Vegetation/Land cover

CORINE Land Cover (CLC), a geographic land cover/land use database was used. CLC describes land cover (and partly land use) according to a nomenclature of 44 classes organized hierarchically in three levels. The first level (5 classes) corresponds to the main categories of the land cover/land use (artificial areas, agricultural land, forests and semi-natural areas, wetlands, water surfaces). The second level (15 classes) covers physical and physiognomic entities at a higher level of detail (urban zones, forests, lakes…). Final level 3 is composed of 44 classes. CLC was elaborated based on the visual interpretation of satellite images (SPOT, LANDSAT TM and MSS). Ancillary data (aerial photographs, topographic or vegetation maps, statistics, local knowledge) were used to refine interpretation and the assignment of the territory into the categories of the CORINE Land Cover nomenclature. The smallest surfaces mapped (mapping units) correspond to 25 hectares. Linear features less than 100 m in width are not considered. The scale of the output product was fixed at 1:100.000. Thus, the location precision of the CLC database is 100 m. As most of the study area is covered by forests (> 80%) two additional digital maps were used to better characterize forested areas in terms of soil erosion: map of forest associations in the scale 1:50.000 and the map of forest development stages (indicated by the diameter of the stems), provided by the Slovenian Institute for Forest Management and Slovenian Forest Service, respectively.

Precipitation

Precipitation data were provided by the Environmental Agency of the Republic of Slovenia (ARSO) as daily, monthly and yearly precipitation. Long-term (1961-2007) precipitation data from the 11 gauging posts within the study area were used in the present study. The gauging posts are: Kneške Ravne, Rut, Podbrdo, Bukovo, Novaki, Na Stanu, Vojsko, Mrzla Rupa, Idrija, Črni vrh nad Idrijo and Cerkno.

6.5.3 Generic steps

Geographical Information System (GIS) was used as a fundamental support to the dataset and was applied to generate the coefficients used in the EPM. The overview of the GIS data used and the generic steps involved for the purpose of soil erosion modeling are shown in the flow-chart in Fig. 77 and discussed in this section as follows.

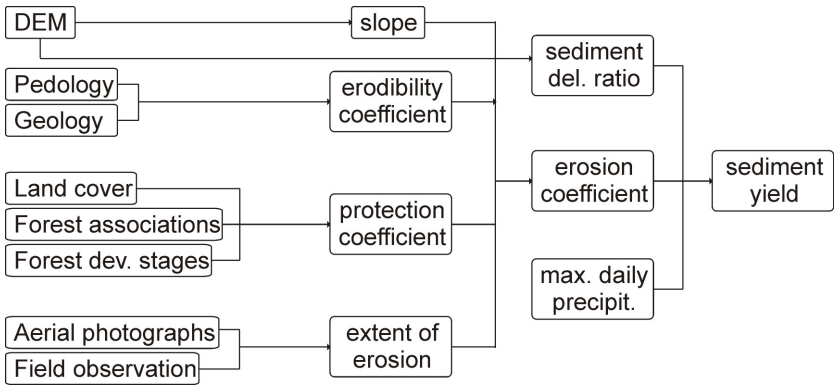

Figure 77: *Flow chart for the EPM – GIS data overview for the purpose of the erosion modeling.*

- All three descriptive variables used in the EPM (K_x, K_y and K_o) were calculated as the sub-area weighted averages for each hydrographic unit, using the advantages of GIS tools. Based on these averages, the coefficient of erosion (K_z) was calculated for each hydrographic unit.
- The K_z erosion coefficient was determined with equation 26, which is strictly related to the erosion, vegetation rule in the soil protection, soil use, soil resistance and the catchment slope. The calculated K_z coefficient values range between 0.10 and 0.48 with an average value of 0.18. According to the EPM erosion categorization (Gavrilović, 1988), these values correspond with the slight and medium erosion category, respectively. In general, higher erosion coefficients were calculated for the units of the upstream reaches, mostly due to the steep relief and less protected surfaces.
- The K_x coefficient related to the soil resistance to the erosion was defined on the basis of the lithology and the pedology of individual hydrographic subunit. In fact, this parameter predicts the erodibility of the outcropping rocks and sediments. However, the resistance of a soil to erosion depends on many factors such as content of organic matter, its mineralogical composition, content of clasts and stage of development. The infiltration capacity of soil is also important as in humid climates, like that in the study area, soil erosion is mainly driven by rainfall. Moreover, in Slovenia, the bedrock is the most important pedogenetic factor. Therefore, for the determination of the soil erodibility coefficient, two thematic maps were used: geological and pedological. Based on the overlay of these two maps, the attributes for K_x were parameterized according to the values in Table 10.
- In the EPM, the influence of land cover/land use on soil erosion is taken into account by the soil protection coefficient (K_x). The CORINE Land Cover (CLC) geographic database was used to determine the land cover/land use classes in the study area. The values for the soil protection coefficient were then parameterized for each of the classes according to the values in Table 10. In the Idrijca River catchment, more than 80% of the area is covered by forests. Forests play an important role in protection of soil erosion. The CORINE Land Cover database divides forests on the third level into three classes only (broad-leaved, coniferous and mixed forests, respectively). However, more than by the type of forest, soil erosion is influenced by the forest associated parameters such the undergrowth, the canopy, root quantities and stem diameter. The amount of precipitation that is intercepted by foils and branches, and the quantity of roots that penetrate the soil, vary between different vegetation associations, and thereby their protective qualities against soil erosion. Root quantities and interception capacities change with the development stage and phenology of the vegetation. Therefore, vegetation associations and vegetation development stages were considered when assessing the soil protection coefficients for forests. For this purpose, two additional thematic map layers were used: forest associations and forest development stages. In the forest association map, 22 different forest associations were found in the study area. In the forest development stages map, forests are divided into 5 classes based on the age and steam diameter. The two maps were combined into one and the soil protection coefficient value assigned for each combination of the forest association/development stage.
- Erosion and stream network development coefficient (K_o) was determined based on the fieldwork observations, aerial photographs and descriptions given in Table 10.
- Averages slope for each hydrographic unit was determined. For this purpose digital elevation data (raster 25 m x 25 m) was imported into terrain modeling software (ArcGIS) and the average slope for each of the 64 polygons in the Idrijca River catchment was calculated.
- Precipitation data provided by the Slovenian Environmental Agency (ARSO) were used.

Altogether, data from 11 meteorological stations in the Idrijca River catchment collected in the 1961-2007 period were gathered. For the calculation of the annual volume of detached soil due to surface erosion, maximum daily precipitation data from these stations were used. As a result of complex relief and variable meteorological conditions, the precipitation in the region is heterogeneous both spatially and temporally. Based on the precipitation-altitude relationship, maximum daily precipitation used in the model was calculated for each hydrographic subunit, taking the average altitude of the subunit into account.

– The erosion rate, as calculated for each hydrographic unit, was then summed to provide the erosion rate for the whole catchment.

– Only a fraction of eroded soil passes through channel system and contributes to sediment yield while some of it deposit in water channels. Sediment yield is quantified by the sediment delivery ratio, expressed as the percent of gross soil erosion by water that is delivered to a particular point in the drainage system. In the present study, sediment delivery ratios (*SDR*) were calculated separately for each hydrographic unit using equation (28). Perimeters (*O*), average height distances (*D*) and the lengths (*L*) of the hydrographic units used for the *SDR* calculation were derived from the digital elevation model using standard GIS operations. Calculated sediment delivery ratios are relatively high due to course texture of soils in the uppermost reaches of the catchment, steep hills gravitating directly to the torrents, the shapes of the hydrographic units and diverse hydrographic network.

6.6 GIS mercury emission model

In recent years, many efforts were diverted to scale up atmospheric Hg emissions from naturally enriched areas (Gustin et al., 2003; Engle and Gustin, 2002; Engle et al., 2001). Gustin (2003) estimated natural Hg emission from Nevada and California based upon the observed Log–Log relationship between daily average Hg fluxes and soil mercury concentrations. Engle and Gustin (2002) used in situ Hg emission flux measurements and the diurnal Gaussian Distribution of Hg fluxes to scale up Hg emissions for the naturally enriched soil in Nevada and California. These works were mainly carried out in desert areas. However, Idrijca River catchment is located in an area with relatively humid and rainy weather. Mercury evaporating from soil in our study area is, obviously, differently day-to-day due to the cloudy weather. Since it never rains in desert, the Gaussian distribution model could be used to present the daily distribution pattern of Hg fluxes and a simple Log–Log model originates from relationship between soil Hg concentrations and Hg flux could be obtained (Gustin, 2003). However, these approaches are not applicable in our study area simply because the daily weather in the Idrijca River catchment area is variable, which is significantly different from the weather in deserts of California and Nevada, USA.

To scale-up Hg emissions from the Idrija mercury mine area at the catchment scale, mercury emission model was built using the advantages of the geographical information system technology (GIS). Point source fluxes obtained by the laboratory flux measurement system (section 5.6) were incorporated into a GIS model. The GIS was employed to spatially model the effect of different parameters controlling the variability of Hg emissions. The amount of Hg vapor emitted from the surface is strongly controlled by substrate Hg concentration, vegetation cover, light intensity, moisture and temperature. For the latter three factors diurnal, daily and seasonal variations must be taken into account. The purpose of the emission model was to scale-up the annual emissions at the catchment scale. Therefore, it was necessary to adjust the measured fluxes to be representative of an average daily and seasonally fluxes. The overview of the GIS data used and the generic steps involved in the building of the mercury emission model is given in Fig. 6.5 and discussed here as follows.

The laboratory flux measurement experiment revealed the two most important factors that influence the magnitude of mercury air/surface fluxes; substrate Hg concentration and temperature, respectively. Therefore, based on the experiment's results, empirical correlation between the flux and the temperature and soil concentration, respectively, was established. An approach similar to that reported by Zhang et al. (2001) and Gbor et al. (2006) was used, as follows. As suggested by Zhang et al. (2001), the air/surface exchange of mercury may be considered as a surface physicochemical process comprising desorption (adsorption) of Hg from (to) soil particle surfaces and subsequent diffusion through soil pores:

$$F_{Hg} = r_{Hg} = -\frac{d[Hg]}{dt} = k[Hg]_s^n \tag{30}$$

where:

F_{Hg} … the Hg emission flux

r_{Hg} … rate of Hg air/surface exchange (ng Hg m^{-2} hr^{-1})
$[Hg]_s$ … soil Hg concentration (µg Hg g^{-1})
t … time (h),
k … rate constant of the overall Hg air/surface exchange process
n … reaction order.

Hence, the Arrhenius equation can be applied to obtain the link between the kinetic rate constant of this process and the soil temperature:

$$\ln(k) = -\frac{E_a}{R \cdot T_s} + const. \tag{31}$$

where:

E_a … apparent activation energy required for the ongoing of the overall process,
R … gas constant (8.314472 J K^{-1} mol^{-1})
T_s … soil temperature (K)

In the case of continuous emission, $[Hg]_s$ is considered to remain constant. Therefore, the air/surface exchange reaction can be considered as pseudo first order and:

$$k' = k[Hg]_s \tag{32}$$

By the substitution of F_{Hg} for the rate constant the common flux-temperature relationship can be extended to include Hg concentration in soil:

$$\ln F_{Hg} = -\frac{E_a}{R \cdot T_s} + \ln[Hg]_s + \lambda \tag{33}$$

where λ is a constant.

As shown by the laboratory flux chamber experiment (section 5.6), the magnitude of the surface-air mercury exchange does not depend only on the total mercury concentrations but also on the binding form of mercury in the individual soil. The later results in different activation energies required for the overall process to occur. Therefore, the study area (Idrijca River catchment) was separated into three groups: (1) the most mercury contaminated area between the towns of Idrija and Spodnja Idrija, (2) contaminated alluvial plains downstream from the town of Idrija, and (3) remaining area of the catchment less contaminated with mercury (soil concentrations below 25 µg g^{-1}).

Different values for the activation energies calculated from the Hg flux-temperature relationship observed during the flux chamber experiment were used for each of the three areas: 109, 105 and 98 kJ mol^{-1}, respectively. Using additional data on Hg flux for different Hg soil concentrations from the laboratory flux measurement experiment, λ was obtained as 44.91, 41.94 and 41.80, respectively. Both E_a and λ values were calculated based on the results obtained under dark conditions. Hence, when applying these values in equation 33, no effect of solar radiation which can significantly enhance the flux during the daylight hours is taken into account. Therefore, an additional term had to be included in equation 33. Based on the results reported by Carpi and Lindberg (1998) that measured Hg flux from forest soil and artificially shaded soil, equation 33 was revised to include the Hg flux-solar radiation relationship:

$$\ln F_{Hg} = -\frac{E_a}{R \cdot T_s} + \ln[Hg]_s + \lambda + 0.003 \cdot R_Z \tag{34}$$

where R_I is the solar energy reaching the soil surface (W m^{-2}).

As major part of our study area is covered by forests, it must be taken into account that on its way through the plant canopy, solar radiation passes through successive layers of leaves. In the process, its intensity decreases exponentially with increasing plant cover, in accordance with the *Lambert-Beer*

extinction law. Therefore, the decrease in radiation can be calculated by the following extinction equation:

$$R_z = R_o \cdot e^{-k \cdot LAI} \tag{35}$$

where

R_o … solar radiation at the top of the canopy
k … extinction coefficient (0.65-1 for forests)
LAI … leaf area index (total leaf area per unit ground area)

Generic steps:

- To scale-up the yearly emissions of mercury from soil at the catchment scale the mercury fluxes were calculated for each hydrographic subunit, using equation (34).
- Calculations were based on the knowledge about spatial distribution of mercury in soil, average monthly temperatures and intensity of solar radiation reaching the soil surface (Fig. 78).
- Simulations were performed using the average monthly temperatures for the months of January, April, July and October. These months are representative of the seasonal meteorological variation in the domain.
- Adjustments for the influence of solar radiation on the mercury flux were made based on the average monthly solar radiation energy for the same for months. Solar radiation data used are the result of the modeling described into more detail in Zakšek et al. (2005) and Kastelec et al. (2007).
- Each hydrographic subunit was divided into part covered with forest and part without forest canopy. For the part covered with the forest canopy, intensity of solar radiation reaching the forest surface was calculated by equation (35). For the extinction coefficient k value of 0.65 was selected. Leaf Area Index (LAI) data for the months of January, April, July and October was obtained from MODIS satellite products (ftp://primavera.bu.edu/pub/datasets/MODIS).
- Calculated hourly emission fluxes were then summed for the entire month in each hydrographic subunit to show the spatial distribution of the emission. Annual emissions were estimated as three times of the four-month's sum.

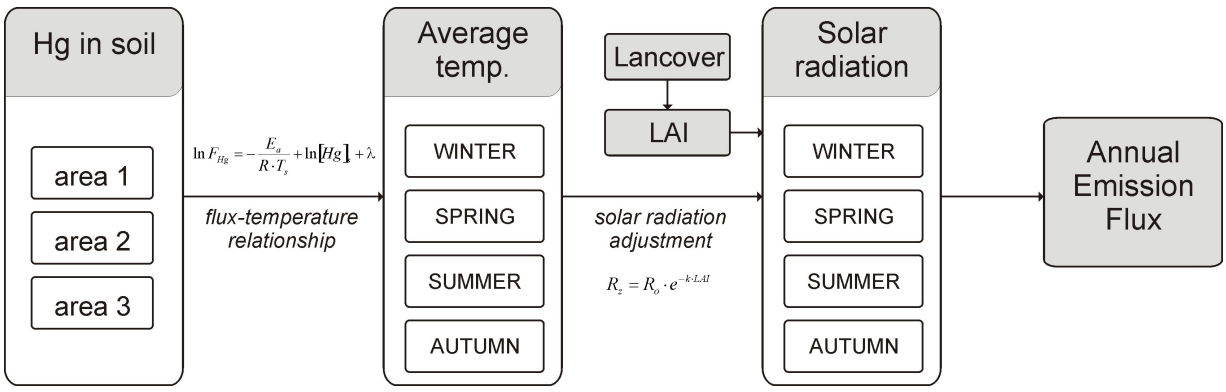

Figure 78: *Flow chart of the mercury emission model.*

6.7 Mass balance model results

6.7.1 Exchange of mercury between surface and atmosphere

6.7.1.1 Atmospheric deposition

As it can be seen from the results presented in section 5.5.3, there were no significant spatial variations in mercury concentrations observed, in both the precipitation and the throughfall. Furthermore, spatial differences in calculated deposition rates could not be explained by the distance from the local pollution sources in the catchment. However, spatial distribution of Hg atmospheric deposition was studied for two precipitation events only. Therefore, to estimate long-term (annual) atmospheric mercury load to soils at the catchment scale, average values obtained at location Idrija were used. At this site mercury concentrations in both the precipitation and the throughfall were measured more frequently from October 2006 to September 2007. In this way, variability in Hg deposition due to the varying meteorological conditions was taken into account.

For the sum of wetfall and dryfall, values of 19.4±15.8 ng m^{-2} day^{-1} for particulate Hg (PHg), 16.4±13.5 ng m^{-2} day^{-1} for dissolved Hg (DHg) and 0.57±0.41 ng m^{-2} day^{-1} for methlymercury (MeHg) were used. For the net throughfall, values of 65.5±33.8 ng m^{-2} day^{-1} for particulate Hg (PHg), 15.8±20.2 ng m^{-2} day^{-1} for dissolved Hg (DHg) and 0.81±0.35 ng m^{-2} day^{-1} for methlymercury (MeHg) were used. Atmospheric deposition was calculated for each hydrographic subunit.

In Table 11 total annual atmospheric deposition (kg $year^{-1}$) to the Idrijca River catchment due to the wetfall, dryfall and throughfall, calculated as the sum of all 64 hydrographic subunits is given.

Table 11: *Total annual atmospheric deposition to the Idrijca River catchment.*

	Wetfall + Dryfall		*Throughfall*	
Mercury species	Deposition rate ng m^{-2} day^{-1}	Deposited kg $year^{-1}$	Deposition rate ng m^{-2} day^{-1}	Deposited kg $year^{-1}$
PHg	19.4	4.2	65.5	11.0
DHg	16.4	3.5	15.8	2.70
MeHg	0.60	0.12	0.40	0.06

Although the dry deposition of mercury was not measured directly, the dry Hg flux can be estimated using the measured concentrations of different Hg species in air and previously published deposition velocities. Measurements of aerosol Hg (TPM) at Idrija site range from 15-68 pg m^{-3}, with an average value of 47 ± 24 pg m^{-3} (n = 5). The calculated fluxes of aerosol Hg, using a commonly cited deposition velocity of 0.1 cm s^{-1} (e.g. Guentzel et al., 1998), range from 1.3-5.9 ng m^{-2} day^{-1}. These estimates are less than 15 % of the measured rates of rainfall total Hg deposition and less than 30 % of measured particle bound Hg deposition (PHg in Table 11), suggesting that aerosol Hg deposition is only a small part of dry deposition. However, it must be noted that the results of SEM/EDXS microscopy of rainfall revealed the presence of cinnabar particles with a 5 µm diameter. As noted by Rea et al. (2001), coarse aerosol particles (> 2 µm) can strongly influence the deposition flux of an element because the velocity increases with aerodynamic diameter, and have a proportionally greater impact on dry deposition than fine particles.

Measurements of divalent reactive gaseous Hg (RGM) performed at Idrija site range from 10-24 pg m^{-3}, with an average value of 19 ± 7 pg m^{-3} (n = 5). The estimated dry deposition flux of RGM, using a commonly cited deposition velocity of 2 cm s^{-1} (e.g. Guentzel et al., 1998), range from 18-42 ng m^{-2} day^{-1}. These estimates are similar to measured rainfall Hg deposition, suggesting that dry deposition of Hg could account for majority of the total atmospheric Hg deposition (both wet and dry) in the Idrija region. However, it must be emphasized that the uncertainties associated with such estimates are large.

6.7.1.2 Emission

Mercury emissions from the surfaces of the Idrijca River catchment were scaled-up as described in section 6.6. Calculations were performed for the average meteorological conditions for the months of January, April, July and October. Calculated hourly emissions fluxes were summed for the entire month for each hydrographic subunit. Annual emissions were estimated as three times of the four-month's sum.

The results of the mercury emission model revealed that annually approximately 44 kg of mercury is emitted from the surface of the Idrijca River catchment. However, it must be noted that in this calculation point sources that can significantly contribute to the overall budget are not included. In the Idrija region, the most important point source of mercury to the atmosphere is the most mercury polluted area around the former smelting complex. At this locations mercury surface-air fluxes reaching up to 27 μg m^{-2} h^{-1} were measured during the mid-day summer. To scale-up fluxes from this site, the extent of polluted area should be known. As the pollution extent is unknown, annual mercury emission from this site was estimated based on the measurements performed by Grönlund et al. (2005) where an average flux from the area of the smelter was calculated to approximately 2-4 g h^{-1}. This would then result in 17-34 kg of Hg emitting annually. However, it must be noted that during the measurement campaign performed by Grönlund et al. (2005) comparatively low concentrations and fluxes were observed at Idrija due to reduced ambient temperatures and rainfall. Therefore, annual amount of mercury emitted from the area of the smelter might be even higher.

6.7.2 Loads to catchment tributary system and riverine transport

In this section calculated terrestrial mercury loads to the Idrijca River and its tributary system are presented and discussed. Calculated soil erosion rates and sediment yields, the result of EPM erosion model, are presented in section 6.7.2.1. In section 6.7.2.2, predicted mercury loads in particulate and dissolved phase, as a result of soil erosion and surface runoff, respectively, are given.

6.7.2.1 Erosion

Calculated erosion rates and sediment yields for the Idrijca River catchment are shown in Table 12. Erosion rates and sediment yields were calculated by the EPM model for 64 hydrographic subunits (flow direction considered), using one value of each parameter for one subunit. It was estimated that at the catchment scale, approximately 160 000 m^3 $year^{-1}$ of soil is eroded which results in the sediment yield to the Idrijca River system of approximately 83 000 m^3 $year^{-1}$ in an average hydrological year.

Calculated specific erosion rates per unit area vary between 180 and 1480 m^3 km^{-2}, with the average being 320 m^3 km^{-2}. This is close to the average reported for the Republic of Slovenia (Mikoš, 1995; Komac and Zorn, 2005). The highest specific erosion rates (> 700 m^3 km^{-2}) were calculated for the most northern parts of the study area in the Bača River subcatchment. In these parts, rain has the highest intensity, hills are very steep and are gravitating directly to the torrents. Moreover, in these parts there is more open spaces with little or no vegetation which results in higher erosion rates calculated, compared to other parts of the study area.

With the EPM model average annual sediment production and sediment yield to the Idrijca River and its tributary system were calculated. In this case, the term sediment is used for the soil which has been transported from the position of its origin and deposited elsewhere due to certain erosive processes. The EPM calculated sediment volume includes both the bed load and suspended load. In order to estimate annual mercury outflow from the catchment associated with the sediment, these two loads must be separated. However, reliable measuring of bed load is possible only by the geodetic survey of the sediment deposits. Therefore, it was assumed similar as by other authors (e.g. Kodrič, 1999; Globevnik et al., 2003) that approximately 25 % of calculated annual sediment yield is trapped in the catchment as a bed sediment, the rest 75 % being in suspended phase. Taking this assumption into account, the EPM model results were verified with the $C_{ss}(Q)$ rating curve (suspended sediment vs. discharge) for the measuring station where enough data for both the suspended sediment concentrations and discharge was available; the Hotešček measuring station on the Idrijca River, about 40 km downstream of the town of Idrija (location No. 12 in Fig. 6). In Slovenia, the monitoring of the suspended load transport is performed by the Environmental Agency of the Republic of Slovenia (ARSO). The data on total suspended sediment concentrations (*TSS*) and discharge (Q) provided by the ARSO for the period 1990–2007 were combined with the data obtained within the present study. At station Hotešček, water discharge of the Idrijca River is measured continuously, while the TSS is measured sporadically.

Table 12: *Erosion rates and sediment yields for individual hydrographic subunits of the Idrijca River catchment.*

HG unit	F_w (km^2)	P_{max}	F_{sl} (%)	K_x (-)	K_y (-)	K_o (-)	K_z (-)	Wp (m^3 year^{-1})	Wp specif. (m^3 km^{-2})	SDR (-)	Gy (m^3 year^{-1})	Gy specif. (m^3 km^{-2})	Xe (kg km^{-2} year^{-1})*
1	20.3	195	45.5	0.22	0.64	0.25	0.13	3651	180	0.43	1582	78	270163
2	14.5	196	57.2	0.19	0.59	0.25	0.12	2230	153	0.49	1101	76	230146
3	36.7	198	27.5	0.23	0.56	0.25	0.10	4603	125	0.15	690	19	187981
4	21.0	183	52.2	0.20	0.53	0.20	0.10	2398	114	0.43	1029	49	171333
5	22.1	183	42.7	0.22	0.64	0.25	0.13	3734	169	0.33	1215	55	253053
6	5.9	185	40.7	0.26	0.79	0.20	0.17	1545	262	0.36	557	94	392557
7	1.1	166	39.3	0.19	0.67	0.20	0.10	117	109	0.20	23	22	163001
8	2.0	175	40.0	0.18	0.65	0.20	0.10	215	108	0.27	59	30	162749
9	11.6	186	47.7	0.20	0.52	0.20	0.10	1270	109	0.52	661	57	163793
10	6.8	174	53.8	0.22	0.51	0.25	0.11	863	127	0.34	290	43	190403
11	4.7	185	50.9	0.26	0.58	0.20	0.13	860	183	0.44	380	81	273964
12	6.1	182	55.0	0.23	0.58	0.25	0.13	1084	176	0.44	472	77	264361
13	7.3	202	46.8	0.22	0.59	0.25	0.12	1251	171	0.65	813	111	257229
14	7.9	202	52.6	0.21	0.57	0.25	0.11	1250	158	0.55	691	87	236620
15	8.8	188	54.6	0.27	0.61	0.25	0.17	2225	253	0.41	921	105	379493
16	10.5	183	54.9	0.27	0.57	0.20	0.14	2093	199	0.54	1139	108	298832
17	2.2	183	51.5	0.25	0.58	0.25	0.14	411	186	0.39	160	72	279099
18	6.2	178	58.5	0.23	0.57	0.25	0.13	1047	170	0.40	418	68	254847
19	2.5	192	47.9	0.25	0.80	0.25	0.19	801	317	0.53	428	170	476209
20	14.0	178	57.1	0.26	0.72	0.25	0.19	4010	285	0.44	1783	127	428192
21	10.3	191	51.7	0.26	0.62	0.20	0.15	2176	211	0.58	1262	122	316462
22	12.2	190	53.3	0.26	0.62	0.20	0.15	2739	225	0.55	1513	125	338108
23	3.3	189	44.6	0.26	0.75	0.25	0.18	945	286	0.51	477	144	428679
24	3.9	183	50.3	0.29	0.62	0.25	0.18	1051	268	0.45	470	120	402705
25	13.8	178	44.2	0.26	0.77	0.20	0.17	3509	254	0.54	1878	136	380293
26	6.9	185	48.9	0.31	0.70	0.25	0.20	2336	340	0.44	1029	150	509879
27	9.4	201	39.2	0.22	0.72	0.25	0.14	1995	212	0.48	950	101	318016
28	4.3	204	48.9	0.25	0.66	0.25	0.16	1112	256	0.46	512	118	383787
29	10.7	198	50.0	0.26	0.76	0.25	0.19	3468	325	0.57	1990	186	487205
30	3.7	168	54.5	0.32	0.52	0.25	0.17	858	229	0.36	310	83	343251
31	10.1	182	47.1	0.30	0.63	0.25	0.18	2696	267	0.53	1430	142	400867
32	10.3	183	49.7	0.27	0.54	0.25	0.14	1975	192	0.56	1106	108	288538
33	34.0	178	46.8	0.27	0.56	0.20	0.13	5895	173	0.49	2900	85	260225
34	21.6	179	40.8	0.28	0.65	0.20	0.15	4546	211	0.59	2661	123	316415
35	9.2	170	44.7	0.25	0.64	0.20	0.14	1622	176	0.51	834	90	263564
36	3.1	159	43.5	0.25	0.87	0.20	0.19	787	254	0.29	229	74	381077
37	5.0	172	59.3	0.19	0.51	0.25	0.10	550	109	0.45	248	49	163985
38	9.3	179	63.4	0.26	0.50	0.25	0.13	1623	175	0.52	844	91	262833
39	18.6	180	55.0	0.20	0.65	0.25	0.13	3220	174	0.53	1710	92	260330
40	12.5	210	36.8	0.25	0.61	0.25	0.13	2558	204	0.64	1630	130	306698
41	5.2	199	33.3	0.23	0.62	0.25	0.12	824	158	0.50	413	79	237067
42	14.1	204	63.0	0.21	0.50	0.25	0.11	2083	147	0.67	1405	99	221192
43	8.1	208	48.5	0.48	0.79	0.25	0.36	7286	894	0.62	4522	555	1341575
44	4.2	217	63.5	0.53	0.60	0.25	0.33	3531	837	0.61	2148	509	1254947
45	1.8	212	64.5	0.22	0.66	0.25	0.15	460	251	0.48	220	120	376147
46	2.6	189	58.5	0.32	0.74	0.25	0.24	1174	452	0.31	363	140	677912
47	4.9	219	61.2	0.23	0.73	0.25	0.17	1573	319	0.64	1011	205	479204
48	2.4	207	73.2	0.48	0.56	0.25	0.30	1643	678	0.56	916	378	1016976
49	3.3	199	59.3	0.23	0.68	0.25	0.16	852	255	0.52	440	132	382230
50	9.8	205	56.7	0.23	0.69	0.25	0.16	2545	258	0.60	1520	154	387704
51	6.2	188	66.2	0.22	0.70	0.25	0.16	1510	245	0.42	636	103	366878
52	6.0	214	62.2	0.44	0.73	0.25	0.33	4953	824	0.60	2972	495	1236660
53	10.0	219	65.1	0.39	0.82	0.25	0.34	8747	876	0.60	5248	526	1313932
54	6.0	218	63.6	0.35	0.84	0.25	0.31	4537	757	0.63	2855	476	1134955
55	10.3	190	69.5	0.26	0.70	0.25	0.20	3487	337	0.59	2071	200	505697
56	7.2	181	59.0	0.24	0.61	0.25	0.15	1468	204	0.44	641	89	305869
57	10.1	176	56.6	0.23	0.64	0.20	0.14	1871	184	0.45	847	83	276698
58	8.7	181	62.5	0.24	0.66	0.25	0.17	2154	247	0.50	1078	123	369884
59	3.4	198	73.7	0.23	0.72	0.25	0.19	1073	317	0.54	582	172	475220
60	4.6	220	74.0	0.53	0.64	0.25	0.38	4774	1029	0.55	2626	566	1542951
61	4.9	220	61.0	0.68	0.69	0.25	0.48	7298	1476	0.60	4379	886	2213904
62	7.4	213	58.3	0.51	0.81	0.25	0.42	8564	1160	0.55	4710	638	1740230
63	7.1	195	71.6	0.23	0.63	0.25	0.16	1784	251	0.60	1071	150	376180
64	15.0	176	55.0	0.27	0.59	0.20	0.15	3082	206	0.56	1726	115	308399
SUM								158593			82797		

* soil bulk density was set to 1.5 g cm^{-3}

For location Hotešček on the Idrijca River, annual TSS load was first calculated based on the sediment rating curve, an empirical relation between the water discharge and the TSS concentration. This is a common method of estimating sediment loads in the absence of continuous measurements. The relationship between the suspended sediment concentration (C_{SS} in g m^{-3}) and the river discharge (Q in m^3 s^{-1}) was calculated as follows:

$$C_{SS} = aQ^b \tag{36}$$

where the coefficients a and b are derived from the coefficients of the linear regression calculated between *TSS* and *Q*. The coefficients *a* and *b* are 1.2985 and 0.787 for station Hotešček (Fig. 79). Using the long term average monthly discharges for the Hotešček station, the corresponding average monthly TSS concentrations and loads were calculated using Eq. 6.28. The annual TSS load was then calculated by summing the monthly loads. In this way, annual suspended sediment load of 12 317 tons was obtained. By the EPM model, for the cross-section at the Hotešček measuring station, annual sediment yield of 40 215 m^3 was calculated. Assuming that the bulk density of eroded soils is 1.5 g cm^{-3} and that 75 % of total annual sediment yield is in suspended phase, this results in a suspended sediment load of 45 242 tons. It can be seen from these numbers that TSS loads calculated by the rating curve are of the same order of magnitude as those calculated by the EPM. However, in this way, only about 25 % of the annual sediment yield calculated by the EPM model can be explained.

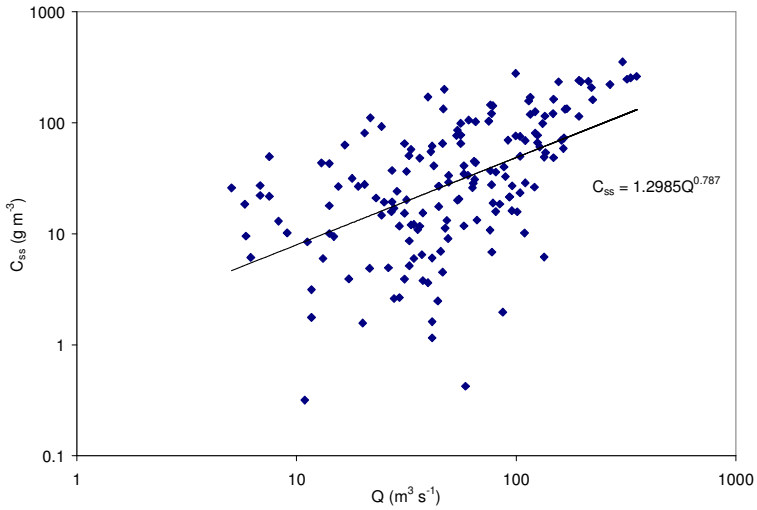

Figure 79: *Suspended sediment rating curve for the Hotešček measuring station.*

At the Hotešček measuring station suspended sediment concentrations are measured only occasionally, mostly for low and medium discharges and only for very few flood-events (Knific, 1996). Obviously, the relationship between the discharge change and the concentration of suspended material in a specific time is not entirely linear. The highest concentration of the sediment frequently occurs just before the peak of the high water wave. The analysis of the monitoring results of the suspended load transport accomplished for Slovenian rivers showed that about 70 % of the material is transported during the periods of high water stages (Ulaga, 2005). In the river systems with the torrential characteristics such as Idrijca River catchment this effect is even more pronounced. In such systems, the rating curve method underestimates the periods of high water stages when most of the TSS load occurs. Therefore, additional approach was used to calculate TSS loads, using the Beale's Ratio Estimator (*BRE*). Beale's Ratio Estimator was developed for situations with an abundance of flow information and relatively little concentration data. The Ratio Estimator assumes a positive relationship between concentration and flow, and the variance in concentration is proportional to the magnitude of flow (Preston et al., 1989). The estimate is derived by multiplying the mean measured loads by the ratio of the average flow for the year, divided by the average flow on days when concentrations were measured (Dolan et al., 1981). The equation is given as:

$$L_{Beale} = Q \cdot \frac{L}{Q_L} \cdot \left[\frac{1 + \frac{S_{LQ}}{N \cdot L \cdot Q_L}}{1 + \frac{S_{QQ}}{N \cdot Q^2}} \right] \tag{37}$$

where Q, L, Q_L, S_{LQ} and S_{QQ} are given by equations 38 to 42:

$$Q = \frac{\sum_{t=1}^{Year} Q_t}{Q_{Year}} \quad \ldots \text{ average water discharge in the defined time interval} \tag{38}$$

$$L = \frac{\sum_{i=1}^{N} (C_i \cdot Q_i)_i}{N} \quad \ldots \text{ average of the sampled load} \tag{39}$$

$$Q_L = \frac{\sum_{i=1}^{N} Q_i}{N} \quad \ldots \text{ average of the discharges when samples were collected} \tag{40}$$

$$S_{LQ} = \frac{\sum_{i=1}^{N} \left[(Q_i - Q_L) \cdot (L_i - L) \right]}{N} \tag{41}$$

$$S_{QQ} = \frac{\sum_{i=1}^{N} (Q_i - Q_L)^2}{N} \tag{42}$$

By the Beale's Ratio Estimator, a statistical method that incorporates the ratio of the covariance of load with discharge to the variance of discharge, annual suspended sediment loads for years 1999-2007 were calculated. The calculated loads range from 14 250 – 72 580 t year^{-1}, with an average being 45 020 t year^{-1} for location Hotešček. These values are comparable with the calculated values by the EPM model and can be considered as s reasonable agreement between the measured and computed/modeled values.

It must be noted, however, that the suspended sediment transport dynamic in the river system is much more complex. Not only the soil erosion but also the processes such as river bank erosion, sediment deposition and resuspension can significantly contribute to the calculated loads. The riverine transport and dispersion of mercury (either dissolved in water or bound to suspended sediments) is strongly effected by the hydrodynamic circulation. As this is changing permanently with time, the following categories must be distinguished: (1) annual average circulation; (2) seasonally averaged circulation; (3) short term current pattern. The annual average circulation is responsible for the long-term transport of mercury. Often the short but strong events, e.g. high river discharge can have very important effect on mercury transport, especially on the transport of the river bottom sediment, which cannot be resuspended until a critical flow velocity is attained (Rajar, 2001). For illustration, a flood wave on the Idrijca River, which was observed in September 2007 is shown in Fig. 80. The water discharge and sediment transport, partly measured, partly calculated by approximate methods, was then used for an attempt to calculate mercury loads during the event. At the Hotešček gauging station, two flood peaks were observed, the first with 184 and the second with 157 m^3 s^{-1}. These values correspond to the discharge of a 2-year return period. The total calculated amount of suspended sediment transported into the Soča River during the described event was about 15.500 tons. Taking the range of measured concentration of mercury bound in suspended matter into account (20-50 µg g^{-1}), the total amount of mercury in its particulate form carried into the Soča River during the observed 48 hours of the event is between 310 and 780 kg.

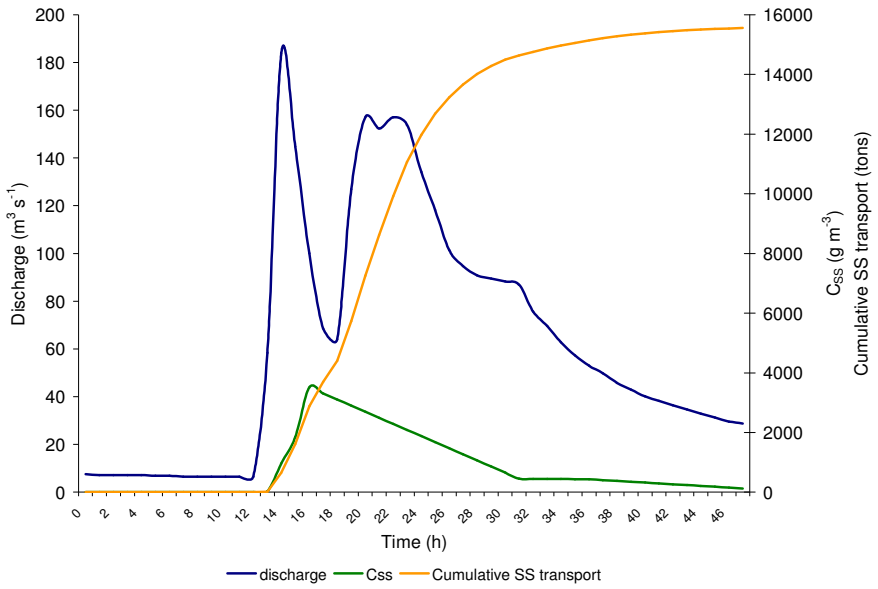

Figure 80: *Sediment transport by the 19/09/2007 flood wave – Hotešček measurement station.*

These results are in a relatively good agreement with the results of Žagar et al. (2006) that modeled mercury transport and transformation processes in the Idrijca and Soča River system. In that work, a 1-D aquatic model MeRiMod was used to simulate hydrodynamics and sediment transport, with the main focus on high discharge conditions. Simulations of several flood events with different recurrence periods (from Q_5 to Q_{500}) were performed. In this way, Žagar et al. (2006) calculated the outflow of suspended sediment from the Idrijca River to Soča River with a typical Q_{100} flood wave at about 7200 tons.

In order to estimate mercury outflow from the catchment associated with such extreme events, a good knowledge about mercury concentration in both suspended and riverbed sediment is needed. During such events, not only the soil erosion but also the riverbed and riverbank erosion are much higher. Flood waves with recurrence period of more than 100 years expectedly cause morphological changes of river reaches. Therefore it is supposed that such flood waves are able to transport material from deeper layers of the riverbed and overbank sediment. It is known from the previous studies of the Idrijca River sediments (e.g. Gosar et al., 1997; Kocman et al., 2004, Žibret and Gosar, 2006) that coarser sediment fraction contain higher Hg concentrations which are likely activated during such events. Moreover, deeper layers of the overbank sediments also contain higher concentrations of Hg (Kocman et al., 2004; Žibret and Gosar, 2006). It is very likely that during such extreme events concentrations of particulate Hg exceed 100 µg g^{-1}, which would then result in much higher mercury outflow from the Idrijca River system under such conditions (2-5 folds).

It must be noted, however, that the flood wave shown in Fig. 80 is not very representative for the Idrijca River. Extremly high concentrations of suspended sediment at relatively low discharges (< 200 m^3 s^{-1}) measured at station Hotešček during this event (up to 3500 g m^{-3}) are the consequence of the catastrophic flooding and landslides that occurred in the Cerknica River subcatchment. Therefore, to include the processes of river bed and river bank erosion in the annual mass balance calculation, outflow of mercury from the catchment due to these processes was calculated based on the flood wave with recurrence period of 2 years (Q_2). TSS load was calculated by the sediment rating curve (Eq. 36). The total calculated amount of suspended sediment transported into the Soča River during the flood wave shown in Fig. 81 is about 1700 tons. Considering particulate Hg concentration of 100 µg g^{-1} due to the resuspension of more Hg abounded sediments under such conditions, the amount of Hg transported would reach 170 kg.

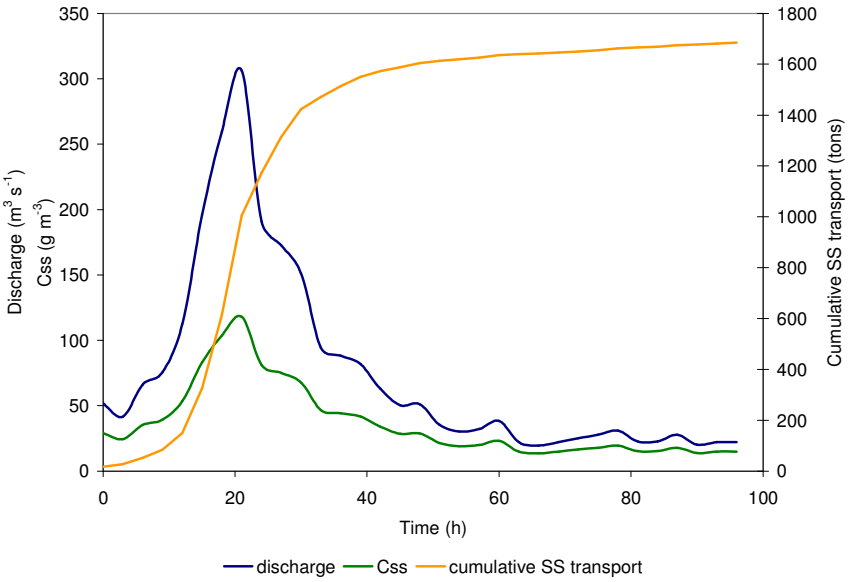

Figure 81: *Sediment transport by the Q_2 flood wave – Hotešček measurement station.*

6.7.2.2 Mercury in dissolved and particulate phase

In the mass balance model, two mercury soil phases were taken into account: dissolved (Hg in soil water) and particulate (Hg bound in soil particles) phase, respectively. The total loss of mercury from the soil is the sum of the loss rates due to leaching, runoff, erosion and volatilization. These loss rates, expressed as the product of a loss rate constant, were calculated according to the procedures described in section 6.3. As a result, total mercury load to the Idrijca River catchments tributary system is the sum of loadings including dissolved Hg lost from the surficial soil layers through surface runoff and particulate bound Hg lost through water runoff erosion.

In Table 13 data that served as an input to the model, as well as calculated annual Hg loads to the Idrijca River and its tributary system are given for each of the 64 hydrographic subunits. Input data include average Hg concentrations in soils, Hg atmospheric deposition rate, Hg emission flux from the surfaces, enrichment factors due to the texture of eroded soil, annual amount of surface runoff and annual amount of infiltration. Results for annual Hg loads to the river system are divided into erosion and runoff loads. Unit area loads are given as well (Table 13).

As it can be seen from Table 13, the total annual mercury loading to the Idrijca River and its tributaries is 953 kg. The predicted mercury load is delivered in the aquatic environment primarily through eroded soil (933 kg Hg year^{-1}). Assuming that 25 % of sediment yield as a consequence of soil erosion is trapped in the catchment as bed sediment, this would then result in 233 kg Hg year^{-1} deposited as a bed load and 700 kg Hg year^{-1} in suspended sediment phase delivered out of the catchment. As it can be seen from Table 13, due to the high variability in spatial distribution of mercury in soil, Hg loads to the river system are the highest in the area of the mercury mine. For example, the area between the towns of Idrija and Spodnja Idrija that represent less than 5 % of the catchment contribute approximately 25 % of total annual mercury load to the Idrica River and its tributaries. At the catchment scale, calculated mercury load in the dissolved phase due to the surface runoff represents only 2 % (19.3 kg Hg year^{-1}) of total load.

The results of the model are in a good agreement with the speciation analysis of mercury in river water performed near the Idrijca River outflow (location Hotešček) discussed in section 5.1.2.3. It was observed that during the high water discharges, relative contribution of particulate bound mercury can arise up to more than 99 %. On the other hand, concentrations of dissolved mercury species remained rather constant, regardless to the hydrological conditions. Therefore, dissolved Hg load calculated based on the measured data and water discharge were compared to the results of the model. Taking the average concentration of dissolved Hg measured at the outflow of the Idrijca River into account (9.3 ng L^{-1}) and the average long term annual discharge (31.3 m^3 s^{-1}, sum of discharges for stations Hotešček and Bača pri Modreju), this results in 9.2 kg of dissolved Hg outflow annually. The results of the model are higher for a factor of 2.

Table 13: *Annual mercury loads to the Idrijca River and its tributary system.*

	Input data							Hg load to water body			
HG unit	**Area (km^2)**	**Hg soil concentration ($mg\ kg^{-1}$)**	**Hg atmos. deposition ($\mu g\ m^{-2}\ year^{-1}$)**	**Hg emission flux ($\mu g\ m^{-2}\ year^{-1}$)**	**enrichment ratio (-)**	**Runoff (cm)**	**Infiltration (cm)**	**Erosion ($g\ year^{-1}$)**	**Runoff ($g\ year^{-1}$)**	**Total Hg load ($g\ year^{-1}$)**	**Area load ($mg\ m^{-2}\ year^{-1}$)**
1	20.3	1.6	40.4	25.7	2.11	90	145	8059	293	8352	0.41
2	14.5	1.4	42.7	21.7	2.07	86	148	4727	173	4899	0.34
3	36.7	0.7	33.5	10.9	2.03	59	143	1385	144	1528	0.04
4	21.0	3.1	39.9	48.8	2.04	58	143	9637	372	10009	0.48
5	22.1	3.6	36.5	59.4	2.10	58	122	13992	465	14457	0.65
6	5.9	16	35.6	254.6	2.21	73	107	28697	671	29368	4.97
7	1.1	14	40.4	222.5	2.05	68	111	1006	102	1108	1.03
8	2.0	130	34.1	634.7	2.04	77	103	23291	786	24077	12.18
9	11.6	20	39.1	316.2	2.03	70	129	39714	1615	41329	3.55
10	6.8	142	38.5	676.6	2.06	71	107	126939	2747	129686	19.09
11	4.7	6.9	37.1	112.0	2.14	73	116	8404	237	8640	1.83
12	6.1	9.1	39.1	145.2	2.12	71	115	13580	398	13978	2.27
13	7.3	2.7	38.9	43.7	2.09	76	128	6925	151	7076	0.97
14	7.9	0.4	39.2	6.8	2.07	78	105	915	26	941	0.12
15	8.8	4.7	36.5	77.1	2.18	76	105	14275	315	14590	1.66
16	10.5	14	40.2	225.7	2.16	70	110	52097	1033	53130	5.06
17	2.2	31	38.2	501.9	2.13	69	112	15848	472	16321	7.39
18	6.2	26	40.1	412.1	2.11	73	104	34207	1155	35362	5.74
19	2.5	25	36.0	404.3	2.22	66	96	35251	411	35662	14.14
20	14.0	20	34.5	321.1	2.22	62	86	115626	1696	117322	8.35
21	10.3	14	37.5	222.5	2.16	63	98	56115	887	57002	5.53
22	12.2	5.3	36.0	86.1	2.17	64	88	26000	413	26413	2.17
23	3.3	11	30.2	176.8	2.20	56	85	16559	193	16752	5.06
24	3.9	5.0	29.0	85.4	2.20	54	79	7814	106	7919	2.02
25	13.8	4.3	31.0	72.2	2.21	55	71	26785	329	27113	1.96
26	6.9	4.8	28.1	81.1	2.24	59	71	16477	194	16671	2.43
27	9.4	5.0	31.8	83.4	2.13	62	84	15157	289	15447	1.64
28	4.3	5.0	32.9	82.3	2.17	72	78	8235	154	8390	1.93
29	10.7	3.8	33.0	63.6	2.22	69	82	25399	281	25679	2.40
30	3.7	7.2	34.7	117.6	2.18	52	73	7272	141	7413	1.98
31	10.1	6.9	29.7	116.4	2.20	63	85	32485	438	32923	3.26
32	10.3	7.5	33.6	123.6	2.13	66	96	26420	506	26926	2.62
33	34.0	3.7	35.6	61.3	2.13	68	90	34742	866	35608	1.05
34	21.6	0.8	30.7	13.5	2.17	72	106	6953	125	7078	0.33
35	9.2	3.2	31.4	53.8	2.15	70	107	8629	208	8837	0.96
36	3.1	4.0	31.6	66.7	2.23	73	102	3063	90	3153	1.02
37	5.0	0.5	39.2	8.0	2.03	109	68	377	27	404	0.08
38	9.3	0.4	38.8	6.6	2.12	109	70	1098	41	1139	0.12
39	18.6	0.3	39.4	5.5	2.12	100	79	1862	64	1925	0.10
40	12.5	0.5	36.8	7.6	2.12	86	99	2420	50	2470	0.20
41	5.2	0.5	37.2	7.4	2.07	78	134	583	19	601	0.12
42	14.1	0.5	40.1	7.4	2.06	90	138	2021	59	2080	0.15
43	8.1	0.2	38.1	3.3	2.44	85	100	3313	14	3327	0.41
44	4.2	0.2	35.9	3.3	2.42	82	110	1558	7	1565	0.37
45	1.8	0.2	42.5	3.2	2.16	73	113	146	3	149	0.08
46	2.6	0.2	37.3	3.3	2.30	78	104	251	4	255	0.10
47	4.9	0.3	40.3	4.3	2.22	76	110	900	10	910	0.18
48	2.4	0.2	38.7	3.3	2.36	77	115	657	4	660	0.27
49	3.3	0.2	37.6	3.1	2.17	73	110	278	5	283	0.08
50	9.8	0.9	39.5	14.8	2.17	79	105	4553	72	4624	0.47
51	6.2	0.1	38.8	1.7	2.18	81	100	220	5	226	0.04
52	6.0	0.2	32.9	2.9	2.39	83	124	1860	9	1869	0.31
53	10.0	0.1	35.7	2.1	2.40	84	138	2403	11	2413	0.24
54	6.0	0.1	36.0	2.2	2.37	103	137	1371	8	1380	0.23
55	10.3	0.2	41.3	3.5	2.24	80	111	1525	18	1543	0.15
56	7.2	0.8	36.7	12.9	2.15	79	100	1636	45	1681	0.23
57	10.1	0.5	38.3	8.6	2.15	64	116	1452	34	1486	0.15
58	8.7	0.2	38.5	3.6	2.19	79	122	788	15	803	0.09
59	3.4	0.2	42.8	3.8	2.22	98	138	465	8	473	0.14
60	4.6	0.2	31.2	3.1	2.43	121	168	1777	10	1787	0.39
61	4.9	0.3	29.8	4.7	2.52	125	173	4529	17	4546	0.92
62	7.4	0.6	37.9	9.3	2.48	101	149	10016	42	10058	1.36
63	7.1	0.5	41.4	7.3	2.18	92	148	1615	30	1645	0.23
64	15.0	2.0	33.9	33.4	2.17	76	115	11346	231	11577	0.77
SUM								933697	19343	953041	

Considering the robustness of the modeling approach (catchment scale, no temporal variability…) agreement within the factor of 2 can be considered as acceptable. However, there are several likely reasons for the discrepancy. First, in the model soil water partition coefficients were used to calculate the fractions of mercury in the dissolved and particulate phase, respectively. This is a highly sensitive parameter, which can vary over many orders of magnitude. Site specific partition coefficients used were derived from the soil leaching experiments during which conditions were used that do not represent the actual situation in the nature.

Second, the amount of surface runoff used to calculate the runoff rate constant is a result of modeling where average long term meteorological conditions which can vary significantly from year to year were used. Another important source of uncertainty is the estimation of average subunit-wide soil mercury concentrations, especially for the hydrographic subunits with elevated soil mercury concentrations. Moreover, there were not enough measurements of mercury in river water performed under higher water discharges to investigate the distribution of dissolved mercury phases under such conditions and to validate the model.

Both the modeled and measured results suggest that majority of mercury in soil is firmly bound to the organic matter and is susceptible to leaching and runoff mostly by being attached in/to particles. Only a small part of mercury (most probably bound to dissolvable organic ligands) may partition to runoff in the dissolved phase. These assumptions were further confirmed by the percent of soil retention calculated as the ratio between the atmospheric mercury deposition and the riverine mercury flux. For the area that is drained by the Trebušica and Bača River, respectively, where there are no direct anthropogenic influences, it was calculated that more than 98 % of mercury deposited from the atmosphere is retained in soil. These results suggest that the atmospheric input of mercury to soil exceeds the amount leached, and the amount of mercury partitioning to runoff is only a small fraction of the amount of mercury stored in soil.

6.7.3 Mass balance evaluation

In Fig. 82 annual mass balance of mercury in the Idrijca River catchment is shown. The following processes are included: atmospheric deposition due to the wetfall, dryfall and throughfall; emissions from the soil surface, runoff of dissolved phases and erosion of particulate bound Hg.

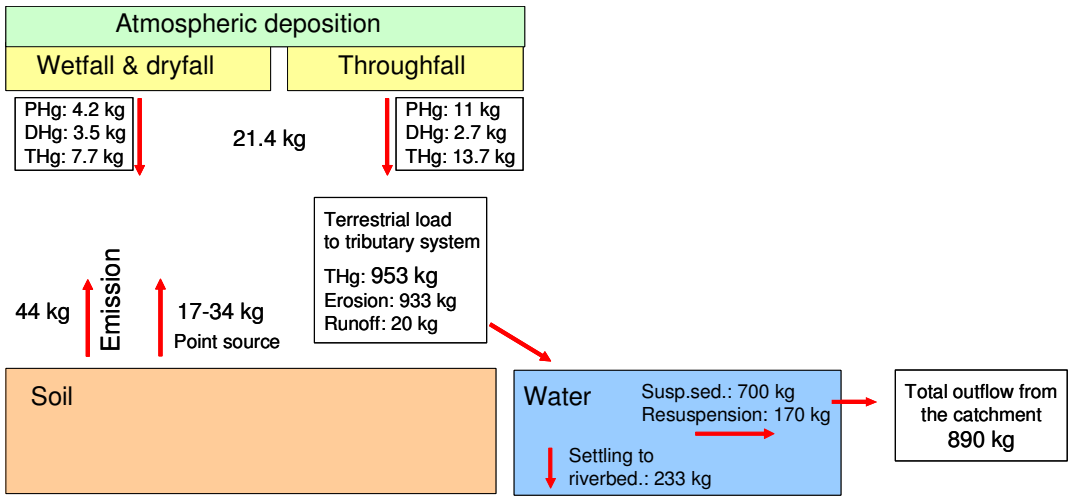

Figure 82: *Annual mass balance of mercury in the Idrijca catchment.*

As it can be seen from Fig. 82, on an annual basis, soil erosion acts as the major terrestrial source of mercury to the Idrijca River and its tributaries. It was estimated that of total 933 kg of particle bound mercury entering the aquatic system due to surface erosion, 700 kg of Hg is transported with the suspended sediments along the Idrijca River in the Soča River. The difference of 233 kg is deposited within the catchment as a riverbed sediment. Due to the surface runoff, additional amount of 20 kg of mercury in the dissolved phase is carried along the Idrijca River annualy. Due to the resuspension of contaminated river sediments of the Idrijca River, approximately 170 kg of mercury is transported to the Soča River with a typical flood wave that can be expected in an average hydrological year. Therefore, the total annual riverine outflow of mercury from the Idrijca River catchment is estimated at 890 kg.

7 Conclusions

Mercury pollution in the Idrijca River catchment, a result of five centuries of mining and ore processing operations in this area, was studied in order to better understand the cycling of mercury at the Idrijca River catchment scale, gaining an understanding of its chemical and transport processes, and to place this knowledge in the context of the global mercury cycle. The main conclusions of this work are as follows.

The results of mercury analysis in river water revealed that even more then 10 years after the end of the mining operations in this region, concentrations in the Idrijca River remain elevated. The distribution of mercury in both Idrijca River and its tributaries is greatly influenced by the distance from the mining sites in the town of Idrija. These results suggest that contaminated soils, Hg-laden material and tailings near the Idrija mine continue to supply Hg to the Idrijca river system. Mercury speciation in water samples obtained under different hydrological conditions indicated the importance of resuspension of Hg from the river bed on its riverine transport. The partitioning of Hg between dissolved and particulate phases was mostly controlled by the concentrations of suspended solids (TSS) and dissolved organic carbon (DOC). As shown by the SEM/EDXS microscopy, at this mercury contaminated site a significant part of the Hg particulate phase in water can be due to the cinnabar particles present.

The results of the spatial and vertical distribution of mercury in soils revealed that at the catchment scale, atmospheric deposition influenced the accumulation of mercury in soils the most. In general, higher THg concentrations were observed in the organic rich topsoil layers and on the hill slopes, as results of the weathering and erosion processes. MeHg in soils showed no correlation with THg concentrations, supporting the assumption of the enhanced demethylation process in Hg reach environments. In the Idrija region, MeHg production seems to be more efficient in low THg abounded soils in which demethylation processes are minimized. Fractionation of water soluble mercury in aqueous soil phase revealed the majority of mercury in soil water is present as species bound to organic matter or suspended mineral particles rather than water-soluble ionic species or in dissolved gaseous form.

Measurements of Hg^0 in the air in Idrija and surroundings revealed that the former smelting plant remains the main source of Hg in air over the Idrija Valley. In the town of Idrija, 2-3 fold higher concentrations of TPM and RGM were measured compared to background sites. These two mercury species then dominate the atmospheric deposition. At mercury polluted site such as Idrija, elevated concentrations of mercury bound in/to particulates in air (TPM) is most probably the result of local mercury sources and fine particulate matter ejected from contaminated surfaces due to the eolian erosion.

Measurements of mercury in precipitation revealed that Hg concentrations depend mostly on the duration, frequency and the amount of precipitation. The results of speciation analysis in precipitation showed that both particulate and dissolved Hg forms are removed by precipitation. Mercury concentrations in throughfall were significantly higher than the associated event precipitation. Particulate bound Hg presented the majority of the total Hg concentrations in the throughfall, suggestsing that at this specific mine polluted site dry deposition is mostly governed by the deposition of Hg containing aerosols.

The laboratory flux measurement experiment revealed the two mostimportant factors that influence the magnitude of mercury air-surface fluxes: substrate Hg concentration and temperature, respectively. The magnitude of the surface-air mercury exchange does not depend only on the total mercury concentrations but also on the binding form of mercury in the individual soil. The later results in different activation energies required for the overall process to occur.

The results of the mercury mass balance model suggest that in the Idrijca River catchment erosion and surface runoff are the main inputs of mercury into the Idrijca River tributary system (953 kg $year^{-1}$). The total average annual riverine outflow of mercury from the Idrijca River catchment was estimated at 890 kg. Both the modeled and measured results suggested that majority (> 98%) of mercury in soil is firmly bound to the organic matter and is susceptible to leaching and runoff mostly by being attached in/to particles. Taking the calculated inputs and outputs of mercury to/from the catchment into account, it can be concluded that the quantity of mercury stored in the Idrijca River catchments soils and sediments significantly exceeds the annual quantity of mercury leaving the catchment. Therefore, without suitable remediation actions reduction of mercury pollution in the area can not be expected.

8 Acknowledgements

I would like to address special thanks to my advisor dr. Milena Horvat who introduced me in the world of mercury and guided me through the all necessary steps to arrive to the final version of this thesis. I want to thank for all the support and encouragements that she gave me.

A special thank to dr. Tjaša Kanduč and dr. Nives Ogrinc for the many helpful dialogues and comments I have received regarding the general water geochemistry. I am also deeply grateful to my colleagues from the Department of Environmental Sciences for their support and stimulation.

I would also like to thank the members of my thesis committee for giving me some substantial arguments. I would like to show my gratitude to the Slovenia Research Agency for providing funds to support this research through the Young Researchers Program.

Finally, to my girls Nataša and Živa, and the little Gal - thank you all for being around.

9 References

Amiotte Suchet, P.; Probst, J.L. Modelling of atmospheric CO_2 consumption by chemical weathering of rocks: Application to the Garonne, Congo and Amazon basins. *Chemical Geology* **107**: 205-210, (1993).

Araguas-Araguas, L.; Fröhlich, K. ; Rozanski, K. Deuterium and oxygen-18 isotope composition of precipitation and atmospheric moisture. *Hydrological Processes* **14**: 1341–1355, (2000).

Babiarz, C.L.; Hurley, J.P.; Hoffmann, S.R.; Andren, A.W.; Shafer, M.M.; Armstrong, D.E. Partitioning of total mercury and methylmercury to the colloidal phase in freshwaters. *Environmental Science & Technology* **35**: 4773 -4782, (2001).

Bahlmann, E.; Ebinghaus, R.; Ruck, W. Development and application of a laboratory flux measurement system (LFMS) for the investigation of the kinetics of mercury emissions from soils. *Journal of Environmental Management* **81**: 114-125, (2006).

Barkay, T.; Wagner-Döbler, I. Microbial transformations of mercury: potentials, challenges, and achievements in controlling mercury toxicity in the environment. *Advances in applied microbiology* **57**: 1-52, (2005).

Bazzoffi, P. Methods for net erosion measurement in watersheds as a tool for the validation of models in central Italy. In: *Workshop on Soil Erosion and Hillslope Hydrology with Emphasis on Higher Magnitude Events, Leuven.* (Leuven, 1985).

Berner, E.K.; Berner, R.A. Global Environment: Water, Air and Geochemical cycles. In: Sumner, M.E. (ed.) *Handbook of Soil Science*. (Prentice Hall, New York, 1996).

Beyer Portner, N. Erosion des bassins versant alpins suisses par ruissellement de surface. PhD Thesis. (Laboratoire de Constructions Hydrauliques-LCH, No. 1815, Lausanne, 1998).

Biester, H.; Gosar, M.; Covelli, S. Mercury speciation in sediments affected by dumped mining residues in the drainage area of the Idrija mercury mine, Slovenia. *Environmental Science and Technology* **34**: 3330-3336, (2000).

Biester, H.; Gosar, M.; Müller, G. Mercury speciation in tailings of the Idrija mercury mine. *Journal of Geochemical Exploration* **65**: 195-204, (1999).

Biester, H.; Muller, G.; Scholer, H.F. Binding and mobility of mercury in soils contaminated by emissions from chlor-alkali plants. *The Science of the Total Environment* **284**: 191-203, (2002).

Bloom, N.S.; Watras, C.J. Observations of methylmercury in precipitation. *The Science of the Total Environment* **87-88**: 199-207, (1989).

Bloom, N.S.; Preus, E.; Katon, J.; Hiltner M. Selective extractions to assess the biogeochemically relevant fractionation of inorganic mercury in sediments and soils *Analytica Chimica Acta* **479**: 233-248, (2003).

Boardman, J. Soil erosion by water: problems and prospects for research. In: Anderson, M.G.; Brooks, S.M. (eds.) *Advances in hillslope processes*. 489–527 (Wiley, Chichester, 1996).

Bonzongo, V.; Lyons, W.B.; Hines, M.E.; Warwick, J.J.; Faganeli, J.; Horvat, M.; Lechler, P.J.; Miller, J.R. Mercury in surface waters of three mine-dominated river systems: Idrija river, Slovenia, Carson river, Nevada and Madeira river, Brazilian Amazon. *Geochemistry: Exploration, Environment, Analysis* **120**: 111-120, (2002).

Brown, S.; Saito, L.; Knightes, C.; Gustin, M. Calibration and evaluation of a Mercury model for a western stream and constructed wetland. *Water, Air, and Soil Pollution* **182**: 275-290, (2007).

Buser, S. *Geological Map of Slovenia*. In: *Encyclopedia of Slovenia*. *No. 8*. (Mladinska knjiga, Ljubljana, 1987).

Byrne, A.R.; Kosta, L. Studies on the distribution and uptake of mercury in the area of mercury mine Idrija. *Vestnik slovenskega kemijskoga društva* **17**: 5-11, (1970).

Cardona-Marek, T.; Schaefer, J.; Ellickson, K.; Barkay, T.; Reinfelder, J.R. Mercury speciation, reactivity,

and bioavailability in a highly contaminated estuary, Berry's Creek, New Jersey Meadowlands. *Environmental Science & Technology* **41**: 8268–8274, (2007).

Carpi, A.; Lindberg, S.E. Application of a teflon™ dynamic flux chamber for quantifying soil mercury flux: Tests and results over background soil. *Atmospheric Environment* **32**: 873-882, (1998).

Celo, V.; Lean, D.R.S.; Scott, S.L. Abiotic methylation of mercury in the aquatic environment. *Science of the Total Environment* **368**: 126– 137, (2006).

Chen, J.; Wang, F.; Xia, X.; Zhang L. Major element chemistry of the Changjiang (Yangtze River). *Chemical Geology* **187**: 231-255, (2002).

Covelli, S.; Faganeli, J.; Horvat, M.; Brambati, A. Porewater distribution and benthic flux measurements of mercury and methylmercury in the Gulf of Trieste (Northern Adriatic Sea). *Estuarine, Coastal and Shelf Science* **48**: 415-428, (1999).

Čar, J. Mineralized Rocks and Ore Residues in the Idrija Region. In: Miklavčič, M. (ed.) *Idrija as a Natural and Anthropogenic Laboratory: Mercury as a Global Pollutant. Proceeding, 24 May 1996, Idrija, Slovenia*. 10–15 (1998).

Čar, J.; Dizdarevič, T. Pisna poročila o vplivu rudarjenja na naravno okolje v Idriji do konca 18. stoletja. *Idrijski razgledi* **48**: 14-25, (2003).

Dai, T.; Manguerra, H. User's guide for WCS mercury tool. (Tetra Tech, Inc., Fairfax, 2000). Available at http://wcs.tetratech-ffx.com/Documentation/index.htm

Dizdarevič, T. The influence of mercury production in Idrija mine on the environment in the Idrija region and over a broad area. *RMZ - Materials and Geoenvironment* **48**: 56–64, (2001).

Dolan, D.M.; Yui, A.K; Geist, R.D. Evaluation of river load estimation methods for total phosphorus. *Journal of Great Lakes Research* **7**: 207–214, (1981).

Dyrssen, D.; Wedborg, M. The sulfur–mercury (II) system in natural waters. *Water, Air, and Soil Pollution* **56**: 507–519, (1991).

EIONET - European Environment Information and Observation Network. http://eionet-en.arso.gov.si (accessed 11 Nov 2005).

EU. *Ambient Air Pollution by Mercury (Hg) Position Paper*, October 2001.

Engle, M.A.; Gustin, M.S. Scaling up atmospheric mercury emissions from three naturally enriched areas: Flowery Peak, Nevada, Peavine Peak, Nevada and Long valley Caldera, California. *The Science of the Total Environment* **290**: 91–104, (2002).

Epstein, S.; Mayeda, T.K. Variation of O 18 content of waters from natural sources. *Geochimica et Cosmochimica Acta* **4**: 213-224, (1953).

Ericksen, J.A.; Gustin, M.S.; Schorran, D.E.; Johnson D.W.; Lindberg, S.E.; Coleman, J.S. Accumulation of atmospheric mercury in forest foliage. *Atmospheric Environment* **37:** 1613–1622, (2003).

Faganeli, J; Horvat, M.; Covelli, S.; Fajon, V.; Logar, M.; Lipej, L.; Čermelj, B. Mercury and methylmercury in the Gulf of Trieste (northern Adriatic Sea). *The Science of the Total Environment* **304**: 315-326, (2003).

Falnoga, I.; Jereb, V.; Smrkolj, P. Hg and Se in foodstuffs grown near a Hg-mining area. *Journal de Physique* **170**: 447-450, (2003).

Fanetti, D.; Vezzoli, L. Sediment input and evolution of lacustrine deltas: The Breggia and Greggio rivers case study (Lake Como, Italy). *Quaternary International* **173–174:** 113–124, (2007).

Ferrara, R.; Mazzolai, B. A dynamic flux chamber to measure mercury emission from aquatic systems. *The Science of the Total Environment* **215**: 51–57, (1998).

Ferrara, R.; Mazzolai, B.; Edner, H.; Svanberg, S.; Wallinder, E. Atmospheric mercury sources in the Mt. Amiata area, Italy. *The Science of the Total Environment* **213**: 13–23, (1998).

Ferrara, R.; Mazzolai, B.; Lanzillotta, E.; Nucaro, E.; Pirrone, N. Temporal trends in gaseous mercury evasion from the Mediterranean seawaters. *The Science of the Total Environment* **259**: 183–190, (2000).

Frančišković-Bilinski, S.; Bilinski, H.; Tibljaš, D.; Rantitsch, G. Effects of mercury mining regions from NW Dinarides on quality of stream sediments. *Fresenius Environmental Bulletin* **14**: 913-927, (2003).

Gabriel, M.C.; Williamson, D.G. Principal biogeochemical factors affecting the speciation and transport of mercury through the terrestrial environment. *Environmental Geochemistry and Health* **26**: 421–434, (2004).

Gavrilović, S. Inženjering o bujičnim tokovima i eroziji. (Savez građevinskih inženjera i tehničara Jugoslavije, Beograd, 1972).

Gavrilović, S. Bujični tokovi i erozija (Torrents and erosion). (Građevinski kalendar, Beograd, 1976). 159–311.

Gavrilovic, Z. The use of an empirical method (erosion potential method) for calculating sediment production and transportation in unstudied or torrential streams. Paper presented at the international conference on river regime. (Institute for the Development of Water Resources, ''Jaroslav Cerni'', Belgrade, 1988).

Gbor, P.K.; Wen, D.; Meng, F.; Yang, F.; Zhang, B.; Sloan, J.J. Improved model for mercury emission, transport and deposition. *Atmospheric Environment* **40**: 973–983, (2006).

Gibbs, R.J. Mechanisms controlling world water chemisty. *Science* **170**: 1088-1090, (1970).

Gieskes, J.M. The alkalinity-total carbon dioxide system in sweater. In: Goldberg E.D. (ed.) *The Sea, Volume 5: Marine Chemistry.* 123-151 (John Wiley and Sons, New York, 1974).

Gillis, A.A.; Miller, D.R. Some local environmental effects on mercury emission and absorption at a soil surface, *The Science of the Total Environment* **260**: 191-200, (2000).

Gilmour, C.C.; Henry, E.A. Mercury methylation in aquatic systems affected by acid deposition. *Environmental Pollution* **71**: 131-169, (1991).

Globevnik, L.; Holjevic, D.; Petkovšek, G.; Rubinic, J. Applicability of the Gavrilović method in erosion calculation using spatial data manipulation techniques. In: *Erosion prediction in ungauged basins: integrating methods and techniques. Proceedings of an international symposium, Sapporo, Japan, 8-9 July 2003.* (IAHS Press, Sapporo, 2003).

Gnamuš, A.; Byrne, A.R.; Horvat, M. Mercury in the soil–plant–deer– predator food chain of a temperate forest in Slovenia. *Environmental Science & Technology* **34**: 3337–3345, (2000).

Gosar, M.; Pirc, S.; Bidovec, M. Mercury in the Idrijca River sediments as a reflection of mining and smelting activities of the Idrija mercury mine. *Journal of Geochemical Exploration* **58**: 125-131, (1997).

Gosar, M.; Šajn, R.; Biester, H. Binding of mercury in soils and attic dust in the Idrija mercury mine area (Slovenia). *The Science of the Total Environment* **369**: 150–162, (2006).

Gosar, M.; Pirc, S.; Šajn, R.; Bidovec, M.; Mashyanov, N.R.; Sholupov, S.E. Distribution of mercury in the atmosphere over Idrija, Slovenia. *Environmental Geochemistry and Health* **19**: 101-110, (1997).

Gray, J.E.; Theodorakos, P.M.; Bailey, E.A.; Turner, R.R. Distribution, speciation, and transport of mercury in stream-sediment, stream-water, and fish collected near abandoned mercury mines in southwestern Alaska, USA, *The Science of the Total Environment* **260**: 21-33, (2000).

Grigal, D.F. Inputs and outputs of mercury from terrestrial watersheds: a review. *Environmental Reviews* **10**: 1-39, (2002).

Groenlund, R.; Edner, H.; Svanberg, S.; Kotnik, J.; Horvat, M. Mercury emissions from the Idrija mercury mine measured by differential absorption Lidar techniques and a point monitoring absorption spectrometer. *Atmospheric Environment* **39**: 4067–4074, (2005).

Guentzel, J.L.; Landing, W.M.; Gary, U.; Gill, A.; Pollman, C.D. Mercury and major ions in rainfall, throughfall, and foliage from the Florida Everglades. *The Science of the Total Environment* **213**: 43-51, (1998).

Guimarães, J.R.D.; Meili, M.; Malm, O.; de Souza Brito, E.M. Hg methylation in sediments and floating meadows of a tropical lake in the Pantanal floodplain, Brazil. *The Science of the Total Environment* **213**: 165-175, (1998)

Guo, L.; Santschi, P.H. Ultrafiltration technique and its applications to sampling and characterization of aquatic colloids. In: Wilkinson, K.J.; Lead, J.R. (eds.) *Environmental Colloids and Particles: Behaviour, Separation and Characterisation. Series on Analytical and Physical Chemistry of Environmental Systems*. (Wiley, 2007).

Gustin, M.S. Are mercury emissions from geologic sources significant? A status report. *The Science of the Total Environment* **304**: 153–167, (2003).

Gustin, M.S.; Taylor, G.E.; Maxey, R.A. Effect of temperature and air movement on the flux of elemental mercury from substrate to the atmosphere. *Journal of Geophysical Research* **102**: 3891-3898, (1997).

Gustin, M.S.; Coolbaugh, M.F.; Engle, M.A.; Fitzgerald, B.C.; Keislar, R.E.; Lindberg, S.E.; Nacht, D.M.; Quashnick, J.; Rytuba, J.J.; Sladek, C.; Zhang, H.; Zehner, R.E. Atmospheric mercury emissions from

mine wastes and surrounding geologically enriched terrains. *Environmental Geology* **43**: 339–351, (2003).

Hall, B.D.; Manolopoulos, H.; Hurley, J.P.; Schauer, J.J.; St. Louis, V.L.; Kenski, D.; Graydon, J.; Babiarz, C.L.; Clecknera, L.B.; Keeler, G.J. Methyl and total mercury in precipitation in the Great Lakes region. *Atmospheric Environment* **39**: 7557–7569, (2005).

Hammerschmidt, C.R.; Lamborg, C.H.; Fitzgerald, W.F. Aqueous phase methylation as a potential source of methylmercury in wet deposition. *Atmospheric Environment* **41**: 1663–1668, (2007).

Hedges, J.I. Global biogeochemical cycle: progress and problem. *Marine Chemistry* **39**: 67-93, (1992).

Hess, A. *Verteilung, Mobilität und Verfügbarkeit von Hg in Böden und Sedimenten am Beispiel zweier hochbelasteter Industriestandorte*. (Heidelberger Geowissenschaftliche Abhandlungen, Heidelberg, 1993).

Hines, M.E.; Horvat, M.; Faganeli, J.; Bonzongo, J.-C.J.; Barkay, T.; Major, E.B.; Scott, K.J.; Bailey, E.A.; Warwick, J.J.; Lyons, W.B. Mercury biogeochemistry in the Idrija river, Slovenia from above the mine into the Gulf Trieste. *Environmental Research* **83**: 129-139, (2000).

Hissler, C.; Probst, J.-L. Chlor-alkali industrial contamination and riverine transport of mercury: Distribution and partitioning of mercury between water, suspended matter, and bottom sediment of the Thur River, France. *Applied Geochemistry* **21**: 1837–1854, (2006).

Holland, H.D. *The Chemistry of the Atmosphere and Oceans*. (Wiley - Interscience, New York, 1978).

Horvat, M. Determination of methylmercury in biological reference materials. *Water, Air, and Soil Pollution* **56**: 95-102, (1991).

Horvat, M. Mercury analysis and speciation in environmental samples. In: Baeyens, W.R.G.; Ebinghaus, R; Vasiljev, R. (eds.) *Global and regional mercury Cycles: Sources, Fluxes and Mass balances.* 1-31 (Kluwer Academic Publishers, Dordrecht, 1996)

Horvat, M.; Byrne, A.R. Preliminary study of the effects of some physical parameters on the stability of methylmercury in biological samples. *Analyst* **117**: 665-668, (1992).

Horvat, M.; Lupšina, V. Determination of total mercury in coal fly ash by gold amalgamation cold vapour atomic absorption spectrometry. *Analytica Chimica Acta* **243**: 71-79, (1991).

Horvat, M.; Byrne, A.R.; May, K. A modified method for the determination of methylmercury by gas chromatography. *Talanta* **37**: 207-212, (1990).

Horvat, M.; Liang, L.; Bloom, N. Comparison of distillation with other current isolation methods for the determination of methylmercury compounds in low-level environmental samples, Part 1: Sediments. *Analytica Chimica Acta* **281**: 135-152, (1993a).

Horvat, M.; Liang, L.; Bloom, N. Comparison of distillation with other current isolation methods for the determination of methylmercury compounds in low-level environmental samples, Part 2: Water. *Analytica Chimica Acta* **282**: 153-168, (1993b).

Horvat, M.; Lupšina, V.; Pihlar, B. Determination of total mercury in coal fly ash by gold amalgamation cold vapour atomic absorption spectrometry. *Analytica Chimica Acta* **24**: 71-79, (1991).

Horvat, M.; May, K.; Stoeppler, M.; Byrne, A.R. Comparative studies of methylmercury determination in biological and environmental samples. *Applied Organometallic Chemistry* **2**: 850-860, (1988).

Horvat, M.; Zvonarič, T.; Stegnar, P. Determination of mercury in seawater by cold vapour atomic absorption spectroscopy. *Acta Adriatica* **28**: 59-63, (1987).

Horvat, M.; Kotnik, J.; Logar, M.; Fajon, V.; Zvonarić, T.; Pirrone, N. Speciation of mercury in surface and deep-sea waters in the Mediterranean sea. *Atmospheric Environment* **37**: 93-108, (2003).

Horvat, M.; Jereb, V.; Fajon, V.; Logar, M.; Kotnik, J.; Faganeli, J.; Hines, M.E.; Bonzongo, J.-C. Mercury distribution in water, sediment and soil in the Idrijca and Soča river systems. *Geochemistry: Exploration, Environment, Analysis* **2**: 287-296, (2002).

Hunter, K.A.; Kim, J.P.; Reid, M.R. Factors influencing the inorganic speciation of trace metal cations in fresh waters. *Marine and Freshwater Research* **50**: 367-372, (1999).

Ittekkot, V. Global trends in the nature of organic matter in the river suspensions. *Nature* **332**:436-438, (1988).

Jing, Y.D.; He, Z.L.; Yang, X.E. Effects of pH, organic acids, and competitive cations on mercury desorption in soils. *Chemosphere* **69**: 1662-1669, (2007).

Kanduč, T.; Szramek, K.; Ogrinc, N.; Walter, L.M. Origin and cycling of riverine inorganic carbon in the Sava River watershed (Slovenia) inferred from major solutes and stable carbon isotopes. *Biogeochem* **86**: 137-154, (2007).

Kastelec, D.; Rakovec, J.; Zaksek, K. *Sončna Energija v Sloveniji* (Založba ZRC, ZRC SAZU, Ljubljana, 2007).

Keeler, G.J.; Gratz, L.E.; Al-Wali, K. Long-term atmospheric mercury wet deposition at Underhill, Vermont. *Ecotoxicology* **14**: 71–83, (2005).

Kim, K.H.; Lindberg, S.E. Design and initial tests of a dynamic enclosure chamber for measurements of vapour phase mercury fluxes over soils. *Water, Air, and Soil Pollution* **80**: 1059–1068, (1995).

Knific, J. Poročilo o kalnosti vodotokov za leta 1991 do 1996. Report. (Hidrometeorološki zavod RS, Ljubljana).

Kocman, D.; Horvat, M.; Kotnik, J. Mercury fractionation in contaminated soils from the Idrija mercury mine region. *Journal of Environmental Monitoring* **6**: 696–703, (2004).

Kocman, D.; Bloom, N.S.; Akagi, H.; Telmer, K.; Hylander, L.; Fajon, V.; Jereb, V.; Jaćimović, R.; Smodiš, B:, Ikingura, J.R.; Horvat, M. Preparation and characterization of a soil reference material from a mercury contaminated site for comparability studies. *Journal of Environmental Monitoring* **81**: 146-154, (2006).

Kodrič, T. Ureditvena dela na hudourniku Lajtna grapa v povodju Bače. Diplomska naloga. (Univerza v Ljubljani, FGG, Ljubljana, 1999). 51 p.

Kolbezen, M.; Pristov, J. *Površinski Vodotoki in Vodna Bilanca Slovenije.* (Ministry of Environment and Physical Planning, Ljubljana, 1998).

Komac, B.; Zorn, M. Soil erosion on agricultural land in Slovenia – measurements of rill erosion in the Besnica valley. *Acta geographica Slovenica* **45**: 53–86, (2005).

Kosta, L.; Byrne, A.R.; Zelenko, V.; Stegnar, P.; Dermelj, M.; Ravnik, V. Studies on uptake, distribution and transformations of mercury in living organisms in the Idrija region and comparative areas. *Vestnik slovenskega kemijskega drustva* **21**: 49–76, (1974).

Kot, F.S.; Matyushkina, L.A. Distribution of mercury in chemical fractions of contaminated urban soils of Middle Amur, Russia. *Journal of Environmental Monitoring* **4**: 803-808, (2002).

Kotnik, J.; Horvat, M.; Dizdarevič, T. Current and past mercury distribution in air over the Idrija Hg mine region, Slovenia. *Atmospheric Environment* **39**: 7570-7579, (2005).

Kotnik, J.; Horvat, M.; Fajon, V.; Gibičar, D.; Kocman, D. Reference method for the determination of Hg deposition. IJS – Working report 9828, (2008).

Kotnik, J.; Horvat, M.; Tessier, E.; Ogrinc, N.; Monperrus, M.; Amouroux, D.; Fajon, V.; Gibičar, D.; Žižek, S.; Sprovieric, F.; Pirrone, N. Mercury speciation in surface and deep waters of the Mediterranean Sea. *Marine Chemistry* **107**: *13-30*, (2007).

Lamborg, C.H.; Fitzgerald, W.F.; O'Donnell, J.; Torgersen, T. An examination of global-scale mercury biogeochemistry using a non-steady state compartment model which features interhemispheric gradients in the atmosphere as constraints. *Geochimica et Cosmochimica Acta* **66**: 1-14, (2002).

Larcher, W. Physiological Plant Ecology: Ecophysiology and Stress Physiology of Functional Groups (Springer-Verlag, Berlin Heilderberg New York, 2003).

Liang, L.; Horvat, M.; Bloom, N.S. An improved method for speciation of mercury by aqueus phase ethylation, room temperature precollection, GC separation and CV AFS detection. *Talanta* **41**: 371-379, (1994).

Likar, J.; Cigale, M.; Režun, B. Long-term deformation processes in the wider area of the closed Idrija Mercury Mine. In: Van Cotthem, A.; Charlier, R.; Thimus, J.-F.; Tshibangu, J.-P. (eds) *EUROCK 2006 – Multiphysics Coupling and Long Term Behavior in Rock Mechanics*. 331-336 (Taylor & Francis Group, London, 2006).

Lin, C.-J.; Pehkonen, S.O. The chemistry of atmospheric mercury: a review. *Atmospheric Environment* **33**: 2067-2079, (1999).

Lindberg, S.E.; Stratton, W.J. Atmospheric mercury speciation: concentration and behavior of reactive gaseous mercury in ambient air. *Environmental Science and Technology* **32**: 49-57, (1998).

Lindberg, S.E.; Zhang, H.; Gustin, M.; Vette, A.; Marsik, F.; Owens, J.; Casimir, A.; Ebinghaus, R.; Edwards, G.; Fitzgerald, G.; Kemp, J.; Kock, H.; London, J.; Majewski, M.; Poissant, L.; Pilote, M.;

Rasmussen, P.; Schaedlich, F.; Schneeberger, D.; Sommar, J.; Turner, R.; Wallschlager, D.; Xiao, Z. Increases in mercury emissions from desert soils in response to rainfall and irrigation. *Journal of Geophysical Research* **104**: 879–21, (1999).

Lindqvist, O.; Rodhe, H. Atmospheric mercury - a review. *Tellus* **27B**: 136-159, (1985).

Lu, J.Y.; Schroeder, W.H.; Berg, T.; Munthe, J.; Schneeberger, D.; Schaedlich, F. Device for sampling and determination of total particulate mercury in ambient air. *Analytical Chemistry* **70**: 2403-2408, (1998).

McKay, D.; Wania, F.; Schoroeder, W.H. Prospects for modeling the behavior and fate of mercury, globally and in aquatic systems. *Water, Air, and Soil Pollution* **80**: 941–950, (1995).

Meili, M. Mercury in lakes and rivers. *Metal Ions in Biological Systems* **34**: 21–51, (1997).

Meybeck, M. River water quality: Global ranges, time and space variabilities, proposals for some redefinitions. *Verhandlungen - Internationale Vereinigung für theoretische und angewandte Limnologie* **26**: 81-96, (1996).

Mikoš, M. Spatial interrelations of erosion-related phenomena. *Gozdarski vestnik* **9**: 342–351, (1995).

Mikoš, M.; Fazarinc, R.; Ribičič, M. Sediment production and delivery from recent large landslides and earthquake-induced rock falls in the Upper Soča River Valley, Slovenia. *Engineering Geology* **84**: 1-13, (2006).

Miklavčič, V. *Mercury in the Town of Idrija (Slovenia) After 500 Years of Mining and Smelting*. In: Ebinghaus, R.; Turner, R.R.; Lacedra, L.D.; Vasiljev, O.; Salomons, W. (eds.) *Mercury Contaminated Sites.* 259-270. (Springer-Verlag, Berlin, 1999).

Mlakar, I. Osnovni parametri proizvodnje rudnika Idrija skozi stoletja do danes. *Idrijski Razgledi* **19**: 1-40, (1974).

Morel, F.M.M.; Kraepiel, A.M.L.; Amyot, M. The chemical cycle and bioaccumulation of mercury. *Annual Review of Ecology and Systematics* **29**: 543-566, (1998).

Morrison, J.; Brockwell, T.; Merren, T.; Fourel, F.; Phillips, A.M. On-line high-precision stable hydrogen isotopic analyses on nanoliter water samples. *Analytical Chemistry* **73**: 3570 -3575, (2001).

Mosbaek, H.; Tjell, J.C.; Sevel, T. Plant uptake of airborne mercury in background areas. *Chemosphere* **17**: 1227–1236, (1988).

Mrak, J. Vpliv potresa na erozijske procese v dolini Tolminke. Diplomska naloga. 56. (Univerza v Ljubljani, FGG, 1999).

Mullins, J.A.; Carsel, R.F.; Scarbrough, J.E.; Ivery, A.M. PRZM-2, A model for predicting pesticide fate in the crop root and unsaturated soil zones: users manual for release 2.0. EPA/600/R-93/046. (US Environmental Protection Agency, Athens, 1993).

Munthe, J. Aqueous oxidation of elemental Hg by O_3. *Atmospheric Environment* **26A**: 1461-1468, (1992).

Munthe, J.; Bodaly, R.A.; Branfireun, B.A.; Driscoll, C.T.; Gilmour, C.C.; Harris, R.; Horvat, M.; Lucotte, M.; Malm O. Recovery of mercury-contaminated fisheries. *Ambio* **36**: 33-44, (2007).

Nyberg, L.; Prevodnik, A. A pilot study of soil erosion in the close environment of Idrija, Western Slovenia. MSc Thesis in geoinformatics. 159. (TRITA-GEOFOTO Stockholm, Royal Institute of Technology, Department of Geodesy and Photogrammetry, Stockholm, 1999).

O'Driscoll, N.J.; Poissant, L.; Canrio, J.; Ridal, J.; Lean, D.R.S. Continuous analysis of dissolved gaseous mercury and mercury volatilization in the upper St. Lawrence River: exploring temporal relationships and UV attenuation. *Environmental Science & Technology* **41**: 5342 -5348, (2007).

Ogrin, D. Modern climate change in Slovenia. In: Orožen Adamič, M. (ed.). *Slovenia: a geographical overview*. 45-50 (Association of the Geographical Societies of Slovenia: Založba ZRC, Ljubljana, 2004).

Pacyna, E.G.; Pacyna, J.M.; Pirrone, N. European emissions of atmospheric mercury from anthropogenic sources in 1995. *Atmospheric Environment* **35**: 2987–2996, (2001).

Pacyna, E.G.; Pacyna, J.M.; Fudala, J.; Strzelecka-Jastrzab, E.; Hlawiczka, S.; Panasiuk, D. Mercury emissions to the atmosphere from anthropogenic sources in Europe in 2000 and their scenarios until 2020. *The Science of the Total Environment* **370**: 147-156, (2006).

Palinkaš, L.A.; Pirc, S.; Miko, S.F.; Durn, G.; Namjesnik, K.; Kapelj, S. *The Idrija Mercury Mine, Slovenia, a Semi-millennium of Continuous Operation: an Ecological Impact.* In: Richardson, M. (ed.) *Environmental Toxicology Assessment.* 317-341 (Taylor & Francis, London, 1995).

Peckenham, J.M.; Kahl, J.S.; Mower, B. Background Mercury Concentrations in River Water in Maine, U.S.A. *Environmental Monitoring and Assessment* **89**: 129–152, (2003).

Petkovšek, G. Procesno modeliranje erozije tal. *Acta hydrotechnica* **18**: 1–18, (2000).

Pintar, J.; Mikoš, M.; Verbovšek, V. Elementi okolju prilagojenega urejanja vodotokov: alternativa utesnjevanju æivih naravnih procesov v toge objekte. In: Simonovič, S. (ed.) *2. kongres o vodah Jugoslavije*. 800-814. (FAGG, Ljubljana, 1986).

Pirrone, N.; Keeler, G.J.; Nriagu, J.O. Regional differences in worldwide emissions of mercury to the atmosphere. *Atmospheric Environment* **30**: 2981–2987, (1996).

Pirrone, N.; Ferrara, R.; Hedgecock, I.M.; Kallos, G.; Mamane, Y.; Munthe, J.; Pacyna, J.M.; Pytharoulis, I.; Poissant, L.; Pilote, M. Mercury concentrations in single event precipitation in southern Quebec. *The Science of the Total Environment* **213**: 65-72, (1998).

Sprovieri, F.; Voudouri, A.; Wangberg, I. Dynamic processes of mercury over the Mediterranean region: results from the Mediterranean Atmospheric Mercury Cycle System (MAMCS) project. *Atmospheric Environment* **37**: 21–39, (2003).

Poissant, L.; Casimir, A. Water-air and soil-air exchange rate of total gaseous mercury measured at background sites. *Atmospheric Environment* **32**: 883-893, (1998).

Preston, S.D.; Bierman, V.J. Jr; Silliman, S.E. An evaluation of methods for the estimation of tributary mass loads. *Water Resources Research* **25**:1379-1389, (1989).

Rajar, R. Hydrology of the Idrijca and Soča rivers and the Gulf of Trieste. *RMZ - Materials and Geoenvironment* **48**: 49-55, (2001).

Ravichandran, M.. Interactions between mercury and dissolved organic matter - a review. *Chemosphere* **55**: 319–331, (2004).

Rea, A.W.; Lindberg, S.E.; Keelera, G.J. Dry deposition and foliar leaching of mercury and selected trace elements in deciduous forest throughfall. *Atmospheric Environment* **35**: 3453–3462, (2001).

Remy, S.; Prudent, P.; Hissler, C.; Probst, J.L.; Krempp, G. Total mercury concentrations in an industrialized catchment, the Thur River basin (north-eastern France): geochemical background level and contamination factors. *Chemosphere* **52**: 635–644, (2003).

Renneberg, A.J.; Dudas, M.J. Transformations of elemental mercury to inorganic and organic forms in mercury and hydrocarbon co-contaminated soils. *Chemosphere* **45**:1103–1109, (2001).

Roy, S.; Gaillardet. J.; Allegre, C.J. Geochemistry of dissolved and suspended loads of the Seine River, France: anthropogenic impact, carbonate and silicate weathering. *Geochimica et Cosmochimica Acta* **63**:1277-1292, (1999).

Sanemasa, I. The solubility of elemental mercury vapor in water. Bulletin *of the Chemical Society of Japan* **48**: 1975-1978, (1975).

Schäfer, J.; Blanc, G.; Audry, S.; Cossa, D.; Bossy, C. Mercury in the Lot–Garonne River system (France): Sources, fluxes and anthropogenic component. *Applied Geochemistry* **21**: 515-527, (2006).

Schlüter, K. Sorption of inorganic mercury and monomethyl mercury in an iron–humus podzol soil of southern Norway studied by batch experiments. *Environmental Geology* **30**: 266-279, (1997).

Schlüter, K. Review: evaporation of mercury from soils. An integration and synthesis of current knowledge. *Environmental Geology* **39**: 249-271, (2000).

Schnoor, J. L. *Environmental Modelling*. 682. (John Wieley & Sons Inc., New York, 1996).

Scholtz, M.T.; Van Heyst, B.J.; Schroeder, W.H. Modelling of mercury emissions from background soils. *The Science of the Total Environment* **304***:* 185–207, (2003).

Schroeder, W.H.; Munthe J. Atmospheric mercury - An overview. *Atmospheric Environment* **32**: 809-822, (1998).

Schroeder, W.H.; Munthe, J.; Lindquist, O. Cycling of mercury between water, air and soil compartments in the environment. *Water, Air, and Soil Pollution* **48**: 337–347, (1989).

Schroeder, W.H.; Yarwood, G.; Niki, H. Transformation processes involving Hg species in atmosphere - results from a literature survey. *Water, Air, and Soil Pollution* **56**: 653-666, (1991).

Schuster, E. The behavior of mercury in the soil with special emphasis on complexation and adsorption processes - a review of the literature. *Water, Air, and Soil Pollution* **56**: 667–680, (1991).

Schwesig, D.; Matzner, E. Pools and fluxes of mercury and methylmercury in two forested catchments in

Germany. *The Science of the Total Environment* **260**: 213-223, (2000).

Sholupov, S.E.; Ganeyev, A.A. Zeeman atomic-absorption spectrometry using high-frequency modulated light polarization. *Spectrochimica Acta, Part B-Atomic Spectroscopy* **50**: 1227–1236, (1995).

Slemr, F.; Schuster, G.; Seiler, W. Distribution, speciation and budget of atmospheric mercury. *Journal of Atmospheric Chemistry* **3**: 407-434, (1985).

Song, X.; Van Heyst, B. Volatilization of mercury from soils in response to simulated precipitation. *Atmospheric Environment* **39:** 7494–7505, (2005).

Stein, E.D.; Cohen, Y.; Winer, A.M. Environmental distribution and transformation of mercury compounds. *Critical reviews in environmental science and technology* **26**: 1-43, (1996).

Stumm, W. *Chemistry of the solid-water interface.* (Wiley Interscience, New York, 1992).

Širca, A.; Rajar, R.; Harris, R.; Horvat, M. Mercury transport and fate in the Gulf of Trieste (Northern Adriatic) – a two-dimensional modeling approach. *Environmental Modelling and Software* **14**: 645–655, (1999a).

Širca, A.; Horvat, M.; Rajar, R.; Covelli, S.; Žagar, D.; Faganeli, J. Estimation of mercury mass balance in the Gulf of Trieste. *Acta Adriatica* **40**: 75–85, (1999b).

Tazioli, A. Evaluation of erosion in equipped basins: preliminary results of a comparison between the Gavrilovic model and direct measurements of sediment transport. *Environmental Geology* Online First, (2008). DOI 10.1007/s00254-007-1183-y

Ulaga, F. Trendi spreminjanja pretokov slovenskih rek. *Dela* **18**: 93-114, (2002).

Ulaga, F. Suspended sediment transportation in Slovene rivers. *Ujma* **20**: 144-150, (2006).

Ullrich, S.M.; Tanton, T.W.; Abdrashitova, S.A. Mercury in the aquatic environment: a review of factors affecting methylation. *Critical Reviews in Environmental Science and Technology* **31**: 241–293, (2001).

United Nations Environmental Programme Chemicals. *Global Mercury Assessment*. UNEP Chemicals, Geneva, (2002).

US Environmental Protection Agency. *Water Quality Standards; Establishment of Numeric Criteria for Priority Toxic Pollutants; States' Compliance.* (Federal Register, 1992).

US Environmental Protection Agency. *Mercury Study Report to Congress*. EPA-452/R-97-005

Vreča, P.; Brenčič, M.; Leis, A. Comparison of monthly and daily isotopic composition of precipitation in the coastal area of Slovenia. *Isotopes in Environmental and Health Studies*. **43**: 307–321, (2007).

Vrščaj, B.; Lobnik, F. Establishment of digital soil MAP of Slovenia in the scale 1:25.000. *Zbornik Biotehniške Fakultete* **73**: 287-300, (1999).

Wallschläger, D.; Desai, M.V.M.; Wilken, R.-D. The role of humic substances in the aqueous mobilization of mercury from contaminated floodplain soils. *Water, Air, and Soil Pollution* **90**: 507–520, (1996).

Wängberg, I.; Fajon, V.; Horvat, M.; Ogrinc, N. Atmospheric mercury at Mediterranean coastal stations. *Environmental fluid mechanics* **8**: 101-116, (2008).

Xiao, Z.F.; Munthe, J.; Schroeder, W.H.; Lindquist, O. Vertical fluxes of volatile mercury over forest soil and lake surfaces in Sweden. *Tellus* **43B**: 267–279, (1991).

Yamamoto, M. Simulation of elemental mercury oxidation in the presence of chloride ion in aquatic environments. *Chemosphere* **32**: 1217-1224, (1996).

Yin, X.; Balogh, S.J. Mercury concentrations in stream and river water: an analytical framework applied to Minnesota and Wisconsin (USA). *Water, Air, and Soil Pollution* **138**: 79-100, (2002).

Zakšek, K.; Podobnikar, T.; Oštir, K. Solar radiation modelling. *Computers and Geosciences* **31**: 233-240, (2005).

Zhang, H.; Lindberg, S.E.; Marsik, F.J.; Keeler, G.J. Mercury air/surface exchange kinetics of background soils of the Tahquamenon River watershed in the Michigan Upper Peninsula. *Water, Air, and Soil Pollution* **126**: 151–169, (2001).

Žagar, D.; Knap, A.; Warwick, J.J.; Rajar, R.; Horvat, M.; Četina, M. Modelling of mercury transport and transformation processes in the Idrijca and Soča river system. *Science of the Total Environmen*t **368**: 149– 163, (2006).

Žibret, G.; Gosar, M. Calculation of the mercury accumulation in the Idrijca River alluvial plain sediments. *The Science of the Total Environment* **368**: 291-297, (2006).

Žižek, S.; Guevara, S.R.; Horvat, M. Validation of methodology for determination of the mercury methylation potential in sediments using radiotracers. *Analytical and Bioanalytical Chemistry,* in press, (2008).

Index of Figures

Index of Tables

APPENDIX A

Table 14**:** *Chemical and isotopic data for the Idrijca River and its tributaries* (17.11.2006).

Loc.	Idrijca River	T(°C)	pH	DO(%)	Alkalinity (mM L^{-1})	Ca (mM)	Mg (mM)	Na (mM)	K (mM)	Si (mM)	SO_4 (mM)	Cl (mM)	DOC (mM)	δC_{POC}(‰)
1	Belca	8.8	8.17	107.4	4.35	1.05	0.76	0.06	0.02	0.03	0.07	0.04	0.52	-26.7
3	Podroteja	8.0	7.96	92.4	3.88	1.23	0.68	0.06	0.01	0.02	0.06	0.07	0.66	-25.7
6	Idrija	6.5	7.73	97.1	3.93	1.16	0.78	0.07	0.01	0.02	0.08	0.07	0.00	
8	Travnik	8.5	8.34	86.4	4.01	1.18	0.94	0.08	0.02	0.02	0.14	0.08	0.09	-27.9
10	Reka	9.0	8.06	82.7	3.99	1.26	0.97	0.12	0.06	0.02	0.35	0.11	0.00	-27.8
12	Hotešček	9.5	8.82	99.9	4.21	1.26	1.03	0.09	0.01	0.02	0.37	0.08	0.17	
14	Idrijca bef. Soča	9.6	8.26	106.2	4.66	1.26	1.00	0.11	0.03	0.02	0.38	0.10	0.49	
Loc.	Idrijca R. tribut.													
2	Zala													
4	Ljubevšca	8.3	8.29	102.0	5.10	1.37	1.09	0.33	0.04	0.05	0.17	0.31	0.23	-27.6
5	Nikova	8.4	8.23	88.1	4.70	1.38	0.89	0.23	0.04	0.04	0.14	0.19	0.00	-27.5
7	Kanomljica	8.2	8.34	99	4.08	1.26	0.90	0.07	0.02	0.03	0.21	0.06	1.57	-26.7
9	Cerknica	9.5	8.19	94.6	3.63	1.35	0.51	0.38	0.05	0.09	0.09	0.78	0.37	-26.6
11	Trebušica	8.6	7.77	88.6	3.89	1.01	0.86	0.05	0.01	0.02	0.07	0.03	0.53	-27.3
13	Bača	9.2	8.29	95.1	3.09	1.17	0.34	0.08	0.02	0.06	0.10	0.04	1.13	-26.8

Table 15: *Chemical and isotopic data for the Idrijca River and its tributaries (17.05.2007)*

Loc.	Idrijca River	T(°C)	pH	Alkalinity (mM L^{-1})	Ca (mM)	Mg (mM)	Na (mM)	K (mM)	Si (mM)	SO_4 (mM)	Cl (mM)	DOC (mM)	δC_{POC}(‰)
1	Belca	9.0	8.43	4.21	0.82	0.74	0.05	<LOD	<LOD	0.04	0.03	0.40	-27.8
3	Podroteja	7.3	7.92	4.20	0.93	0.75	0.07	<LOD	<LOD	0.05	0.07	1.83	-28
6	Idrija	10.8	8.43	4.33	1.15	0.87	0.11	0.05	0.02	0.11	0.10	0.33	-26.9
8	Travnik	11.4	8.44	4.43	1.00	1.22	0.10	0.02	0.02	0.72	0.10	1.10	-28.1
10	Reka	11.7	8.29	4.26	1.01	0.89	0.11	0.02	0.03	0.36	0.11	1.29	-27.1
12	Hotešček	13.0	8.82	4.27	1.16	0.85	0.10	0.05	<LOD	<LOD	<LOD	1.50	-27.3
14	Idrijca bef. Soča	12.7	8.77	4.20	1.15	0.84	0.11	0.05	0.02	<LOD	<LOD	0.42	-28.1
Loc.	Idrijca R. tribut.												
2	Zala	10.6	8.09	4.87	1.27	0.98	0.17	0.04	0.03	0.07	0.15	0.24	-31.3
4	Ljubevšca	10.2	8.54	5.04	1.32	1.05	0.30	0.05	0.07	0.10	0.29	0.70	-27.6
5	Nikova	10.1	8.67	4.81	1.31	0.91	0.20	0.06	0.04	0.10	0.13	0.35	-27.5
7	Kanomljica	10.8	8.29	4.33	1.23	0.87	0.08	0.05	0.04	0.15	<LOD	0.26	-26.7
9	Cerknica	11.8	8.35	3.52	1.25	0.47	0.19	0.06	0.10	0.19	0.12	0.20	-26.6
11	Trebušica	11.6	8.37	4.01	1.00	0.85	0.06	0.04	0.02	0.05	0.03	0.13	-27.3
13	Bača	12.2	8.40	3.15	1.18	0.32	0.08	0.05	0.07	0.08	<LOD	0.53	-26.8

Table 16: *Mercury speciation in Idrijca River and its tributaries.*

Date	Location	THg	DHg	PHg	RHg	DGM
17/11/2006	Belca	0.81	0.28	0.54	0.28	0.15
	Podroteja	1.68	0.96	0.72	0.50	0.18
	Ljubevšča	26.0	19.5	6.47	9.82	1.62
	Nikova	49.7	41.8	7.91	11.6	1.56
	Idrija	54.8	31.7	23.0	10.7	1.73
	Kanomljica	41.1	3.69	37.4	1.07	0.36
	Travnik	47.6	34.6	12.9	11.6	2.69
	Cerknica	4.60	1.26	3.34	0.14	0.15
	Reka	28.8	24.0	4.77	7.59	1.35
	Trebušica	0.34	0.20	0.14	-	-
	Hotešček	10.8	8.68	2.12	4.17	1.16
	Bača	0.20	0.05	0.15	-	-
	Idrijca bef. Soča	11.3	8.68	2.65	2.38	1.09
17/05/2007	Belca	0.76	0.26	0.49	0.15	0.18
	Zala	32.8	3.51	29.27	1.90	0.94
	Podroteja	0.69	0.25	0.43	0.13	0.20
	Ljubevšča	12.0	7.69	4.33	2.96	1.48
	Nikova	49.8	27.0	22.9	5.16	1.49
	Idrija	283	143	140	33.1	23.7
	Kanomljica	3.53	1.09	2.44	0.52	0.70
	Travnik	44.2	19.74	24.50	5.23	3.24
	Cerknica	3.87	0.25	3.62	1.13	0.19
	Reka	32.3	16.7	15.6	2.96	2.16
	Trebušica	0.43	0.21	0.22	0.19	-
	Hotešček	22.3	7.67	14.7	1.72	2.05
	Bača	0.23	0.14	0.10	-	-
	Idrijca bef. Soča	14.3	9.38	4.95	0.91	1.60
23/01/2007	Hotešček	26.0	10.7	15.3	3.05	
28/05/2007	Podroteja	3.49	0.91	2.58	0.62	0.37
	Idrija	125	69.8	55.1	13.1	5.77
	Reka	98.6	34.7	63.9	5.55	2.25
	Hotešček	51.7	9.97	41.74	4.10	1.91
19/09/2007	Hotešček	708	6.75	702	3.78	1.10

Table 17: *Mercury speciation in the Idrija air (pg Hg m^{-3}).*

Date	GEM	RGM	TPM	TRM (%)	TPM (%)
19/20 Sept.06	9647	23	55	0.24	0.57
20 Sept.06	12568	24	27	0.19	0.21
20/21 Sept.06	8600	12	68	0.14	0.79
21 Sept.06	9298	23	15	0.25	0.16
21/22 sep.06	7902	10	68	0.13	0.87

Table 18**:** *Mercury speciation in the precipitation in Idrija (ng L^{-1}).*

IDRIJA Open Air	THg	PHg	DHg	RHg	DGM
24/10/2006	11.1	4.43	6.64	3.30	0.27
27/10/2006	24.4	21.5	2.88		0.37
22/11/2006	3.15	2.07	1.09		
01/12/2006	6.18	3.15	3.03		
10/12/2006	6.28	1.51	4.77	0.50	0.18
18/12/2006	9.16	7.23	1.93		
23/01/2007	23.8	11.0	12.8	2.20	
25/01/2007	3.33	1.31	2.02	0.60	
10/02/2007	7.04	3.16	3.88		
19/02/2007	5.32	3.34	1.98		
25/02/2007	4.20	1.80	2.40	1.25	
08/03/2007	8.45	2.91	5.54	1.40	
21/03/2007	9.18	3.98	5.20	1.12	
31/07/2007	28.5	23.9	4.67	3.44	0.32
12/08/2007	5.60	2.54	3.06		
12/09/2007	14.2	9.80	4.44		
19/09/2007	6.90	2.83	4.07	2.32	0.69

Table 19: *Mercury deposition in Idrija (ng m^{-2} day^{-1}).*

IDRIJA Open Air	THg dep	PHg dep	DHg dep	RHg dep	DGM dep
24/10/2006	55.9	22.4	33.6	16.67	1.36
27/10/2006	57.5	50.7	6.80		0.87
22/11/2006	29.9	19.6	10.3		
01/12/2006	13.0	6.61	6.38		
10/12/2006	26.2	6.33	19.9	2.09	0.74
18/12/2006	22.3	17.6	4.70		
23/01/2007	84.4	38.9	45.4	7.78	
25/01/2007	75.9	29.8	46.0	13.7	
10/02/2007	29.2	13.1	16.1		
19/02/2007	18.3	11.5	6.81		
25/02/2007	22.3	9.55	12.7	6.63	
08/03/2007	16.3	5.62	10.7	2.70	
21/03/2007	18.7	8.13	10.6	2.29	
31/07/2007	67.6	56.6	11.1	8.15	0.76
12/08/2007	14.9	6.74	8.12		
12/09/2007	11.3	7.80	3.54		
19/09/2007	44.9	18.4	26.5	15.10	4.49

Table 20**:** *Mercury speciation in the throughfall in Idrija (ng L^{-1}).*

IDRIJA Forest	THg	PHg	DHg	RHg	DGM
27/10/2006	30	17	13		
25/02/2007	31	27	3.9	1.8	
08/03/2007	81	73	8.8	2.8	
21/03/2007	14	8.5	5.9	2.1	
31/07/2007	29	11	19	4.5	0.6
12/08/2007	125	80	45		
12/09/2007	75	63	12		
19/09/2007	24	14	11	5.3	1.5

Table 21**:** *Mercury depostion in the throughfall in Idrija (ng m^{-2} day^{-1}).*

	THg dep	PHg dep	DHg dep	RHg dep	DGM dep
27/10/2006	70	40	31		
25/02/2007	120	105	15	7.0	
08/03/2007	111	99	12	3.8	
21/03/2007	29	17	12	4.3	
31/07/2007	69	25	44	11	1.4
12/08/2007	138	89	50		
12/09/2007	59	50	10		
19/09/2007	158	90	69	34	9.8

APPENDIX B

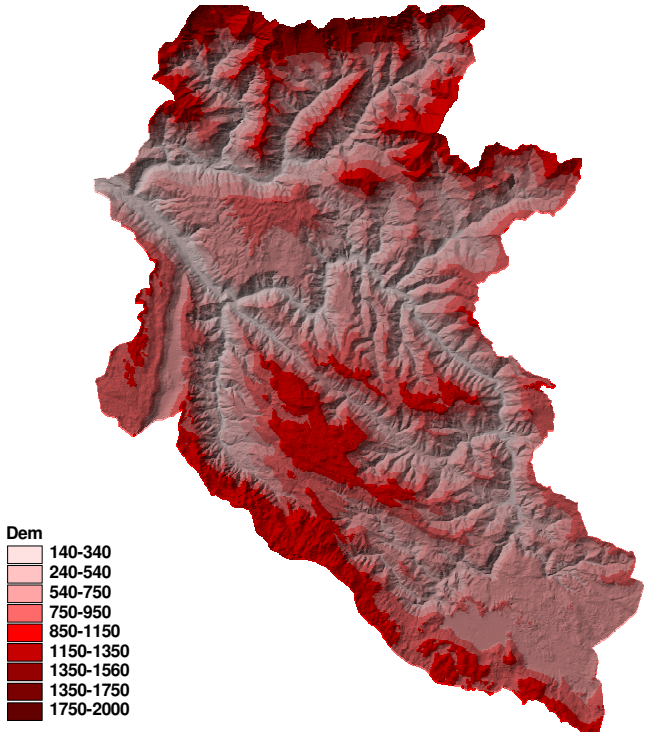

Figure 81*: Digital elevation model.*

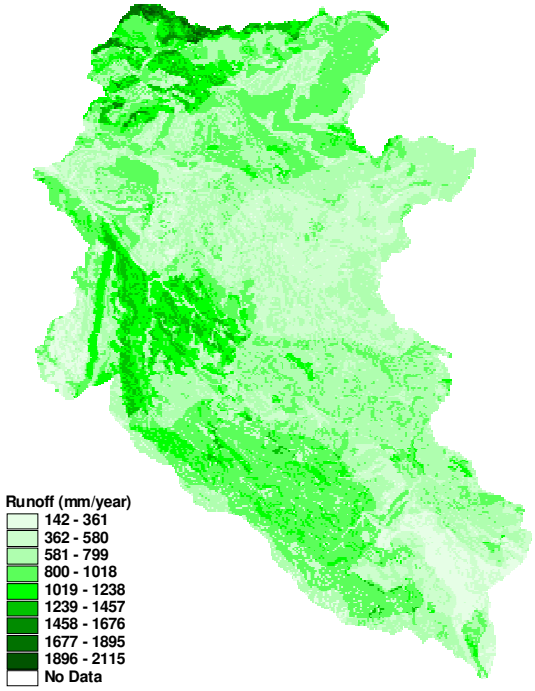

Figure 82: *Runoff map.*

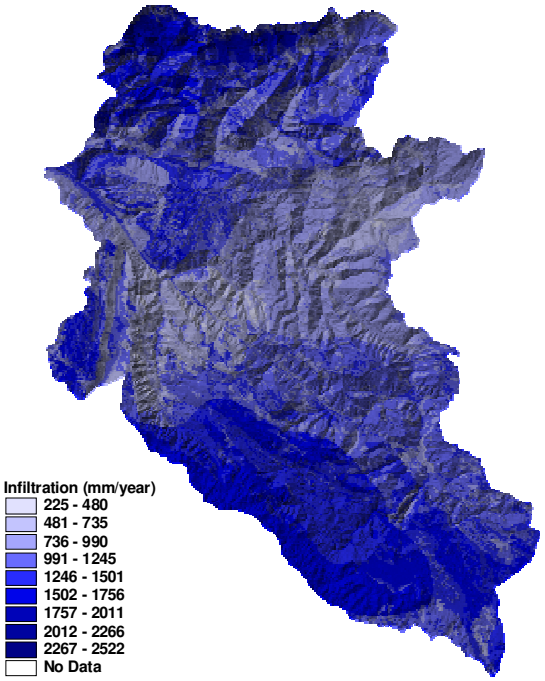

Figure 83*: Infiltration map.*

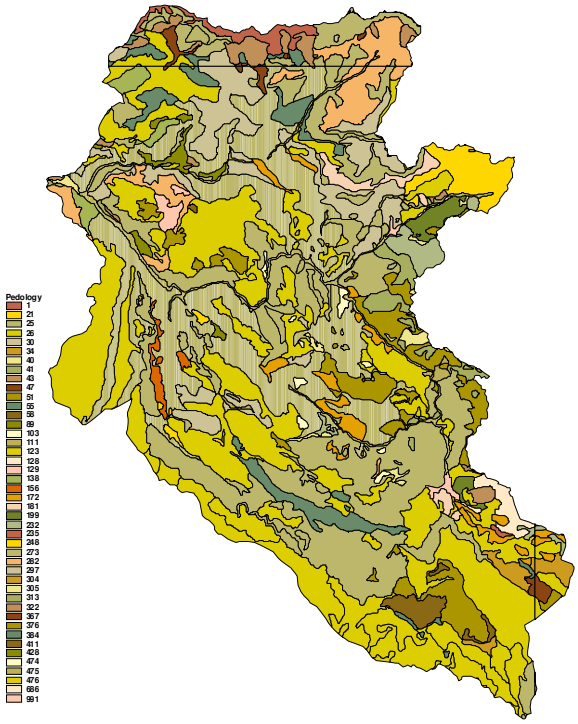

Figure 84**:** *Map of pedosystematic units.*

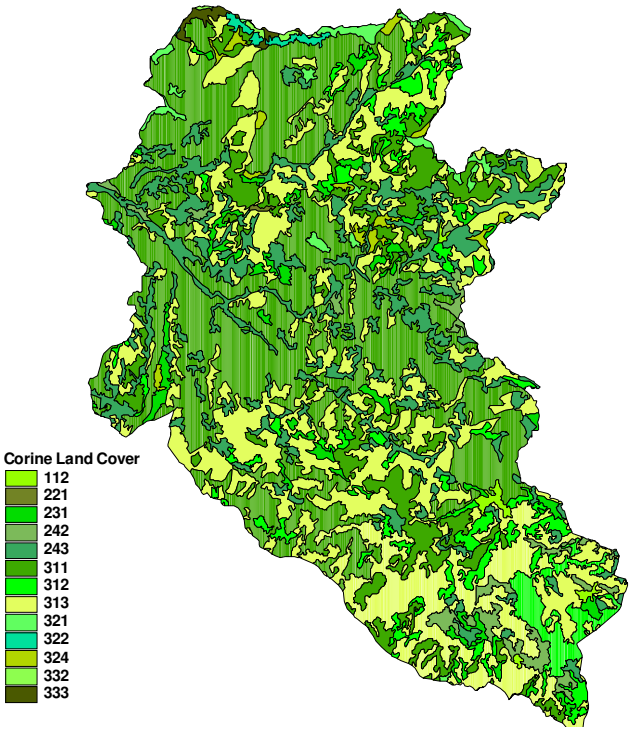

Figure 85*: Corine land cover.*

APPENDIX C

PAPER

Mercury fractionation in contaminated soils from the Idrija mercury mine region

David Kocman,* Milena Horvat and Jože Kotnik

Jožef Stefan Institute, Jamova 39, SI-1001 Ljubljana, Slovenia

Received 9th March 2004, Accepted 20th May 2004
First published as an Advance Article on the web 7th July 2004

Mercury (Hg) fractionation was investigated in contaminated soil in the Idrija Hg-mine region, Slovenia. The main aim of this study was to test and apply sequential extraction and quantification of different Hg phases in order to estimate the mobility and potential bioavailability of Hg in contaminated soils. Separation of Hg phases was performed by means of a selective sequential extraction procedure complemented by volatilization of elemental mercury (Hg^0). The influence of temperature, moisture and storage on Hg^0 volatilization was also investigated. The total Hg concentrations varied between 8.4 and 415 mg kg^{-1} and were up to 40-fold higher than the maximum permissible set by Slovenian legislation. Fractionation measurements indicated cinnabar as the predominant Hg fraction, followed by Hg^0. Accumulation of cinnabar predominantly occurred in coarse grained flood plain sediments, where on average it constituted more than 80% of total Hg. In contrast non-cinnabar fractions were found to be enriched in areas where fine grained material was deposited, reaching up to 60% of total Hg. The strong positive correlation (R^2 = 0.71–0.99) among non-cinnabar fractions suggested that these fractions predominantly control the mobility and potential bioavailability of Hg. Sample pretreatment before fractionation influenced the partition of Hg between different fractions, and therefore fractionation in fresh, nontreated samples is suggested. In addition, the specificity of the extraction steps needs further attention, as it was shown that some extraction steps, such as the organo-chelating Hg fraction, do not provide meaningful results. This further suggests that protocols for mercury fractionation need further harmonization in order to improve the comparability of the results and their use in risk assessment. Volatile mercury fluxes averaged between 0.04 and 6.5 ng g^{-1} h^{-1}. Good agreement (R^2 = 0.81–0.95) was found between the non-cinnabar fractions and evaporation of Hg^0. Both the temperature and sample moisture had significant effects on mercury volatilization. The results in this study were obtained at 70 °C, which may be somewhat high, in particular for bacterial activity which may also play an important role in Hg volatilization. Therefore it is strongly suggested that further optimisation of the protocol to assess Hg volatilization from soil is required.

1. Introduction

Although the production of mercury (Hg) at the Idrija mercury mine stopped in 1994, more than 500 years of mining and ore processing operations left behind intense pollution of nearly all environmental compartments.[1–4] Total Hg concentrations in polluted soils, sediments and the tailings have been well documented,[5–7] but little is known about the speciation and mobility of Hg in solids.[8] The Idrija ore deposit, the origin of Hg in the Idrija region, is classified as a monomineral deposit, as most of the mercury appears in the form of cinnabar (HgS ~ 70%) and only to a relatively smaller extent in the form of native mercury (Hg ~ 30%).[9] Cinnabar is accumulated in coarse grained river sediments, while non-cinnabar Hg forms are enriched in fine grained flooded soils.[10] The predominant Hg species in older tailings is cinnabar, whereas in tailings of the 20th century the amount of cinnabar decreases.[11]

The biogeochemical and especially the ecotoxicological significance of Hg input is determined by its specific binding form and coupled reactivity rather than by its accumulation rate in the solid material.[12] Consequently, these are the parameters that have to be determined in order to assess the potential for Hg transformation processes (such as methylation, reduction, demethylation), and to improve data for environmental risk assessment. One of the aims of the study presented here was differentiation of Hg compounds in soils into different behavioural classes by the sequential extraction scheme adopted from Bloom *et al.*[13] The sequential extraction scheme consisted of six steps, including (a) water soluble (F1), (b) 'human stomach acid' soluble (F2), (c) organo-chelated (F3), (d) elemental Hg (F4), (e) mercuric sulfide (F5) and (f) residual fraction (F6).

Emissions of volatile mercury species from natural sources are believed to be a significant contributor to the atmospheric burden of mercury and were found to be greater than estimated in global models.[14,15] In contrast to anthropogenic point sources of atmospheric Hg, natural sources are long lived ($>10^4$ years) and their emissions enter the global atmospheric Hg pool. In the past decade significant progress has been made in development of methods for the measurements of mercury emissions. Experimental studies have been carried out using both dynamic flux chambers and micro-meteorological methods.[16,17] The mercury concentration in the substrate was found to be the dominant factor controlling emissions and may be used to predict emissions from regions of mercury enrichment.[18] Other parameters, such as rock type, degree of hydrothermal alteration and the presence of heat sources and geological structures, also control the magnitude of Hg emissions from natural sources, while micro-meteorological parameters especially light, temperature and precipitation dictate daily trends.[19] A good model should simulate all the processes in their proper importance, but as no *ideal* model of mercury soil-to-atmosphere emission exists, it is most important to know the relative importance of different parameters. The work reported here was intended to contribute toward further understanding of the exchange of mercury between soil and the atmosphere, and for making estimates of the contributions of mercury emissions from background and mercury-contaminated soil to the atmospheric load of mercury. For this purpose a simple mercury volatilization simulation

DOI: 10.1039/b403625e

experiment was applied. The study focuses on the estimation of the amount of volatile mercury in soil and on the influence of temperature and sample moisture content on mercury volatilization.

2. Materials and methods

2.1. Sampling and sample pre-treatment

Forest soil was collected (Fig. 1) in the town of Idrija in the vicinity of the smelter (S1) and meadow soil on the Pront hill (S2). One soil sample mixed with tailings (S3) was collected in the town of Idrija. Flood plain samples were collected along the river Idrijca in the town of Idrija (S4) and downstream where the Idrijca merges with the river Bača (S5). All samples were taken by means of a stainless steel auger at a depth of 0–10 cm. A composite sample (made from 5 samples) was collected for each of the 5 locations within an area of about 25 m^2 at each location and stored in polyethylene containers. On the flood plain at the confluence of the rivers Idrijca and Bača, a 1-m-deep profile was also sampled at depths of 50 (S6) and 100 cm (S7).

Two types of samples were investigated: fresh and homogenized. For this reason samples were divided in two parts. The fresh part was stored under refrigeration until analysis. In the other part, larger particles, *e.g.* stones and plant residues, were first removed. Then the samples were dried to constant weight at 35 °C in a drying oven for approximately 3 days. Samples were then ground and homogenized in an agate mortar, and sieved through a mesh of 200 μm pore size. Total Hg concentrations were measured on homogenized samples. In applying the sequential extraction procedure, both fresh and homogenized samples were analyzed. The procedure for simulation of mercury volatilization from soils was applied to fresh samples. A separate aliquot of fresh sample was dried at 105 °C to constant weight for the determination of moisture content. The results of measurements were expressed on a dry weight basis.

2.2. Reagents

Merck (Darmstadt, Germany) suprapur acids and deionised water obtained from a Millipore Milli Q system were used for the preparation of samples, extraction solutions and standards. All other chemicals were of analytical reagent grade. A standard stock solution of mercury was obtained from Merck. A fresh working standard solution was prepared daily by dilution of the stock solution with hydrochloric acid and Milli Q water. Whatman glass microfibre filters of 47 mm diameter and 0.20 μm pore size were used for filtration.

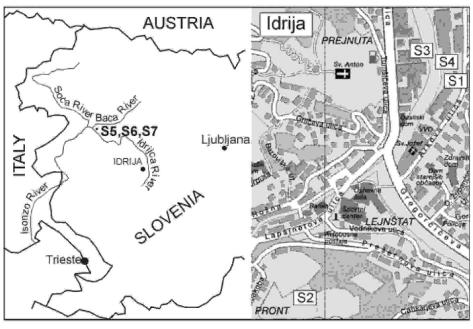

Fig. 1 Sampling sites (S1–S7).

2.3. Characterisation of samples

Samples were characterised according to different agronomic parameters: pH, moisture content, organic matter content, organic carbon content, cation exchange capacity, total nitrogen, total phosphorus and texture. The concentrations of various macroelements were ascertained by atomic absorption in the case of calcium and magnesium, and atomic emission in the case of sodium and potassium.

2.4. Determination of total mercury

Total Hg concentrations in samples were determined by cold vapour atomic absorption spectrometry (CVAAS). After overnight decomposition with nitric, hydrochloric and hydrofluoric acid in a closed Teflon® vial at 125 °C, mercury was reduced with $SnCl_2$, amalgamated on a gold trap and flushed by air from the heated trap into the measuring cell of a LCD Milton Roy mercury detector.[20] Quality control included reagent blanks to assess contamination and triplicate samples to check precision. One certified reference material (CRM) and one reference material (RM) were also used to assess accuracy: CRM BCR 580, Estuarine sediment, obtained from the Institute for Reference Materials and Measurements (IRMM) and RM IAEA 405, Trace elements and methylmercury in estuarine sediment, obtained from the International Atomic Energy Agency (IAEA).

2.5. Selective sequential extraction procedure

The five-step sequential extraction procedure described by Bloom *et al.*[13] was followed. Analyses were performed on all seven soil samples. For an internal check on the procedure an additional step was applied. After the sequential extraction steps, the residual mercury content was determined by digestion with nitric, hydrochloric and hydrofluoric acid. The sequential extraction procedure uses the following six steps, in the same order as presented in Fig. 2.

Extractions were carried out using 1.0000 ± 0.0001 g of moist sample. The sample weight to extractant volume ratio was of 1 to 100. 100 mL of extractant was added to the solid and subjected to end-over-end shaking at 250 rpm for 18 ± 4 h. The vials were then centrifuged at 3800 rpm for 10 min, and the supernatant liquid decanted for filtration through a membrane filter of 0.20 μm pore size. The extract was then placed in a clean Teflon® bottle and oxidized by adding 5 mL of 0.2 M BrCl. Total Hg in the oxidized fraction extract was determined using $SnCl_2$ reduction, trap gold amalgamation and CVAAS. In the subsequent extraction steps the procedure was repeated. Owing to the very low expected Hg values in some fractions, the filters were rinsed with HNO_3, HCl and deionised water before filtration to avoid contamination. For the last fraction (F6) a filtration step was not applied because HF solution dissolves glass microfibre membranes.

Quality control included reagent blanks to assess contamination and duplicate sample S5 to check precision. Concentrations of Hg in steps 1–6 were also summed and compared to total Hg concentrations.

2.6. Method for simulation of mercury volatilization from soils

As mentioned above, simulation of mercury volatilization from soil was performed on fresh samples. A sample was placed in a flow of Hg-free nitrogen in a Teflon® evaporation vessel connected to a water separation bottle and a gold sand trap (Fig. 3). The gold sand trap was then removed and analyzed by thermal desorption, double amalgamation and cold vapour atomic fluorescence spectrometry (CVAFS). This kind of experimental design allowed manipulation of the environmental conditions and measurement of the response with high resolution. The temperature within the evaporation vessel was

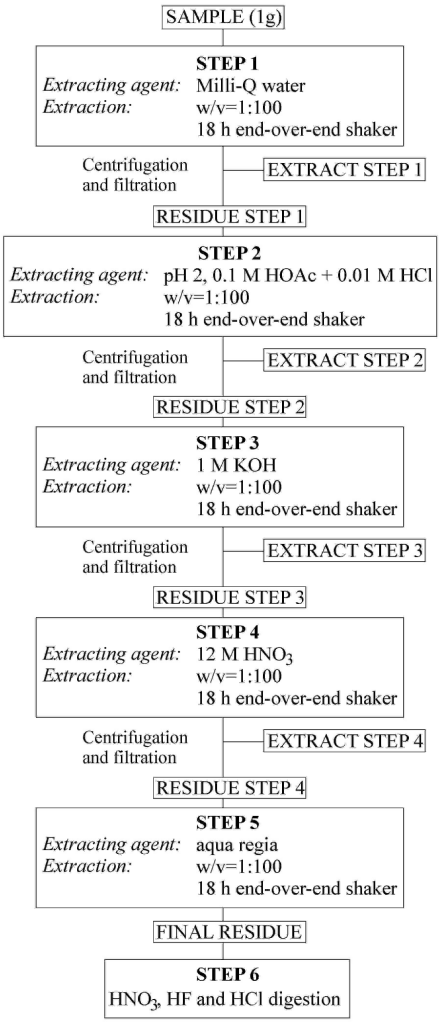

Fig. 2 Sequential extraction method followed in the present study.

modified by the heater and rain/flood simulated by addition of deionised water. The detection limit for the system, calculated as three times the standard deviation of typical mean blank levels of the mercury-collection traps, was 25 pg. The analytical system was calibrated by injecting known volumes of Hg^0-saturated air (Tekran Model 2505 Mercury vapour calibration unit) into the system using an air-tight gas syringe. The quality control included reagent blanks to assess contamination and triplicate samples to check precision. Additionally, the experiment was repeated after six months to establish the effect of sample storage (under refrigeration at 4 °C) and the influence of the moisture on mercury volatilization without heating.

3. Results and discussion

3.1. Characterisation of samples

According to their different agronomic parameters, presented in Table 1, samples can be divided into two groups; samples of alluvial plains and others. There is a significant difference between these two groups. Samples of alluvial plains contain less potassium, organic carbon and organic matter, have a higher C/N ratio and somewhat lower cation exchange capacity when compared with others. As regards texture, alluvial plain samples are coarse grained, while fine grained material prevails in other samples. The pH value of all samples is slightly above 7. Exceptions are sample S3, with a pH slightly below 7, and sample S2, with a significantly lower pH value than 7. This suggests that samples S2 and S3 originate from soil which was not evolved on the limestone bedrock, as was the case with other samples. The amounts of potassium and phosphorus accessible to plants in the samples indicate that sampling was not conducted in areas of intensive agriculture or that the samples were taken from deeper layers. Nitrogen increases as the degree of mineralization increases. As regards cationic macroelements, calcium is the most abundant, followed by magnesium, potassium and sodium, in all the samples.

3.2. Total mercury concentrations

The main aim of the present study was to improve our understanding of mercury mobility and potential bioavailability in soils of the Idrija region by means of selective extraction. That is why sampling sites were chosen at places where a number of measurements of total Hg had been made in the past. The results presented here confirm the findings of the previous studies.[5–7] Total Hg concentrations in samples determined using a mixture of nitric, hydrochloric and hydrofluoric acid are presented in Table 2. Concentrations are expressed on a dry weight basis. Slovenian legislation[21] defines the critical value for total mercury concentration in soil at 10 mg Hg kg^{-1}. It is

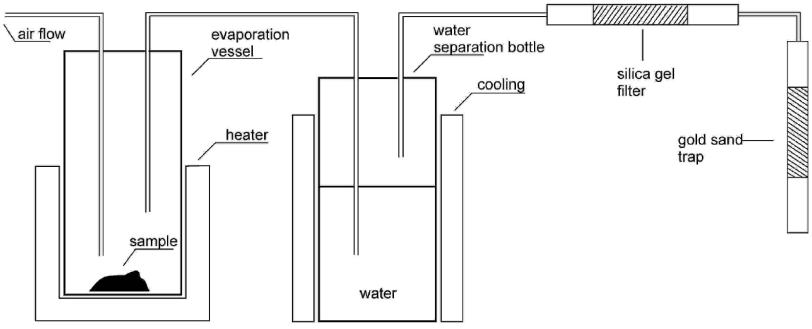

Fig. 3 Design of the system for measuring soil Hg volatilization.

Table 1 Agronomic characteristics of the soil samples

Location[a]	S1	S2	S3	S4	S5	S6	S7
pH in KCl (−)	7.2	4.4	6.5	7.2	7.3	7.5	7.5
pH in water (−)	7.6	5.3	7.2	7.7	7.6	7.8	7.9
Phosphorus – P_2O_5/mg 100 g^{-1}	8.6	5.2	1.6	6.6	5.1	5	2.9
Potassium – K_2O/mg 100 g^{-1}	10.8	14.5	8.2	6	5	4.2	4.2
Organic matter (%)	7.9	4.9	1.2	2.7	3.9	2.2	2.4
Total N (%)	0.54	0.35	0.08	0.11	0.18	0.08	0.09
C/N ratio (−)	8.5	8.1	8.7	14.2	12.6	15.9	15.5
H^+/mekv 100 g^{-1}	5.04	20.41	3.79	0.98	1.91	0.05	15.5
Na^+/mekv 100 g^{-1}	0.0018	0.0019	0.0015	0.0014	0.0015	0.0015	0.0013
K^+/mekv 100 g^{-1}	0.105	0.159	0.078	0.05	0.036	0.027	0.026
Ca^+/mekv 100 g^{-1}	24.8	6.04	8.33	16.16	19.25	14.22	14.74
Mg^+mekv 100 g^{-1}	8.46	4.38	5.8	5.52	4.33	6.42	5.92
Cationic exchange capacity	38.4	31.1	18	22.7	25.5	20.7	21.1
org. C (%)	4.6	2.8	0.7	1.6	2.3	1.3	1.4
% sand	39.1	23.9	42	80	72.8	78.8	75.8
% silt	36.7	49.3	29	9.3	15.5	12.6	14
% clay	24.2	26.8	29	10.7	11.7	8.6	10.2

[a] S1–S7 sampling sites (Fig. 1).

evident from the data of Table 2 that the total concentrations of mercury in all the samples investigated exceeded the limit value for the total concentration of mercury in soil, except sample S3. The highest T-Hg values were measured in the immediate vicinity of the former mine-smelter complex (S1) and beneath the mine-smelter on the flood plain of the river Idrijca (S4). The origin of mercury at these two locations differ. Mercury in the forest soil close to the smelting house mainly originates from atmospheric deposition of Hg, while in the alluvial ground Hg originates from deposition of particles, in which Hg is present as Hg sulfide.[10] Downstream, where the Idrijca merges with the Bača (S5), Hg concentrations are about 3-fold lower but still very high. These very high Hg concentrations reflect active Hg transport from mining sites and recent and past deposition of Hg enriched particles close to the turbulent water flow. The soil depth profile at this location showed an increase of Hg from about 76 mg kg^{-1} at the surface to about 175 mg kg^{-1} at 50 cm depth. Farther down at 100 cm depth, the concentrations decreased to around 144 mg kg^{-1}. The profile was not deep enough to reach sediments deposited before the beginning of mining operations, hence the mercury content was high throughout the profile. It is questionable if this sequence shows sedimentation in chronological order due to erosion and re-deposition of sediments typical of fluvial flood plains. However, other cores taken from the same site show a similar course of Hg enrichment.[5,10,22] Although the meadow in Idrija at S2 was never under the direct influence of the mine or the smelter, total Hg concentrations at this site are rather high due to native mercury-bearing carboniferous clastic rocks. The lowest total Hg values were measured in the soil sample S3, since this soil was brought from a non-contaminated area and mixed with young tailings of the 20th century, treated by very efficient roasting techniques used in the last decades of the Idrija mine operation.

Table 2 Total Hg concentrations (mg Hg kg^{-1}) and relative standard deviations (RSD) of triplicate measurements of soil samples S1–S7 and certified reference material (CRM)

Sample name	T-Hg (average)	RSD (%)
S1	333.0	2.6
S2	47.0	9.2
S3	8.9	3.1
S4	369.0	8.5
S5	76.0	21.5
S6	175.0	14.9
S7	144.0	13.9
BCR 580[a]	134.3	0.42
IAEA 405[b]	0.82	1.5

[a] BCR 580, Estuarine sediment (certified value = 132 ± 3 mg Hg kg^{-1}). [b] IAEA 405, Estuarine sediment (reference value = 0.81 ± 0.04 mg Hg kg^{-1}).

3.3. Volatile mercury

Fig. 4 shows the results obtained for mercury volatilization from heated fresh soils. The amount of Hg evaporated during each individual one-hour interval is plotted and the line displays trend over time. It should be emphasized that each result in the plot is the average of three independent determinations. The precision varied from 15 to 30%. Mercury fluxes were measured for 14 h in one-hour intervals following the procedure described above. At the beginning, mercury fluxes were measured at 70 °C. The expectation was that more than 95% of volatile mercury would vaporise within the first six hours at 70 °C. In contrast to this expectation, significant Hg fluxes were also measured over longer periods. As shown in Fig. 4, there is a similar trend in all samples. The highest fluxes were determined in the first hour. Afterwards, during the second and third hour, fluxes gradually decreased. During the next three hours, when samples were already dry, fluxes within one-hour intervals became constant. This fact indicates the influence of moisture on mercury emission. After six hours the samples were cooled down and fluxes measured for two hours at room temperature. Mercury fluxes at room temperature were 3 to 10-fold lower, showing no significant difference when the two one-hour intervals were compared. The sudden flux decrease in comparison with fluxes measured at 70 °C indicated the importance of temperature on mercury emission. To confirm the influence of both moisture and temperature on mercury emission, samples were remoistened (sample weight to water volume was 1 to 1), heated at 70 °C once again and mercury fluxes measured for another six hours. The trend observed in the first six hours of the experiment was repeated (with a correlation coefficient $R^2 = 0.94$). Once again, the highest fluxes were measured in the first two hours (during the eighth and tenth hour respectively), then a gradual decrease followed until the fluxes become constant. To test the importance of total Hg concentrations on mercury volatilization, the sum of 14-hours fluxes was plotted against total Hg determined in these samples, as shown in Fig. 5. A very strong correlation between these two variables is evident from this plot. Considering the very high total Hg concentrations, the fact that only a (small) part of all the available volatile mercury was removed during the mercury volatilization experiment and that natural sources are long lived, it is likely that mercury emissions from mercury-contaminated soil in the Idrija region

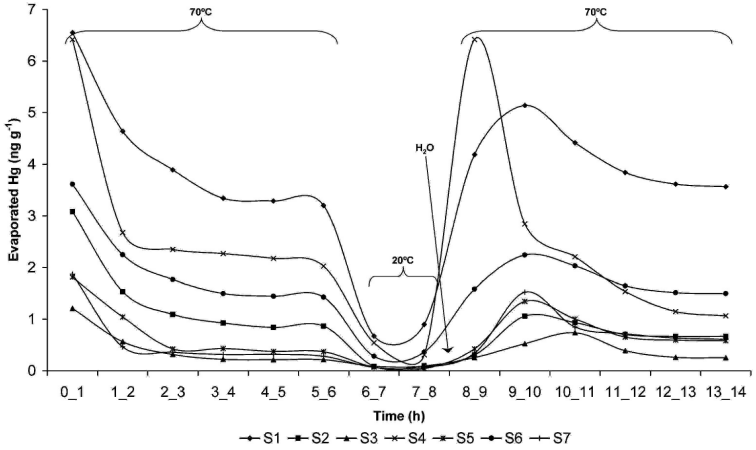

Fig. 4 Results of Hg volatilization simulation experiment (one-hour intervals).

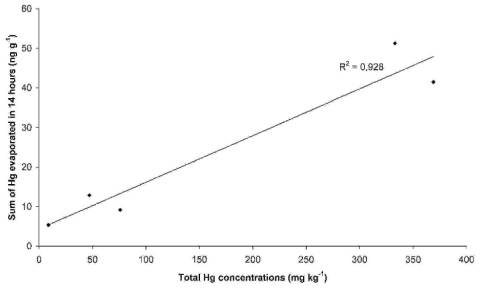

Fig. 5 Sum of 14-hours Hg fluxes *vs.* total Hg concentrations in S1–S5 soil samples.

will remain the main contributor to the atmospheric load of mercury for quite some time.

The experiment described here was repeated after six months on samples S1–S5 (Fig. 6). Compared to the previous experiment an additional step was introduced to check the effect of moisture on Hg volatilization at room temperature. After six hours at 70 °C and the next two hours at room temperature, the samples were moistened and fluxes measured at room temperature for another two hours before being heated to 70 °C for an additional hour. The aim was to establish the effect of sample storage and the influence of moisture on mercury volatilization without heating. Comparison of the results obtained during the first six hours before and after six months storage showed a very high correlation (R^2 = 0.99) when the sum of intervals was compared. On the other hand, there was a great disagreement when one-hour intervals were

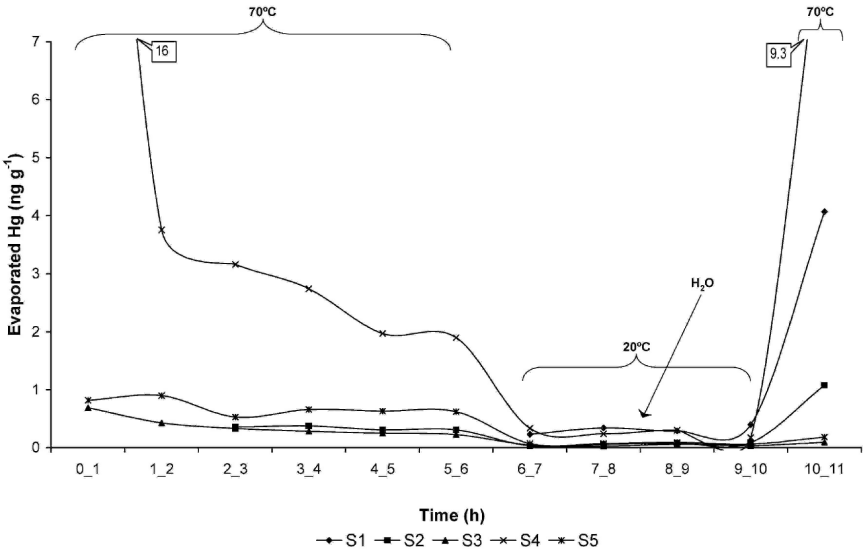

Fig. 6 Results of mercury volatilization simulation experiment (one-hour intervals); after six months.

compared. Additionally, moistened samples showed no expected increase in mercury flux at room temperature when compared to dry ones. This could be due to changes that occurred in the samples during storage, or due to a very small difference between dry and moist sample flux that was close to the detection limit of the method. Another reason could be due to bacterial inactivity. Bacteria are responsible for Hg reduction and volatilization in soil, but were killed during heating at 70 °C.

3.4. Application of the sequential extraction scheme

As mentioned above, the sequential extraction scheme was applied to two types of samples, fresh and homogenized. The results obtained from homogenized samples differ from the fresh ones (Fig. 7). Evidently there must be some kind of alteration of mercury during homogenization of the samples, particularly in the case of fractions F1, F2 and F3. Since the samples were dried at 35 °C, the amount of water soluble mercury (F1) was found to be somewhat lower in the fresh samples S1–S3. This is not the case with alluvial plain samples (S4–S7), as samples were frequently under the influence of flowing water. That is why higher concentrations in fraction F1 were measured in homogeneous samples at these sites. The amount of organo-chelated mercury (F3) was lower in homogeneous dry samples due to the removal of plant residues, roots and other organic particles during grinding and sieving in the homogenization process. The amount of elemental mercury (F4) was also found to be lower in homogeneous samples, as a part of the Hg^0, which is typical of this fraction, evaporated while samples were dried. Comparison of the amounts of Hg obtained during the second step (F2) showed no significant difference between fresh and homogenized samples. In the case of fraction F5, differences were mainly found among samples most abundant in cinnabar as a result of poor homogeneity.

The results discussed below were obtained from fresh samples, representing the actual situation in nature. All concentrations determined in a particular extraction step were higher than their corresponding detection limit of the analytical method. The sum of the six fractions was reasonably similar to the total content obtained after digestion of the homogenised sample with nitric, hydrofluoric and hydrochloric acid.

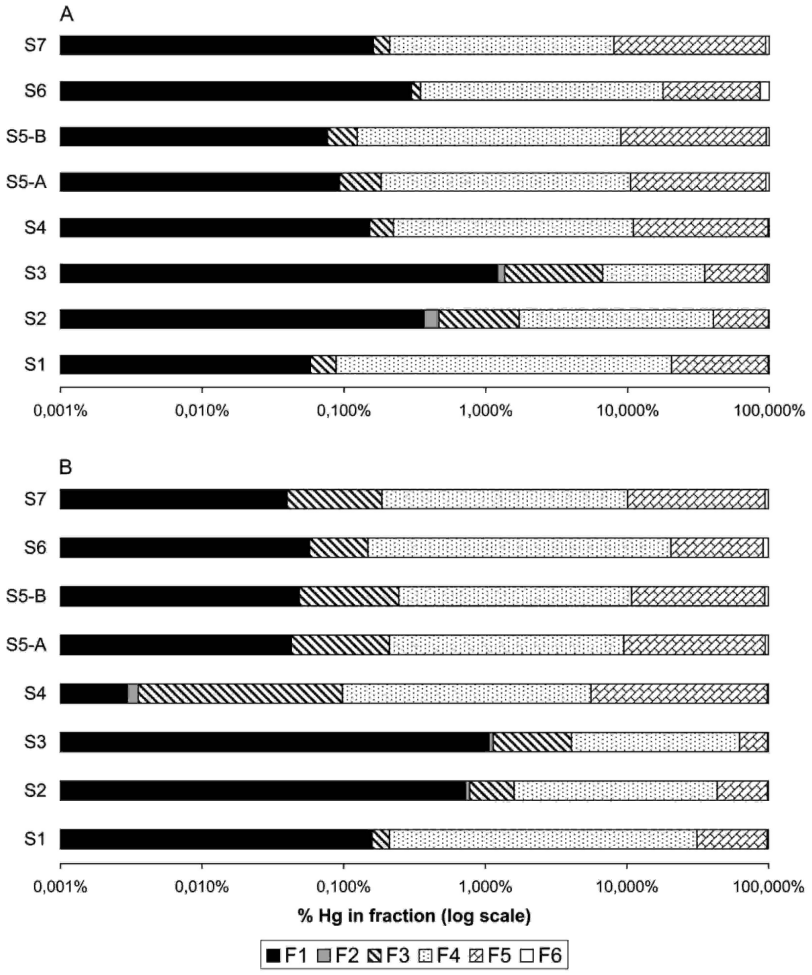

Fig. 7 Sequential extraction results obtained from (A) homogenized and (B) fresh samples.

Recoveries of 80–105% were reached in most cases, which is very similar to those recorded for the same extraction scheme.[23] Comparison of two parallel determinations of the sample S5 (S5-A and S5-B) in each particular step showed good agreement. It is evident from the data of Fig. 7 that values varied from 0 to 10%. Bigger differences were observed among fractions most abundant in Hg, which is most probably due to the presence of insoluble cinnabar particles. These data confirmed that the precision of the analytical work is acceptable, especially if we consider poor homogeneity of the samples and the fact that during the sequential extraction process minor losses of the sample may occur.

The distribution of mercury in the fractions differs with the type of sample, although there are similarities in some cases. Hg was principally distributed between the cinnabar (F5) and elemental (F4) fraction, as mentioned in the literature.[10,11] Although the percentage of the first three fractions is rather small, absolute values of these mobile Hg fractions are quite high due to very high total Hg values in soils in the Idrija region. In general, samples can be divided into two groups: samples of flood plains and others. There is a significant difference between these two groups. In the first, the water soluble fraction of Hg was found to be somewhat higher (up to 1%) at sites that are not directly under the influence of flowing water, while in the flood plain samples water soluble Hg did not exceed 0.06%. This was expected, since frequent river flooding washes away water soluble forms of Hg. Hg carried downstream is available for transformation in both the Soča/Isonzo river system and in the marine environment of the Gulf of Trieste.[24–26] The lowest quantities of Hg were extracted during the second extraction step at pH 2. This *in vitro* procedure was created to simulate bioaccessibility of metals contained in geological solids within the acidic environment of the mammalian gastrointestinal tract. Nevertheless, absolute quantities of Hg in the second fraction were rather high due to high total Hg values in the samples. The third, organo-chelated Hg fraction, is presumably the most important one, as it is most strongly correlated with methylation potential.[13] The expectation was that fraction F3 would be more abundant in samples with a higher amount of organic matter, as Hg that appears in this fraction is associated mostly with humic organic matter. On the contrary, the results showed a decline in the amount of organo-chelated Hg with increasing percentage of organic matter. Thus, the only significant fraction F3 was measured in samples S2–S4 (between 0.3 and 0.46 mg kg^{-1}), containing less than 4% of organic matter. Such unspecific leaching casts doubt on whether all Hg extracted during extraction step 3 is really organo-chelated, which provides a note of caution against relying too heavily on the measured recoveries. The measurements of the Hg after fourth extraction step may be interpreted as an estimate of total Hg^0. This assumption was also confirmed by the very high correlation ($R^2 = 0.81$) between the relative amount of fraction F4 and relative amount of Hg evaporated during the volatilization experiments described above. Between 30 and 60% of the Hg was recovered in the fourth fraction at sampling sites S1–S3, while less than 10% (with the exception of S6) was recovered at flood plain sites. High Hg^0 values in meadow soil (S2) can be explained by native mercury-bearing rocks, while Hg^0 at sampling site S1 which is located close to the smelting house mainly originates from the Hg^0 condensed during the ore roasting process. As expected, the most abundant fraction (up to 93%) in all samples, with the exception of S3, is fraction F5, representing mostly cinnabar. The sixth, the additional fractionation step, showed that between 2 and 8% of Hg was not recovered in the first five fractions. This remaining fraction after *aqua regia* digestion is insoluble Hg bound to crystalline metal ores such as bauxite and hematite.

Grain size effect on the content of fractions. To investigate the effect of sample grain size on fraction content, Pearson correlation coefficients (r) and determination coefficients (R^2) between the individual fraction content and sample grain size (texture) were calculated. From the correlation coefficient values presented in Table 3 it is clear that there was a significant grain-size effect on the fraction contents. Fractions F1, F2 and F4 were positively correlated with the amount of clay and negatively correlated with the amount of sand. On the contrary, fraction F5, the cinnabar fraction, was in negative correlation with the amount of clay and in positive correlation with the amount of sand. On the basis of texture, samples can be classified into two groups. Samples from alluvial plains (S4–S7) were in the first group, composed mainly of sand and larger particles than sand. In the second group were the samples with clay and silt particles dominating (S1–S3). There is a significant difference between these two groups, as cinnabar is especially concentrated in coarse grained alluvial samples, where it constitutes on average more than 73% of total Hg. In contrast, non-cinnabar fractions were found to be enriched in areas where fine grained material was deposited, reaching up to 62% of total Hg.

Relations between relative amounts of fractions in the samples analyzed. An analysis of the relations between the fractions within the samples revealed a high degree of correlation between them (Table 3). An increased amount of any one fraction F1, F2, F3 or F4 lead to an increase of the remaining three fractions. On the other hand, an increased amount of fraction F5 resulted in decreased amounts of fractions F1 to F4. This suggested that most chemical processes involved in mercury cycling in the soil occur within the non-cinnabar mercury forms (F1–F4), as cinnabar (F5) is a very resistant insoluble form of mercury that does not enter in the mercury cycle. Biogeochemical conversion between non-cinnabar mercury forms provides the basis for mercury's complex distribution pattern in the soil, for its biological enrichment, and its atmospheric enrichment as well.

Relation between the relative amount of mercury in the fractions and the relative amount of evaporated mercury. To test the importance of different forms of mercury on mercury emission, correlations between the relative amount of the

Table 3 Correlations among different Hg fractions, texture and Hg fluxes

	F1 (%)	F2 (%)	F3 (%)	F4 (%)	F5 (%)	Sand (%)	Clay (%)	Hg flux[a]
F1 (%)		0.9948[b]	0.9146[b]	0.9435[b]	−0.9306[b]	−0.7536[b]	0.8601[b]	0.9505[b]
F2 (%)	0.9896[c]		0.9277[b]	0.9086[b]	−0.8983[b]	−0.6952[b]	0.8119[b]	0.9497[b]
F3 (%)	0.8364[c]	0.8606[c]		0.8398[b]	−0.8448[b]	−0.4762[b]	0.6872[b]	0.9770[b]
F4 (%)	0.8902[c]	0.8255[c]	0.7053[c]		−0.9919[b]	−0.8248[b]	0.9136[b]	0.9019[b]
F5 (%)	0.8660[c]	0.8069[c]	0.7137[c]	0.9838[c]		0.7677[b]	−0.8575[b]	−0.8859[b]
Sand (%)	0.5680[c]	0.4832[c]	0.2268[c]	0.6803[c]	0.5893[c]		−0.9506[b]	−0.6248[b]
Clay (%)	0.7398[c]	0.6592[c]	0.4722[c]	0.8347[c]	0.7352[c]	0.9036[c]		0.8127[b]
Hg flux[a]	0.9034[c]	0.9019[c]	0.9546[c]	0.8133[c]	0.7849[c]	0.3903[c]	0.6606[c]	

[a] Relative amount of Hg evaporated in 14 h during the volatilization simulation experiment. [b] Pearson product moment correlation coefficient (r). [c] Determination coefficient (R^2).

fractions in the samples and the relative amount of volatile mercury obtained during the emission simulation experiment were investigated, as mercury surface-to-atmosphere exchange is one of the most important factors affecting the mobility of mercury. High correlations (R^2 = 0.78–0.95) were observed as shown in Table 3. The relative amount of volatile (mainly Hg^0) mercury increased when the relative amount of the F1, F2, F3 and F4 fractions increased, and decreased when the percentage of F5 fraction increased. The suggestion is that Hg bound in the fractions F1 to F4 is mobile and potentially bioavailable, while Hg bound in fraction F5 is not, and therefore less harmful to the environment.

4. Conclusions

Despite the fact that mining activity in the Idrija region has finished, analyses of mercury content in different soils showed a high degree of contamination. Sources of contamination are natural rock containing mercury, deposits of residues from combustion or erosion and deposition of contaminated sediments by the river Idrijca. 41 to 51 mg kg^{-1} were found in soil samples taken in the area which is not under the direct influence of mining activity, and 322 to 345 mg kg^{-1} in samples taken nearby the smeltery. High amounts of mercury (60 to 415 mg kg^{-1}) were also detected in samples from the alluvial plains downstream of Idrija. The reason could be the high transport ability of the river Idrijca river during floods. Analyses of the vertical soil profile at the confluence of the rivers Bača and Idrijca showed higher amounts of mercury occurring at depths of 0.5 and 1 m than at the surface. This is due to a different mining technology during the formation of those sediments.

The simulation of the mercury vaporization from soil revealed that soil temperature and to a less extent added moisture are the main factors affecting the evaporation of mercury. The high correlation between the amount of mercury evaporated and total mercury in the samples indicates that elevated amounts of mercury in the air are not only consequences of anthropogenic impact but also the result of the geochemical characteristics of the region. Based on the results, which show that a constant evaporation rate is obtained after 6 hours, we recommend that the procedure to assess the potential for mercury volatilization from soils should be completed after this period of time. Our experiments were conducted at 70 °C, which seems to be high, as in nature temperatures rarely achieve such high values. We suggest that further investigations need to be performed to optimize the selected temperature. This is supported by the fact that bacteria may also be responsible for Hg reduction and volatilization, and the selected temperature should not destroy the bacterial activity, as may be the case at 70 °C. Sample storage also showed a great influence on the results obtained.

Sequential extraction of soils revealed that cinabarite and elemental mercury prevail. The amount of cinabarite increased linearly with the amount of course-grained component in the soil. With increase in the amount of non-cinabarite fractions the ratio of vaporized elemental mercury increased. The high correlations (R^2 = 0.71–0.99) between the amounts of water soluble mercury, acid soluble mercury, organic complex bonded mercury and elemental mercury indicate that processes of mercury transformation occur mainly between these species. In nature, the amount of these species, which are potentially bioavailable, is considerably lower than the total mercury content. Our results suggest that data on the amount of the mobile fraction of mercury are more relevant than data on total mercury content. The total mercury concentrations are high due to high contents of cinabarite, which is not soluble and does not enter the processes of mercury transformation. One of the very important conclusions of this work is also related to the effect of the sample preparation procedure and unspecific leaching on the results obtained by the sequential extraction. This suggests that further development and standardization of the method is of paramount importance to obtaining results comparable with other studies. In addition, the results of laboratory analyses should be compared by *in situ* measurements.

References

1 L. Kosta, A. R. Byrne, V. Zelenko, P. Stegnar, M. Dermelj and V. Ravnik, *Acta Chim. Slov.*, 1974, **21**, 49.
2 I. Mlakar and M. Drovenik, *Geologija*, 1971, **14**, 67.
3 R. Planinc, O. Bajt, M. Horvat, J. Faganeli and B. Gorenc, *Acta Chim. Slov.*, 1993, **40**, 349.
4 M. Horvat, S. Covelli, J. Faganeli, M. Logar, V. Mandič, R. Rajar, A. Širca and D. Žagar, *Sci. Total Environ.*, 1999, **237**(238), 43.
5 M. Gosar, S. Pirc and M. Bidovec, *J. Geochem. Explor.*, 1997, **58**, 125.
6 V. Miklavčič, in *Idrija as a natural and anthropogenic laboratory: Mercury as a major pollutant*, ed. V. Miklavčič, Idrija Mercury Mine, Idrija, 1998, pp. 6–9.
7 A. Gnamuš, M. Zupan and R. Šajn, *RMZ – Mater. Geoenviron.*, 2001, **48**, 94.
8 J. Čar, in *Idrija as a natural and anthropogenic laboratory: Mercury as a major pollutant*, ed. V. Miklavčič, Idrija Mercury Mine, Idrija, 1998, pp. 10–15.
9 T. Dizdarević, *RMZ – Mater. Geoenviron.*, 2001, **48**, 56.
10 H. Biester, M. Gosar and S. Covelli, *Environ. Sci. Technol.*, 2000, **34**, 3330.
11 H. Biester, M. Gosar and G. Müller, *J. Geochem. Explor.*, 1999, **65**, 195.
12 Ph. Quevauviller, in *Methodologies in Soil and Sediment Fractionation Studies*, ed. Ph. Quevauviller, The Royal Society of Chemistry, Cornwall, 2002, v.
13 N. S. Bloom, E. Preus, J. Katon and M. Hiltner, *Anal. Chim. Acta*, 2003, **479**, 233.
14 M. T. Scholtz, B. J. Heyst and W. H. Schroeder, *Sci. Total Environ.*, 2003, **304**, 185.
15 R. Ferrara, B. E. Maserti, M. Anderson, H. Edner, P. Ragnarson, S. Svanberg and A. Hernandez, *Atmos. Environ.*, 1998, **32**, 3897.
16 A. Carpi and S. E. Lindberg, *Atmos. Environ.*, 1998, **32**, 873.
17 K. H. Kim, S. E. Lindberg and T. P. Meyers, *Atmos. Environ.*, 1995, **29**, 267.
18 M. S. Gustin, S. E. Lindberg, K. Austin, M. Coolbaugh, A. Vetter and Z. Zhang, *Sci. Total Environ.*, 2000, **25**, 961.
19 M. S. Gustin, *Sci. Total Environ.*, 2003, **304**, 153.
20 M. Horvat, V. Lupšina and B. Pihlar, *Anal. Chim. Acta*, 1991, **243**, 71.
21 Official Gazette of Slovenia, No. 68/96, T.02/1, Ljubljana, 1996.
22 M. Horvat, V. Jereb, V. Fajon, M. Logar, J. Kotnik, J. Faganeli, M. E. Hines and J.-C. Bonzongo, *Geochem.: Explor., Environ., Anal.*, 2002, **2**, 287.
23 N. S. Bloom and J. Katon, *Application of selective extractions to the determination of mercury speciation in mine tailings and adjacent soils*, Proceedings of the EPA Workshop on Hg Releases from Mining, November 28–30, San Francisco, 2000, pp. 79–83.
24 M. Horvat, B. Kontić, J. Kotnik, N. Ogrinc, V. Jereb, V. Fajon, M. Logar, J. Faganeli, T. Dizdarević, R. Rajar, A. Širca, G. Petkovšek and D. Žagar, *Crit. Rev. Anal. Chem.*, in press.
25 J. C. Bonzongo, W. B. Lyons, M. E. Hines, J. J. Warwick, J. Faganeli, M. Horvat, P. J. Lechler and J. R. Miller, *Geochem.: Explor., Environ., Anal.*, 2002, **2**, 111.
26 M. E. Hines, M. Horvat, J. Faganeli, J.-C. J. Bonzongo, T. Barkay, E. B. Major, K. J. Scott, E. A. Bailey and J. J. Warwick, *Environ. Res.*, 2000, **83**, 129.

Preparation and characterization of a soil reference material from a mercury contaminated site for comparability studies

David Kocman[a,*], Nicolas S. Bloom[b], Hirokatso Akagi[c], Kevin Telmer[d], Lars Hylander[e], Vesna Fajon[a], Vesna Jereb[a], Radojko Jaćimović[a], Borut Smodiš[f], Justinian R. Ikingura[g], Milena Horvat[a]

[a]*Department of Environmental Sciences, Jožef Stefan Institute, Jamova 39, 1001 Ljubljana, Slovenia*
[b]*Frontier Geosciences Inc., 414 Pontius Ave North, Seattle, WA 98109, USA*
[c]*National Institute for Minamata Disease Laboratory, Japan*
[d]*School of Earth and Ocean Sciences, University of Victoria, Victoria, Canada V8W 3P6*
[e]*Limnological Department, Uppala University, Sweden*
[f]*Division of Human Health, International Atomic Energy Agency, Wagramerstrasse 5, P.O. Box 100, A-1400 Vienna, Austria*
[g]*Department of Geology, University of Dar es Salaam, P.O. Box 35052, Dar es Salaam, Tanzania*

Received 21 May 2004; received in revised form 24 February 2005; accepted 30 September 2005
Available online 6 June 2006

Abstract

The preparation and characterization of a soil reference material (SOIL-1) from a site polluted with mercury due to the past mercury mining in Idrija, Slovenia is reported. Homogeneity tests and intercomparison exercises for total (T-Hg) and methylmercury (MeHg) were performed. In addition, selective sequential extraction was applied for Hg fractionation, and multielemental analyses were performed by k_0 standardization neutron activation analysis (k_0-INAA) and inductively coupled mass spectrometry (ICP-MS) for other trace elements. Comparison of different analytical methods, as well as the distribution of data were critically evaluated using descriptive statistics and analysis of variance (ANOVA). Due to the nugget effect (cinnabar particles representing more than 90% of the mercury), homogeneity for T-Hg determination was difficult to achieve. The intercomparison exercise indicated that in order to obtain comparable results for total mercury (T-Hg) sample decomposition by HF must be performed. These data are then in good agreement with non-destructive methods such as k_0-INAA. Accepted reference values calculated taking into account the results obtained by six and three laboratories, respectively, were $67.1 \pm 11.3\,\mathrm{mg\,kg^{-1}}$ for T-Hg and $4.0 \pm 1.3\,\mathrm{ng\ g^{-1}}$ for MeHg (95% confidence intervals). However, the results obtained for Hg fractionation displayed significant differences in the organically bound fraction and elemental Hg. Results obtained by two laboratories using totally different analytical protocols for other elements showed excellent agreement for most elements. In summary, the results obtained for the SOIL-1 sample were of sufficient quality to suggest its use for quality control in laboratories dealing with mercury contaminated soils.

Keywords: Reference material; Mercury; Soils

1. Introduction

Soils and sediments are known to be accumulation pools for metals. Regarding mercury pollution, these environmental compartments are also critical from another point of view—they are important sites where Hg(II) is methylated to the most toxic Hg compound—methylmercury $MeHg^+$. Mercury in soil can also undergo other important transformation mechanisms such as reduction to elemental Hg and demethylation of $MeHg^+$. It is generally accepted that there is still a gap in our knowledge of the biogeochemistry of Hg in soils and sediments. In addition there is a lack of suitable "matrix" reference materials (RMs) for mercury analysis and speciation in contaminated soils. Only a few of them are certified, with

*Corresponding author.
E-mail address: david.kocman@ijs.si (D. Kocman).

0301-4797/$ - see front matter © 2006 Elsevier Ltd. All rights reserved.
doi:10.1016/j.jenvman.2005.09.024

concentrations ranging from 20 ng g^{-1} to about 6 μg g^{-1} with uncertainties from 8% to 31%. The stated concentrations refer to either "aqua regia extractable", "boiling HNO_3" or "cold HNO_3 extractable" mercury (IAEA, 1995). The present status of Hg in sediments is slightly better—there are a few RMs certified for both total (T-Hg) and methylmercury (MeHg), but they are mostly of marine origin (Horvat, 1999). Clearly, the existing RMs do not cover the needs for Hg studies and monitoring in contaminated areas where T-Hg concentrations are elevated (above several tens of μg g^{-1}).

Therefore, the aim of our work was to prepare a RM suitable for Hg studies in contaminated sites. Polluted soil (SOIL-1) from an area close to the Idrija mercury mine, Slovenia, was chosen. That soil is contaminated with Hg due to continuous deposition of particles enriched with Hg during flood events. Such a sample is representative of areas where mercury transport and deposition is governed by river hydrology, which is typical in a number of mercury contaminated environments. The work was conducted by the International Atomic Energy Agency (IAEA) and IJS in the framework of an IAEA Coordinated Research Project (CRP) "Health impacts of mercury cycling in contaminated environments studied by nuclear techniques". In this paper, the preparation and characterization of SOIL-1 by means of sample homogeneity measurements and interlaboratory studies are reported. All laboratories of the CRP participants were encouraged to participate in the data quality intercomparison exercises by analyzing total and MeHg in the samples by their usual techniques. The sample was also analyzed in two laboratories for other elements using INAA and ICP-MS methods. Further characterization included differentiation of Hg compounds in SOIL-1 into different behavioral classes by a sequential extraction scheme adopted from Bloom et al. (2003).

2. Methodology

2.1. Preparation of SOIL-1

2.1.1. Origin of SOIL-1

About 100 kg of soil sample was collected in polyethylene containers on 27th February 2001 from the grassland at Bača pri Modreju that is frequently flooded by the river Idrijca (Fig. 1). Surface soil was taken by a plastic shovel. The sample was then transported to the Department of Environmental Sciences at the Jožef Stefan Institute, Ljubljana for further preparation. The same sampling site has been regularly monitored since 1995 and the concentrations of total Hg were reported to be in the range between 40 and 50 mg kg^{-1} dry weight, while MeHg concentrations varied from 3 to 5 ng g^{-1}.

2.1.2. Preparation of bulk material and bottling

The soil was air dried at 40 °C in a drying oven for 3 days. Samples were then ground and homogenized in a rotating ceramic ball mill for 60 min, sieved first through a 1.4 mm screen and then through a 250 μm screen. Since the preliminary data on bulk homogeneity indicated noticeable non-homogeneities, it was decided to re-homogenize the samples. The results were still not satisfactorily homogeneous, therefore sieving through a 125 μm screen had to be conducted. The whole content of the sample was then homogenized in a plastic rotating container for 3 days. Based on demonstrated homogeneity of the bulk material for a 500 mg sample the material was sub-sampled into 300 polyethylene bottles (100 mL), each containing about 70 g of sample. A flow chart for soil preparation is shown in Fig. 2.

2.1.3. Homogeneity studies

2.1.3.1. Bulk homogeneity test. In order to ensure the suitability of the material for an intercomparison, preliminary tests were performed for T-Hg at different particle sizes and sample intakes. To test the homogeneity of the material prior to final bottling, between-bottle homogeneity was verified based on aliquots from 10 bottles taken randomly. Due to high Hg concentrations the initial bulk homogeneity test was done on a 200 mg sample intake for <250 μm particle size. Total Hg was analyzed by cold vapor atomic absorption spectrophotometry (CV AAS) after digestion of the samples with nitric and sulfuric acid at 70 °C for 12 h in a closed Teflon digestion vessel on a LCD Milton Roy instrument (Horvat et al., 1991). The digested samples of <250 particle size and 200 mg sample intake were also measured by a SANSO SEISHAKUSHO CV AAS Hg analyzer, Instrument Model 910, Japan, without amalgamation to check for possible interferences during the measurement step. A repeated bulk homogeneity test was done on the <125 μm fraction with the same sample intake. Due to relatively poor homogeneity the sample intake was increased to 500 mg, which resulted in more acceptable CVs.

2.1.3.2. Final homogeneity test. A final homogeneity test was conducted after completion of the bottling of the sample material. A more rigorous digestion was employed, as the bulk homogeneity test did not come up with fully satisfactory results. Samples were analyzed by CV AAS after complete dissolution by a mixture of hydrofluoric, nitric and hydrochloric acids at 135 °C for 12 h. The between-bottle homogeneity was tested by the determination of T-Hg based on sample weights of 100 mg taken from six bottles. The within-bottle homogeneity was assessed by three replicate determinations on the content of each bottle.

2.2. Intercomparison exercise

An intercomparison exercise was conducted between the participating laboratories on SOIL-1. This study was intended to give the laboratories responsible for mercury analyses an opportunity to check the accuracy of their analytical results and analytical performance.

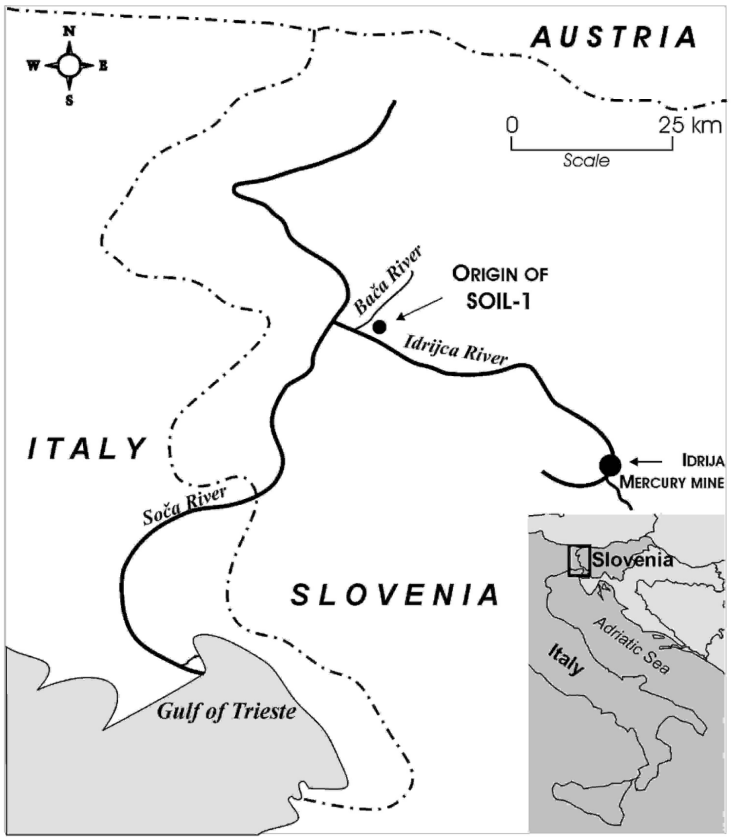

Fig. 1. Origin of SOIL-1 material.

The bottles of sample material were dispatched to all CRP participants and other laboratories interested in participating. Participating laboratories were requested to determine T-Hg and MeHg by their routine procedures. The IAEA and IJS were also interested in receiving results for any other element(s) that participating laboratories determined routinely. Participating laboratories were requested to make at least three, but preferably six, independent replicate determinations and to report all results, including the average weight of the sample taken for analysis, the concentration of each independent replicate determination, the arithmetic mean and the standard deviation of the replicate determinations and the detection limit of the method. Additionally, information requested included a summary of quality control procedures routinely employed within their laboratory, the results for Certified RMs analyzed concurrently and the instrumental method used for the quantitative determination.

In total, six laboratories from six countries participated in this intercomparison exercise. Total Hg results were provided by six laboratories, methylmercury by three and multielemental results by two. The analytical methods used by different laboratories accompanied by a short description are summarized in Table 1.

2.3. *Sequential extraction procedure*

A six-step sequential extraction scheme (SES) was applied to SOIL-1 in two laboratories (Frontier Geosciences Inc., Seattle and IJS, Ljubljana). Analyses were performed on 9 and 4 replicate samples, respectively. The SES consisted of six steps: including (a) water soluble (F1), (b) "human stomach acid" soluble (F2), (c) organo-chelated (F3), (d) elemental Hg (F4), (e) mercuric sulfide (F5) and residual fraction (F6). The sequential extraction procedure steps and the reagents used are described in Table 2.

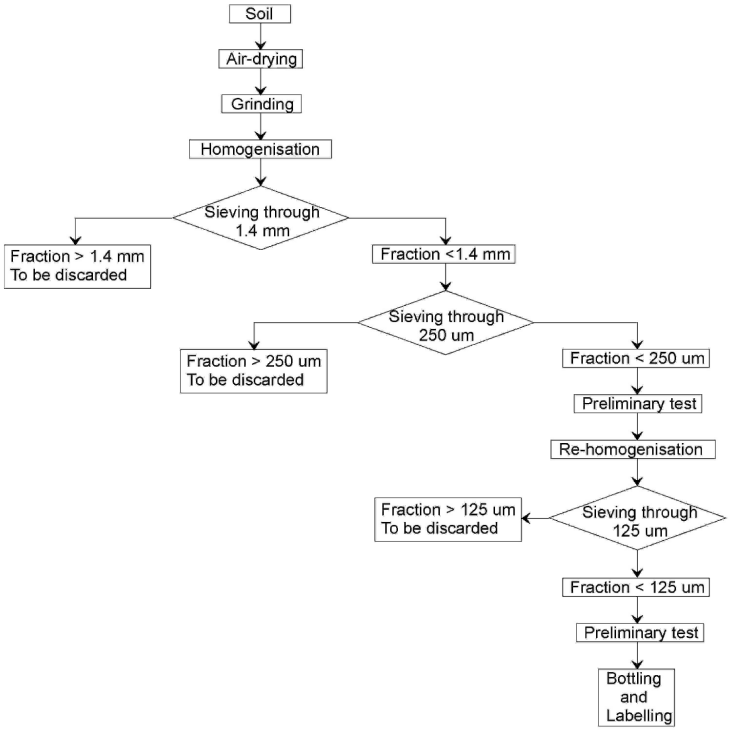

Fig. 2. Flow chart for the preparation of the SOIL-1.

Extractions were carried out using 0.4 g of sample. The sample weight to extractant volume ratio was 1–100. A total of 40 mL of extractant was added to the solid and subjected to end-over-end shaking at 250 rpm for 18 ± 4 h. The vials were then centrifuged at 3800 rpm for 10 min, and the supernatant liquid decanted for filtration through a membrane filter of 0.20 μm pore size. The extracted solution was then placed in a clean Teflon bottle and oxidized by adding 5 mL of 0.2 M BrCl. Total Hg in the oxidized extracted solution was determined using $SnCl_2$ reduction, gold trap amalgamation and CVAAS. In the subsequent extraction steps the above procedure was repeated. Owing to the very low expected Hg values in some fractions, the filters were rinsed with HNO_3, HCl and deionised water before filtration to avoid contamination. This SES is described in more detail elsewhere (Bloom et al., 2003).

The soil was prepared initially for comparability studies by the CRP participants. However, it was hoped that the material if satisfactory could serve a wider function to scientists working in the field of soil and environmental contamination.

3. Results and discussion

3.1. Homogeneity studies

3.1.1. Bulk homogeneity

The coefficients of variation (CV) obtained from replicate T-Hg analyses of different particle sizes and sample weights are presented in Table 3. The between bottles CVs revealed that the results obtained from the sample of the particle size <250 μm were not satisfactory. Re-homogenization and sieving through 125 μm pore size showed no better results when 200 mg of sample was analyzed. A larger sample intake (500 mg) showed a lower CV (about 7%), which was considered satisfactory based on the fact that soil samples from areas impacted by mining activities cannot be prepared completely homogeneous due to the nugget effect.

3.1.2. Final homogeneity

The homogeneity test was done with three replicate determinations in six individual bottles. The between-bottles CV was 16.8% and within-bottles CVs varied

Table 1
Analytical methods used by participating laboratories accompanied with a short description

Code	Institution	Analyses	Detection	Digestion method
1A	IJS, Slovenia	T-Hg	CV AAS	HNO_3/H_2SO_4 digestion, $SnCl_2$ reduction, amalgamation
1B	IJS, Slovenia	T-Hg	CV AAS	$HF/HNO_3/HCl$ digestion, $SnCl_2$ reduction, amalgamation
1C	IJS, Slovenia	T-Hg multielemental	k_0-INAA	Thermal neutron flux irradiation in 250 kW TRIGA Mark II reactor, HPGe calibrated detector
1D	IJS, Slovenia	MeHg	CV AFS	$KBr/H_2SO_4/CuSO_4$ leaching, solvent extraction by CH_2Cl_2, derivatisation, ethylation, gas chromatography, pyrolysis
2	University of Dar es Salaam, Tanzania	T-Hg	CV AAS	HNO_3 digestion
3	Syddansk Universitet, Denmark	T-Hg	FAAS	Thermal decomposition at 550 ºC
4A	NIMD, Japan	T-Hg	CV AAS	HNO_3 digestion
4B	NIMD, Japan	MeHg	GC ECD	Acid leaching, solvent extraction of dithizonates
5A	University of Victoria, Canada	T-Hg	CV AFS	Aqua-regia (HCl/HNO_3) digestion with 0.01% $K_2Cr_2O_7$
5B	University of Victoria, Canada	multielemental	ICP MS	Aqua-regia (HCl/HNO_3) digestion with 0.01% $K_2Cr_2O_7$
6A	Frontier Geoscience, USA	T-Hg	CV AFS	$HF/HNO_3/HCl$ digestion, $SnCl_2$ reduction, amalgamation
6B	Frontier Geoscience, USA	MeHg	CV AFS	$KBr/H_2SO_4/CuSO_4$ leaching, solvent extraction by CH_2Cl_2, derivatisation, ethylation, gas chromatography, pyrolysis

Table 2
Sequential extraction scheme (SES): steps, reagents and fraction descriptions

Step	Reagents	Fraction description	Typical Hg species
F1	Milli-Q water	Water soluble	$HgCl_2$, $HgSO_4$
F2	pH 2 HCl/HOAc	"Human stomach acid" soluble	HgO
F3	1 N KOH	Organo-chelated	Hg in humic acids, Hg_2Cl_2
F4	12 N HNO3	Elemental	Hg^0, Hg_2Cl_2
F5	Aqua regia	Cinnabar	HgS, m-HgS, HgSe, HgAu
F6	$HF/HCl/HNO_3$	Residual	mineral lattice bound

Table 3
Bulk homogeneity test results

Sample intake (mg)	Particle size (μm)	n[a]	Average T-Hg (mg kg^{-1})	CV (%)[b]
200	<250	3	58.6	11.9
200	<250	3	56.3[c]	11.9
200	<125	1	47.1	11.0
500	<125	1	50.5	7.3

[a]Number of replicates in each of 10 bottles.
[b]Coefficient of variation.
[c]Without amalgamation.

between 10% and 18%. An F-test at a significance level of 0.05 did not detect any difference between the within- and between-bottle variances. Although the material homogeneity test showed poorer homogeneity than expected, for both the between- and within bottle homogeneity, the heterogeneity was measurable and, therefore, we concluded that the material was suitable for use as an intercomparison sample.

3.2. Intercomparison exercise results

3.2.1. Total mercury

The results obtained from participating laboratories were evaluated using statistical and graphical methods, including descriptive statistics and analysis of variance (ANOVA). For each of the data sets, the range of determinations, arithmetic means and standard deviations were compiled, based on the laboratory means. Some data were rejected on the basis of difficulties reported by the laboratories (e.g. too small a sample weight, high Hg vapor pressure, calibration range, no acceptable quality control, etc.).

The remaining laboratory data were used to calculate an overall arithmetic mean, standard deviation and 95% confidence interval. A summary of the results is presented in Fig. 3, which depicts S-plots showing all the laboratory mean values in order of increasing concentration, based on at least three independent determinations. It is evident from this plot that the data are relatively spread out with CV varying between 4% and 19%. In most cases CVs were about 10%, which is attributed to the relatively high heterogeneity of the material. For the determination of total Hg, most of the laboratories used a wet digestion procedure, followed by cold vapor techniques with detection by AAS or AFS. One laboratory used thermal decomposition (Lab code 3) and one non-destructive k_0-instrumental neutron activation analysis (k_0-INAA) (Lab code 1C). Out of eight reported datasets, three showed statistically significant different means for total Hg. (i.e., using ANOVA and the least significant difference multiple range test at $P = 0.05$) (Miller and Miller, 1993). Two of them showed higher values (Lab codes 1C and 6A) and one of them was significantly lower (Lab code 1A). Lower results were observed when wet digestion using H_2SO_4/HNO_3 acids followed by CV AAS was employed (Lab code 1A). The reason for the lower results obtained may be due to the incompleteness of the H_2SO_4/HNO_3 acid digestion where Hg could not be totally leached from the HgS (cinnabar). Lower results may also be a consequence of volatilization losses during an incorrect digestion procedure, as described in the literature (Trimm et al., 1998). Higher results were observed in the case of total sample digestion using HF (Lab codes 1B, 6A) and non-destructive k_0-INAA (Lab code 1C). Total decomposition with a mixture of acids including hydrofluoric acid is well known to produce higher results for heavy metals including mercury (Wyse et al., 2004). Also k_0-INAA showed good performance on environmental samples such as soil, sediments and sewage sludge in the past, especially when elevated mercury values ($>1\,mg\,kg^{-1}$) were involved (Jaćimović and Horvat, 2004), as is the case in our study. Methods employed by other laboratories were based on acid leaching without the presence of HF (Lab codes 1A, 2, 4A, 5A) and one thermal decomposition method (Lab code 3). Only Lab 1A showed a statistically significant difference for total Hg when these laboratories (Lab code 1A, 2, 3, 4A and 5A) were compared.

Although the data for Lab codes 1C, 1A and 6A were statistically different from the other results, we only excluded data for the lowest concentrations of total Hg (Lab. Code 1A). This decision was based on the fact that the same laboratory also reported data based on dissolution of the sample with the use of HF. All other data were then used for calculation of the mean value and 95% confidence intervals. Accepted laboratory means varied between 62.3 and $82.1\,mg\,kg^{-1}$. The recommended value is $67.1\,mg\,kg^{-1}$ with the 95% confidence interval from 55.8 to $78.4\,mg\,kg^{-1}$.

3.2.2. Methylmercury

Data obtained from three independent laboratories varied from 2.3 to $5.6\,ng\,g^{-1}$. These results are in accordance with previous observations at the location where the material for SOIL-1 was taken (Horvat et al., 2002). A summary of the results is presented in Fig. 4, which depicts S-plots showing the laboratory mean values in increasing concentrations. All laboratories' CVs are less than 7%. Methods used by laboratories 1D and 6B were practically the same. The protocol is based on acid

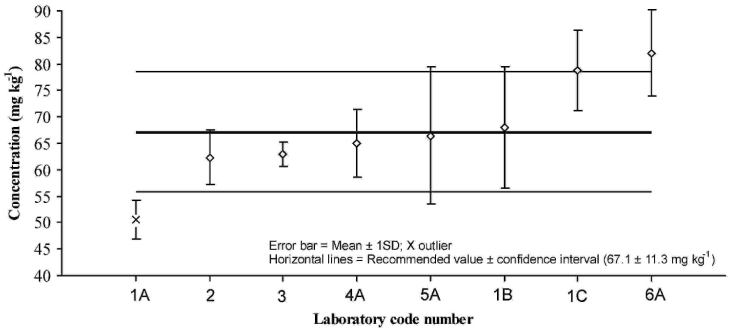

Fig. 3. Figure of laboratory T-Hg mean values, standard deviations and 95% confidence interval.

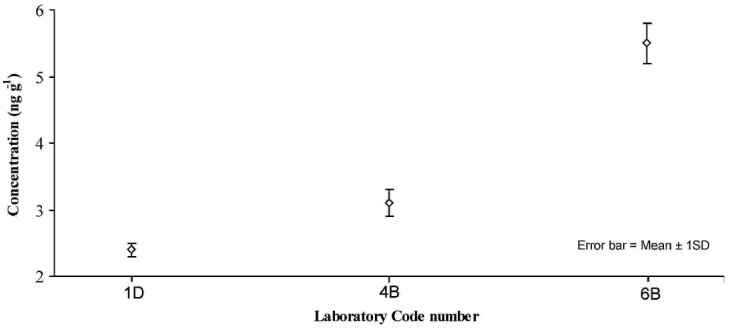

Fig. 4. Figure of laboratory MeHg mean values and standard deviations.

Table 4
Comparison of laboratory code no. 1 and no. 6 SES results

Fraction	Laboratory			
	Lab code no.1 ($n = 4$)[a]		Lab code no.6 ($n = 9$)	
	Average T-Hg (mg kg^{-1})	CV (%)	Average T-Hg (mg kg^{-1})	CV (%)
F1	0.032	36	0.018	5.7
F2	0.002	40	0.0013	21
F3	0.106	26	1.02	4
F4	5.87	3	3.43	7.3
F5	64.8	4	67.8	9.3
F6	0.032	35	—	—

[a] n, Number of replicates.

leaching, solvent extraction, derivatization by ethylation and detection by gas chromatography, pyrolysis and CV AFS detection (Logar et al., 2002). However, the results differ significantly. This difference could be attributed to the artifact MeHg production during the extraction step (Hintelmann et al., 1997), although the use of $KBr/H_2SO_4/CuSO_4$ leaching should practically be artifact free (Bloom et al., 1997). These differences deserve further attention; as shown in a study by Liang et al. (2004), the recovery of MeHg in soil may be significantly affected by the amount of sample intake and extraction reagents used. Slight changes in analytical protocols may affect the results. The results presented in Fig. 4 are for information purposes only and might be useful to those that intend to use this material for method development and comparability studies.

3.3. Results for sequential extraction

The results of sequential extraction obtained from both laboratories revealed cinnabar (F5) and elemental Hg (F4) as the predominant fractions, followed by organo-chelated (F3), water soluble (F1) and "human acid" soluble (F2) mercury. The sum of all fractions was similar to the total content obtained after digestion of the homogenized sample with nitric, hydrofluoric and hydrochloric acid. Recoveries of 80–105% were reached in most cases. The difference between the sum of species and T-Hg can be due in part to small losses during the SES extraction (<5%) and unleachable Hg bound in the rock lattice. The latter was confirmed in one laboratory by the determination of the residual mercury content after digestion with nitric, hydrochloric and hydrofluoric acid. Trace amounts of mercury were measured (between 32 and 42 μg kg^{-1}). Comparison of parallel determination in each particular step showed a good agreement. The CV values varied from 3% to 9% in the case of elemental (F4) and cinnabar (F5) fractions. Bigger differences were observed among fractions less abundant in Hg (more than 30%), which can be related to analytical uncertainties.

Comparison of the results using the same SES protocol is shown in Table 4. A significant disagreement was observed for F3, where IJS reported 10 times lower values than Frontier Geosciences, while for fraction F4 the values reported by the IJS were higher by a factor of 2. The differences are difficult to interpret and it is suggested that further research is needed to confirm the suitability of the proposed fractionation scheme for soil samples.

3.4. Multielemental analysis results

In addition, multielemental analysis results obtained by two laboratories using k_0-INAA and ICP-MS are given in Table 5. The results are presented as the average values of three and six independent determinations, respectively, accompanied with relative standard deviations (RSD) and detection limits. Thirty-seven elements were determined

Table 5
Summary of the results of k_0-INAA and ICP-MS multielemental analyses

Analyte	k_0-INAA ($n = 3$)			ICP-MS ($n = 6$)		
	Mean (mg kg^{-1})	RSD (%)	LOD (mg kg^{-1})	Mean (mg kg^{-1})	RSD (%)	LOD[a] (mg kg^{-1})
Ag	<0.3		0.3			
As	9.3	1.18	0.4			
Au	<0.002		0.002			
Ba	197.0	1.52	10	200.6	3.2	0.28
Be				1.5	15.9	0.06
Bi				1.3	13.3	0.01
Br	6.1	0.98	0.3			
Ca	96739.0	1.38	500			
Ce						
Cd	2.0	0.00	1.50			
Ce	54.7	2.74	0.3			
Co	6.6	0.76	0.03			
Cr	36.4	1.37	0.5			
Cs	5.2	0.39	0.06	5.1	4.5	0.25
Dy				4.1	7.6	0.01
Er				2.4	4.8	0.01
Eu	0.8	3.57	0.1	0.8	4.4	0.03
Fe	19678.0	0.64	30			
Ga	<20		20			
Gd				4.8	6.9	0.56
Hf	5.5	0.72	0.05	3.0	5.4	0.01
Hg	78.75	7.62	0.2			
Ho				0.8	2.7	0.005
K	14431.0	2.75	500			
La	27.9	2.15	0.03	26.8	5.9	0.01
Li				32.5	8.0	1.47
Lu				0.3	4.4	0.01
Mo	1.4	23.53	0.5	1.2	6.7	0.14
Na	5479.0	0.55	15			
Nb				18.3	10.5	0.11
Nd	27.1	5.90	1	23.7	6.2	0.03
Pb				44.8	7.7	0.03
Pr				6.6	3.2	0.01
Rb	71.3	1.40	2	75.0	5.5	0.5
Sb	2.7	2.62	0.03			
Sc	7.6	0.53	0.005	7.6	7.9	0.05
Se	<0.4		0.4			
Sm	4.6	1.32	0.01	4.7	4.2	0.04
Sn	<20		20			
Sr	128.0	3.91	20	134.0	2.8	0.48
Ta	0.8	0.66	0.03	0.8	3.1	0.003
Tb	0.7	1.54	0.03	0.7	9.1	0.004
Te	1.0	19.80	0.9			
Th	10.0	1.00	0.05	10.2	10.2	0.02
Tl				0.5	7.0	0.05
Tm				0.3	4.5	0.01
U	3.2	2.21	0.05	3.4	5.6	0.01
V				49.1	5.7	0.06
W	2.2	2.74	1			
Y				25.9	4.6	0.01
Yb	2.4	1.67	0.05	2.3	6.9	0.03
Zn	88.5	5.42	2			
Zr	234.0	3.85	40	103.4	9.2	0.02

[a]LOD, limit of detection.

using k_0-INAA and 32 elements using ICP-MS. The RSD for all of the elements that are well measured by these two methods are quite low, less than 10%. This indicates that these elements are homogeneously distributed in SOIL-1 as opposed to Hg where significant heterogeneity was observed due to the specific nature of SOIL-1. The comparison of the results obtained by k_0-INAA and ICP-MS showed generally excellent agreement. However, there were some differences, since ICP-MS showed somewhat lower results for Hf and Zr.

4. Conclusions

Mercury polluted soil (SOIL-1) from the Idrija mercury mine region, Slovenia, was prepared and characterized for T-Hg and MeHg. Bulk homogeneity tests showed that it is very difficult to assure sufficient homogeneity for mercury determination in soils from Hg contaminated sites. This is probably due to the nugget effect, a term which describes particles of small size with a high amount of Hg (most probably cinnabar particles), as it was shown by a sequential extraction procedure that more than 90% of the mercury is contained in the cinnabar (F5) fraction. Moreover, the intercomparison exercise underscored the importance of complete decomposition of this kind of material with HF or the use of non-destructive methods such as k_0-INAA for obtaining accurate results for T-Hg. MeHg measurements obtained from different laboratories showed that the improvement of analytical procedures for MeHg in soil deserves further attention.

Two sets of data for multielemental analysis indicated that Hg in the SOIL-1 is distributed differently from other matrix elements. Considering the nature of the SOIL-1 sample (e.g. mercury mining), heterogeneity of Hg at the 17% level is acceptable and therefore the material is suggested for comparability studies. However, the generalization of such an assumption for other contaminated samples, prepared for similar purposes, should be made with caution, taking the origin of the sample into consideration.

Acknowledgments

This work was supported by the IAEA through contract 10879/R1 "Biogeochemistry of mercury in the contaminated environment in the wider Idrija region and the Gulf of Trieste using nuclear techniques".

References

Bloom, N.S., Colman, J.A., Barber, L., 1997. Artifact formation of methyl mercury during aqueous distillation and alternative techniques for the extraction of methyl mercury from environmental samples. Fresenius Journal of Analyical Chemistry 358, 371–377.

Bloom, N.S., Preus, E., Katon, J., Hiltner, M., 2003. Selective extractions to assess the biogeochemically relevant fractionation of inorganic mercury in sediments and soils. Analytica Chimica Acta 479, 233–248.

Hintelmann, H., Falter, R., Ilgen, G., Evans, R.D., 1997. Determination of artifactual formation of monomethylmercury (CH_3Hg^+) in environmental samples using stable Hg^{2+} isotopes with ICP-MS detection: calculation of contents applying species specific isotope addition. Fresenius J. Anal. Chem. 358, 363–370.

Horvat, M., 1999. Current status and future needs for biological and environmental reference materials certified for methylmercury compounds. Chemosphere 39, 1167–1179.

Horvat, M., Miklavčič, V., Pihlar, B., 1991. Determination of total mercury in coal fly ash by gold amalgamation cold vapour atomic absorption spectrometry. Analytica Chimica Acta 243, 71–79.

Horvat, M., Jereb, V., Logar, M., Kotnik, J., Faganeli, J., Hines, M.E., Bonzongo, J.C., 2002. Mercury distribution in water, sediment and soil in the Idrijca and Soča river systems. Geochemical Exploration and Environmental Analysis 2, 287–296.

IAEA, 1995. Survey of reference materials. Vol. 1: Biological and environmental reference for trace elements, nuclides and micro-contaminants. IAEA-TECDOC-854, Vienna.

Jaćimović, R., Horvat, M., 2004. Determination of total mercury in environmental and biological samples using k_0-INAA, RNAA and CV AAS/AFS techniques: advantages and disadvantages. Journal of Radioanalytical and Nuclear Chemistry 259, 385–390.

Liang, L., Horvat, M., Feng, X., Shang, L., Li, H., Pang, P., 2004. Re-evaluation of distillation and comparison with HNO_3 leaching/solvent extraction for isolation of methylmercury compounds from sediment/soil samples. Applied Organometallic Chemistry 18, 264–270.

Logar, M., Horvat, M., Akagi, H., Pihlar, B., 2002. Simultaneous determination of inorganic mercury and methylmercury compounds in natural waters. Analytical and Bioanalytical Chemistry 374, 1015–1021.

Miller, J.C., Miller, J.N., 1993. Statistics for Analytical Chemistry. Ellis Horwood Limited, West Sussex, UK.

Trimm, D.L., Beiro, H., Parker, J., 1998. Comparison of digestion techniques in analyses for total metals in marine sediments. Bulletin of the Environmental Contamination and Toxicology 60, 425–432.

Wyse, E.J., Coquery, M., Azemard, S., de Mora, S.J., 2004. Characterisation of trace elements and methylmercury in an estuarine sediment reference material, IAEA-405. Journal of Environmental Monitoring 6, 48–57.